

**New developments in  
sentinel lymph node biopsy for  
early-stage oral cancer**

Rutger Mahieu



# **New developments in sentinel lymph node biopsy for early-stage oral cancer**

Nieuwe ontwikkelingen in de schildwachtlierprocedure  
bij vroeg-stadium mondholtekanker

**Rutger Mahieu**

ISBN: 978-94-6496-338-0

Cover concept: Rutger Mahieu

Cover background: Klaas Jonkman ([www.klaasjonkman.com](http://www.klaasjonkman.com))

Cover: Ilse Modder ([www.ilsemodder.nl](http://www.ilsemodder.nl))

Layout: Ilse Modder ([www.ilsemodder.nl](http://www.ilsemodder.nl))

Printed and published by: Gildeprint - Enschede ([www.gildeprint.nl](http://www.gildeprint.nl))

The author gratefully acknowledges the financial support for printing this thesis by: Stichting ORLU, Michel Keijzerfonds, ChipSoft, Daleco Pharma B.V., ExamVision, Guerbet, Makker Hoortoestellen, MDS Medical, Mediplast, MediTop, NRG PALLAS, PI Medical, QuaMedical, Soluvos Medical B.V., Sonova Audiological Care Nederland B.V., Tristel, Tromp Medical B.V., Vivisol.

# **New developments in sentinel lymph node biopsy for early-stage oral cancer**

**Nieuwe ontwikkelingen in de schildwachtklierprocedure bij  
vroeg-stadium mondholtekanker**  
(met een samenvatting in het Nederlands)

## **Proefschrift**

ter verkrijging van de graad van doctor aan de  
Universiteit Utrecht  
op gezag van de  
rector magnificus, prof. dr. H.R.B.M. Kummeling,  
ingevolge het besluit van het College voor Promoties  
in het openbaar te verdedigen op

donderdag 3 april 2025 des middags te 2.15 uur

door

**Rutger Mahieu**

geboren op 1 april 1993  
te Blaricum

**Promotor:**

Prof. dr. R. de Bree

**Copromotor:**

dr. B. de Keizer

**Beoordelingscommissie:**

Prof. dr. P.J. van Diest (voorzitter)

Prof. dr. M.G.E.H. Lam

dr. R.A. Valdés Olmos

Prof. dr. M.R. Vriens

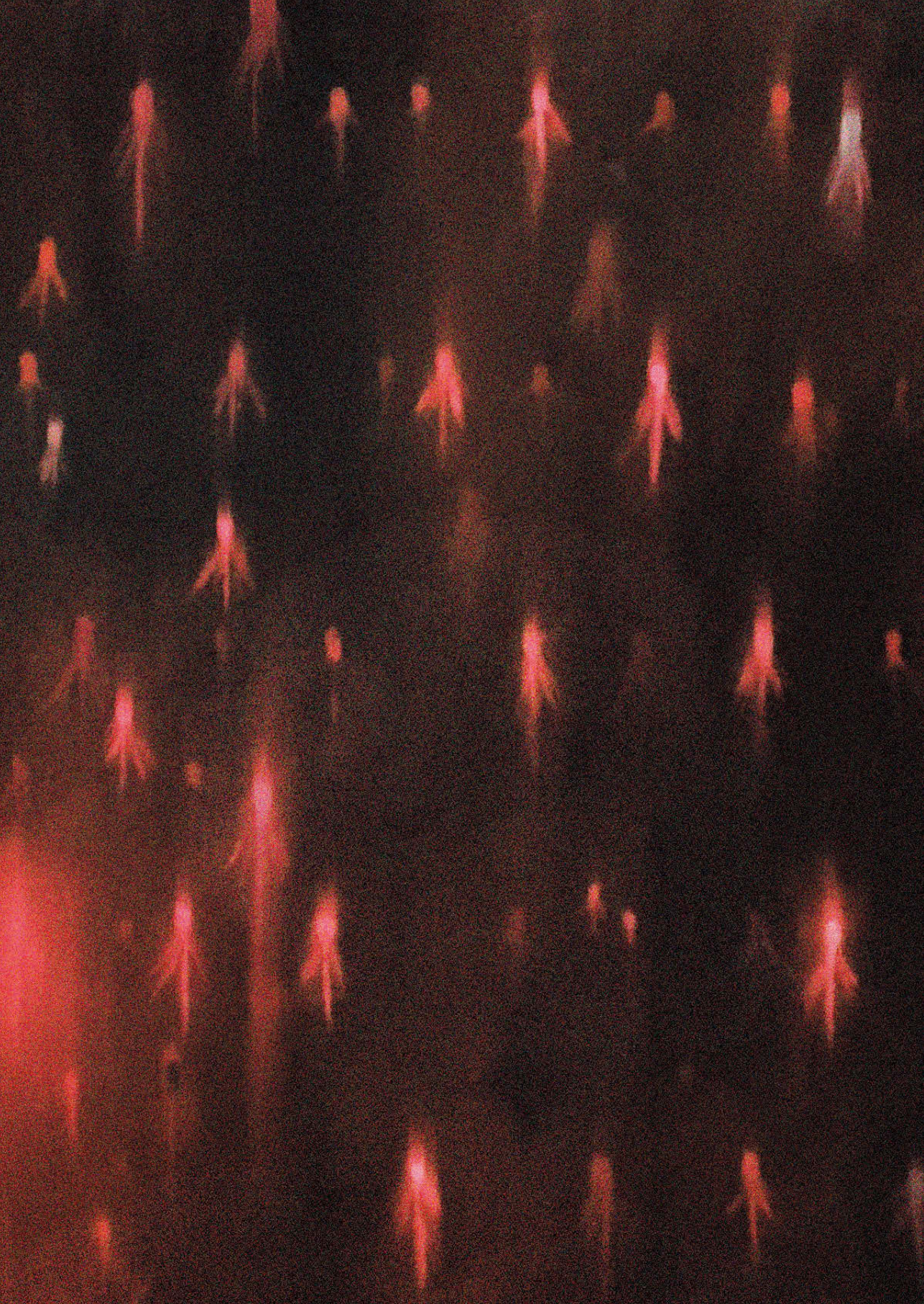
Prof. dr. M.J.H. Witjes

# Table of contents

Chapter 1	General introduction and outline of this thesis	9
<b>Conventional procedure</b>		
Chapter 2	Contralateral regional recurrence in lateralized or paramedian early-stage oral cancer undergoing sentinel lymph node biopsy - comparison to a historic elective neck dissection cohort <i>Front Oncol. 2021 Apr 23;11:644306</i>	25
Chapter 3	Evaluation of a streamlined sentinel lymph node imaging protocol in early-stage oral cancer <i>Ann Nucl Med. 2021 Dec;35(12):1353-1360</i>	47
<b>Novel tracers and imaging techniques</b>		
Chapter 4	The potential of the Crystal Cam handheld gamma-camera for preoperative and intraoperative sentinel lymph node localization in early-stage oral cancer <i>Eur Arch Otorhinolaryngol. 2023 Dec;280(12):5519-5529</i>	65
Chapter 5	Sentinel lymph node detection in oral cancer: a within-patient comparison between [ <sup>99m</sup> Tc]Tc-tilmanocept and [ <sup>99m</sup> Tc]Tc-nanocolloid <i>Eur J Nucl Med Mol Imaging. 2021 Mar;48(3):851-858</i>	87
Chapter 6	Diagnostic accuracy of [ <sup>99m</sup> Tc]Tc-tilmanocept compared to [ <sup>99m</sup> Tc]Tc-nanocolloid for sentinel lymph node identification in early-stage oral cancer <i>Clin Otolaryngol. 2021 Nov;46(6):1383-1388</i>	109
Chapter 7	New developments in imaging for sentinel lymph node biopsy in early-stage oral cavity squamous cell carcinoma <i>Cancers (Basel). 2020 Oct 20;12(10):3055</i>	123
Chapter 8	Sentinel lymph node detection in early-stage oral squamous cell carcinoma using magnetic resonance lymphography: a pilot study <i>J Clin Med. 2024 Nov 22;13(23):7052</i>	159
Chapter 9	CT lymphography using Lipiodol® for sentinel lymph node biopsy in early-stage oral cancer <i>J Clin Med. 2022 Aug 31;11(17):5129</i>	183

Chapter 10	Within-patient comparison between [ <sup>68</sup> Ga]Ga-tilmanocept PET/CT lymphoscintigraphy and [ <sup>99m</sup> Tc]Tc-tilmanocept lymphoscintigraphy for sentinel lymph node detection in oral cancer: a pilot study <i>Eur J Nucl Med Mol Imaging. 2022 May;49(6):2023-2036</i>	205
Chapter 11	[ <sup>68</sup> Ga]Ga-tilmanocept PET/CT lymphoscintigraphy: a novel technique for sentinel lymph node imaging <i>Eur J Nucl Med Mol Imaging. 2021 Apr;48(4):963-965</i>	229
Chapter 12	Summary, general discussion and future perspectives	237
Chapter 13	Nederlandse samenvatting	253
<b>Appendices</b>		
	<i>List of publications</i>	268
	<i>Acknowledgments   Dankwoord</i>	270
	<i>About the author   Curriculum Vitae</i>	275

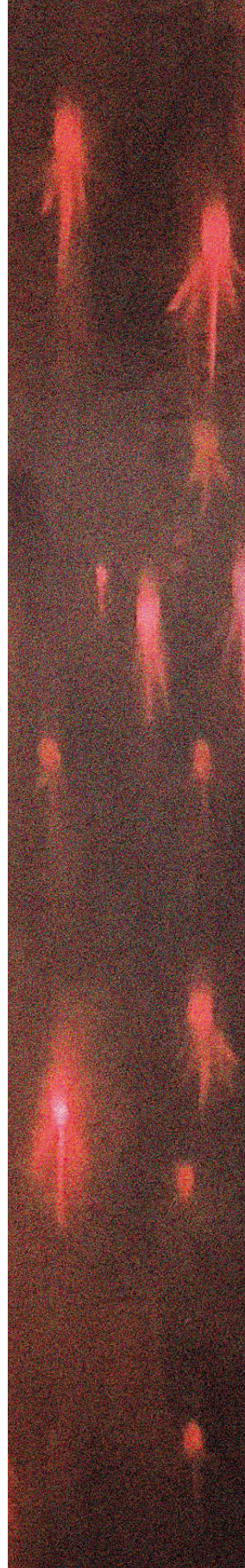




# 1

General introduction and outline  
of this thesis

---



Oral cavity cancer is a significant cause of morbidity and mortality worldwide. The most common type of cancer in the oral cavity is squamous cell carcinoma, representing over 90% of all oral cancers [1, 2]. Oral squamous cell carcinoma (OSCC) arises from the epithelium of the oral cavity and is strongly associated with tobacco and alcohol use [3]. Unfortunately, despite efforts and public campaigns to decrease the prevalence of smoking, a proportional decrease in incidence of OSCC has not yet been observed (Figure 1) [1, 4]. In the Netherlands alone, approximately 1000 patients are newly diagnosed with OSCC each year [4].

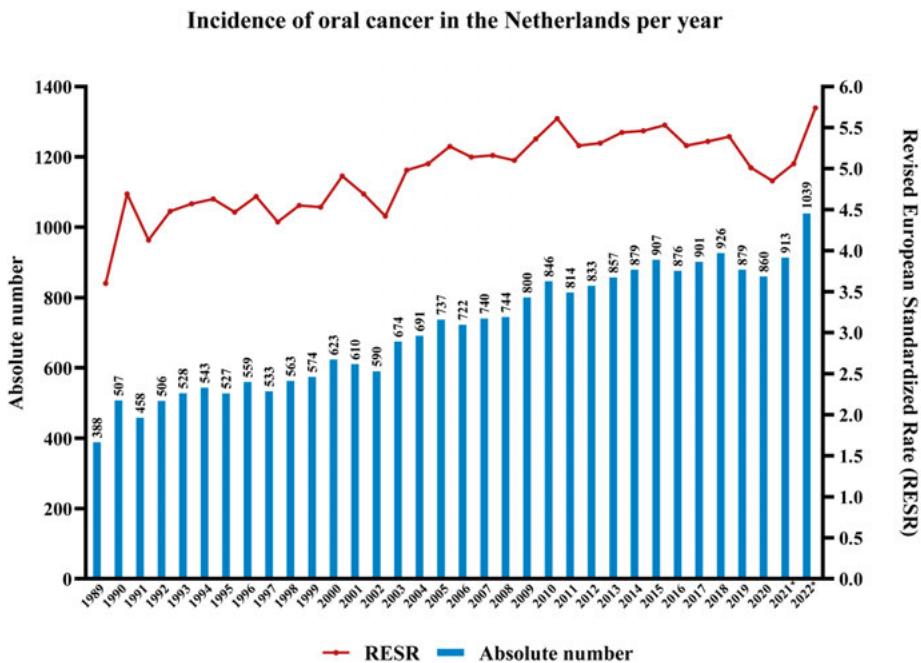


**Figure 1.** Incidence of oral cancer in the Netherlands per year. Bars represent the absolute number of patients diagnosed with oral cancer for each year. Line represents Revised European Standardized Rate (RESR; new cases per 100.000 people per year, corrected for age distribution in the European population in 2010). \*Provisional data. Data retrieved from Integraal Kankercentrum Nederland (IKNL) [4].

Staging of patients with OSCC is of vital importance, as it defines the choice of treatment as well as the patient's prognosis. The extent of the tumor (T), the presence of cervical lymph node metastases (N) and distant metastases (M), referred to as TNM-classification, determine the stage at presentation [5, 6]. OSCCs have a proclivity to metastasize through lymphatics to regional lymph nodes first, rather than to spread hematogenously [7]. Presence of regional lymph node metastases has proven to significantly increase the risk for distant metastasis and is regarded one of the foremost prognostic factors in OSCC; nearly reducing survival by half

[7]. Therefore, accurate detection of cervical lymph node metastases is critical for prognosis prediction and, more importantly, for therapy planning.

Evaluation of the cervical lymph nodes generally entails clinical examination and imaging of the head and neck, using conventional imaging techniques such as computed tomography (CT), magnetic resonance imaging (MRI), ultrasound (US) and fluorodeoxyglucose-positron emission tomography/computed tomography ( $[^{18}\text{F}]$  FDG-PET/CT) [8, 9]. However, assessing cervical lymph node involvement with these imaging modalities is mainly based on morphologic criteria (i.e., size, border irregularity and inhomogeneous patterns), and in case of  $[^{18}\text{F}]$ FDG-PET/CT also on glucose consumption, all of which do not always reflect the presence of malignancy correctly [10-12]. Ultrasound-guided fine-needle aspiration cytology (USgFNAC) has shown superior diagnostic accuracy for detecting lymph node metastases, but still has its limitations. First of all, the diagnostic accuracy of USgFNAC is strongly dependent on the experience and skills of the ultrasonographer and cytopathologist. Furthermore, owing to its inability to detect small metastatic deposits and susceptibility to sampling error (i.e., metastatic deposits missed by fine-needle aspiration), the sensitivity of USgFNAC is inherently limited [13]. Taking the limitations of these conventional diagnostic procedures into account, OSCC patients who clinically and radiologically show no signs of lymph node metastasis (cN0: clinically negative neck) still have a substantial risk of harboring (occult) nodal metastases in the neck, which is reported to be around 20-30% [13-14].

The most optimal treatment regimen for patients with such a considerable risk of occult nodal metastases has been widely debated, particularly in surgically treated patients in whom the neck does not need to be accessed for managing the primary tumor. Since in early-stage OSCC (cT1-T2N0) it is usually not necessary to approach the neck when the primary tumor can be resected transorally and no reconstruction is necessary, a long lasting controversy is ongoing regarding management of the clinically negative neck in these patients. Should all patients be treated prophylactically by surgically removing the most at-risk cervical nodal basins (i.e., elective neck dissection), or can the neck be left untreated with a “watchful-waiting” follow-up policy [15]? The rationale for elective treatment of neck is based on the premise that occult metastases will progress into clinically manifest metastases if the neck is left untreated, whereas delayed treatment of lymph node metastases is associated with more extensive treatment of the neck, a poorer oncological outcome and reduced survival rates [7, 12, 15, 16]. Conversely, the main argument against elective neck dissection is that a considerable proportion of patients (70-80%) are subjected to treatment that they do not need, increasing the risk of surgical complications and potentially causing unnecessary morbidity, among which shoulder dysfunction [7, 17]. Furthermore,

surgical resection of the most at-risk cervical nodal basins may involve the removal of one of the physical barriers that may prevent distant metastases in the event of a local recurrence or second primary tumor, which are not uncommon in patients with OSCC [18, 19].

In the heat of the debate arose a diagnostic procedure: sentinel lymph node biopsy (SLNB). A procedure that has been introduced in a variety of tumor types over the last few decades, including OSCC, in an attempt to avoid futile comprehensive prophylactic treatment of the at-risk nodal basins while not jeopardizing the chance of regional control and survival [20, 21].

## Sentinel lymph node biopsy

The sentinel lymph node (SLN) concept is fundamentally built on the theory of orderly spread of tumor cells within the lymphatic system. In other words, SLNB is based on the premise that lymph flow from the primary tumor travels sequentially to the first draining lymph node (i.e., SLN) and then on to the other regional lymph nodes (i.e., higher echelon nodes, HENs; Figure 2).

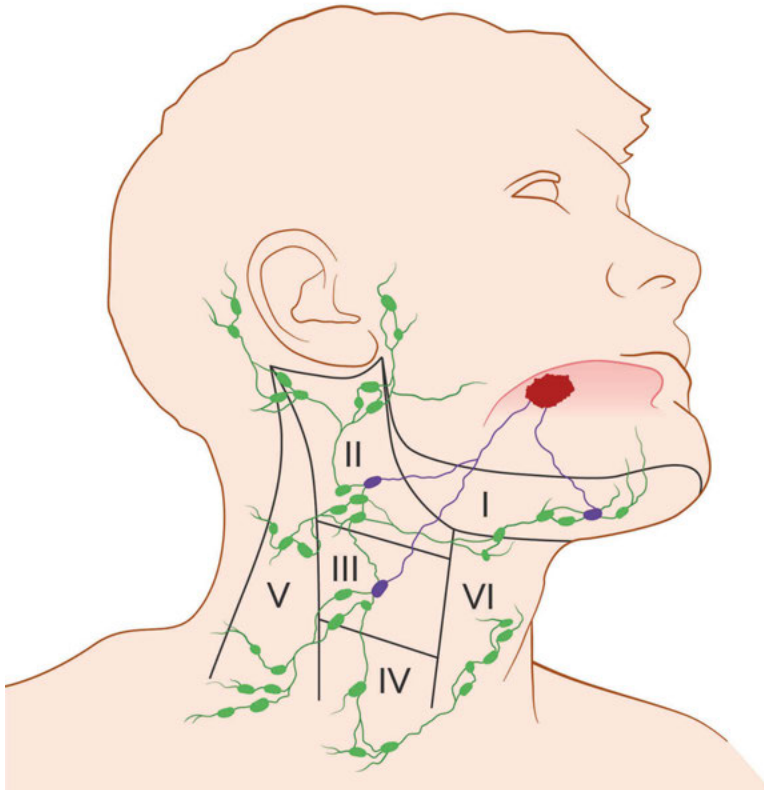


**Figure 2.** Lymphatic drainage of a tumor of the tongue with a total of three SLNs (*purple*). Any successive lymph nodes in order of lymphatic drainage (*green*) are considered HENs. Lymph node levels of the neck (I-VI) as delineated by the American Academy of Otolaryngology and Head and Neck Surgery (AAO-HNS) [22].

Hence, the SLN is the lymph node that has the highest risk of harboring metastasis and reflects the histopathological status of the rest of the nodal basin accordingly [21]. That is, SLN(s) without metastases would preclude malignant involvement of the regional lymph nodes and justifies clinical follow-up of the neck. If a SLN does harbor metastasis, however, malignant cells may have spread from the SLN to lymph nodes located further down the lymphatic system (HENs). Therefore, a

complementary treatment of the regional nodal basin is warranted when a metastatic SLN is present.

The conventional SLNB procedure consists of three steps: identification, surgical extirpation and histopathological evaluation of SLNs (Figure 3) [23-25].

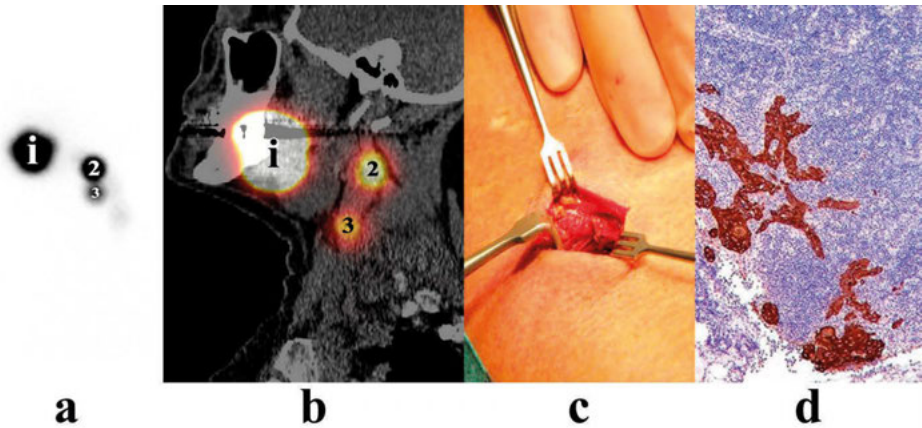


**Figure 3.** Steps of SLNB procedure: (a) planar static scintigraphy following peritumoral injection of  $^{99m}\text{Tc}[\text{Tc}]$ -nanocolloid in a patient with OSCC of the oral tongue on the left side. (b) Corresponding SPECT/CT images in the same patient. Both planar static scintigraphy as well as SPECT/CT depicting the hotspot of the injection site (*i*) as well as a SLN in level II (2) and level III (3) of the ipsilateral neck. (c) Surgical extirpation of the designated SLNs via a small incision. (d) Histopathological examination of extirpated SLN(s).

In order to identify SLNs, a radioactive tracer is injected around the tumor. Mainly throughout Europe, this radiotracer consists of nanocolloid labeled to the gamma-emitting radioisotope technetium-99m ( $^{99m}\text{Tc}$ ) [23, 24]. The administered radiotracer (e.g., [ $^{99m}\text{Tc}$ ]Tc-nanocolloid), which migrates towards and accumulates in SLNs can subsequently be visualized by a gamma-camera. This imaging procedure, referred to as lymphoscintigraphy, generally includes early dynamic and static scintigraphy (0 – 30 minutes post-injection; Figure 3a) followed by late static scintigraphy and single photon emission computed tomography/computed tomography (SPECT/CT, approximately 2 hours post-injection; Figure 3b). Subsequently, lymphoscintigraphic images are evaluated by a nuclear physician, who designates depicted hotspots (i.e., region with radioactive uptake) as either injection site, SLN or HEN. Only the location of hotspots considered to be SLNs are marked on the overlying skin using the conventional gamma-camera and a cobalt-57 ( $^{57}\text{Co}$ ) penpoint marker. Lymphoscintigraphy can be carried out either the day of surgical extirpation (single-day protocol) or the day before surgery (two-day protocol), adjusting the administered radioactive dosage accordingly [24].

During surgery, the SLNs as identified by lymphoscintigraphy are mainly localized through gamma-tracing using a handheld gamma-probe [25]. In addition, to further aid the surgeon in tracking SLNs intraoperatively, several portable gamma-detecting imaging devices have been developed, such as freehand SPECT and portable gamma-cameras, allowing for real-time image-guided SLN localization [26-28]. Besides, fluorescent dyes, among which indocyanine green (ICG), can be merged with a variety of radiotracers. The resulting hybrid tracer (e.g., ICG- $^{99m}\text{Tc}$ ]Tc-nanocolloid) facilitates optical fluorescence guidance when using a near-infrared camera, while still enabling radioguided SLN localization [29]. Nowadays, this hybrid approach for intraoperative SLN localization is routinely used in most Dutch head-and-neck cancer centers.

Postoperatively, the surgically harvested SLNs are subjected to meticulous histopathological examination, including step-serial-sectioning (section thickness 150-500  $\mu\text{m}$ ), hematoxylin-eosin staining and immunohistochemistry with pancytokeratin antibody (AE1/AE3) staining, designed to detect micrometastases and even isolated tumor cells with high sensitivity [23].

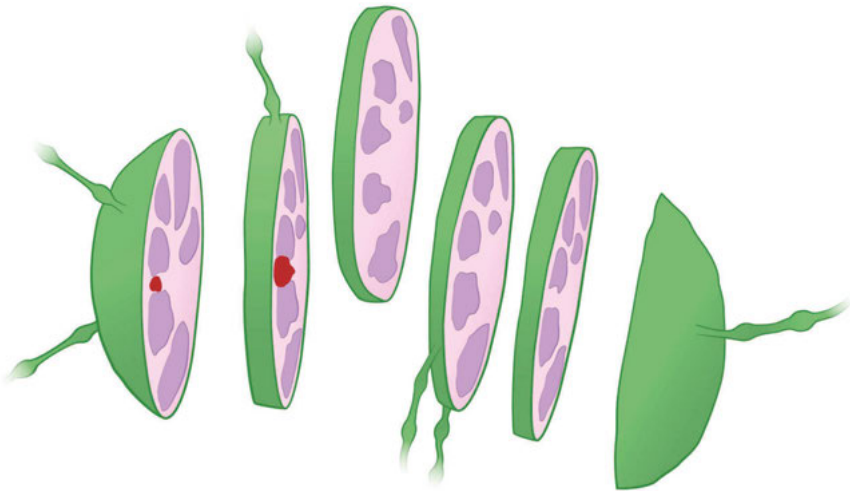


**Figure 4.** Histopathological examination of extirpated SLN(s) by step-serial-sectioning, hematoxylin-eosin staining and immunohistochemistry; revealing (micro)metastatic disease (*red immunostained lesion*).

Using this approach, SLNB has proven to be a reliable staging procedure for the clinically negative neck in early-stage OSCC patients with a pooled sensitivity of 87% (95% CI: 85-89%) and a negative predictive value (NPV) of 94% (95% CI: 93%-95%) [30]. In recent randomized controlled trials, comparing SLNB with elective neck dissection in early-stage cN0 OSCC, SLNB showed similar locoregional-free,

disease-specific and overall survival rates as elective neck dissection, demonstrating the oncologic equivalence between a SLNB and elective neck dissection approach in these patients [31-34]. Although elective neck dissection has the benefit of being a single-stage procedure, without need for specific facilities (i.e., radiopharmaceutical and nuclear medicine department, advanced histopathology), SLNB has the benefit of assessing individual lymphatic drainage patterns. In doing so, SLNB is able to reveal aberrant lymphatic drainage and detect any lymph node metastases beyond the cervical nodal levels generally addressed by elective neck dissection (e.g., skip metastases or contralateral nodal metastases in lateralized OSCC) [21, 35]. Furthermore, SLNB has proven to provide significantly superior postoperative functional results as well as considerable shorter hospital stay when compared to patients who underwent elective neck dissection [17, 32]. Besides, given current evidence, SLNB followed by complementary neck dissection or watchful-waiting appears to be the most cost-effective strategy regarding the management of cN0 in early-stage OSCC [36, 37]. On account of the established oncologic equivalence as well as the advantages of SLNB over elective neck dissection, SLNB is implemented in the Dutch national guidelines as the preferred treatment strategy for cN0 in early-stage OSCC [38].

Nevertheless, challenges remain for SLNB, especially in OSCC, that need to be addressed to enhance its diagnostic accuracy and consequently further improve patient's disease-free survival as well as quality-of-life and reduce health-related costs to a greater extent [16, 17, 36, 39].

# Challenges for sentinel lymph node biopsy in oral cancer

In OSCC, often multiple lymph nodes with radioactive uptake (i.e., hotspots) are revealed on lymphoscintigraphy. Although multiple true SLNs exist in many OSCC patients, owing to the complex lymphatic system and abundance of lymph nodes in the neck, some hotspots may actually represent HENs as the administered radiotracer is not always completely retained in SLNs and may therefore migrate towards and accumulate in HENs. The limited resolution of lymphoscintigraphy impedes the visualization of connecting lymphatic vessels in the majority of cases, which can complicate the discrimination of hotspots between relevant SLN and irrelevant HEN [40]. These difficulties in determining whether a hotspot is either a SLN or HEN have been demonstrated by interobserver variabilities in defining SLNs [41]. Falsely considering HENs as SLNs can induce unnecessary surgical exploration of the neck, with its accompanying morbidity and risk of complications, which may hamper a complementary neck dissection in case of metastatic involvement of SLNs [42]. Moreover, mistakenly designating SLNs as HENs can lead to neglect of true SLNs that are potentially harboring metastases. As a consequence, patients may be incorrectly staged negative for the presence of nodal disease (i.e., false-negative outcome), thereby erroneously omitting the treatment required for the regional nodal basin.

Another limitation of SLNB, caused by the inadequate resolution of lymphoscintigraphy using conventional [<sup>99m</sup>Tc]Tc-radiotracers, arises in situations where SLNs are located in close vicinity of the radiotracer injection site. In these cases, activity residing at the radiotracer injection site may conceal neighboring SLNs and thus impede distinction between SLN and injection site. This particular circumstance, known as the shine-through phenomenon, considerably increases the risk of missing metastatic SLNs (Figure 5) [43-46]. Especially tumor subsites with close spatial relation to SLNs, such as the floor-of-mouth or vestibule-of-mouth, are prone to the shine-through phenomenon. Hence, the accuracy of SLNB has proven to be significantly lower in these subsites (e.g., floor-of-mouth: sensitivity 63%, NPV 90%), compared to other OSCC subsites (sensitivity 86%, NPV 95%) [42].

Until these limitations of SLNB are resolved, occult nodal metastasis remain undetected (shine-through phenomenon) or neglected (falsely considering SLN as HEN) and therefore untreated following SLNB in 5-6% of early-stage OSCC patients [30, 43]. Considering that any untreated nodal metastasis will inevitably develop into clinical manifestation of disease, which usually entails more comprehensive surgery as well as more frequently adjuvant radiotherapy and even reduced chances of survival, there is still a need for technological advancements to overcome these

1

limitations of SLNB in early-stage OSCC [16, 47].

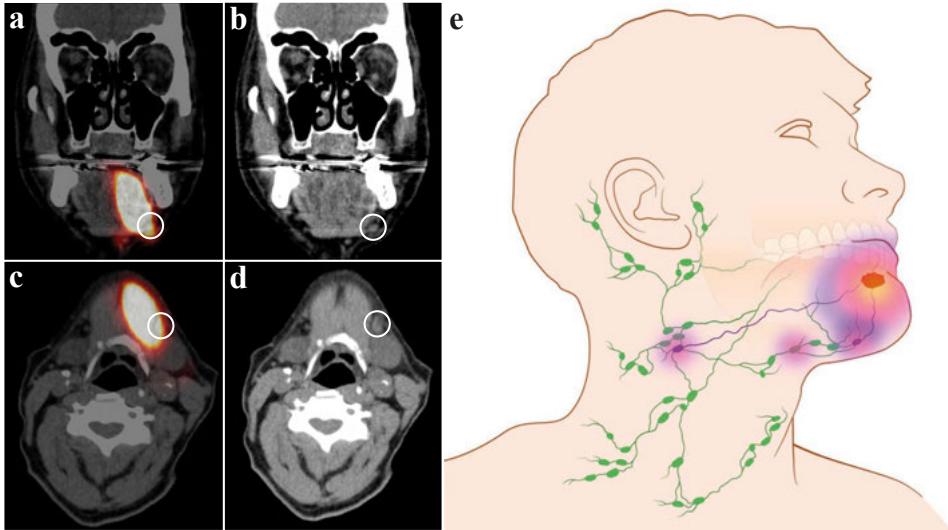


**Figure 5.** Shine-through phenomenon in a patient with floor-of-mouth cancer. (a,c) Coronal and axial SPECT/CT images: radiation flare of the tracer injection site overshines a sentinel lymph node located in cervical lymph node level Ib (*white circle*). (b,d) Coronal and axial low-dose CT images of same patient: (sentinel) lymph node located in cervical lymph node level Ib that could not be differentiated from the hotspot originating from tracer injection site on SPECT/CT (*white circle*). (e) Schematic illustration of shine-through phenomenon.

## Outline of this thesis

This thesis is dedicated to enhancing the current SLNB procedure, in particular in early-stage OSCC.

In **chapter 2** the overall rate of occult contralateral nodal metastasis in lateralized or paramedian early-stage OSCC patients in a large retrospective Dutch multicenter cohort ( $n = 816$ ) is described. To assess whether SLNB provides improved control over the contralateral clinically negative neck compared to an elective neck dissection strategy in these patients, we compare the rate of contralateral regional recurrences between patients who underwent SLNB and patients who underwent elective neck dissection. Finally, disease-specific survival between patients in whom occult contralateral nodal metastases were detected by SLNB or bilateral elective neck dissection and patients who developed contralateral regional recurrence are compared.

**Chapter 3** describes a retrospective within-patient study that evaluates a streamlined lymphoscintigraphy protocol in 77 early-stage OSCC patients, in an attempt to reduce lymphoscintigraphy acquisition time and its associated patient burden and costs, without interfering with its diagnostic accuracy.

In **chapter 4** the use of the Crystal Cam handheld gamma-camera for both preoperative and intraoperative SLN localization in a prospective monocenter cohort of 53 patients undergoing SLNB is evaluated.

In **chapters 5 and 6** a new radiotracer for SLN identification ( $[^{99m}\text{Tc}]\text{Tc-tilmanocept}$ ) is compared to the routinely used radiotracer at our institute ( $[^{99m}\text{Tc}]\text{Tc-nanocolloid}$ ). In these head-to-head comparative prospective studies, 20 patients underwent lymphoscintigraphy using both the routinely used radiotracer ( $[^{99m}\text{Tc}]\text{Tc-nanocolloid}$ ) as well as the new radiotracer ( $[^{99m}\text{Tc}]\text{Tc-tilmanocept}$ ). The diagnostic accuracy of SLNB using  $[^{99m}\text{Tc}]\text{Tc-tilmanocept}$  is reported, with histopathological examination of excised SLNs and any complementary neck dissection specimens, as well as a follow-up of at least 12 months as reference standard.

**Chapter 7** provides a review of the literature on several novel SLNB imaging techniques for early-stage OSCC: MR lymphography, CT lymphography, PET/CT lymphoscintigraphy and contrast-enhanced lymphosonography. Their reported diagnostic accuracy is described, and their relative merits, disadvantages and potential applications are outlined.

The following chapters (**chapters 8 – 10**) report the results of the prospective within-patient comparison studies, each comprising a small number of patients ( $n = 10$ ), on some of the novel SLNB imaging techniques in early-stage OSCC as described in the review of the literature (**chapter 7**). In these studies, patients underwent conventional lymphoscintigraphy using  $^{99m}\text{Tc}$ -labeled radiotracers as well as MR lymphography using gadolinium (**chapter 8**), CT lymphography using Lipiodol® (**chapter 9**) or [ $^{68}\text{Ga}$ ]Ga-tilmanocept PET/CT lymphoscintigraphy (**chapter 10**). Corresponding images of conventional lymphoscintigraphy and the respective novel SLNB imaging modality were evaluated in each patient, particularly comparing SLN identification rate as well as visualization of connecting lymphatic vessels between both modalities.

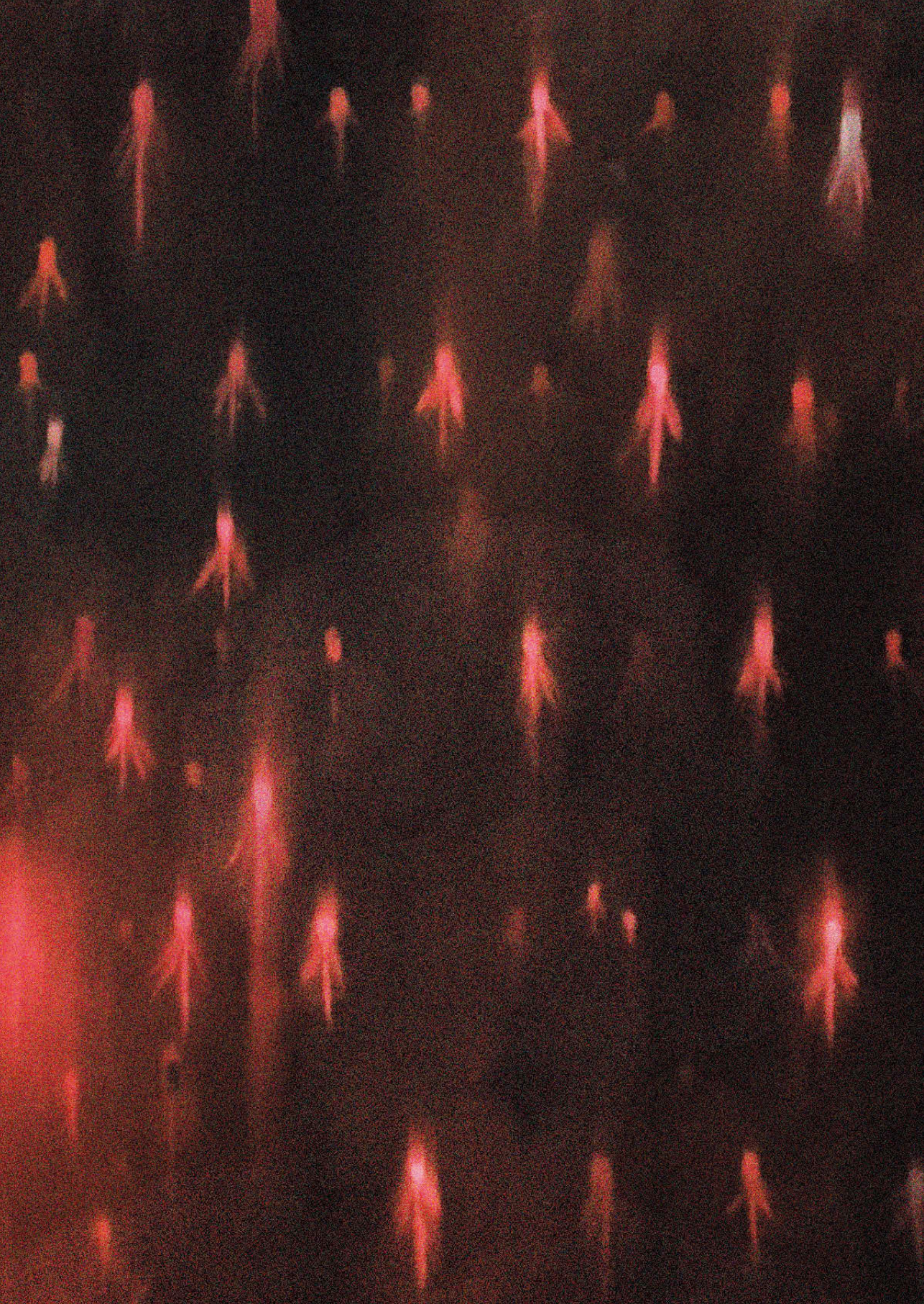
Finally, **chapter 11** provides a further description of the relative advantages of [ $^{68}\text{Ga}$ ]Ga-tilmanocept PET/CT lymphoscintigraphy and its potential implementations in oncologic healthcare.

## References

- Zanoni DK, Montero PH, Migliacci JC, et al. Survival outcomes after treatment of cancer of the oral cavity (1985-2015). *Oral Oncol.* 2019;90:115-121. doi:10.1016/j.oraloncology.2019.02.001
- Pulte D, Brenner H. Changes in survival in head and neck cancers in the late 20th and early 21st century: a period analysis. *Oncologist.* 2010;15(9):994-1001. doi:10.1634/theoncologist.2009-0289
- Hashibe M, Brennan P, Chuang SC, et al. Interaction between tobacco and alcohol use and the risk of head and neck cancer: pooled analysis in the International Head and Neck Cancer Epidemiology Consortium. *Cancer Epidemiol Biomarkers Prev.* 2009;18(2):541-550. doi:10.1158/1055-9965.EPI-08-0347
- Integraal Kankercentrum Nederland (IKNL). Incidentie hoofd-hals kanker. Accessed 29<sup>th</sup> of January 2024 via <https://iknl.nl/kankersoorten/hoofd-halskanker/registratie/incidentie>.
- Amin MB, Greene FL, Edge SB, et al. The Eighth Edition AJCC Cancer Staging Manual: Continuing to build a bridge from a population-based to a more “personalized” approach to cancer staging. *CA Cancer J Clin.* 2017;67(2):93-99. doi:10.3322/caac.21388
- Brierley JD, Gospodarowicz M, Wittekind C. UICC TNM Classification of Malignant Tumours. 8<sup>th</sup> ed. Chichester, United Kingdom: Wiley; 2017.
- de Bree R, Takes RP, Shah JP, et al. Elective neck dissection in oral squamous cell carcinoma: Past, present and future. *Oral Oncol.* 2019;90:87-93. doi:10.1016/j.oraloncology.2019.01.016
- de Bondt RB, Nelemans PJ, Hofman PA, et al. Detection of lymph node metastases in head and neck cancer: a meta-analysis comparing US, USgFNAC, CT and MR imaging. *Eur J Radiol.* 2007;64(2):266-272. doi:10.1016/j.ejrad.2007.02.037
- Brouwer J, de Bree R, Comans EF, Castelijns JA, Hoekstra OS, Leemans CR. Positron emission tomography using [<sup>18</sup>F]fluorodeoxyglucose (FDG-PET) in the clinically negative neck: is it likely to be superior? *Eur Arch Otorhinolaryngol.* 2004;261(9):479-483. doi:10.1007/s00405-003-0727-3
- de Bondt RB, Nelemans PJ, Bakers F, et al. Morphological MRI criteria improve the detection of lymph node metastases in head and neck squamous cell carcinoma: multivariate logistic regression analysis of MRI features of cervical lymph nodes. *Eur Radiol.* 2009;19(3):626-633. doi:10.1007/s00330-008-1187-3
- Kim SJ, Pak K, Kim K. Diagnostic accuracy of F-18 FDG PET or PET/CT for detection of lymph node metastasis in clinically node negative head and neck cancer patients; A systematic review and meta-analysis. *Am J Otolaryngol.* 2019;40(2):297-305. doi:10.1016/j.amjoto.2018.10.013
- de Bree R, de Keizer B. Comparison of different diagnostic approaches in the management of the clinically negative neck in early oral cancer patients. *Cancer.* 2021;127(12):1959-1962. doi:10.1002/ncr.33443
- de Bree R, Takes RP, Castelijns JA, et al. Advances in diagnostic modalities to detect occult lymph node metastases in head and neck squamous cell carcinoma. *Head Neck.* 2015;37(12):1829-1839. doi:10.1002/hed.23814
- Nieuwenhuis EJ, Castelijns JA, Pijpers R, et al. Wait-and-see policy for the N0 neck in early-stage oral and oropharyngeal squamous cell carcinoma using ultrasonography-guided cytology: is there a role for identification of the sentinel node? *Head Neck.* 2002;24(3):282-289. doi:10.1002/hed.10018
- de Bree R, de Keizer B, Civantos FJ, et al. What is the role of sentinel lymph node biopsy in the management of oral cancer in 2020? *Eur Arch Otorhinolaryngol.* 2021;278(9):3181-3191. doi:10.1007/s00405-020-06538-y
- D’Cruz AK, Vaish R, Kapre N, et al. Elective versus therapeutic neck dissection in node-negative oral cancer. *N Engl J Med.* 2015;373(6):521-529. doi:10.1056/NEJMoa1506007
- van Hinte G, Sancak T, Weijs WLJ, et al. Effect of elective neck dissection versus sentinel lymph node biopsy on shoulder morbidity and health-related quality of life in patients with oral cavity cancer: A longitudinal comparative cohort study. *Oral Oncol.* 2021;122:105510. doi:10.1016/j.oraloncology.2021.105510
- Leemans CR, Tiwari R, Nauta JJ, van der Waal I, Snow GB. Recurrence at the primary site in head and neck cancer and the significance of neck lymph node metastases as a prognostic factor. *Cancer.* 1994;73(1):187-190. doi:10.1002/1097-0142(19940101)73:1<187::aid-cncr2820730132>3.0.co;2-j

19. Mroueh R, Nevala A, Haapaniemi A, Pitkaniemi J, Salo T, Mäkitie AA. Risk of second primary cancer in oral squamous cell carcinoma. *Head Neck*. 2020;42(8):1848-1858. doi:10.1002/hed.26107
20. Nieweg OE, Uren RF, Thompson JF. The history of sentinel lymph node biopsy. *Cancer J*. 2015;21(1):3-6. doi:10.1097/PPO.0000000000000091
21. de Bree R, Nieweg OE. The history of sentinel node biopsy in head and neck cancer: From visualization of lymphatic vessels to sentinel nodes. *Oral Oncol*. 2015;51(9):819-823. doi:10.1016/j.oraloncology.2015.06.006
22. Robbins KT, Shaha AR, Medina JE, et al. Consensus statement on the classification and terminology of neck dissection. *Arch Otolaryngol Head Neck Surg*. 2008;134(5):536-538. doi:10.1001/archotol.134.5.536
23. Alkureishi LW, Burak Z, Alvarez JA, et al. Joint practice guidelines for radionuclide lymphoscintigraphy for sentinel node localization in oral/oropharyngeal squamous cell carcinoma. *Ann Surg Oncol*. 2009;16(11):3190-3210. doi:10.1245/s10434-009-0726-8
24. Giammarile F, Schilling C, Gnanasegaran G, et al. The EANM practical guidelines for sentinel lymph node localisation in oral cavity squamous cell carcinoma. *Eur J Nucl Med Mol Imaging*. 2019;46(3):623-637. doi:10.1007/s00259-018-4235-5
25. Schilling C, Stoeckli SJ, Vigili MG, et al. Surgical consensus guidelines on sentinel node biopsy (SNB) in patients with oral cancer. *Head Neck*. 2019;41(8):2655-2664. doi:10.1002/hed.25739
26. Vermeeren L, Valdés Olmos RA, Klop WM, Balm AJ, van den Brekel MW. A portable gamma-camera for intraoperative detection of sentinel nodes in the head and neck region. *J Nucl Med*. 2010;51(5):700-703. doi:10.2967/jnumed.109.071407
27. Vidal-Sicart S, Paredes P, Zanón G, et al. Added value of intraoperative real-time imaging in searches for difficult-to-locate sentinel nodes. *J Nucl Med*. 2010;51(8):1219-1225. doi:10.2967/jnumed.110.074880
28. Heuveling DA, van Weert S, Karagozoglou KH, de Bree R. Evaluation of the use of freehand SPECT for sentinel node biopsy in early stage oral carcinoma. *Oral Oncol*. 2015;51(3):287-290. doi:10.1016/j.oraloncology.2014.12.001
29. KleinJan GH, van Werkhoven E, van den Berg NS, et al. The best of both worlds: a hybrid approach for optimal pre- and intraoperative identification of sentinel lymph nodes. *Eur J Nucl Med Mol Imaging*. 2018;45(11):1915-1925. doi:10.1007/s00259-018-4028-x
30. Liu M, Wang SJ, Yang X, Peng H. Diagnostic efficacy of sentinel lymph node biopsy in early oral squamous cell carcinoma: a meta-analysis of 66 studies. *PLoS One*. 2017;12(1):e0170322. doi:10.1371/journal.pone.0170322
31. Sundaram PS, Subramanyam P. Effectiveness of sentinel lymph node scintigraphy and intraoperative gamma probing with gold standard elective neck dissection in patients with N0 oral squamous cell cancers. *Nucl Med Commun*. 2019;40(11):1138-1147. doi:10.1097/MNM.0000000000001090
32. Garrel R, Poissonnet G, Moyà Plana A, et al. Equivalence randomized trial to compare treatment on the basis of sentinel node biopsy versus neck node dissection in operable T1-T2N0 oral and oropharyngeal cancer. *J Clin Oncol*. 2020;38(34):4010-4018. doi:10.1200/JCO.20.01661
33. Hasegawa Y, Tsukahara K, Yoshimoto S, et al. Neck dissections based on sentinel lymph node navigation versus elective neck dissections in early oral cancers: a randomized, multicenter, and noninferiority trial. *J Clin Oncol*. 2021;39(18):2025-2036. doi:10.1200/JCO.20.03637
34. Gupta T, Maheshwari G, Kannan S, Nair S, Chaturvedi P, Agarwal JP. Systematic review and meta-analysis of randomized controlled trials comparing elective neck dissection versus sentinel lymph node biopsy in early-stage clinically node-negative oral and/or oropharyngeal squamous cell carcinoma: Evidence-base for practice and implications for research. *Oral Oncol*. 2022;124:105642. doi:10.1016/j.oraloncology.2021.105642
35. Mahieu R, den Toom IJ, Boeve K, et al. Contralateral regional recurrence in lateralized or paramedian early-stage oral cancer undergoing sentinel lymph node biopsy-comparison to a historic elective neck dissection cohort. *Front Oncol*. 2021;11:644306. doi:10.3389/fonc.2021.644306
36. Govers TM, Takes RP, Baris Karakullukcu M, et al. Management of the N0 neck in early stage oral squamous cell cancer: a modeling study of the cost-effectiveness. *Oral Oncol*. 2013;49(8):771-777. doi:10.1016/j.oraloncology.2013.05.001
37. de Kerangal Q, Kapso R, Morinière S, Laure B, Bonastre J, Moya-Plana A. Sentinel lymph node biopsy versus selective neck dissection in patients with early oral squamous cell carcinoma: A cost analysis. *J Stomatol Oral Maxillofac Surg*. 2022;123(3):372-376. doi:10.1016/j.jormas.2021.05.003

38. Federatie Medisch Specialisten. Management negatieve hals mondholtecarcinoom. Richtlijndatabase. Accessed 31<sup>st</sup> of August 2023 via [https://richtlijndatabase.nl/richtlijn/hoofd-halstumoren/management\\_negatieve\\_hals\\_mondholtecarcinoom.html](https://richtlijndatabase.nl/richtlijn/hoofd-halstumoren/management_negatieve_hals_mondholtecarcinoom.html).
39. Mahieu R, Krijger GC, Ververs FFT, de Roos R, de Bree R, de Keizer B. [<sup>68</sup>Ga]Ga-tilmanocept PET/CT lymphoscintigraphy: a novel technique for sentinel lymph node imaging. *Eur J Nucl Med Mol Imaging*. 2021;48(4):963-965. doi:10.1007/s00259-020-05101-5
40. Mahieu R, de Maar JS, Nieuwenhuis ER, et al. New developments in imaging for sentinel lymph node biopsy in early-stage oral cavity squamous cell carcinoma. *Cancers (Basel)*. 2020;12(10):3055. doi:10.3390/cancers12103055
41. Flach GB, van Schie A, Witte BI, et al. Practice variation in defining sentinel lymph nodes on lymphoscintigrams in oral cancer patients. *Eur J Nucl Med Mol Imaging*. 2014;41(12):2249-2256. doi:10.1007/s00259-014-2843-2
42. Heuveling DA, Flach GB, van Schie A, et al. Visualization of the sentinel node in early-stage oral cancer: limited value of late static lymphoscintigraphy. *Nucl Med Commun*. 2012;33(10):1065-1069. doi:10.1097/MNM.0b013e3283571089
43. den Toom IJ, Boeve K, Lobeek D, et al. Elective neck dissection or sentinel lymph node biopsy in early stage oral cavity cancer patients: the Dutch experience. *Cancers (Basel)*. 2020;12(7):1783. doi:10.3390/cancers12071783
44. Alkureishi LW, Ross GL, Shoaib T, et al. Sentinel node biopsy in head and neck squamous cell cancer: 5-year follow-up of a European multicenter trial. *Ann Surg Oncol*. 2010;17(9):2459-2464. doi:10.1245/s10434-010-1111-3
45. Pedersen NJ, Jensen DH, Hedbäck N, et al. Staging of early lymph node metastases with the sentinel lymph node technique and predictive factors in T1/T2 oral cavity cancer: A retrospective single-center study. *Head Neck*. 2016;38 Suppl 1:E1033-E1040. doi:10.1002/hed.24153
46. Stoeckli SJ, Huebner T, Huber GF, Broglie MA. Technique for reliable sentinel node biopsy in squamous cell carcinomas of the floor of mouth. *Head Neck*. 2016;38(9):1367-1372. doi:10.1002/hed.24440
47. Flach GB, Tenhagen M, de Bree R, et al. Outcome of patients with early stage oral cancer managed by an observation strategy towards the N0 neck using ultrasound guided fine needle aspiration cytology: No survival difference as compared to elective neck dissection. *Oral Oncol*. 2013;49(2):157-164. doi:10.1016/j.oraloncology.2012.08.006



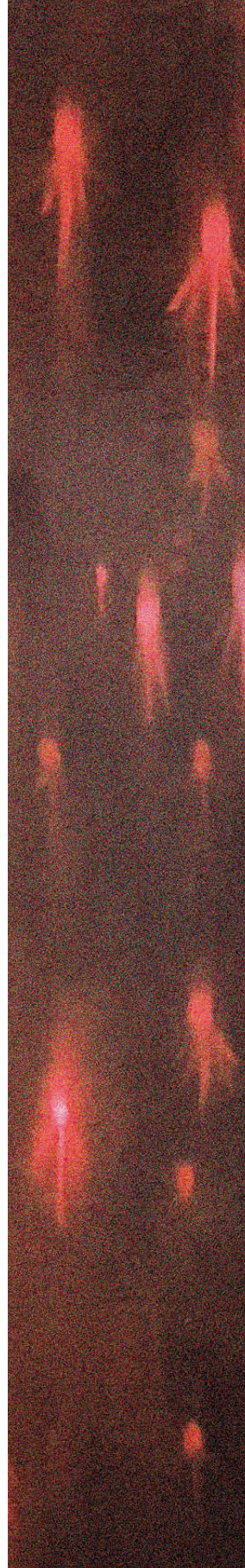
# 2

## Contralateral regional recurrence in lateralized or paramedian early-stage oral cancer undergoing sentinel lymph node biopsy - comparison to a historic elective neck dissection cohort

---

Rutger Mahieu, Inne J. den Toom, Koos Boeve, Daphne Lobeek,  
Elisabeth Bloemena, Maarten L. Donswijk, Bart de Keizer,  
W. Martin C. Klop, C. René Leemans, Stefan M. Willems,  
Robert P Takes, Max J.H. Witjes, Remco de Bree.

*Front Oncol. 2021 Apr 23;11:644306*



# Abstract

## Introduction

Nowadays, two strategies are available for the management of the clinically negative neck in early-stage (cT1-2N0) oral squamous cell carcinoma (OSCC): elective neck dissection (END) and sentinel lymph node biopsy (SLNB). SLNB stages both the ipsilateral and the contralateral neck in early-stage OSCC patients, whereas the contralateral neck is generally not addressed by END in early-stage OSCC not involving the midline. This study compares both incidence and hazard of contralateral regional recurrences (CRR) in those patients who underwent END or SLNB.

## Materials and Methods

A retrospective multicenter cohort study, including 816 lateralized or paramedian early-stage OSCC patients, staged by either unilateral or bilateral END ( $n = 365$ ) or SLNB ( $n = 451$ ).

## Results

The overall rate of occult contralateral nodal metastasis was 3.7% (30 of 816); the incidence of CRR was 2.5% (20 of 816). Patients who underwent END developed CRR during follow-up more often than those who underwent SLNB (3.8 vs. 1.3%;  $p = 0.018$ ). Moreover, END patients had a higher hazard for developing CRR than SLNB patients ( $HR = 2.922$ ;  $p = 0.030$ ). In addition, tumor depth-of-invasion was predictive for developing CRR ( $HR = 1.922$ ;  $p = 0.009$ ). Five-year disease-specific survival in patients with CRR was poor (42%) compared to patients in whom occult contralateral nodal metastases were detected by SLNB or bilateral END (88%), although not statistically different ( $p = 0.066$ ).

## Conclusion

Our data suggest that SLNB allows for better control of the contralateral clinically negative neck in patients with lateralized or paramedian early-stage OSCC, compared to END as performed in a clinical setting. The prognosis of those in whom occult contralateral nodal metastases are detected at an earlier stage may be favorable compared to those who eventually develop CRR, which highlights the importance of adequate staging of the contralateral clinically negative neck.

## Introduction

In patients with early-stage (cT1-2N0) oral squamous cell carcinoma (OSCC) occult metastases are present in 20-30% of patients with a clinically negative neck, despite advanced diagnostic imaging modalities [1-3].

As watchful-waiting in these patients has been associated with a poor prognosis, especially when compared to those in whom the clinically negative neck was electively treated [1], two strategies are available for management of the clinically negative neck in early-stage OSCC: elective neck dissection (END) and sentinel lymph node biopsy (SLNB) [3-6]. Although END is considered the best approach by many [5], SLNB has proven to reliably stage the clinically negative neck in early-stage OSCC with a pooled sensitivity and negative predictive value of 87% and 94%, respectively [4, 7-9]. While END has the benefit of being a single-stage procedure, without need for specific facilities (e.g., nuclear medicine, advanced histopathology), SLNB is less invasive for the 70-80% of patients without metastatic neck involvement and has overall lower morbidity rates, better quality of life and lower health-care costs compared to END [10-13].

Furthermore, SLNB allows assessment of individual lymphatic drainage patterns and is able to detect aberrant drainage patterns [14, 15]. This feature is of particular benefit in OSCC, since even lateralized OSCC occasionally metastasizes to contralateral cervical lymph nodes (2.7% [95% CI 1.2-4.2%]) [8, 9, 14, 16-21]. Studies reported contralateral or bilateral lymphatic drainage patterns in 13-23% of lateralized OSCC patients, as detected during the SLNB procedure [8, 9, 14, 22].

Thus, SLNB stages the contralateral clinically negative neck in (lateralized) early-stage OSCC patients as well, whereas the contralateral clinically negative neck is generally not addressed by END in early-stage OSCC not involving the midline (i.e., lateralized or paramedian tumors).

Although the reported incidence of contralateral lymph node metastases in these patients is relatively low, underdiagnosis of the contralateral clinically negative neck is undesirable, especially since the presence of contralateral lymph node metastasis from OSCC has been associated with poor disease-specific survival (DSS) [16, 23, 24].

Therefore, this study aimed to assess whether SLNB allows for better control of the contralateral neck as compared to END, in early-stage OSCC not involving the midline. Accordingly, this study compares both incidence and hazard of contralateral regional recurrences (CRR) in those who underwent either END or SLNB as performed in daily

clinical practice. Furthermore, this study compares the prognosis of those in whom occult contralateral nodal metastases were detected at an earlier stage by SLNB or bilateral END (pN2c) and those who eventually developed CRR.

## Materials and methods

### Ethical considerations

This study abided the Declaration of Helsinki and was approved by UMC Utrecht's Ethics Committee (no. 17/766) and all participating centers. The Internal Review Board waived requirement for signed informed consent forms for all subjects [4]. Samples and data were handled according to General Data Protection Regulation.

### Patients

Patients without a history of head and neck cancer requiring treatment of the neck (i.e., neck dissection, neck irradiation) were included from five Dutch Head and Neck Cancer centers. In these centers SLNB is currently part of standard oncological care in regard to staging the clinically negative neck in early-stage OSCC patients. Data were extracted from two large retrospective cohorts (END-cohort and SLNB-cohort), which have been extensively described by den Toom et al. [4].

For this study, only patients with early-stage OSCC (cT1-2N0) not involving the midline (i.e., lateralized or paramedian), were included in this study (AJCC UICC TNM-staging 7<sup>th</sup> Edition). Paramedian tumors were classified as tumors located adjacent to, but not involving, the midline. In all patients, clinical nodal staging was confirmed by palpation, imaging (i.e., ultrasound, CT and/or MRI) and, in case of suspected lymph nodes, ultrasound-guided fine-needle aspiration cytology.

Patients who underwent unilateral END for tumors from which the specific location was missing, were included. In these cases, it was estimated that performing unilateral END, instead of bilateral END, was on the basis of non-involvement of the midline. Patients who underwent bilateral END for confirmed lateralized or paramedian early-stage OSCC were included as well.

Patients were excluded if they underwent bilateral END for tumors from which the specific location was missing, as there was insufficient data to reliably assess whether the tumor involved the midline.

Out of 887 patients (END  $n = 399$ , SLNB  $n = 488$ ), 816 patients met the inclusion criteria (END  $n = 365$ , SLNB  $n = 451$ ) (Figure 1).

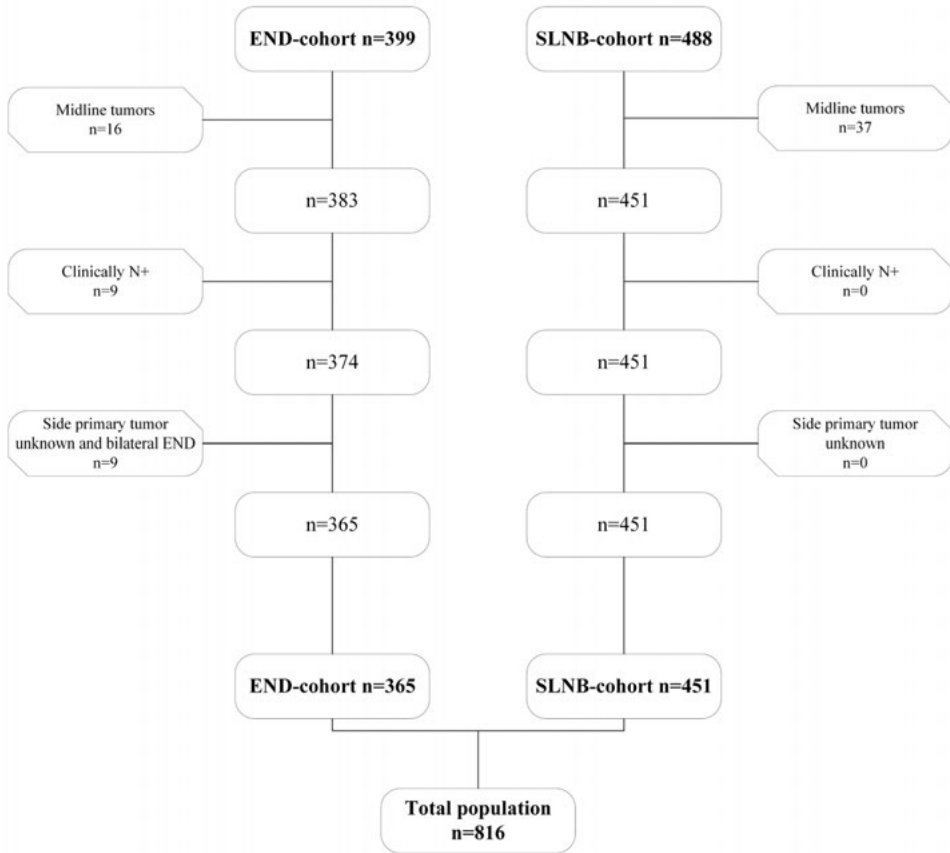


**Figure 1.** Flowchart for inclusion of patients in both the END-cohort ( $n = 365$ ) and the SLNB-cohort ( $n = 451$ ).

### Elective neck dissection (END)

The END-cohort has been previously described by den Toom et al. [4]; early-stage OSCC patients who underwent END between 1990 and 2015 were included in the END-cohort. END was performed as selective- (level I-III/IV;  $n = 294$ ) or modified radical neck dissection (level I-V;  $n = 70$ ). Twenty-eight patients (7.7%) underwent bilateral END for lateralized or paramedian early-stage OSCC. The decision to perform either unilateral or bilateral END was made by the treating physician. The indication for bilateral END was on discretion of the treating physician and multidisciplinary team. END was elected over watchful-waiting when tumor depth-of-invasion (DOI) was estimated  $> 4$  mm [25]. Neck dissection specimens were histopathologically assessed using conventional hematoxylin-eosin staining on formalin-fixed paraffin-embedded tissue.

## **Sentinel lymph node biopsy (SLNB)**

Early-stage OSCC patients who underwent SLNB between 2007 and 2018 were included in the SLNB-cohort. SLNB was performed according to European Association of Nuclear Medicine and Sentinel European Node Trial joint practice guidelines [26-28]. SLNB was elected over watchful-waiting irrespective of tumor DOI. In short, the SLNB procedure consisted of preoperative peritumoral injections with technetium-99m [<sup>99m</sup>Tc]-labeled nanocolloid (80-240 MBq), followed by planar dynamic and static lymphoscintigraphy including SPECT/CT imaging, in a one- or two day protocol. Intraoperative localization and extirpation of SLNs were performed using a handheld gammaprobe. Harvested SLNs were histopathologically assessed using step-serial-sectioning (section thickness 150-500 μm) with hematoxylin-eosin staining and immunohistochemistry [26, 29]. In SLNB-negative patients a wait-and-scan policy was adopted, while SLNB-positive patients underwent complementary neck treatment. The vast majority of SLNB-positive patients underwent neck dissection as complementary neck treatment (85.6%; 89 out of 104). Seven patients (6.7%) underwent complementary neck irradiation and three patients (2.9%) underwent complementary chemoradiation due to irradical resection of the primary tumor ( $n = 2$ ) or presence of extracapsular spread of nodal metastasis ( $n = 1$ ). Radiotherapy was employed only on the affected nodal basin in three patients, whereas in the other seven patients the side and levels involved in neck irradiation was unknown.

## **Contralateral regional recurrence (CRR), pN2c and occult contralateral nodal metastasis**

Regional recurrences that occurred in the contralateral neck of the initial primary tumor, within five years following treatment, were regarded as event for CRR analyses. In addition, CRR in the presence of ipsilateral regional recurrences were regarded as event for CRR analyses as well. Regional recurrences in the presence of local recurrence or second primary tumors were excluded from final analyses, as differentiation between missed nodal metastasis at initial diagnostic work-up and metastasis developed from reseeding local recurrence is unfeasible.

Nodal metastasis detected in the contralateral neck of the primary tumor at time of initial neck staging, by either SLNB or bilateral END, was classified as pN2c, irrespective of the nodal status of the ipsilateral neck.

Occult contralateral nodal metastasis were defined as lymph node metastasis in the contralateral neck of the initial primary tumor, which was detected by either SLNB or bilateral END (i.e., pN2c) or which became clinically manifest during follow-up (i.e., CRR).

## Statistical analysis

All data were analyzed with IBM SPSS Statistics Version 26.0. Data are expressed as mean  $\pm$ SD for continuous variables. Number of cases and percentages are presented for categorical variables.

Independent Samples T-test was applied for parametric continuous variables, Mann-Whitney U test was applied for non-parametric continuous variables and  $\chi^2$ -test was applied for categorical variables. Fisher's exact test was used to compare categorical variables containing small number of cases ( $n \leq 5$ ). Post-hoc testing was conducted in case of statistically significant  $\chi^2$ -test or Fisher's exact test outcomes for categorical variables with  $\geq 3$  groups.

For comparing five-year DSS between patients with occult contralateral nodal metastasis (i.e., pN2c, CRR) and those without, Log-Rank test was conducted and Kaplan-Meier survival curves were computed. Furthermore, five-year DSS were compared between patients in whom contralateral nodal metastases were detected by SLNB or bilateral END (pN2c) and those who eventually developed CRR during follow-up.

To assess independent predictors of CRR over time, Cox-regression analysis was applied (Method: Backward Likelihood Ratio). Variables that showed univariate association with occult contralateral nodal metastasis (i.e., pN2c and/or CRR), at a level of  $p \leq 0.05$ , were included in the proportional hazard regression model. Accordingly, covariates were neck management (SLNB/END), initial ipsilateral pN+-status, location of primary tumor (i.e., paramedian or lateralized), vaso-invasive tumor growth, perineural tumor growth and tumor DOI. Included covariates were analyzed for multicollinearity; variables with correlation of  $\geq 0.5$  were not included in Cox-regression analysis [30].

Missing data were handled by pairwise deletion. A p-value of  $< 0.05$  was regarded statistically significant.

## Results

The SLNB-cohort contained a higher rate of tongue tumors ( $p < 0.001$ ), whereas the END-cohort contained a higher rate of floor-of-mouth tumors ( $p = 0.008$ ) (Table 1). The END-cohort had a higher rate of cT2-staged tumors ( $p < 0.001$ ) and a higher rate of tumors staged pT2 or higher (52.8% vs. 24.6%;  $p < 0.001$ ). Tumor DOI was higher in the END-cohort ( $p < 0.001$ ). Extracapsular spread of nodal metastases was more often present in the END-cohort ( $p < 0.001$ ). Median follow-up was longer for the END-cohort ( $p < 0.001$ ).

### **Contralateral regional recurrences (CRR)**

The overall rate of CRR was 2.5% (20 of 816). Tumor DOI was higher in patients who developed CRR ( $p < 0.001$ ) (Table 2). Vaso-invasive tumor growth was more frequently present in patients who developed CRR ( $p = 0.032$ ). END-patients developed CRR more often (14 of 365; 3.8%) as compared to SLNB-patients (6 of 451; 1.3%) ( $p = 0.021$ ). None of the patients who underwent bilateral END developed CRR. In one patient, CRR was diagnosed in the presence of distant metastasis. CRR was diagnosed in the presence of ipsilateral regional recurrence in one END-patient and in two SLNB-patients. The rate of ipsilateral nodal metastases, as detected by END or SLNB, was higher in those who developed CRR ( $p = 0.018$ ). None of the patients in whom occult contralateral nodal metastases were detected by SLNB or bilateral END (i.e., pN2c) developed CRR. Out of those who developed CRR, 15 patients underwent salvage treatment with curative intent; in three patients no data on salvage treatment was available.

### **Occult contralateral nodal metastasis (i.e., pN2c and CRR)**

The overall rate of occult contralateral nodal metastasis was 3.7% (30 of 816). Patients with paramedian tumors showed a higher rate of contralateral nodal metastases compared to those with lateralized tumors ( $p = 0.018$ ) (Table 3). Tumor DOI was higher in patients with occult contralateral nodal metastasis ( $p < 0.002$ ). Perineural tumor growth and vasoinvasive tumor growth were more often present in those with occult contralateral nodal metastasis ( $p = 0.002$ ,  $p = 0.001$ ). A higher rate of ipsilateral nodal metastases, as detected by SLNB or END, was seen in patients with occult contralateral nodal metastasis ( $p = 0.025$ ). Of those in whom occult contralateral nodal metastasis was detected by either bilateral END or SLNB (i.e., pN2c), ipsilateral nodal metastasis was simultaneously detected in three patients (30%). No significant difference was seen in the rate of occult contralateral nodal metastasis between the END- and SLNB-cohort.

**Table 1.** Patient- and tumor characteristics comparing END- and SLNB-cohort

<i>n</i> = 806	SLNB ( <i>n</i> = 451)	END ( <i>n</i> = 365)	p-value*
Age; mean ( $\pm$ SD)	62.03 ( $\pm$ 11.97)	61.98 ( $\pm$ 12.77)	0.960
<b>Gender</b>			0.533
Male (%)	233 (51.8%)	197 (54.0%)	
<b>Site of primary tumor<sup>a</sup></b>			< 0.001†; 0.003†
Tongue (%)	300 (66.5%)	195 (53.4%)	
Floor-of-mouth (%)	98 (21.7%)	113 (31.0%)	
Buccal Mucosa (%)	34 (7.5%)	35 (9.6%)	
Other (%)	19 (4.3%)	22 (6.0%)	
<b>cT-stage</b>			< 0.001†
T1 (%)	306 (67.8%)	133 (36.4%)	
T2 (%)	145 (32.2%)	222 (63.6%)	
<b>pT-stage<sup>b</sup></b>			< 0.001†
T1 (%)	340 (75.4%)	172 (47.2%)	
T2 (%)	107 (23.7%)	188 (51.5%)	
T3 (%)	4 (0.9%)	3 (0.8%)	
T4 (%)	0 (0%)	2 (0.5%)	
<b>DOI; mean (<math>\pm</math>SD) in mm</b>	5.32 ( $\pm$ 4.28)	6.90 ( $\pm$ 4.19)	< 0.001‡
<b>pN-stage</b>			0.533
pN0 (%)	347 (76.9%)	274 (75.1%)	
pN+ (%)	104 (23.1%)	91 (24.9%)	
<b>pN2c</b>			0.199
Yes (%)	8 (1.8%)	2 (0.5%)	
<b>ECS</b>			< 0.001X
Yes (%)	3 (0.7%)	32 (8.8%)	
<b>Follow-up in years; median (IQR)</b>	2.2 (1.0-4.1)	4.6 (2.5-7.3)	< 0.001‡

SLNB *sentinel lymph node biopsy*, END *elective neck dissection*, SD *standard deviation*, DOI *depth-of-invasion*, ECS *extracapsular spread*, IQR *interquartile range*.

\*Bold script indicates significant value

†  $\chi^2$  test

‡ Independent Samples T-test

X Fisher's Exact Test

‡ Mann-Whitney U test

<sup>a</sup>Significance regards tumors of the tongue and floor-of-mouth tumors

<sup>b</sup>Significance regards tumors staged pT2 or higher

**Table 2.** Characteristics associated with contralateral regional recurrence

<i>n</i> = 816	No CRR ( <i>n</i> = 796)	CRR ( <i>n</i> = 20)	p-value*
<b>Site of primary tumor</b>			0.655
Tongue (%)	481 (60.4%)	14 (70.0%)	
Floor-of-mouth (%)	206 (25.9%)	5 (25.0%)	
Buccal Mucosa (%)	68 (8.5%)	1 (5.0%)	
Other (%)	41 (5.2%)	0 (0%)	
<b>pT-stage<sup>a</sup></b>			0.097
T1 (%)	503 (63.2%)	9 (45.0%)	
T2 (%)	286 (35.9%)	9 (45.0%)	
T3 (%)	5 (0.6%)	2 (10.0%)	
T4 (%)	2 (0.3%)	0 (0%)	
<b>Location primary tumor</b>			0.154
Lateralized	655 (97.4%)	18 (2.6%)	
Paramedian	23 (92.0%)	2 (8.0%)	
DOI; mean ( $\pm$ SD) in mm	5.90 ( $\pm$ 4.21)	9.48 ( $\pm$ 6.11)	< 0.001‡
<b>Non-cohesive growth</b>			0.316
Yes (%)	267 (53.6%)	13 (65.0%)	
<b>Perineural growth</b>			0.071
Yes (%)	110 (18.8%)	7 (35.0%)	
<b>Vasoinvasive growth</b>			0.032X
Yes (%)	51 (8.9%)	5 (25.0%)	
<b>Procedure neck<sup>b</sup></b>			0.021†
SLNB (%)	445 (98.7%)	6 (1.3%)	
Unilateral END (%)	323 (95.8%)	14 (4.2%)	
Bilateral END (%)	28 (100%)	0 (0%)	
<b>pN-stage</b>			0.018†
Ipsilateral pN+ (%)	179 (22.5%)	9 (45.0%)	
<b>pN2c</b>			N.A.
Yes (%)	10 (1.3%)	0 (0%)	
<b>ECS</b>			0.588
Yes (%)	34 (4.3%)	1 (5.0%)	

CRR *contralateral regional recurrence*, DOI *depth-of-invasion*, SD *standard deviation*, SLNB *sentinel lymph node biopsy*, END *elective neck dissection*, ECS *extracapsular spread*, N.A. *not applicable*

\*Bold script indicates significant value

†  $\chi^2$  test

‡ Independent Samples T-test

X Fisher's Exact Test

<sup>a</sup> p-value regards tumors staged pT1 versus pT2 or higher

<sup>b</sup> Significance regards difference in CRR-rate between END- and SLNB-cohort

**Table 3.** Characteristics associated with occult contralateral nodal metastasis (i.e., pN2c and CRR)

<i>n</i> = 816	No contralateral metastases ( <i>n</i> = 786)	Contralateral metastases ( <i>n</i> = 30)	p-value*
<b>Site of primary tumor</b>			0.394
Tongue (%)	474 (60.3%)	21 (70.0%)	
Floor-of-mouth (%)	203 (25.8%)	8 (26.7%)	
Buccal Mucosa (%)	68 (8.7%)	1 (3.3%)	
Other (%)	41 (5.2%)	0 (0%)	
<b>pT-stage<sup>a</sup></b>			0.277
T1 (%)	496 (63.1%)	16 (53.3%)	
T2 (%)	283 (36.0%)	12 (40.0%)	
T3 (%)	5 (0.6%)	2 (6.7%)	
T4 (%)	2 (0.3%)	0 (0%)	
<b>Location primary tumor</b>			<b>0.018X</b>
Lateralized	657 (96.2%)	26 (3.8%)	
Paramedian	21 (84.0%)	4 (16.0%)	
<b>DOI; mean (±SD) in mm</b>	5.90 (±4.21)	8.46 (±5.75)	<b>0.002‡</b>
<b>Non-cohesive growth</b>			0.177
Yes (%)	262 (53.4%)	18 (66.7%)	
<b>Perineural growth</b>			<b>0.002†</b>
Yes (%)	106 (18.3%)	11 (42.3%)	
<b>Vasoinvasive growth</b>			<b>0.001†</b>
Yes (%)	49 (8.6%)	7 (28.0%)	
<b>Procedure neck</b>			0.334
SLNB (%)	437 (98.7%)	14 (3.1%)	
END (%)	349 (95.6%)	16 (4.4%)	
<b>pN-stage<sup>a</sup></b>			<b>0.025†</b>
Ipsilateral pN+ (%)	176 (22.4%)	12 (40.0%)	
<b>ECS</b>			0.133
Yes (%)	32 (4.1%)	3 (10.0%)	

CRR *contralateral regional recurrence*, DOI *depth-of-invasion*, SD *standard deviation*, SLNB *sentinel lymph node biopsy*, END *elective neck dissection*, ECS *extracapsular spread*.

\*Bold script indicates significant value

X Fisher's Exact Test

‡ Independent Samples T-test

†  $\chi^2$  test

<sup>a</sup> p-value regards tumors staged pT1 versus pT2 or higher

## Survival

Figure 2 shows five-year DSS for patients with and without occult contralateral nodal metastasis (i.e., pN2c and CRR). Five-year DSS was significantly shorter for patients who developed CRR as compared to patients without occult contralateral nodal metastasis (42% vs. 92%,  $p < 0.001$ ). No difference in five-year DSS was observed between those in whom occult contralateral nodal metastasis were detected by SLNB or bilateral END (i.e., pN2c), and patients without occult contralateral nodal metastasis (88% vs. 92%;  $p = 0.446$ ). Five-year DSS of patients who developed CRR was worse compared to those in whom occult contralateral metastasis were detected by SLNB or bilateral END (i.e., pN2c), although not statistically significant (42% vs. 88%;  $p = 0.066$ ). Of those who underwent salvage treatment with curative intent for CRR, 67% (10 of 15 patients) died of disease after an average follow-up of 6.1 months following occurrence of CRR.

Mean time of survival in patients who developed CRR was 4.1 years [95% CI 2.29-5.95], whereas mean time of survival of those in whom contralateral nodal metastases were detected by SLNB or bilateral END (i.e., pN2c) was 9.7 years [95% CI 7.37-12.02]. The mean time of survival in patients without occult contralateral nodal metastasis was 19.3 years [95% CI 18.81-19.72].

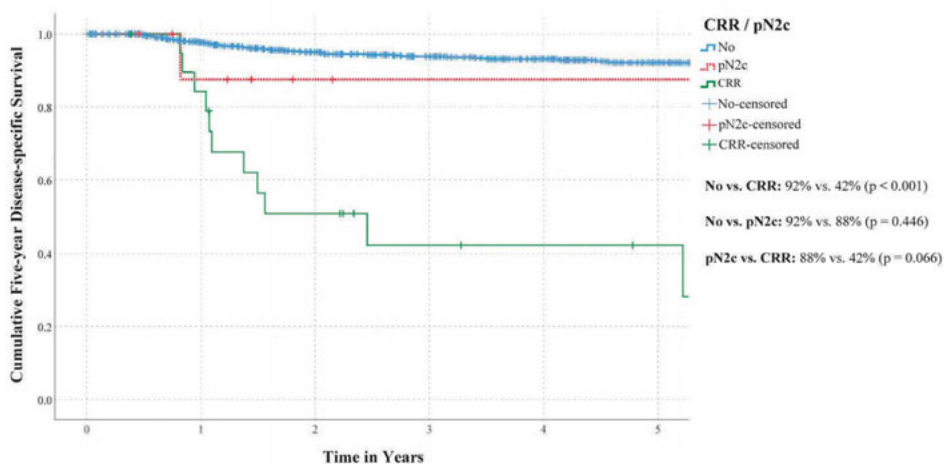


**Figure 2.** Five-year DSS curves for lateralized or paramedian early-stage OSCC patients without contralateral occult nodal metastasis (*blue bold line*) as compared to those with contralateral occult nodal metastasis: initially staged pN2c by SLNB or bilateral END (*red interrupted line*) or CRR (*green line*).

### Hazard for developing contralateral regional recurrence (CRR)

Proportional hazard regression analysis showed that patients who underwent END had a higher hazard for developing CRR as compared to those who underwent SLNB (HR = 2.922 [95% CI 1.11-7.71];  $p = 0.030$ ) (Figure 3). In addition, tumor DOI was significantly associated with development of CRR as well (HR = 2.277 [95% CI 1.44-3.60];  $p < 0.001$ ).

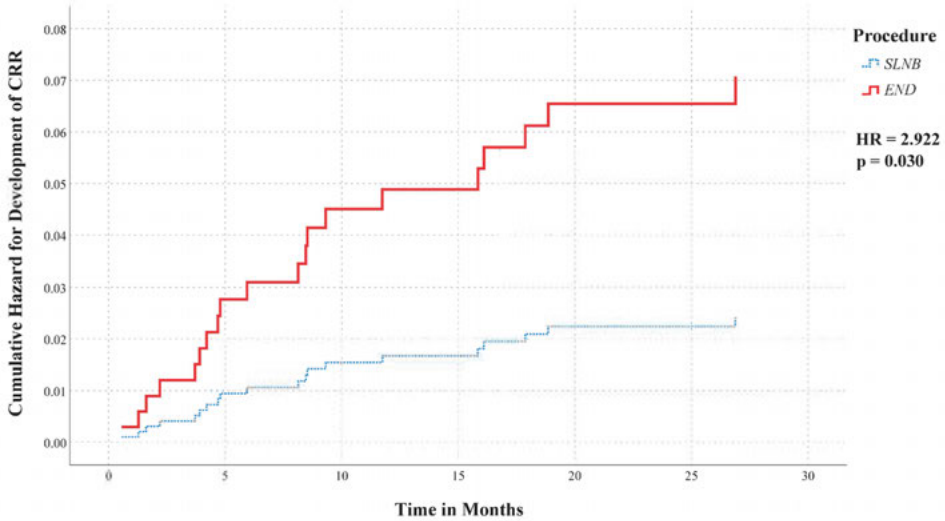


**Figure 3.** Cumulative hazard curve regarding development of CRR in patients with early-stage OSCC not involving the midline, divided by initial management of the neck: elective neck dissection (END; red bold line) or sentinel lymph node biopsy (SLNB; blue interrupted line). A significantly higher hazard for developing CRR was observed for patients who underwent END compared to those who underwent SLNB (HR = 2.922 [95% CI 1.11-7.71]).

## Discussion

This is the first study that evaluated incidence and hazard of CRR in early-stage OSCC not involving the midline (i.e., lateralized and paramedian) and compared these outcomes between patients who underwent either END or SLNB.

The overall incidence of occult contralateral nodal metastasis in this study was 3.7% (30 of 816), which is in concordance with the reported incidence of occult contralateral nodal metastasis in lateralized early-stage OSCC (2.7% [95% CI 1.2-4.2%]) [8, 9, 14, 16-21].

Our results showed higher incidence of CRR in patients who underwent END (3.8%) as compared to those who underwent SLNB (1.3%) ( $p = 0.018$ ). Furthermore, our data showed that patients staged by END had a higher hazard of developing CRR, independent of factors such as tumor DOI, compared to patients staged by SLNB (HR = 2.922 [95% CI 1.11-7.71];  $p = 0.030$ ).

Five-year DSS of patients who developed CRR was poor in our population, in particular when compared to those without occult contralateral nodal metastasis. These findings are in line with previous reports on prognosis of (lateralized) OSCC patients with CRR [16, 23, 24]. Moreover, our results suggest that five-year DSS of patients in whom contralateral nodal metastases were detected at an earlier stage by SLNB or bilateral END (pN2c), may be better than in those who eventually developed CRR. In addition, the successful salvage rate of those who developed CRR was only 33% in our population. This highlights the importance of adequate staging or treatment of the contralateral clinically negative neck.

Nevertheless, elective treatment of the contralateral clinically negative neck in OSCC without midline-involvement remains controversial. This controversy is sustained by the varying incidence of occult contralateral nodal metastasis and CRR among institutions and the accompanying morbidity of (bilateral) END [18-20, 23, 24, 31-34]. In our population, only two patients who underwent bilateral END had occult contralateral nodal metastasis, indicating that 26 of 28 patients (93%) underwent unnecessary contralateral END. With this in mind, it is worth noting that SLNB has the benefit of staging the contralateral clinically negative neck simultaneous with the ipsilateral neck. Accordingly, SLNB is able to avoid overtreatment of the contralateral neck by allowing accurate selection of only those that require treatment of the contralateral neck.

Another predictor for development of CRR in our population was tumor DOI (HR = 2.277 [95% CI 1.44-3.60];  $p < 0.001$ ), which is in agreement with previous findings

by Ganly et al. [35]. In their study, neck failure in the undissected contralateral neck of T1-2N0 oral tongue patients accounted for 39% of all recurrences. Moreover, their results showed that tumor thickness was predicting for CRR. Although tumor thickness and DOI are not equivalent, they have similar prognostic implications for nodal metastases [36]. As a consequence, the higher rate of CRR in our END-cohort may be explained by greater tumor DOI in these patients. Nevertheless, when correcting for DOI in our proportional hazard regression analysis, a significantly higher hazard for developing CRR was observed in END-patients as compared to SLNB-patients.

The limitations of our study remain its retrospective design and the heterogeneity in performing SLNB or END among institutions. Secondly, occult contralateral nodal metastases are uncommon in this population, which irrevocably results in a small number of events for analyses. Accordingly, it could be argued that a larger sample, resulting in more CRR- and pN2c-events for analyses, may result in a significantly better prognosis for those in whom the metastatic involved contralateral neck is correctly staged and treated at an earlier stage, as compared to those who eventually develop CRR. Thirdly, since END-patients were included between 1990 and 2015, a substantial proportion may have been elected for END based on potentially dated therapeutic guidelines or aged diagnostic imaging modalities. Moreover, patients were predominantly selected for END based on estimated tumor DOI > 4 mm, inevitably resulting in higher tumor DOI in the END-cohort. Due to this heterogeneity in therapeutic decision making between both cohorts, they cannot easily be compared, especially since the END-cohort had a higher tumor DOI, higher T-stages, a higher rate of extracapsular spread of nodal metastases and a longer follow-up duration, which might impact the occurrence of occult contralateral nodal metastasis or CRR. Nevertheless, there was no significant difference in the total rate of occult contralateral nodal metastasis (i.e., pN2c and CRR) between both cohorts, which implies that these cohorts can be compared when concerning control of the contralateral clinically negative neck. Furthermore, our proportional hazard regression analysis, which allows adjustment for confounding effects of included variables, showed a higher hazard for developing CRR in the END-cohort, independent of confounding factors such as tumor DOI. In addition, both higher T-stages and presence of extracapsular spread of nodal metastases showed no association with contralateral nodal metastases or CRR in our univariate analyses. Besides, although a longer follow-up was available for END patient compared to SLNB patients, local or regional recurrences are uncommon after 2 years post-treatment [37]. The follow-up duration of the SLNB-cohort was therefore considered long enough for missed occult metastases to become clinically manifest and provides no explanation for the difference in rate of CRR between both cohorts. It could be argued that patients who underwent unilateral END for tumors from which the specific location was missing, should be excluded

from this study. However, since none of these patients developed CRR, excluding them would result in a relatively higher incidence of CRR in the END-cohort, which will presumably induce a distortion of results in favor of SLNB. Fourthly, as there are no clear guidelines in which cases to perform contralateral END in early-stage OSCC, these were likely performed, based on preference of the treating physician and on availability of the latest state-of-the-art imaging modalities. This may introduce some bias, however it reflects daily clinical practice at that time. This strengthens the need for more research to develop evidence-based guidelines on this important topic. Fifthly, in this study the 7<sup>th</sup> TNM-classification was applied, whereas the 8<sup>th</sup> edition has already been implemented [38]. While tumor diameter reflected pT-stage in the 7<sup>th</sup> edition, DOI is newly incorporated for T-stage in the 8<sup>th</sup> edition [36, 39]. Due to missing data on DOI in several cases, our results could not be directly translated to the 8<sup>th</sup> TNM-classification. Finally, some clinical and histopathological factors, that have been associated with contralateral nodal metastasis in OSCC, were not included due to lack of data. These factors include histological grading, surgical margin status, peritumoral inflammation, (adjuvant) radiotherapy to contralateral neck and time of initial diagnosis [24]. In particular, (adjuvant) radiotherapy to contralateral neck could influence the occurrence of CRR in these patients and should therefore be documented and incorporated in further studies. Although non-cohesive growth of the tumor was included as a potential predictor for CRR in our analyses, it was not subdivided by grading of pattern-of-invasion (i.e., cohesive growth, small islands, thin strands and individual tumor cells) [24, 40]. Nevertheless, the correlation between several of these factors (i.e., histological grading, peritumoral inflammation and pattern-of-invasion) and contralateral nodal metastasis is dubious [24].

In conclusion, the incidence of CRR in lateralized or paramedian early-stage OSCC is relatively low (2.5%). As the salvage rate and prognosis of those who develop CRR remain poor, adequate staging of the contralateral clinically negative neck is highly recommended, especially since the prognosis of those in whom occult contralateral nodal metastases are detected at an earlier stage may be favorable compared to those who eventually develop CRR. In our population, a higher incidence of CRR was observed in those who underwent END for lateralized or paramedian early-stage OSCC, as compared to those who underwent SLNB. Furthermore, a higher hazard for developing CRR was observed in patients who underwent END in a clinical setting as compared to patients who underwent SLNB. Accordingly, our data suggest that SLNB allows for better control of the contralateral clinically negative neck in early-stage OSCC not involving the midline.

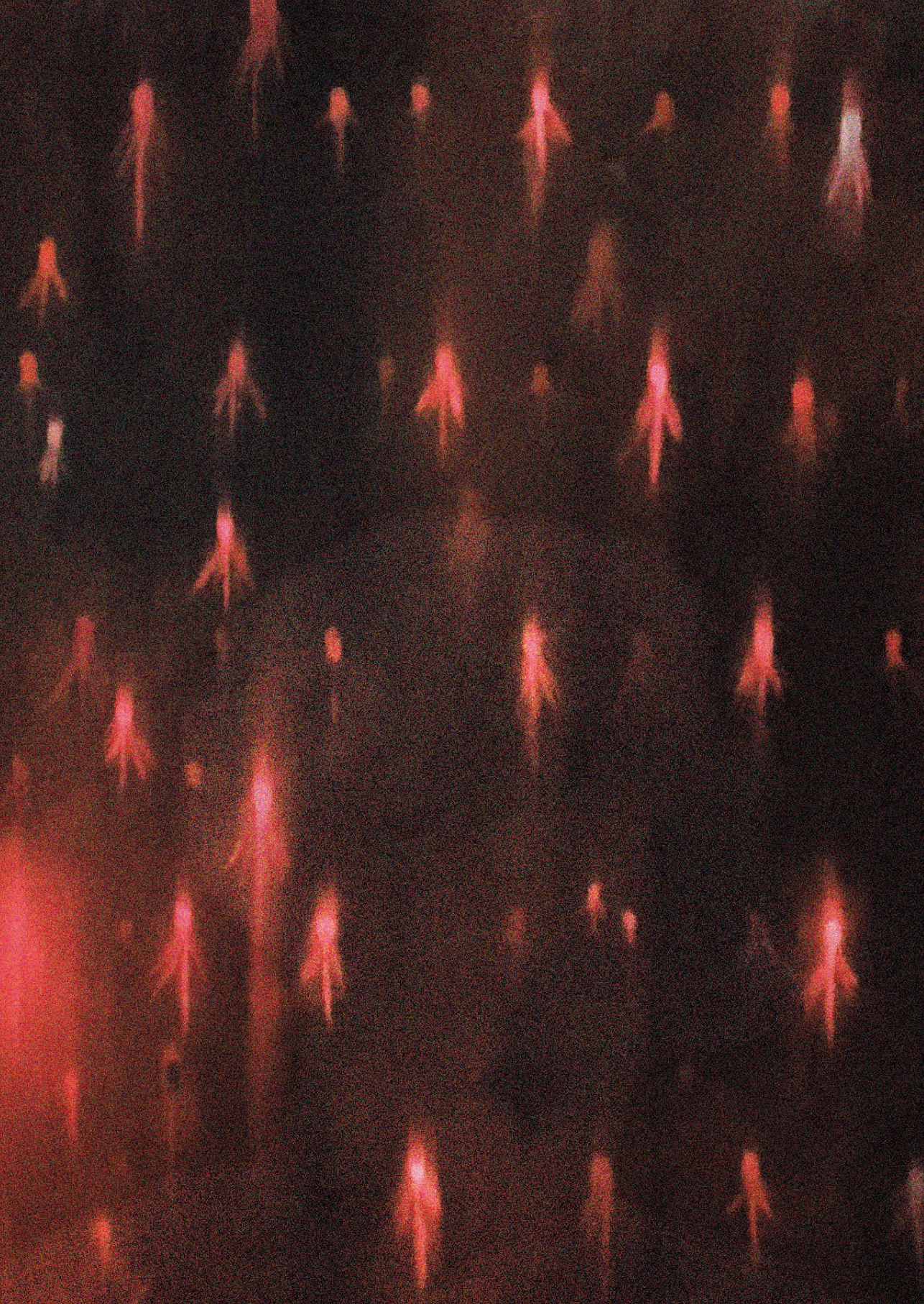
## References

1. D'Cruz AK, Vaish R, Kapre N, et al. Elective versus therapeutic neck dissection in node-negative oral cancer. *N Engl J Med*. 2015;373(6):521-529. doi:10.1056/NEJMoa1506007
2. Abu-Ghanem S, Yehuda M, Carmel NN, et al. Elective neck dissection vs observation in early-stage squamous cell carcinoma of the oral tongue with no clinically apparent lymph node metastasis in the neck: a systematic review and meta-analysis. *JAMA Otolaryngol Head Neck Surg*. 2016;142(9):857-865. doi:10.1001/jamaoto.2016.1281
3. de Bree R, Takes RP, Shah JP, et al. Elective neck dissection in oral squamous cell carcinoma: Past, present and future. *Oral Oncol*. 2019;90:87-93. doi:10.1016/j.oraloncology.2019.01.016
4. den Toom IJ, Boeve K, Lobeek D, et al. Elective neck dissection or sentinel lymph node biopsy in early stage oral cavity cancer patients: the Dutch experience. *Cancers (Basel)*. 2020;12(7):1783. doi:10.3390/cancers12071783
5. Schilling C, Shaw R, Schache A, et al. Sentinel lymph node biopsy for oral squamous cell carcinoma. Where are we now? *Br J Oral Maxillofac Surg*. 2017;55(8):757-762. doi:10.1016/j.bjoms.2017.07.007
6. Cramer JD, Sridharan S, Ferris RL, Duvvuri U, Samant S. Sentinel lymph node biopsy versus elective neck dissection for stage I to II oral cavity cancer. *Laryngoscope*. 2019;129(1):162-169. doi:10.1002/lary.27323
7. Liu M, Wang SJ, Yang X, Peng H. Diagnostic efficacy of sentinel lymph node biopsy in early oral squamous cell carcinoma: a meta-analysis of 66 studies. *PLoS One*. 2017;12(1):e0170322. doi:10.1371/journal.pone.0170322
8. Schilling C, Stoeckli SJ, Haerle SK, et al. Sentinel European Node Trial (SENT): 3-year results of sentinel node biopsy in oral cancer. *Eur J Cancer*. 2015;51(18):2777-2784. doi:10.1016/j.ejca.2015.08.023
9. Flach GB, Bloemena E, Klop WM, et al. Sentinel lymph node biopsy in clinically N0 T1-T2 staged oral cancer: the Dutch multicenter trial. *Oral Oncol*. 2014;50(10):1020-1024. doi:10.1016/j.oraloncology.2014.07.020
10. Schiefke F, Akdemir M, Weber A, Akdemir D, Singer S, Frerich B. Function, postoperative morbidity, and quality of life after cervical sentinel node biopsy and after selective neck dissection. *Head Neck*. 2009;31(4):503-512. doi:10.1002/hed.21001
11. Murer K, Huber GF, Haile SR, Stoeckli SJ. Comparison of morbidity between sentinel node biopsy and elective neck dissection for treatment of the n0 neck in patients with oral squamous cell carcinoma. *Head Neck*. 2011;33(9):1260-1264. doi:10.1002/hed.21622
12. Govers TM, Schreuder WH, Klop WM, et al. Quality of life after different procedures for regional control in oral cancer patients: cross-sectional survey. *Clin Otolaryngol*. 2016;41(3):228-233. doi:10.1111/coa.12502
13. Govers TM, Takes RP, Baris Karakullukcu M, et al. Management of the N0 neck in early stage oral squamous cell cancer: a modeling study of the cost-effectiveness. *Oral Oncol*. 2013;49(8):771-777. doi:10.1016/j.oraloncology.2013.05.001
14. Mølstrøm J, Grønne M, Green A, Bakholdt V, Sørensen JA. Topographical distribution of sentinel nodes and metastases from T1-T2 oral squamous cell carcinomas. *Eur J Cancer*. 2019;107:86-92. doi:10.1016/j.ejca.2018.10.021
15. den Toom IJ, Boeve K, van Weert S, et al. High rate of unexpected lymphatic drainage patterns and a high accuracy of the sentinel lymph node biopsy in oral cancer after previous neck treatment. *Oral Oncol*. 2019;94:68-72. doi:10.1016/j.oraloncology.2019.05.007
16. Koo BS, Lim YC, Lee JS, Choi EC. Management of contralateral N0 neck in oral cavity squamous cell carcinoma. *Head Neck*. 2006;28(10):896-901. doi:10.1002/hed.20423
17. Kurita H, Koike T, Narikawa JN, et al. Clinical predictors for contralateral neck lymph node metastasis from unilateral squamous cell carcinoma in the oral cavity. *Oral Oncol*. 2004;40(9):898-903. doi:10.1016/j.oraloncology.2004.04.004
18. Lim YC, Lee JS, Koo BS, Kim SH, Kim YH, Choi EC. Treatment of contralateral N0 neck in early squamous cell carcinoma of the oral tongue: elective neck dissection versus observation. *Laryngoscope*. 2006;116(3):461-465. doi:10.1097/01.mlg.0000195366.91395.9b
19. Zbären B, Nuyens M, Caversaccio M, Stauffer E. Elective neck dissection for carcinomas of the oral cavity: occult metastases, neck recurrences, and adjuvant treatment of pathologically positive necks. *Am J Surg*. 2006;191(6):756-760. doi:10.1016/j.amjsurg.2006.01.052

20. Nobis CP, Otto S, Grigorieva T, et al. Elective neck dissection in unilateral carcinomas of the tongue: Unilateral versus bilateral approach. *J Craniomaxillofac Surg.* 2017;45(4):579-584. doi:10.1016/j.jcms.2017.01.008
21. Pezier T, Nixon IJ, Gurney B, et al. Sentinel lymph node biopsy for T1/T2 oral cavity squamous cell carcinoma--a prospective case series. *Ann Surg Oncol.* 2012;19(11):3528-3533. doi:10.1245/s10434-011-2207-0
22. Moya-Plana A, Aupérin A, Guerlain J, et al. Sentinel node biopsy in early oral squamous cell carcinomas: Long-term follow-up and nodal failure analysis. *Oral Oncol.* 2018;82:187-194. doi:10.1016/j.oraloncology.2018.05.021
23. Feng Z, Niu LX, Yuan Y, Peng X, Guo CB. Risk factors and treatment of contralateral neck recurrence for unilateral oral squamous cell carcinoma: a retrospective study of 1482 cases. *Oral Oncol.* 2014;50(11):1081-1088. doi:10.1016/j.oraloncology.2014.08.003
24. Fan S, Tang QL, Lin YJ, et al. A review of clinical and histological parameters associated with contralateral neck metastases in oral squamous cell carcinoma. *Int J Oral Sci.* 2011;3(4):180-191. doi:10.4248/IJOS11068
25. Huang SH, Hwang D, Lockwood G, Goldstein DP, O'Sullivan B. Predictive value of tumor thickness for cervical lymph-node involvement in squamous cell carcinoma of the oral cavity: a meta-analysis of reported studies. *Cancer.* 2009;115(7):1489-1497. doi:10.1002/cncr.24161
26. Alkureishi LW, Burak Z, Alvarez JA, et al. Joint practice guidelines for radionuclide lymphoscintigraphy for sentinel node localization in oral/oropharyngeal squamous cell carcinoma. *Ann Surg Oncol.* 2009;16(11):3190-3210. doi:10.1245/s10434-009-0726-8
27. Giammarile F, Schilling C, Gnanasegaran G, et al. The EANM practical guidelines for sentinel lymph node localisation in oral cavity squamous cell carcinoma. *Eur J Nucl Med Mol Imaging.* 2019;46(3):623-637. doi:10.1007/s00259-018-4235-5
28. Schilling C, Stoeckli SJ, Vigili MG, et al. Surgical consensus guidelines on sentinel node biopsy (SNB) in patients with oral cancer. *Head Neck.* 2019;41(8):2655-2664. doi:10.1002/hed.25739
29. Dhawan I, Sandhu SV, Bhandari R, Sood N, Bhullar RK, Sethi N. Detection of cervical lymph node micrometastasis and isolated tumor cells in oral squamous cell carcinoma using immunohistochemistry and serial sectioning. *J Oral Maxillofac Pathol.* 2016;20(3):436-444. doi:10.4103/0973-029X.190946
30. Donath C, Grassel E, Baier D, Pfeiffer C, Bleich S, Hillemacher T. Predictors of binge drinking in adolescents: ultimate and distal factors - a representative study. *BMC Public Health.* 2012;12:263. doi:10.1186/1471-2458-12-263
31. Klingelhöffer C, Gründlinger A, Spanier G, et al. Patients with unilateral squamous cell carcinoma of the tongue and ipsilateral lymph node metastasis do not profit from bilateral neck dissection. *Oral Maxillofac Surg.* 2018;22(2):185-192. doi:10.1007/s10006-018-0690-1
32. Habib M, Murgasen J, Gao K, et al. Contralateral neck failure in lateralized oral squamous cell carcinoma. *ANZ J Surg.* 2016;86(3):188-192. doi:10.1111/ans.13206
33. Liao CT, Huang SF, Chen IH, et al. Risk stratification of patients with oral cavity squamous cell carcinoma and contralateral neck recurrence following radical surgery. *Ann Surg Oncol.* 2009;16(1):159-170. doi:10.1245/s10434-008-0196-4
34. Shimamoto H, Oikawa Y, Osako T, et al. Neck failure after elective neck dissection in patients with oral squamous cell carcinoma. *Oral Surg Oral Med Oral Pathol Oral Radiol.* 2017;124(1):32-36. doi:10.1016/j.oooo.2017.03.003
35. Ganly I, Goldstein D, Carlson DL, et al. Long-term regional control and survival in patients with "low-risk," early stage oral tongue cancer managed by partial glossectomy and neck dissection without postoperative radiation: the importance of tumor thickness. *Cancer.* 2013;119(6):1168-1176. doi:10.1002/cncr.27872
36. Dirven R, Ebrahimi A, Moeckelmann N, Palme CE, Gupta R, Clark J. Tumor thickness versus depth of invasion - Analysis of the 8<sup>th</sup> edition American Joint Committee on Cancer Staging for oral cancer. *Oral Oncol.* 2017;74:30-33. doi:10.1016/j.oraloncology.2017.09.007
37. Hutchison IL, Ridout F, Cheung SMY, et al. Nationwide randomised trial evaluating elective neck dissection for early stage oral cancer (SEND study) with meta-analysis and concurrent real-world cohort. *Br J Cancer.* 2019;121(10):827-836. doi:10.1038/s41416-019-0587-2
38. Brierley JD, Gospodarowicz M, Wittekind C. UICC TNM Classification of Malignant Tumours. 8<sup>th</sup> ed. Chichester, United Kingdom: Wiley; 2017.

39. Lydiatt WM, Patel SG, O'Sullivan B, et al. Head and Neck cancers-major changes in the American Joint Committee on cancer eighth edition cancer staging manual. *CA Cancer J Clin.* 2017;67(2):122-137. doi:10.3322/caac.21389
40. De Silva RK, Siriwardena BSMS, Samaranayaka A, Abeyasinghe WAMUL, Tilakaratne WM. A model to predict nodal metastasis in patients with oral squamous cell carcinoma. *PLoS One.* 2018;13(8):e0201755. doi:10.1371/journal.pone.0201755





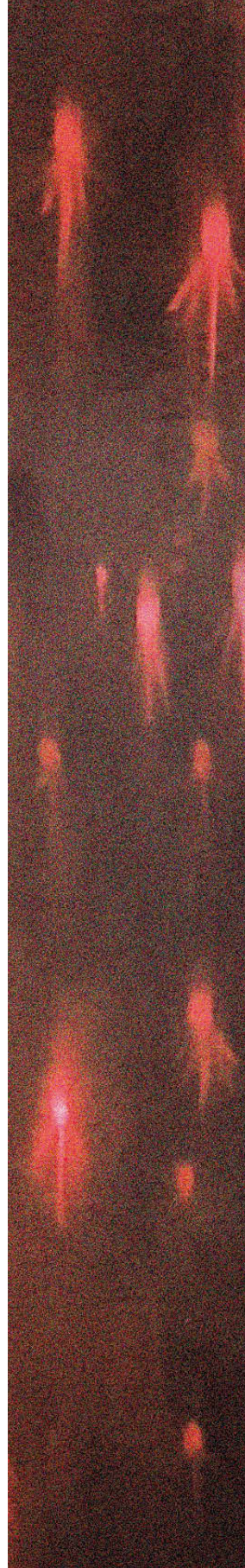
# 3

## Evaluation of a streamlined sentinel lymph node imaging protocol in early-stage oral cancer

---

Michiel Zeeuw, Rutger Mahieu, Bart de Keizer, Remco de Bree.

*Ann Nucl Med. 2021 Dec;35(12):1353-1360*



# Abstract

## Objective

Sentinel lymph node (SLN) mapping for early-stage oral squamous cell carcinoma (OSCC) is comprehensive and consequently time-consuming and costly. This study evaluated the clinical value of several SLN imaging components and analyzed the accuracy for SLN identification using a streamlined SLN imaging protocol in early-stage OSCC.

## Materials and Methods

This retrospective within-patient evaluation study compared both number and localization of identified SLNs between the conventional SLN imaging protocol and a streamlined imaging protocol (dynamic lymphoscintigraphy (LSG) for 10 minutes directly post-injection and SPECT/CT at ~2 hours post-injection). LSG and SPECT/CT images of 77 early-stage OSCC patients, scheduled for SLN biopsy, were evaluated by three observers. Identified SLNs using either protocol were related to histopathological assessment of harvested SLNs, complementary neck dissection specimens and follow-up status.

## Results

A total of 200 SLNs were identified using the streamlined protocol, 12 additional SLNs ( $n = 212$ ) were identified with the conventional protocol in 10 patients. Of those, 9 of 12 SLNs were identified on early static LSG and 3 of 12 SLNs on late static LSG. None of the additionally identified SLNs contained metastases; none of those in whom additional SLNs were identified developed regional recurrence during follow-up. Only inferior alveolar process carcinoma showed a higher rate of additionally identified SLNs with the conventional protocol ( $p = 0.006$ ).

## Conclusion

Early dynamic LSG can be reduced to 10 minutes. Late static LSG may be omitted, except in those with a history of oncological neck treatment or with OSCC featuring slow lymphatic drainage. Early static LSG appeared to be contributory in most OSCC subsites.

## Introduction

Sentinel lymph node (SLN) biopsy has been studied widely and has proven to be reliable in staging the clinically negative neck in early-stage OSCC patients, with a pooled sensitivity and negative predictive value of 87% and 94%, respectively [1-5]. Today, SLN biopsy is implemented as standard oncological care in nearly all Dutch head and neck oncological centers for staging the clinically negative neck in patients with early-stage OSCC [6].

In essence, SLN mapping is initiated by peritumoral injections of a  $^{99m}\text{Tc}$ -labeled radiotracer. Directly post-injection planar dynamic and early static lymphoscintigraphic (LSG) imaging is acquired, followed by late static LSG and SPECT/CT imaging [7-10].

The current SLN imaging protocol in early-stage OSCC is comprehensive. Accordingly, it is associated with high costs, patient discomfort and limited availability of SPECT/CT imaging devices on day-to-day basis [11]. There may be opportunities to develop a protocol which is less costly and time-consuming for both medical professionals and patients.

In 2012, Heuveling et al. already underlined the limited value of late static LSG in early-stage OSCC. The authors stated that late static LSG is only contributory in selected cases and should not be routinely performed [12]. This finding is in concordance with practice guidelines of Alkureishi et al. suggesting that late static LSG should only be performed if early static LSG does not depict any hotspots [8]. More recently, the European Association of Nuclear Medicine (EANM) revised their guidelines by advising that early dynamic LSG should encompass the first 10-15 minutes post-injection, instead of 30 minutes as performed in our institution [9].

In an attempt to streamline the current SLN imaging protocol, this study evaluated the clinical relevance of several routinely performed SLN imaging components, as performed in our institution. Furthermore, this study compares the accuracy for SLN identification using a streamlined SLN imaging protocol with the conventional SLN imaging protocol, in early-stage OSCC patients.

# Materials and methods

## Ethical considerations

This study abided the Declaration of Helsinki and was approved by the Ethics Committee (no. 19-397). Requirement for informed consent was waived by the Internal Review Board. Pathological, imaging and clinical data were dealt with in accordance to General Data Protection Regulation.

## Patients

Patients with early-stage OSCC (cT1-3N0), who underwent SLN biopsy in our institution between December 2017 and March 2020, were included in this study (AJCC UICC TNM-staging 8<sup>th</sup> Edition) [13, 14]. Patients with a primary tumor staged cT3 were only included when tumor dimensions  $\leq 4$  cm [13]. Clinical nodal staging was confirmed by at least ultrasound; ultrasound-guided fine needle aspiration cytology was performed in case of suspected lymph nodes.

Patients were excluded if the administered dosage in megabecquerel (MBq) was not in line with the most recent guidelines of the EANM [9].

## Sentinel lymph node imaging procedure

All patients underwent planar static and dynamic LSG and SPECT/CT imaging the day prior surgery (two-day protocol) or the day of surgery (single-day protocol) on a Siemens Symbia T16 SPECT/CT scanner, using “low- and medium energy” (LME) collimators. A total of 2-4 peritumoral injections were administered with a <sup>99m</sup>Tc-labeled radiotracer (i.e., nanocolloid, tilmanocept). For the two-day protocol  $\sim 120$  MBq (3.24 mCi) [<sup>99m</sup>Tc]Tc-nanocolloid or  $\sim 74$  MBq (2.0 mCi) [<sup>99m</sup>Tc]Tc-tilmanocept was administered, whereas for the single-day protocol  $\sim 50$  MBq (1.35 mCi) [<sup>99m</sup>Tc]Tc-nanocolloid was administered. Directly post-injection planar dynamic LSG was acquired in anterior view (128  $\times$  128 matrix; 60 frames of 30 seconds). Then, early planar static LSG was acquired in anterior view (256  $\times$  256 matrix; 240 seconds) and anterior-oblique view from both sides (256  $\times$  256 matrix; 480 seconds), with additional Co-57 flood source images (3  $\times$  30 seconds) for contour detection. 3D SPECT/CT was acquired at 90-120 minutes post-injection, for a total duration of 35 minutes, on a 128  $\times$  128 matrix (pixel spacing, 3.9  $\times$  3.9 mm), with 128 angles, 20 s per projection, over a non-circular 360° orbit (CT:110 kV, 40 mAs eff., 16  $\times$  1.2 mm). SPECT images were reconstructed using clinical reconstruction software (Siemens Flash3D), with attenuation and scatter correction (6 iterations, 8 subsets, 5 mm Gaussian filter). SPECT/CT imaging was immediately followed by late planar static LSG with flood field images (256  $\times$  256 matrix; 3  $\times$  240 s, 3  $\times$  30 s) [15]. Identified SLN(s) were marked on the corresponding overlying skin with a Co-57 pen point marker.

## Surgery, histopathological assessment and follow-up

Intraoperatively, the marked SLN(s) were localized under at least handheld gamma-probe guidance, accompanied by surgical extirpation. Extirpated SLN(s) were subjected to histopathological assessment according to SLN biopsy protocol (i.e., step-serial-sectioning, hematoxylin-eosin staining and immunohistochemistry) [8, 16]. For those in whom SLN(s) were negative for metastasis, a wait-and-scan policy was adopted. SLN biopsy-positive patients, however, underwent complementary treatment of the neck (i.e., neck dissection and/or (chemo)radiotherapy). Complementary neck dissection specimens were routinely assessed for additional lymph node metastases by histopathological examination. Follow-up visits were scheduled according to standard oncological care.

## Streamlined imaging protocol

For the streamlined protocol, selected conventional imaging components were omitted or its acquisition time was reduced (Table 1; Figure 1). Planar dynamic LSG was reduced to 10 minutes. Then, SPECT/CT images, acquired ~2 hours post-injection, were analyzed. Both early and late planar static LSG were omitted for the streamlined protocol.

**Table 1.** Components and duration of the conventional and streamlined SLN imaging protocol

	Conventional protocol	Streamlined protocol
<b>Early planar dynamic LSG (minutes)</b>	30:00	10:00
<b>Early planar static LSG (minutes)</b>		
Anterior view	4:30	Omitted
Anterior-oblique view L+R	9:00	Omitted
<b>SPECT/CT (minutes)</b>	35:00	35:00
<b>Late planar static LSG (minutes)</b>		
Anterior view	4:30	Omitted
Anterior-oblique view L+R	9:00	Omitted
<b>Total (minutes)</b>	92:00	45:00

SLN: *sentinel lymph node*; LSG: *lymphoscintigraphy*; L: *left*; R: *right*

## Evaluation

Both imaging protocols were evaluated retrospectively by 3 observers with considerable experience in analyzing LSG and SPECT/CT images for SLN mapping in early-stage OSCC (Figure 1). In case of discrepancies between observers as a joint team deciding unanimously, consensus was obtained through discussion.

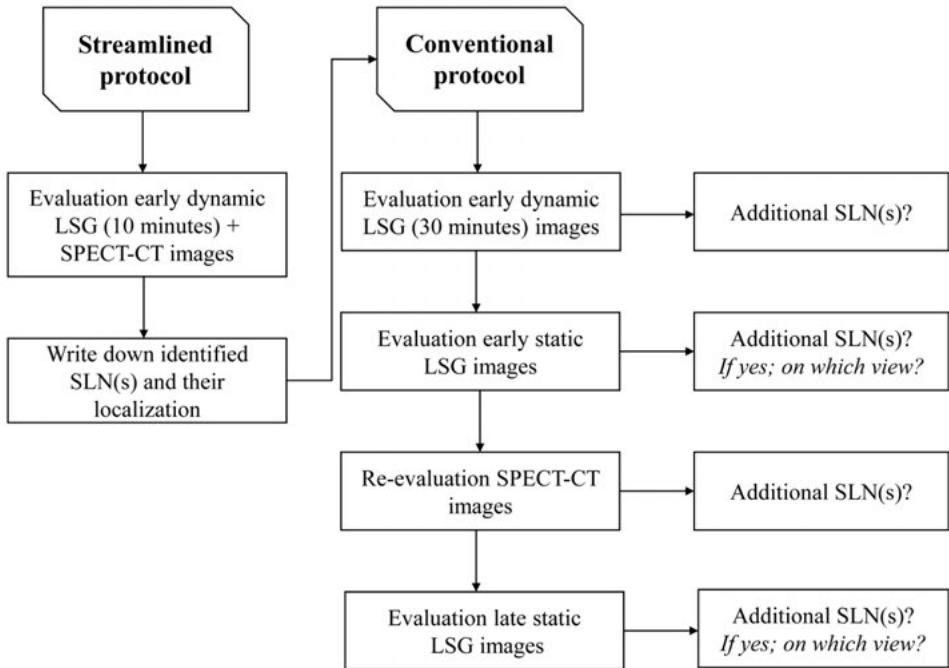


**Figure 1.** LSG: *lymphoscintigraphic*, SLN: *sentinel lymph node*

First, the observers were asked to classify visualized lymph nodes as “yes”, “no” or “potential” as to being SLNs based on the streamlined protocol. Subsequently, all lymph nodes classified as “potential” had to be labeled “yes” or “no”, indicating the advice on its surgical extirpation.

Secondly, the individual components of the conventional imaging protocol were evaluated in consecutive order. The observers were asked to identify whether additional SLNs were identified for each component. If any additional SLNs were identified, the observers were asked on which view (e.g., anterior-posterior, anterior-oblique) the additional SLNs were first identified.

To identify false-negative outcomes of the streamlined imaging protocol, identified SLN(s) using either imaging protocol were related to histopathological status of harvested SLNs. Furthermore, in case of additional lymph node metastases in complementary neck dissection specimens, their corresponding location was correlated to images from either imaging protocol. Finally, for those who developed regional nodal recurrence during follow-up, the corresponding location of the regional nodal recurrence was correlated to images from either imaging protocol as well. Regional nodal recurrences in presence of local tumor recurrence or second primary tumors were not considered suitable for such correlation, since differentiation

between missed occult nodal metastasis by SLN biopsy and metastasis developed from reseeding tumors is unfeasible. Regional nodal recurrences that occurred in a side of the neck which was initially staged positive for nodal metastasis by SLN biopsy, were not considered false-negative outcomes, as such a regional recurrence is considered to be a consequence of insufficient complementary treatment rather than inadequate SLN biopsy.

### **Statistical analyses**

All data were analyzed with IBM SPSS Statistics Version 26.0. For categorical variables the number of cases and its percentage were calculated. Continuous parametric variables are presented as mean ( $\pm$ SD), whereas non-parametric variables are presented as median with interquartile range (IQR).

To assess whether not identifying all SLNs with the streamlined protocol was associated with patient-, tumor- or imaging characteristics, univariate analyses were applied. Independent Samples T-test was applied for parametric continuous variables (i.e., tumor size) and Mann-Whitney U test for non-parametric continuous variables (i.e., DOI and administered radioactive dosage). For categorical variables (i.e., tumor localization, clinical T-stage and used radiotracer) Chi-square Tests were applied; in case of variables with small samples ( $n \leq 5$ ) Fisher's Exact Test was used (i.e., midline involvement and one-/two-day imaging protocol). In case of significant association for categorical variables with  $\geq 3$  groups, subsequent post-hoc analyses were conducted.

Finally, Spearman's rank-order correlation was used to assess the association between both amount as well as location of identified SLNs per patient with both SLN imaging protocols.

A p-value  $\leq 0.05$  was considered to be statistically significant.

## Results

Out of a total of 92 patients, 77 patients were included in this study. In those excluded ( $n = 15$ ), the administered dosage in megabecquerel (MBq) was not in line with the most recent guidelines of the EANM [9].

Of those included in this study, 9 (11.7%) had undergone previous neck treatment for head and neck malignancies (Table 2). Of all primary tumors, the majority was located in the tongue (59.7%). Most patients presented with tumors clinically staged T1- or T2 (92.2%). SLN biopsy showed cervical lymph node metastases in 19 (24.7%) patients. Mean follow-up time after surgery was 14.9 ( $\pm 7.2$ ) months.

A total of 200 SLNs were identified using the streamlined imaging protocol; 12 additional SLNs (thus in total 212) were identified with the conventional imaging protocol in 10 patients (Table 3). Figure 2 illustrates how an additional SLN was identified based on early static LSG (anterior-oblique view).

**Table 2.** Patient- and tumor characteristics

Characteristics	<i>n = 77</i>
<b>Gender</b>	
Male (%)	45 (58.4%)
Female (%)	32 (41.6%)
<b>Age at scan; mean (<math>\pm</math>SD) in years</b>	62.5 ( $\pm$ 13.0)
<b>Previous neck treatment</b>	
None (%)	68 (88.3%)
Neck dissection (%)	4 (5.2%)
Radiotherapy (%)	3 (3.9%)
Neck dissection & chemoradiation (%)	2 (2.6%)
<b>Anatomical localization primary tumor</b>	
Tongue (%)	46 (59.7%)
Floor-of-mouth (%)	14 (18.2%)
Buccal mucosa (%)	8 (10.4%)
Retromolar area (%)	5 (6.5%)
Inferior alveolar process (%)	4 (5.2%)
<b>Clinical T-stage primary tumor</b>	
cT1 (%)	31 (40.3%)
cT2 (%)	40 (51.9%)
cT3 (%)	6 (7.8%)

**Table 2.** Continued.

Characteristics	n = 77
<b>Pathological N-stage</b>	
N0 (%)	58 (75.3%)
N1 (%)	8 (10.4%)
N2a (%)	1 (1.3%)
N2b (%)	5 (6.5%)
N2c (%)	3 (3.9%)
N3b (%)	2 (2.6%)
<b>Follow-up time; mean (±SD) in months</b>	<b>14.9 (±7.2)</b>

SD: standard deviation. TNM-staging according to AJCC UICC 8<sup>th</sup> Edition [12, 13].

**Table 3.** Patients with additionally detected SLNs based on conventional imaging components

Nº	Primary tumor	SLNs on streamlined protocol	PA	PA	Additionally identified SLNs	Based on which image	PA extra SLN	Follow-up time (months)	Follow-up status	
1	Tongue (right)	IIa	Right	-	IIB	Right	Early static oblique	-	22	NED
		III	Right	-	IIB	Right	Early static oblique	-		
		III	Left	n.s.r.						
		IV	Right	n.s.r.						
2	Buccal mucosa (left)	III	Right	-	Va	Left	Early static AP	n.s.r.	21	NED
3	Inferior alveolar process (left)	Ib	Left	n.s.r.	IIa	Left	Early static oblique	-	11	Local recurrence
		IIa	Left	+						
4	Inferior alveolar process (right)	None		N.A.	IIa	Right	Early static oblique	-	21	NED
					Ib	Right	Late static oblique	-		
5	Buccal mucosa (left)	Ib	Left	+	IIa	Left	Early static oblique	n.s.r.	19	NED
6	Tongue (right)	IIa	Right	-	Ib	Right	Early static oblique	n.s.r.	16	NED
		III	Right	-						
7	Tongue (left)	IIa	Left	-	Ib	Left	Early static oblique	-	15	NED
8	Retromolar area (right)	IIa	Right	-	IIa	Right	Late static oblique	-	11	NED
9	Floor-of-the-mouth (right)	III	Right	-	IIa	Right	Early static oblique	-	11	NED
		III	Left	-						

**Table 3.** Continued.

Nº	Primary tumor	SLNs on streamlined protocol		PA	Additionally identified SLNs		Based on which image	PA extra SLN	Follow-up time (months)	Follow-up status
10	Inferior alveolar process (left)	Ia	Left	-	III	Left	Late static oblique	n.s.r.	5	NED
		III	Left	-						

SLN: *sentinel lymph node*; PA: *histopathological assessment*; n.s.r.: *not surgically removed*; +: *histopathologically positive*; -: *histopathologically negative*; NED: *no evidence of disease*; N.A.: *not applicable*.

Of the 12 additionally identified SLNs, 9 (75%) were identified on early static LSG and 3 (25%) on late static LSG. All hotspots visualized during early static LSG remained visible on late static LSG. In the 3 patients in whom additional SLNs were identified on late static LSG only, 2 primary tumors were located in the inferior alveolar process and 1 in the retromolar area. The added 20 minutes early dynamic LSG of the conventional protocol did not allow identification of additional SLNs.

None of the additionally identified SLNs were histopathologically positive. In addition, none of the patients in whom additional SLNs were identified by the conventional SLN imaging protocol developed regional nodal recurrence after a mean follow-up of 15.2 ( $\pm 5.6$ ) months. Univariate analyses showed that only the primary tumor site was associated with not identifying all SLNs using the streamlined protocol ( $p = 0.002$ ). Post-hoc analyses showed that only inferior alveolar process carcinoma was associated with not identifying all SLNs using the streamlined protocol ( $p = 0.006$ ). In 3 out of 4 (75%) patients with inferior alveolar process carcinoma, the streamlined SLN imaging protocol did not allow identification of all SLNs. In those 3 patients, 4 additional SLNs were identified. In one of those patients no drainage was observed with the streamlined SLN protocol, however, the conventional SLN imaging protocol allowed identification of 2 SLNs with marginal activity. In the remaining patient with inferior alveolar process carcinoma (25%), no drainage at all was observed on dynamic and static LSG and SPECT/CT images.

Out of those who underwent previous oncological treatment of the neck (i.e., neck dissection and/or (chemo)radiation), additional SLNs were identified by early static LSG in one patient (*patient 2*, selective neck dissection left) and on late static LSG in two patients (*patient 8*, bilateral neck irradiation; *patient 10*, selective neck dissection right).

Finally, Spearman's showed a statistically significant correlation between identified SLNs and their corresponding location using both SLN imaging protocols for each patient ( $r_s = 0.898$ ;  $p < 0.001$ ).

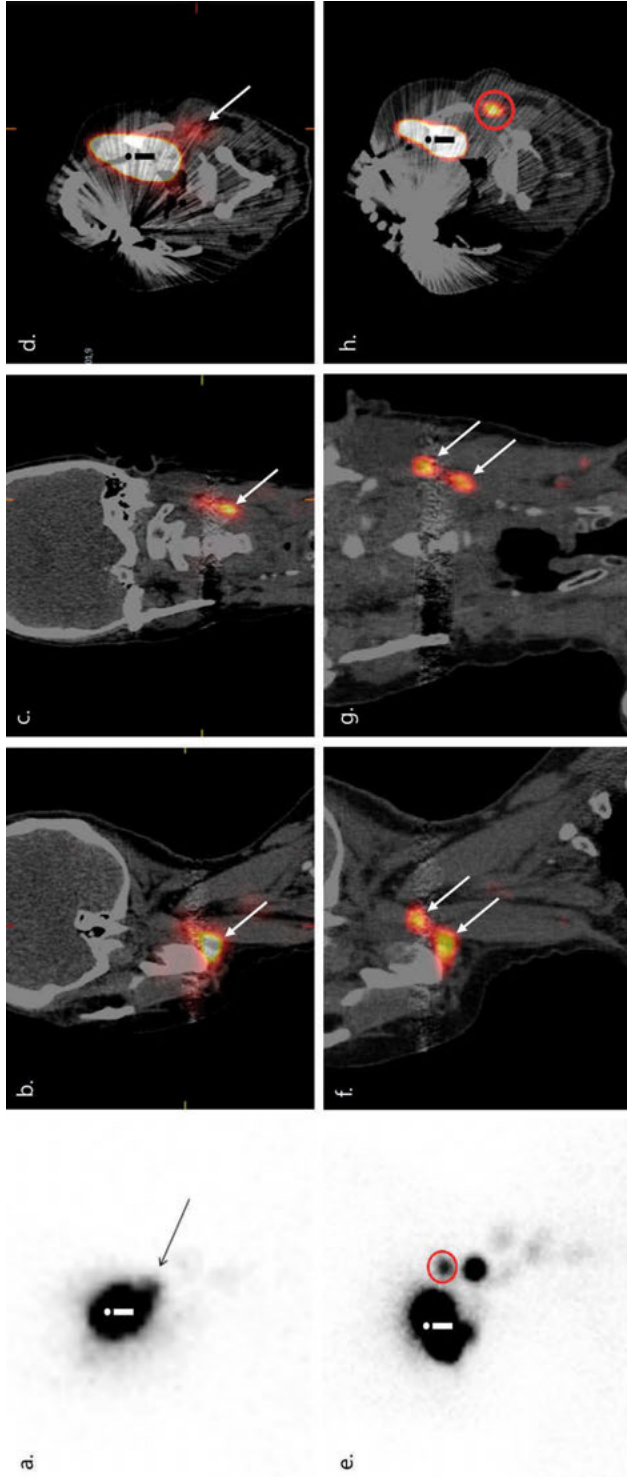


**Figure 2.** A 77-year-old patient (patient 3) with a cT2N0 primary tumor in the inferior alveolar process, located on the left side. Using the streamlined protocol, two SLNs were identified (level Ib left; level IIa left). Written informed consent for publishing these images was obtained from this patient. (a) Planar early dynamic LSG 10 minutes anterior view; one hotspot level Ib left (arrow). (b) SPECT/CT sagittal plane; one large hotspot level IIa (arrow). (c) SPECT/CT coronal plane; one large hotspot level IIa left (arrow). (d) SPECT/CT axial plane; injection site (i) and one large hotspot level IIa left (arrow). (e) Planar early static LSG anterior-oblique view; one additionally identified hotspot level IIa left (red circle). (f) Post-evaluation SPECT/CT reconstruction\* sagittal plane; discrimination between two hotspots level IIa (arrows). (g) Post-evaluation SPECT/CT reconstruction\* coronal plane; discrimination between two hotspots level IIa left (arrows). (h) Post-evaluation SPECT/CT reconstruction\* axial plane; more cranially localized one additionally identified hotspot (red circle). \*SPECT/CT reconstructions were made with ITK-SNAP ([www.itksnap.org](http://www.itksnap.org)) [17]. LSG: lymphoscintigraphy.

## Discussion

The aim of this study was to evaluate the clinical relevance of several components of the conventional SLN imaging protocol and to assess the reliability of a streamlined SLN imaging protocol in early-stage OSCC. Using the streamlined SLN imaging protocol 200 SLNs were identified, whereas the conventional SLN imaging protocol allowed identification of 12 additional SLNs. None of the additionally identified SLNs contained metastases; none of the patients in whom they were identified developed regional nodal recurrence. Early dynamic LSG with a duration of 30 minutes showed no additional diagnostic value over a duration of 10 minutes; no additional SLNs were identified based on evaluation of 20 supplementary minutes of dynamic LSG. This finding is in accordance with the revised guidelines of the EANM, stating that early dynamic LSG should encompass the first 10-15 minutes post-injection [9]. In early-stage breast cancer dynamic LSG was completely omitted from the SLN imaging protocol, without interfering with its diagnostic accuracy, as immediate dynamic LSG had no additional value in identifying SLNs [18-21]. In early-stage OSCC, however, dynamic LSG immediately post-injection is deemed essential, as it allows visualization of lymphatic vessels draining the injection site; assisting the discrimination between SLNs and higher echelon nodes (HEN) in the complex anatomy of the neck with its abundant lymph nodes [8]. Erroneously considering HENs as SLNs induces unnecessary exploration of the neck, with its accompanying morbidity and risk of complications, that may hamper a complementary neck dissection in case of metastatic involvement of SLNs [12]. Therefore, a complete omission of early dynamic LSG is not recommended for the SLN imaging protocol in early-stage OSCC.

Early static LSG allowed for identification of additional SLNs in 8 of 77 (10.4%) patients. Early static LSG was contributory in nearly all OSCC subsites, as for those in whom additional SLNs were identified by early static LSG, the primary tumors were located in the tongue ( $n = 3$ ), buccal mucosa ( $n = 2$ ), inferior alveolar process ( $n = 2$ ) and floor-of-mouth ( $n = 1$ ). Even though none of these additionally identified SLNs were histopathologically positive, nor did any of these patients develop regional nodal recurrence, the omission of early static LSG may lead to a substantial rise in false-negative SLN biopsy outcomes. Moreover, differentiating between either relevant SLN or irrelevant HEN can be facilitated by comparing early static LSG images to SPECT/CT images acquired at ~2 hours post-injection. Accordingly, it is our considered opinion that one should not refrain from early static LSG acquisition for all OSCC subsites.

Late static LSG contributed for 3 of 12 of the additionally identified SLNs (25%) in 3 of 77 patients (3.9%). Thus, out of a total of 212 SLNs, only 3 of 212 SLNs (1.4%)

were identified on late static LSG. Heuveling et al. already underlined the limited value of late static LSG and recommended its acquisition only in patients with tumors featuring slow or limited lymphatic drainage (i.e., buccal mucosa, inferior alveolar process and soft-palate) [12]. This recommendation is mainly in concordance with our results, since in 2 of 4 patients with inferior alveolar process carcinoma (50%) and in 1 of 5 patients with tumors of the retromolar area (20%), additional SLNs were identified on late static LSG. Furthermore, for most prevalent anatomical localizations of OSCC – tongue, floor-of-mouth and buccal mucosa – late static LSG was not contributory in our population. Of those in whom additional SLNs were identified by late static LSG ( $n = 3$ ), two patients had a history of neck dissection or neck irradiation. Still, in one patient (*patient 10*) the additionally identified SLN was detected in the non-dissected neck. Nevertheless, previous treatment of the neck has been known to alter lymphatic drainage patterns and may even decelerate and impede lymphatic drainage [22]. Therefore, late static LSG could also be valuable in those who underwent previous treatment of the neck. In the study of Heuveling et al., late static LSG showed additional SLNs in half of patients with paramedian and midline tumors exhibiting bilateral drainage [12]. Nevertheless, SPECT/CT was not yet available during their evaluation. As in our population no additional SLNs were identified by late static LSG in those with paramedian or midline tumors, late static LSG does not appear to be of additional value in these patients if SPECT/CT imaging is acquired at ~2 hours post-injection.

Although the value of SPECT/CT imaging was not evaluated in this study, SPECT/CT imaging is deemed indispensable for SLN mapping, since it contributes significantly to SLN identification and provides enhanced anatomical orientation [23]. Previously, den Toom et al. demonstrated that the addition of SPECT/CT to planar static LSG resulted in more precise SLN detection and suggested that its beneficial properties in regard of topographical orientation lead to a safer surgical procedure for patients [23].

The major limitation of this study remains its retrospective design, making it irrevocably susceptible to bias. As included patients underwent their oncological treatment relatively recent at our institution, while observers were not blinded during evaluation, the observers might have been prone to recall bias during the evaluation. Moreover, the evaluation was not done independently by the 3 observers, but as a joint team deciding unanimously.

Furthermore, the mean follow-up duration of this population was on average 14.9 months. Although the majority (80%) of (loco)regional recurrences in patients with OSCC occur within 12 months, it is advocated to conduct a follow-up period of at least

24 months to assure that all missed occult nodal metastases have become clinically manifest [24, 25]. A blinded prospective within-patient study with longer follow-up duration, would ascertain more strength of research results.

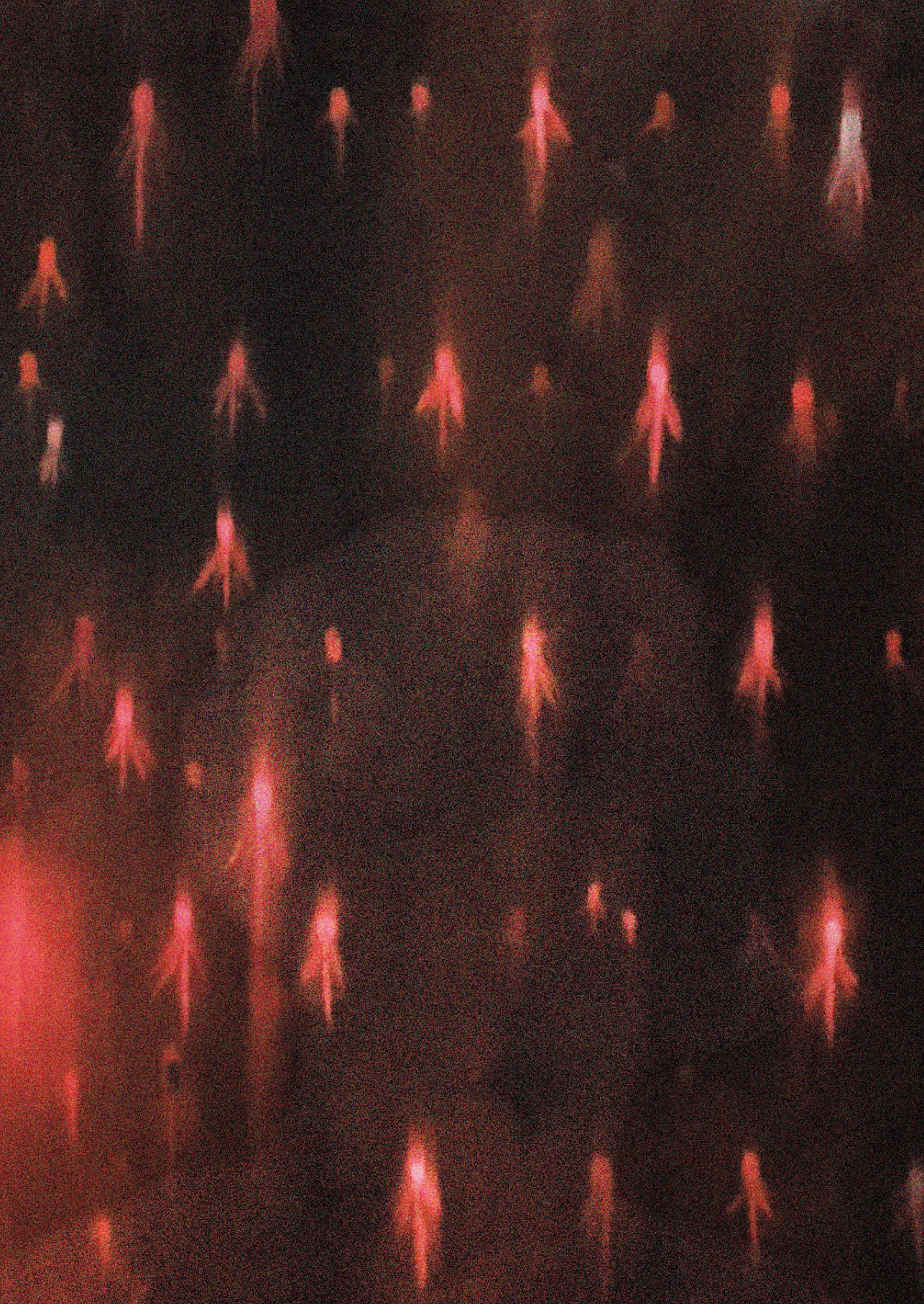
## Conclusion

The results of this study indicate that the conventional SLN imaging protocol, as employed by our institution for early-stage OSCC, can be streamlined without interfering with its diagnostic accuracy. As early static LSG appeared to be valuable in most OSCC subsites, the recommended streamlined protocol would consist of early dynamic LSG for 10 minutes, early static LSG and SPECT/CT imaging at ~2 hours post-injection. In those with OSCC featuring slow or marginal lymphatic drainage (i.e., tumors involving the inferior alveolar process or retromolar area) as well as in those who underwent previous oncological treatment of the neck, late static LSG should be acquired nonetheless. Accordingly, the acquisition time for SLN mapping may be reduced from 92 to 58.5 minutes in the vast majority of early-stage OSCC patients. Consequently, a streamlined SLN imaging protocol may reduce the costs of SLN biopsy altogether and decrease patient discomfort, while facilitating the availability of nuclear imaging devices on a day-to-day basis. Nevertheless, on account of the retrospective nature of this study and its relatively short follow-up duration, a blinded prospective within-patient study, with longer follow-up and histological assessment as reference standard, is required before any definite conclusions can be drawn.

## References

1. Loree JT, Popat SR, Burke MS, Frustino J, Grewal JS, Loree TR. Sentinel lymph node biopsy for management of the N0 neck in oral cavity squamous cell carcinoma. *J Surg Oncol*. 2019;120(2):101-108. doi:10.1002/jso.25494
2. Boeve K, Schepman KJ, Schuurung E, et al. High sensitivity and negative predictive value of sentinel lymph node biopsy in a retrospective early stage oral cavity cancer cohort in the Northern Netherlands. *Clin Otolaryngol*. 2018;43(4):1080-1087. doi:10.1111/coa.13107
3. Den Toom IJ, Heuveling DA, Flach GB, et al. Sentinel node biopsy for early-stage oral cavity cancer: the VU University Medical Center experience. *Head Neck*. 2015;37(4):573-578. doi:10.1002/hed.23632
4. Schilling C, Stoeckli SJ, Haerle SK, et al. Sentinel European Node Trial (SENT): 3-year results of sentinel node biopsy in oral cancer. *Eur J Cancer*. 2015;51(18):2777-2784. doi:10.1016/j.ejca.2015.08.023
5. Liu M, Wang SJ, Yang X, Peng H. Diagnostic efficacy of sentinel lymph node biopsy in early oral squamous cell carcinoma: a meta-analysis of 66 studies. *PLoS One*. 2017;12(1):e0170322. doi:10.1371/journal.pone.0170322
6. den Toom IJ, Boeve K, Lobeek D, et al. Elective neck dissection or sentinel lymph node biopsy in early stage oral cavity cancer patients: the Dutch experience. *Cancers (Basel)*. 2020;12(7):1783. doi:10.3390/cancers12071783
7. Schilling C, Stoeckli SJ, Vigili MG, et al. Surgical consensus guidelines on sentinel node biopsy (SNB) in patients with oral cancer. *Head Neck*. 2019;41(8):2655-2664. doi:10.1002/hed.25739
8. Alkureishi LW, Burak Z, Alvarez JA, et al. Joint practice guidelines for radionuclide lymphoscintigraphy for sentinel node localization in oral/oropharyngeal squamous cell carcinoma. *Ann Surg Oncol*. 2009;16(11):3190-3210. doi:10.1245/s10434-009-0726-8
9. Giammarile F, Schilling C, Gnanasegaran G, et al. The EANM practical guidelines for sentinel lymph node localisation in oral cavity squamous cell carcinoma. *Eur J Nucl Med Mol Imaging*. 2019;46(3):623-637. doi:10.1007/s00259-018-4235-5
10. Flach GB, van Schie A, Witte BI, et al. Practice variation in defining sentinel lymph nodes on lymphoscintigrams in oral cancer patients. *Eur J Nucl Med Mol Imaging*. 2014;41(12):2249-2256. doi:10.1007/s00259-014-2843-2
11. Govers TM, Takes RP, Baris Karakullukcu M, et al. Management of the N0 neck in early stage oral squamous cell cancer: a modeling study of the cost-effectiveness. *Oral Oncol*. 2013;49(8):771-777. doi:10.1016/j.oraloncology.2013.05.001
12. Heuveling DA, Flach GB, van Schie A, et al. Visualization of the sentinel node in early-stage oral cancer: limited value of late static lymphoscintigraphy. *Nucl Med Commun*. 2012;33(10):1065-1069. doi:10.1097/MNM.0b013e3283571089
13. International Consortium for Outcome Research (ICOR) in Head and Neck Cancer, Ebrahimi A, Gil Z, et al. Primary tumor staging for oral cancer and a proposed modification incorporating depth of invasion: an international multicenter retrospective study. *JAMA Otolaryngol Head Neck Surg*. 2014;140(12):1138-1148. doi:10.1001/jamaoto.2014.1548
14. Lydiatt WM, Patel SG, O'Sullivan B, et al. Head and Neck cancers-major changes in the American Joint Committee on cancer eighth edition cancer staging manual. *CA Cancer J Clin*. 2017;67(2):122-137. doi:10.3322/caac.21389
15. den Toom IJ, Mahieu R, van Rooij R, et al. Sentinel lymph node detection in oral cancer: a within-patient comparison between [<sup>99m</sup>Tc]Tc-tilmanocept and [<sup>99m</sup>Tc]Tc-nanocolloid. *Eur J Nucl Med Mol Imaging*. 2021;48(3):851-858. doi:10.1007/s00259-020-04984-8
16. Dhawan I, Sandhu SV, Bhandari R, Sood N, Bhullar RK, Sethi N. Detection of cervical lymph node micrometastasis and isolated tumor cells in oral squamous cell carcinoma using immunohistochemistry and serial sectioning. *J Oral Maxillofac Pathol*. 2016;20(3):436-444. doi:10.4103/0973-029X.190946
17. Yushkevich PA, Piven J, Hazlett HC, et al. User-guided 3D active contour segmentation of anatomical structures: significantly improved efficiency and reliability. *Neuroimage*. 2006;31(3):1116-1128. doi:10.1016/j.neuroimage.2006.01.015
18. Doting MH, Stiekema HM, de Vries J, et al. Immediate dynamic lymphoscintigraphy delivers no additional value to lymphoscintigraphy 3 hr after tracer injection in sentinel lymph node biopsy in breast cancer patients. *J Surg Oncol*. 2007;95(6):469-475. doi:10.1002/jso.20721

19. Keshtgar MR, Ell PJ. Clinical role of sentinel-lymph-node biopsy in breast cancer. *Lancet Oncol.* 2002;3(2):105-110. doi:10.1016/s1470-2045(02)00652-6
20. Lee AC, Keshtgar MR, Waddington WA, Ell PJ. The role of dynamic imaging in sentinel lymph node biopsy in breast cancer. *Eur J Cancer.* 2002;38(6):784-787. doi:10.1016/s0959-8049(01)00471-3
21. Giammarile F, Alazraki N, Aarsvold JN, et al. The EANM and SNMMI practice guideline for lymphoscintigraphy and sentinel node localization in breast cancer. *Eur J Nucl Med Mol Imaging.* 2013;40(12):1932-1947. doi:10.1007/s00259-013-2544-2
22. den Toom IJ, Boeve K, van Weert S, et al. High rate of unexpected lymphatic drainage patterns and a high accuracy of the sentinel lymph node biopsy in oral cancer after previous neck treatment. *Oral Oncol.* 2019;94:68-72. doi:10.1016/j.oraloncology.2019.05.007
23. den Toom IJ, van Schie A, van Weert S, et al. The added value of SPECT-CT for the identification of sentinel lymph nodes in early stage oral cancer. *Eur J Nucl Med Mol Imaging.* 2017;44(6):998-1004. doi:10.1007/s00259-017-3613-8
24. Brands MT, Smeekens EAJ, Takes RP, et al. Time patterns of recurrence and second primary tumors in a large cohort of patients treated for oral cavity cancer. *Cancer Med.* 2019;8(12):5810-5819. doi:10.1002/cam4.2124
25. Garrel R, Poissonnet G, Moyà Plana A, et al. Equivalence randomized trial to compare treatment on the basis of sentinel node biopsy versus neck node dissection in operable T1-T2N0 oral and oropharyngeal cancer. *J Clin Oncol.* 2020;38(34):4010-4018. doi:10.1200/JCO.20.01661



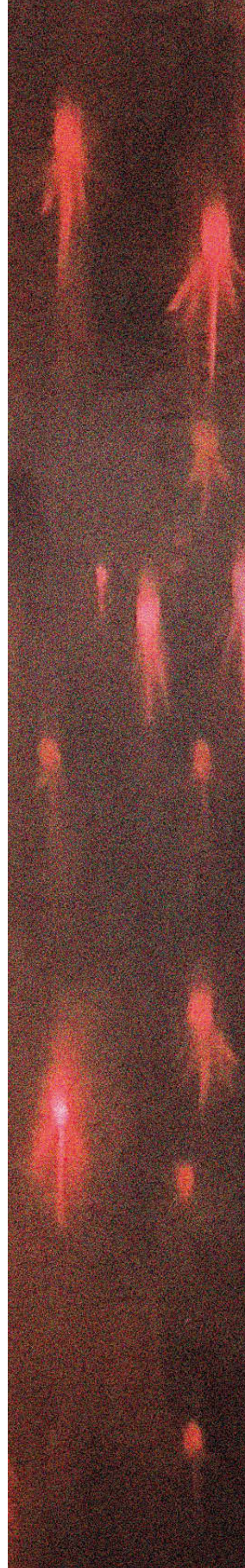
# 4

## The potential of the Crystal Cam handheld gamma-camera for preoperative and intraoperative sentinel lymph node localization in early-stage oral cancer

---

Rutger Mahieu, Bernard M. Tijink, Robert J. J. van Es,  
Bastiaan J. van Nierop, Casper Beijst, Bart de Keizer,  
Remco de Bree.

*Eur Arch Otorhinolaryngol. 2023 Dec;280(12):5519-5529*



# Abstract

## Purpose

Evaluating the Crystal Cam handheld gamma-camera for preoperative and intraoperative sentinel lymph node (SLN) localization in early-stage oral cancer.

## Methods

The handheld gamma-camera was used complementary to conventional gamma-probe guidance for intraoperative SLN localization in 53 early-stage oral cancer patients undergoing SLN biopsy. In 36 of these patients, a blinded comparison was made between preoperative handheld gamma-camera and lymphoscintigraphy outcomes. Of those, the reliability for marking the SLN's location using both handheld gamma-camera and a <sup>57</sup>Co-penpoint marker was evaluated in 15 patients.

## Results

In the entire cohort, the handheld gamma-camera preoperatively detected 116 of 122 (95%) of SLNs identified by lymphoscintigraphy. In those patients where the observer was blinded for lymphoscintigraphy ( $n = 36$ ), 71 of 77 (92%) of SLNs were correctly identified by handheld gamma-camera. Overlooked SLNs by handheld gamma-camera were mainly located near the injection site. The SLN's marked location by handheld gamma-camera and <sup>57</sup>Co-penpoint marker was considered accurate in 42 of 43 (98%) of SLNs. The intraoperative use of the handheld gamma-camera led to the extirpation of 16 additional "hot" lymph nodes in 14 patients, 4 of which harbored metastases, and prevented 2 patients (4%) from being erroneously staged negative for nodal metastasis. In those with follow-up  $\geq 24$  months or false-negative outcomes  $< 24$  months following SLNB, a sensitivity of 82% and negative predictive value of 93% was obtained.

## Conclusion

The Crystal Cam handheld gamma-camera offers reliable preoperative and intraoperative SLN localization and might reduce the risk of missing a malignant SLN during surgery. Detecting SLNs near the injection site by handheld gamma-camera remains challenging.

## Introduction

Over the last decade, sentinel lymph node biopsy (SLNB) is being increasingly advocated for staging the clinically negative neck (cN0) in early-stage oral squamous cell carcinoma (OSCC) [1, 2].

Recent trials have confirmed the less-invasive character of SLNB in OSCC, with lower functional morbidity and similar oncological outcomes when compared to elective neck dissection (END) [3-5].

However, as the rate of false-negative SLNB still varies between 5 and 15%, with its accompanying oncological implications (i.e., comprehensive surgery, adjuvant radiotherapy and reduced disease-specific survival), efforts are made to further improve the accuracy of SLNB, especially in floor-of-mouth cancers [5-10].

Several novel lymphographic techniques have been proposed to improve preoperative identification of sentinel lymph nodes (SLN) [9]. However, tracking the preoperatively identified SLNs during surgery can remain a challenge.

Conventionally, SLNs identified by lymphoscintigraphy (including SPECT/CT) are localized intraoperatively through gamma-tracing using a handheld gamma-probe [11]. Handheld gamma-probes have some limitations as their performance is operator-dependent, lack the ability for visual feedback and provide inadequate contrast for differentiating between neighboring radioactive signals [11, 12]. Especially in cases where SLNs are identified close to the injection site, distinction between SLN and injection site by gamma-probe can be complicated [10-13].

Optical tracers have been suggested, such as various blue dyes and indocyanine green (ICG), but these pose several limitations as well. Since unbound optical tracers appear to flow quickly to SLNs, yet are not retained in lymph nodes, they may washout or migrate to higher-echelon-nodes (HEN) by the time of SLN retrieval [10]. The adjunction of fluorescent dyes to well-known radiotracers (e.g., ICG- $^{99m}\text{Tc}$ -nanocolloid), on the other hand, has shown promising results for intraoperative SLN localization [14-16]. Nevertheless, radioguidance remains the cornerstone of SLN localization, owing to the limited tissue penetration of the fluorescent signal (0.5 – 1 cm), hampering the use of fluorescent dyes for surgical planning or for tracking SLNs from larger distances [10, 15].

Various portable gamma-detecting imaging devices have been developed for visualization of radiotracers (e.g., freehand SPECT, portable gamma-cameras),

allowing for real-time image-guided SLN localization while being less affected by tissue attenuation compared to fluorescence guidance. The complementary use of real-time radioguided imaging to standard handheld gamma-probe guidance has shown to facilitate more accurate and efficient localization of SLNs during surgery [12, 13, 17-21].

However, most portable gamma-cameras and freehand SPECT devices are large in size, costly and occasionally require an additional operator to establish optimal settings. The handheld gamma-camera used in this study (Crystal Cam, Crystal Photonics GmbH, Berlin, Germany) is relatively inexpensive and highly portable, owing to its small size and low weight (see “*Specifications Crystal Cam*”), which can be fully managed by the surgeon in a sterile setting. Previously, the feasibility and utility of this handheld gamma-camera for SLN localization has been described in melanoma and breast cancer patients [22-25].

In this prospective study, the utilization of this handheld gamma-camera is evaluated for preoperative and intraoperative SLN localization in early-stage OSCC patients undergoing SLNB.

# Materials and methods

## Patients

This study was performed in line with the principles of the Declaration of Helsinki and was approved by the University Medical Center Utrecht's Ethics Committee (no. 17/835); informed consent for participation was obtained from all patients.

Between January 2018 and October 2020, a total of 53 patients with clinically T1-T3N0 OSCC scheduled for SLNB were prospectively included (Table 1; TNM Staging AJCC UICC 8<sup>th</sup> Edition [26, 27]). Patients with a tumor clinically staged as T3 were only included when staging was based on depth-of-invasion of > 10 mm and tumor dimensions of > 2 cm and ≤ 4 cm [28]. In all patients, cN0 status was determined by ultrasound of the neck. In those with suspect lymph nodes, ultrasound-guided fine-needle aspiration cytology was performed. The majority of patients (72%) also underwent magnetic resonance imaging of the head and neck as part of their clinical staging.

## Study design

This study was performed in several phases. Figure 1 provides an overview of the study procedures and included patients for each phase of the study.

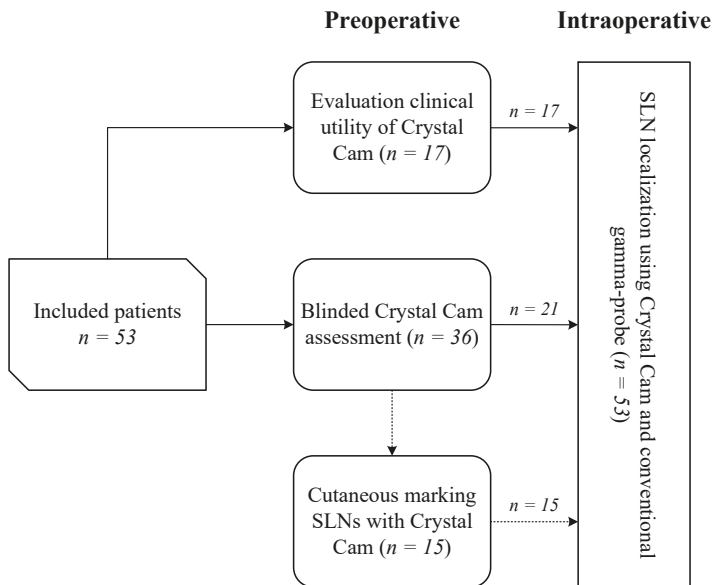


**Figure 1.** Flowchart of study procedures. Dotted arrow represents patients ( $n = 15$ ) who underwent both blinded assessment as well as cutaneous marking of the SLNs' location by handheld gamma-camera and a  $^{57}\text{Co}$ -penpoint marker. n, number; SLN, sentinel lymph node.

First, the clinical utility of this handheld gamma-camera was evaluated in 17 patients (32%), by assessing whether identified SLNs using lymphoscintigraphy could be detected preoperatively with the handheld gamma-camera (Figure 2).

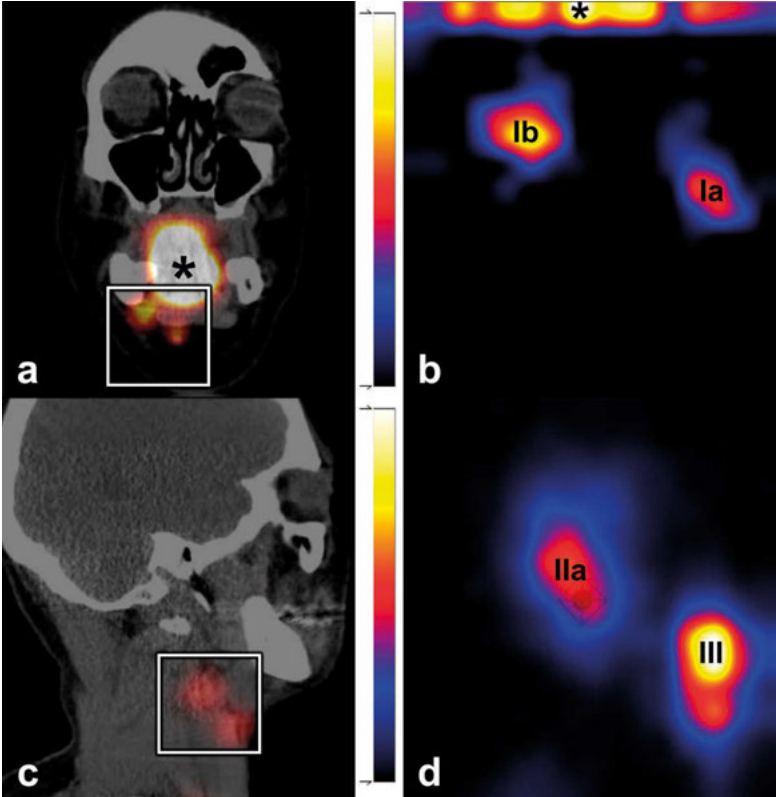


**Figure 2.** Comparison SPECT/CT (a,c) and Crystal Cam handheld gamma-camera images (b,d). Coronal plane of SPECT/CT (a) depicting injection site (\*) and two SLNs located in level Ia and level Ib on the left side. Both SLNs (Ia, Ib) and injection site could be visualized within the field-of-view of the handheld gamma-camera (white square; a,b). Two SLNs as identified by SPECT/CT (c) (sagittal plane; level IIa, III), also detected by handheld gamma-camera (IIa, III) (d).

Subsequently, to evaluate the reliability of SLN identification using the handheld gamma-camera, a blinded comparison was made between preoperative handheld gamma-camera and lymphoscintigraphy outcomes in 36 patients (68%; see “Assessment blinded for lymphoscintigraphy”).

Out of those who underwent blinded SLN assessment by handheld gamma-camera (n = 36), the reliability of SLN localization using the handheld gamma-camera and a <sup>57</sup>Co-penpoint marker was evaluated in 15 patients (42%; see “Cutaneous marking location SLNs”).

In all patients ( $n = 53$ ), the handheld gamma-camera was used complementary to conventional gamma-probe guidance for intraoperative SLN localization (see “Surgical procedure”).

### Specifications

The Crystal Cam is a handheld solid-state gamma-camera with a cadmium zinc telluride detector (thickness: 5 mm), that provides two-dimensional imaging at a field-of-view of  $40 \times 40 \text{ mm}^2$  with  $16 \times 16$  pixels (Figure 3). Its physical dimensions ( $65 \times 65 \times 180 \text{ mm}$ ) and total weight of 0.8 kg, including a collimator and 3 mm lead integrated side shielding, allow for single-handed control of the gamma-camera without an articulated arm. The included low-energy (LE) collimators, which can be changed at runtime, facilitate either high sensitivity (LEHS collimator; Figure 3a) or high resolution (LEHR collimator; Figure 3b) imaging. Both the LEHS and LEHR collimator were used at discretion of the observers. Control and visualization software (Crystal Imager) runs on a standard laptop to which the handheld gamma-camera is connected (Figure 3c). This handheld gamma-camera is able to simultaneously detect both  $^{99m}\text{Tc}$  and  $^{57}\text{Co}$  in different energy windows [23].

In this study, quality controls of the handheld gamma-camera were performed on a regular basis by a nuclear physicist for testing sensitivity, homogeneity, peaking and null-effect.

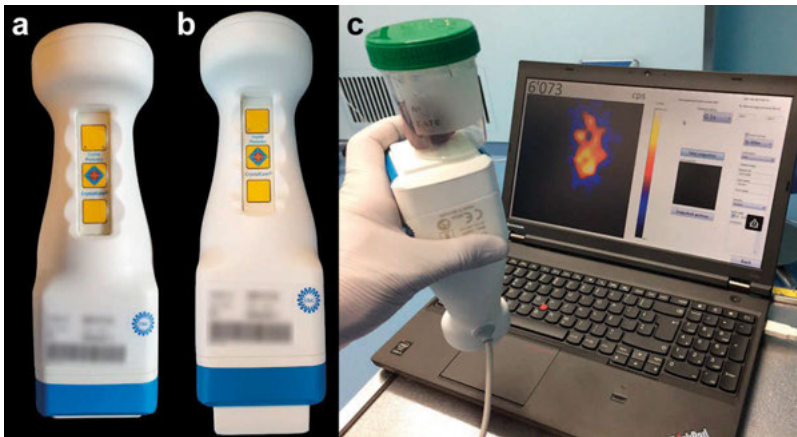


**Figure 3.** Crystal Cam handheld gamma-camera. (a) Equipped with a low-energy high-sensitivity (LEHS) collimator. (b) Equipped with a low-energy high-resolution (LEHR) collimator. (c) Connected to laptop with Crystal Imager software via USB.

## Lymphoscintigraphy

Lymphoscintigraphy including SPECT/CT acquisition were conducted according to EANM guidelines [11]. Following peritumoral injections of a  $^{99m}\text{Tc}$ -labeled radiotracer (i.e., [ $^{99m}\text{Tc}$ ]Tc-nanocolloid or [ $^{99m}\text{Tc}$ ]Tc-tilmanocept) planar static and dynamic scintigraphy as well as SPECT/CT were acquired the day prior to surgery (two-day protocol) or the day of surgery (single-day protocol) on a Siemens Symbia T16 SPECT/CT scanner; equipped with low-medium energy (LME) collimators to limit septal penetration and reduce shine-through [29]. SPECT images were reconstructed using clinical reconstruction software (Siemens Flash3D), with attenuation and scatter correction (6 iterations, 8 subsets, 5 mm Gaussian filter). For the two-day protocol,  $\sim 120$  MBq [ $^{99m}\text{Tc}$ ]Tc-nanocolloid or  $\sim 74$  MBq [ $^{99m}\text{Tc}$ ]Tc-tilmanocept was administered, whereas for the single-day protocol  $\sim 50$  MBq [ $^{99m}\text{Tc}$ ]Tc-nanocolloid was administered.

## Assessment blinded for lymphoscintigraphy

Immediately following lymphoscintigraphy, SLN assessment was preoperatively performed using the handheld gamma-camera by a single observer while blinded for lymphoscintigraphy ( $n = 36$ ; 68%). Identified hotspots using the handheld gamma-camera were recorded and designated as either SLN or HEN on the basis of their location and relative radioactive intensity. Subsequently, the results of lymphoscintigraphy including SPECT/CT, as reviewed by a nuclear physician, were revealed to the blinded observer. Any discrepancies between lymphoscintigraphy and handheld gamma-camera outcomes were registered. If SLNs were missed by blinded assessment using the handheld gamma-camera, an additional assessment was conducted to determine whether missed SLNs could be identified with either the handheld gamma-camera or gamma-probe with information provided by lymphoscintigraphy. In all patients, lymphoscintigraphy was leading in designating SLNs for biopsy.

## Cutaneous marking location SLNs

In 15 patients (28%), the location of the SLNs designated for biopsy by lymphoscintigraphy were first marked on the overlying skin with the handheld gamma-camera and a  $^{57}\text{Co}$ -penpoint marker using its dual-isotope function (Figure 4). Then, with the patient in a similar position, the location of the identified SLNs were marked using the conventional gamma-camera (Siemens Symbia T16 system) and the  $^{57}\text{Co}$ -penpoint marker, according to standard protocol. Subsequently, the location of both cutaneous markings was compared, with cutaneous markings based on the conventional gamma-camera as reference standard. The marked location of SLNs using the handheld gamma-camera was considered accurate if they deviated  $\leq 10$  mm in any direction from the location as marked with the conventional gamma-camera.

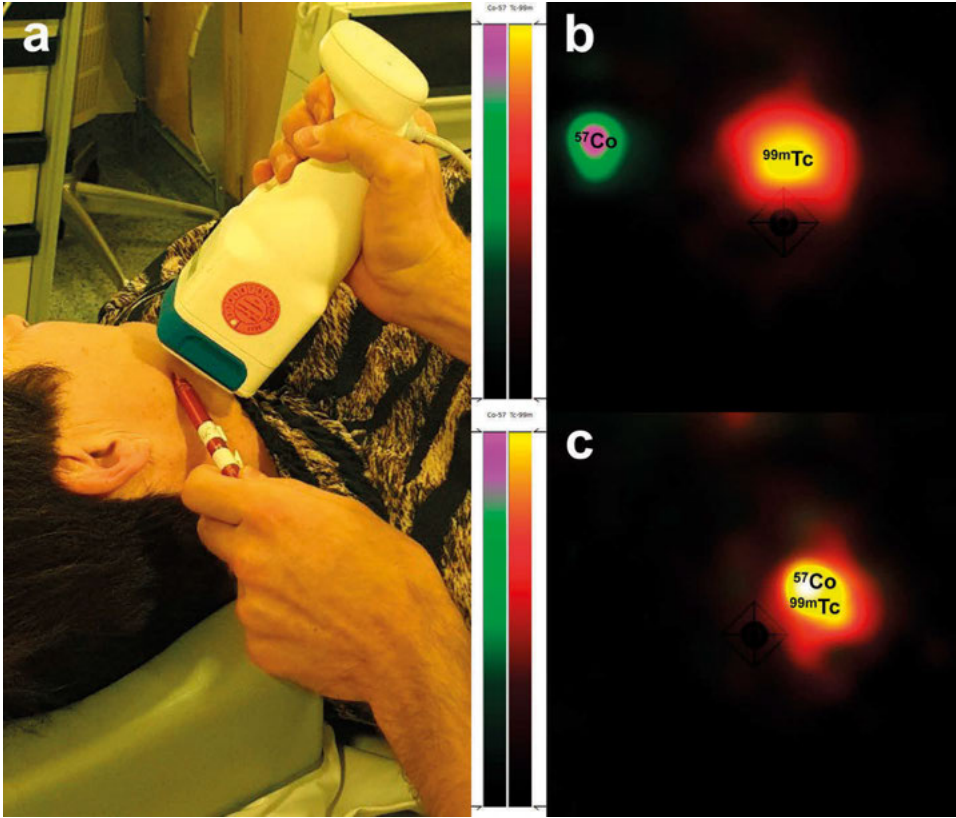


**Figure 4.** (a) Cutaneous marking of the location of SLNs using Crystal Cam handheld gamma-camera and a  $^{57}\text{Co}$ -penpoint marker. To simulate the definite surgical position, the patient is placed in supine position with head slightly extended and rotated to the opposite side. (b) Separate  $^{57}\text{Co}$ -hotspot ( $^{57}\text{Co}$ ) and  $^{99\text{m}}\text{Tc}$ -hotspot ( $^{99\text{m}}\text{Tc}$ ) within the handheld gamma-camera's field-of-view. (c) Overlapping  $^{57}\text{Co}$ -hotspot and  $^{99\text{m}}\text{Tc}$ -hotspot, indicating that the  $^{57}\text{Co}$ -penpoint marker is positioned on the SLN's location.

**Surgical procedure**

Marked SLNs were localized and harvested primarily under conventional portable gamma-probe guidance; the handheld gamma-camera was available to the surgeon on request. During surgery, an experienced operator was present to assist in using the handheld gamma-camera. In 10 patients (19%), also fluorescence guidance was available using ICG- $^{99\text{m}}\text{Tc}$ ]Tc-nanocolloid and near-infrared imaging. The location of harvested SLNs including their radioactive uptake (in counts per second as measured by the portable gamma-probe) were registered. Following extirpation of a SLN and check for residual activity with the gamma-probe, the handheld gamma-camera was used to scan for residual activity (Figure 5).



**Figure 5** Intraoperative use of Crystal Cam handheld gamma-camera.

At the end of SLNB, surgeons were asked whether the handheld gamma-camera further assisted SLN localization when used complementary to conventional portable gamma-probe guidance. To this end, the 3-point subjective scoring system as previously published by Heuveling et al. was adopted [12]: (1) the handheld gamma-camera provided confusing information and was not helpful; (2) the handheld gamma-camera could reliably be used, but provided no additional helpful information; (3) the handheld gamma-camera provided additional helpful information for localization of SLNs.

### **Histopathology and follow-up**

Harvested SLNs were sent for histopathological examination using step-serial-sectioning (section thickness 150  $\mu\text{m}$ ) with hematoxylin-eosin and pan-cytokeratin antibody (AE 1/3) staining [30, 31]. Patients with histopathologically negative SLNs were assigned to a wait-and-scan approach. In those with at least one histopathologically positive SLN, complementary treatment of the affected and adjacent nodal basins was employed (i.e., neck dissection and/or (chemo) radiotherapy). Complementary neck dissection specimens were histopathologically assessed for additional (non-SLN) nodal metastases. Follow-up visits were scheduled according to standard oncological care.

## False-negative SLNB

Isolated regional recurrences that occurred in the side of the neck staged negative by SLNB, within three years following treatment, were regarded as a false-negative outcome for SLNB. Regional recurrences in presence of local recurrence or second primary tumors were not considered false-negative outcomes for SLNB, as differentiation between missed nodal metastasis at initial diagnostic work-up and metastasis developed from a reseeding local recurrence or second primary tumor is unfeasible.

## Analyses

All data were analyzed with IBM SPSS Statistics Version 28.0 (IBM Corp., Armonk, New York, United States). Descriptive statistics are presented as number of cases and percentages for dichotomous and ordinal variables, whereas continuous parametric variables are presented as mean and standard deviation (SD). Non-parametric variables are presented as median with interquartile range (IQR). Fisher's exact test was used to compare categorical variables containing small number of cases ( $n \leq 5$ ).

Spearman's rank-order correlation tests were conducted to determine the association between amount and location of identified SLNs by blinded handheld gamma-camera assessment and lymphoscintigraphy for each patient. On the basis of the false-negative rate for SLNB in this cohort, the sensitivity ( $\text{true-positives} / (\text{true-positives} + \text{false-negatives})$ ) and negative predictive value (NPV;  $(\text{true-negatives} / (\text{true-negatives} + \text{false-negatives}))$ ) were calculated. Overall, a p-value  $\leq 0.05$  was considered to be statistically significant.

## Results

Patient- and tumor characteristics of included patients are listed in Table 1. A total of 10 (19%) patients had a history of head and neck cancer, of which 8 previously underwent oncological treatment of the neck. In the majority of patients, the primary tumor was located in the oral tongue (59%). Most tumors were pathologically classified as pT2 (55%). In one patient the primary tumor (retromolar trigone) was pathologically classified as pT4a on the basis of mandibular invasion.

Patients mainly underwent SLNB by two-day protocol (47 of 53; 89%) using [<sup>99m</sup>Tc] Tc-nanocolloid (33 of 47; 70%). A total of 138 SLNs were harvested, on average 3 per patient (range 0 – 6), of which 15 harbored metastasis (11%). Of those patients with nodal metastases as assessed by SLNB (*n* = 10; 19%), half underwent complementary neck dissection whereas the other half underwent complementary radiotherapy. Two patients underwent adjuvant neck irradiation following complementary neck dissection. None underwent concurrent chemotherapy as part of complementary- or adjuvant therapy.

**Table 1.** Patient- and tumor characteristics.

Characteristics	<i>n</i> = 53
<b>Gender, n (%)</b>	
Female	24 (45%)
<b>Median age (<i>y</i>) (range)</b>	61.5 (29-97)
<b>History of head and neck cancer, n (%)</b>	10 (19%)
<b>Previous oncological treatment of the neck, n (%)</b>	
Neck dissection	6 (11%)
Radiotherapy	1 (2%)
Neck dissection and chemoradiation	1 (2%)
<b>Tumor location, n (%)</b>	
Tongue	31 (59%)
Floor-of-mouth	5 (9%)
Buccal mucosa	7 (13%)
Retromolar trigone	7 (13%)
Lower gum	3 (6%)
<b>Side primary tumor, n (%)</b>	
Left	21 (40%)
Right	30 (56%)
Midline	2 (4%)

**Table 1.** Continued.

Characteristics	<i>n</i> = 53
<b>Radiotracer, n (%)</b>	
Nanocolloid	39 (74%)
Tilmanocept	14 (26%)
<b>Two-day SLNB protocol, n (%)</b>	47 (89%)
<b>Pathological T-stage, n (%)<sup>a</sup></b>	
pT1	19 (36%)
pT2	29 (55%)
pT3	4 (7%)
pT4a	1 (2%)
<b>Median harvested SLNs (range)</b>	3 (0-6)
<b>Histopathological status SLNs, n (%)</b>	
Negative	123 (89%)
Positive	15 (11%)
<b>SLNB outcome, n (%)</b>	
pN0(sn)	43 (81%)
pN+ (sn)	10 (19%)
<b>Complementary neck treatment, n (%)</b>	
Neck dissection	5 (9%)
Radiotherapy	5 (9%)
<b>Pathological N-stage, n (%)<sup>a</sup></b>	
pN1	3 (6%)
pN2b	5 (9%)
pN2c	1 (2%)
pN3b	1 (2%)
<b>Follow-up in months (range)</b>	23 (2 – 49)

*n*, number; *y*, years; *mm*, millimeters; *SD*, standard deviation; *SLNs*, sentinel lymph nodes; *SLNB*, sentinel lymph node biopsy; *ND*, neck dissection; *RT*, radiotherapy.

<sup>a</sup>According to AJCC TNM classification, 8<sup>th</sup> edition.

### Identification of SLNs

In the 17 patients in whom the clinical utility of the handheld gamma-camera was evaluated, 41 out of the 45 SLNs (91%) identified by lymphoscintigraphy were also detected with the handheld gamma-camera. The undetected SLNs (*n* = 4) in two patients were located in levels Ia, IIa, III and V of the ipsilateral neck (Table 2). None of these undetected SLNs could be localized intraoperatively as its radioactive signal was either indistinguishable from the radioactive signal deriving from the injection site or on account of their marginal radioactive uptake. In both patients, there was no evidence of nodal disease at 31 and 35 month follow-up.

4

While blinded for lymphoscintigraphy ( $n = 36$ ), 71 out of 77 SLNs were correctly identified using the handheld gamma-camera (92%). The SLNs as overlooked by blinded handheld gamma-camera assessment were mainly located close to the injection site (levels Ia and Ib); one was located in the previously treated neck and one was located in the contralateral neck of the primary tumor (Table 2). Of the 6 overlooked SLNs by blinded assessment in 5 patients, only 4 were surgically harvested since the other two could not be located intraoperatively by neither handheld gamma-probe nor handheld gamma-camera. Histopathological assessment showed no metastasis in these 4 overlooked SLNs. The two patients in whom the overlooked SLNs could not be harvested intraoperatively showed no evidence of nodal disease 26 and 30 months following SLNB.

In 4 patients a total of 6 hotspots were scored as SLN based on blinded handheld gamma-camera assessment, but designated as HEN based on lymphoscintigraphy. In addition, 2 SLNs were incorrectly identified with the handheld gamma-camera (false-positives): one revealed to be an appendix of the injection site whereas the other appeared to be an intense hotspot in the contralateral neck, which was mistaken for a SLN in the side of the neck being scanned. Overall, there was a strong agreement between SLNs identified using the handheld gamma-camera while blinded for lymphoscintigraphy and the SLNs as ultimately designated for biopsy by lymphoscintigraphy ( $r_s = 0.857$ ,  $p < 0.001$ ).

### **Cutaneous marking location SLNs**

In 15 patients, the location of 43 SLNs designated for biopsy were marked on the overlying skin with the handheld gamma-camera and the  $^{57}\text{Co}$ -penpoint marker. The marked location by handheld gamma-camera deviated on one occasion 15 mm from the location as marked by the conventional gamma-camera and for all other instances on average 1.0 mm (range 0 – 10 mm).

**Table 2.** Undetected and/or overlooked SLNs by Crystal Cam handheld gamma-camera.

Primary tumor	Previous neck treatment	Radiotracer (dosage)	Identified SLNs LSG	Harvested	PA	pN(sn) <sup>a</sup>	Complementary treatment	Follow-up (months)	
Buccal mucosa (left)	SND left	Nanocolloid (126 MBq)	Ila	Right	Yes	-	None	NED (35)	
			V	Left*	No	N.A.			
Tongue (right)	None	Tilmanocept (74 MBq)	Ila	Right*	No	N.A.	Bilateral ND	NED (31)	
			III	Right*	No	N.A.			
			Ia	Left*	No	N.A.			
Lower gum (right)	None	Nanocolloid (117 MBq)	Ib	Left	Yes	+			
			III	Left	Yes	-			
			Ia	Right <sup>*,b</sup>	Yes	-	pN0	None	NED (37)
			Ib	Right <sup>*,b</sup>	Yes	-			
			Ila	Right	Yes	-			
			III	Right	Yes	-			
Buccal mucosa (left)	None	Nanocolloid (122 MBq)	Ib	Left	Yes	+	Unilateral RT	NED (30)	
			Ib	Left <sup>*,b</sup>	No	N.A.			
Tongue (right)	None	Nanocolloid (131 MBq)	Ib	Right <sup>b</sup>	Yes	-	None	NED (29)	
			III	Right	Yes	-			
			Ila	Left	Yes	-			
Tongue (right)	SND right	Nanocolloid (119 MBq)	III	Left	Yes	-			
			Ia	Left	Yes	+	pN0	None	NED (26)
Tongue (right)	None	Nanocolloid (60 MBq)	Ila	Right <sup>*,b</sup>	No	N.A.			
			Ila	Right	Yes	-	pN0	None	NED (20)
			Ila	Left	Yes	-			
			III	Left <sup>b</sup>	Yes	-			

SLN, sentinel lymph node; LSG, lymphoscintigraphy; PA, pathological assessment; SND, selective neck dissection; MBq, megabecquerel; N.A., not applicable; +, histopathologically positive for metastasis; -, histopathologically negative for metastasis; NED, no evidence of disease; ND, neck dissection; RT, radiotherapy.  
<sup>a</sup> According to AJCC TNM classification, 8<sup>th</sup> edition. \* Undetected by handheld gamma-camera. <sup>b</sup> Overlooked by blinded handheld gamma-camera assessment.

## Intraoperative SLN localization

Intraoperatively, based on the information as provided by the complementary use of the handheld gamma-camera, 16 additional “hot” lymph nodes were harvested in 14 patients (26%). Out of these additionally harvested lymph nodes, 4 harbored metastases as confirmed by histopathological assessment (25%) which led to upstaging in 4 patients (8%). On account of these additionally harvested metastatic lymph nodes, two patients underwent complementary treatment of the neck instead of being assigned to a wait-and-scan approach (pN0(sn) to pN1(sn)) and one patient was upstaged from pN1(sn) to pN2b(sn), which had no therapeutic consequences since the patient chose to undergo complementary radiotherapy instead of a complementary neck dissection followed by adjuvant neck irradiation. The remaining patient was upstaged from pN1(sn) to pN3b(sn), yet opted for complementary radiotherapy only and declined a complementary neck dissection or concurrent chemotherapy.

In 29 patients (55%), the surgeon deemed the complementary use of the handheld gamma-camera as “helpful” for localizing SLNs intraoperatively. In the remaining patients ( $n = 24$ ), the performance of the handheld gamma-camera was considered reliable, but did not provide additional helpful information (45%). None regarded the information provided by the handheld gamma-camera as “confusing”.

For the 10 patients in whom also fluorescence guidance was available, the handheld gamma-camera was still considered to be of added value in 4 patients (surgeon score 3; 40%), which did not differ significantly when compared to the rate of patients in whom no fluorescence guidance was available and the handheld gamma-camera was regarded as helpful (58%;  $p = 0.482$ ). In these 10 patients, 2 additional “hot” lymph nodes were harvested on account of information provided by the handheld gamma-camera, none of which harbored metastasis.

## Follow-up

In this cohort, two patients developed an isolated nodal recurrence in the side of the neck staged negative by SLNB at 5 and 6 month follow-up, corresponding with a false-negative rate of 3.8%. Accordingly, in those with follow-up  $\geq 24$  months or false-negative SLNB within 24 month follow-up ( $n = 39$ ), a sensitivity of 82% and a NPV of 93% was obtained. The false-negative rate of SLNB in this cohort without the use of the handheld gamma-camera would have been 7.6% (4 of 53), corresponding with a sensitivity of 64% and a NPV of 87%.

## Discussion

This study evaluated the use of the Crystal Cam handheld gamma-camera in 53 early-stage OSCC (cT1-3N0) patients undergoing SLNB. Overall, this handheld gamma-camera was able to preoperatively detect 95% of SLNs (116 of 122) as identified by conventional lymphoscintigraphy. When blinded for lymphoscintigraphy, 92% of SLNs were correctly identified by handheld gamma-camera. The marked location of SLNs by handheld gamma-camera and  $^{57}\text{Co}$ -penpoint marker was considered accurate in 98% of SLNs. Its complementary use during surgery led to the extirpation of additional “hot” lymph nodes in 14 patients, which ultimately prevented two patients from otherwise being falsely staged negative for nodal disease (4%). The surgeon deemed the complementary use of the handheld gamma-camera helpful for intraoperatively localizing SLNs in 55% of patients.

When considering its accuracy in detecting and localizing SLNs, both preoperatively and intraoperatively, the clinical utility of the Crystal Cam handheld gamma-camera in early-stage OSCC appears similar to several other gamma-detecting imaging devices [12, 13, 17-21, 32]. This handheld gamma-camera proved to be particularly helpful when scanning for residual activity after harvesting a presumed SLN [19, 32]; most additional “hot” lymph nodes (possibly remaining SLNs) were harvested in this manner. Furthermore, in several patients, tracking SLNs under conventional gamma-probe guidance was challenging and time-consuming. In these circumstances, the handheld gamma-camera provided more precise information on the SLN’s position, thus facilitating its localization and extirpation (surgeon score 3). The handheld gamma-camera was even considered helpful in 4 out of the 10 patients in whom fluorescence guidance was also available; its use resulted in the extirpation of 2 additional “hot” lymph nodes in these patients. More efficient SLN localization may decrease the extent of exploration (with its associated postoperative fibrosis and risk of complications) required to harvest SLNs, which benefits an eventual complementary neck dissection, and may reduce the duration of surgery [12, 13, 20]. However, if more “hot” lymph nodes are found and harvested on account of real-time radioguided imaging, the procedure may as well be prolonged [13].

Additionally, the dual-isotope capability of this handheld gamma-camera has shown to enable accurate pre-operative localization of designated SLNs by  $^{57}\text{Co}$ -penpoint marker. Owing to the close proximity of the handheld gamma-camera to the skin, the majority of SLNs can easily be localized and marked by the nuclear physician using this dual-isotope feature. Since the location of SLNs in definite surgical position may slightly differ from the pre-operatively marked location, the handheld gamma-camera can also be used to adjust skin marks intraoperatively [12, 13]. Moreover, as

the  $^{57}\text{Co}$ -penpoint marker is small and can easily be incorporated in a sterile setting using a surgical glove, the dual-isotope feature can even be used after the incision is made to further narrow down the exact location of SLNs. Accordingly, this handheld gamma-camera has been introduced within the clinical care of this institution.

There are a few shortcomings of the handheld gamma-camera used in this study. First, since it only provides a two-dimensional view, no real-time information on the depth of SLNs can be obtained. Second, as demonstrated by the overlooked and undetected SLNs using the handheld gamma-camera in this study, (handheld) gamma-cameras remain susceptible to the shine-through phenomenon and may therefore experience difficulties in detecting SLNs located near the injection site [9, 10, 12]. In addition, detecting SLNs with low radioactive uptake may be challenging. Especially in these situations near-infrared fluorescence imaging can be of added value [12, 14]. Finally, one should be aware of intense radioactive signals originating from the contralateral neck when using the handheld gamma-camera, as these can be mistaken for a hotspot in the side of the neck being scanned. This issue can easily be overcome though by adjusting the view angle of the handheld gamma-camera relative to the hotspot.

Certain limitations of this study have to be acknowledged. Most importantly, since the handheld gamma-camera was used in all patients, several of its potential benefits (e.g., reduced duration of surgery, lower complication rate) cannot be assessed. Obviously, the surgical procedure cannot be performed twice in each patient and considerable interpatient variability renders randomization an unrealistic option. Therefore, determining its additional value on these matters is unfeasible. Secondly, due to the number of surgeons ( $n = 7$ ) having used the handheld gamma-camera intraoperatively, examination bias is inevitable, even though handling this handheld gamma-camera is intuitive and interpretation of its images fairly straightforward [24]. Finally, the variability in radiotracers and radioactive dosage administered as well as protocols used for SLNB (i.e., single-day protocol, two-day protocol) may have affected this study's outcomes.

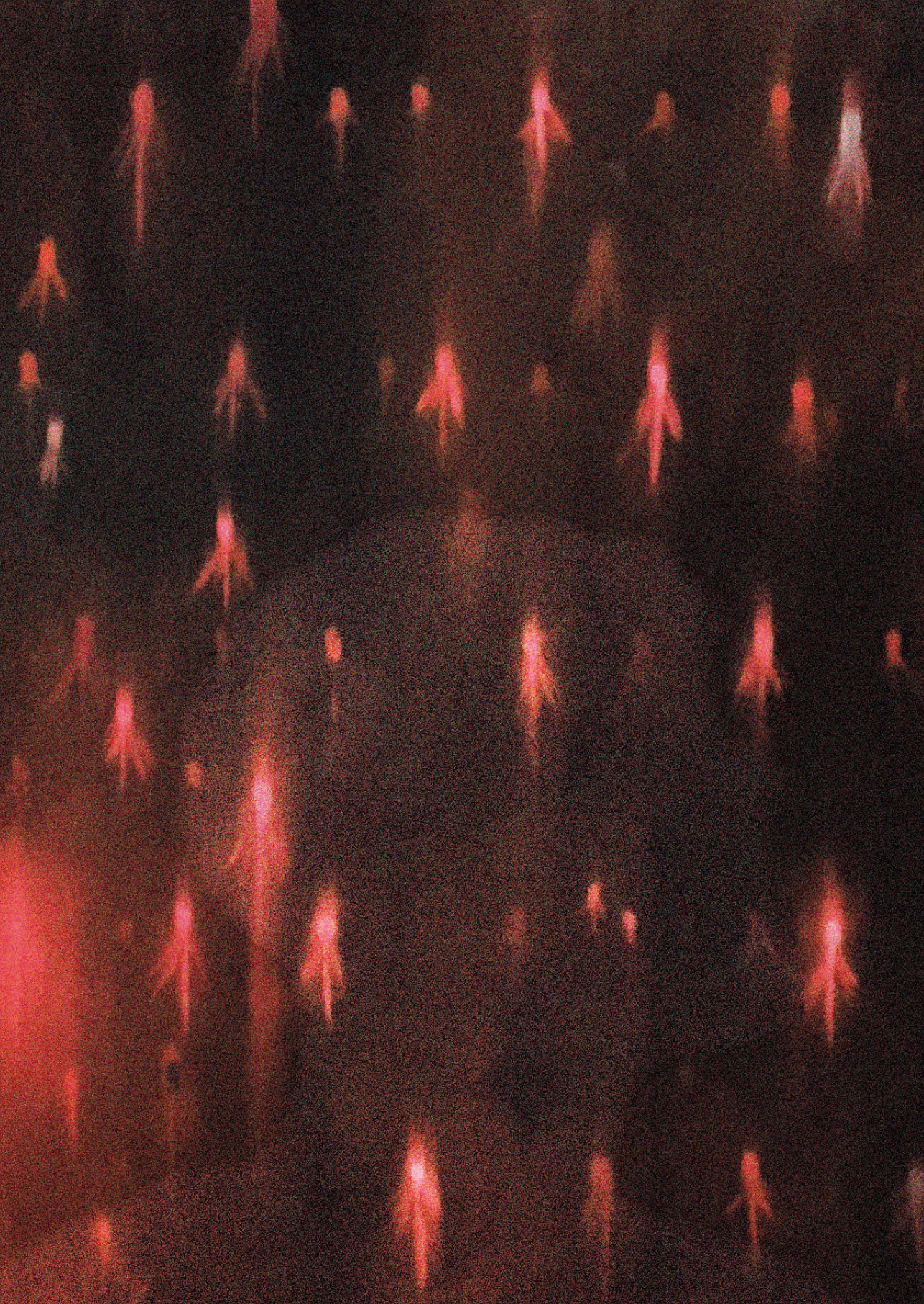
In conclusion, the results of this study demonstrate that the relatively inexpensive and portable Crystal Cam handheld gamma-camera offers reliable preoperative and intraoperative SLN localization in early-stage OSCC patients, which facilitates SLNB and might even reduce the risk of missing a malignant SLN during surgery. Still, detecting SLNs close to the injection site or with low radioactive uptake by handheld gamma-camera can be challenging. In those situations, complementary near-infrared fluorescence imaging may be of additional value.

## References

1. Schilling C, Shaw R, Schache A, et al. Sentinel lymph node biopsy for oral squamous cell carcinoma. Where are we now? *Br J Oral Maxillofac Surg.* 2017;55(8):757-762. doi:10.1016/j.bjoms.2017.07.007
2. de Bree R, de Keizer B, Civantos FJ, et al. What is the role of sentinel lymph node biopsy in the management of oral cancer in 2020? *Eur Arch Otorhinolaryngol.* 2021;278(9):3181-3191. doi:10.1007/s00405-020-06538-y
3. Garrel R, Poissonnet G, Moyà Plana A, et al. Equivalence randomized trial to compare treatment on the basis of sentinel node biopsy versus neck node dissection in operable T1-T2N0 oral and oropharyngeal cancer. *J Clin Oncol.* 2020;38(34):4010-4018. doi:10.1200/JCO.20.01661
4. Hasegawa Y, Tsukahara K, Yoshimoto S, et al. Neck dissections based on sentinel lymph node navigation versus elective neck dissections in early oral cancers: a randomized, multicenter, and noninferiority trial. *J Clin Oncol.* 2021;39(18):2025-2036. doi:10.1200/JCO.20.03637
5. Gupta T, Maheshwari G, Kannan S, Nair S, Chaturvedi P, Agarwal JP. Systematic review and meta-analysis of randomized controlled trials comparing elective neck dissection versus sentinel lymph node biopsy in early-stage clinically node-negative oral and/or oropharyngeal squamous cell carcinoma: Evidence-base for practice and implications for research. *Oral Oncol.* 2022;124:105642. doi:10.1016/j.oraloncology.2021.105642
6. D'Cruz AK, Vaish R, Kapre N, et al. Elective versus therapeutic neck dissection in node-negative oral cancer. *N Engl J Med.* 2015;373(6):521-529. doi:10.1056/NEJMoa1506007
7. Flach GB, Tenhagen M, de Bree R, et al. Outcome of patients with early stage oral cancer managed by an observation strategy towards the N0 neck using ultrasound guided fine needle aspiration cytology: No survival difference as compared to elective neck dissection. *Oral Oncol.* 2013;49(2):157-164. doi:10.1016/j.oraloncology.2012.08.006
8. Miura K, Kawakita D, Oze I, et al. Predictive factors for false negatives following sentinel lymph node biopsy in early oral cavity cancer. *Sci Rep.* 2022;12(1):6917. doi:10.1038/s41598-022-10594-1
9. Mahieu R, de Maar JS, Nieuwenhuis ER, et al. New developments in imaging for sentinel lymph node biopsy in early-stage oral cavity squamous cell carcinoma. *Cancers (Basel).* 2020;12(10):3055. doi:10.3390/cancers12103055
10. Schilling C, Stoeckli SJ, Vigili MG, et al. Surgical consensus guidelines on sentinel node biopsy (SNB) in patients with oral cancer. *Head Neck.* 2019;41(8):2655-2664. doi:10.1002/hed.25739
11. Giammarile F, Schilling C, Gnanasegaran G, et al. The EANM practical guidelines for sentinel lymph node localisation in oral cavity squamous cell carcinoma. *Eur J Nucl Med Mol Imaging.* 2019;46(3):623-637. doi:10.1007/s00259-018-4235-5
12. Heuveling DA, van Weert S, Karagozoglou KH, de Bree R. Evaluation of the use of freehand SPECT for sentinel node biopsy in early stage oral carcinoma. *Oral Oncol.* 2015;51(3):287-290. doi:10.1016/j.oraloncology.2014.12.001
13. Vermeeren L, Valdés Olmos RA, Klop WM, Balm AJ, van den Brekel MW. A portable gamma-camera for intraoperative detection of sentinel nodes in the head and neck region. *J Nucl Med.* 2010;51(5):700-703. doi:10.2967/jnumed.109.071407
14. van den Berg NS, Brouwer OR, Klop WM, et al. Concomitant radio- and fluorescence-guided sentinel lymph node biopsy in squamous cell carcinoma of the oral cavity using ICG-<sup>99m</sup>Tc-nanocolloid. *Eur J Nucl Med Mol Imaging.* 2012;39(7):1128-1136. doi:10.1007/s00259-012-2129-5
15. KleinJan GH, van Werkhoven E, van den Berg NS, et al. The best of both worlds: a hybrid approach for optimal pre- and intraoperative identification of sentinel lymph nodes. *Eur J Nucl Med Mol Imaging.* 2018;45(11):1915-1925. doi:10.1007/s00259-018-4028-x
16. Almhanedi H, McGurk M, Wan S, Schilling C. Novel double injection technique for sentinel lymph node biopsy in oral cancer. *Br J Oral Maxillofac Surg.* 2021;59(10):1296-1301. doi:10.1016/j.bjoms.2021.07.008
17. Schilling C, Gnanasegaran G, Thavaraj S, McGurk M. Intraoperative sentinel node imaging versus SPECT/CT in oral cancer - A blinded comparison. *Eur J Surg Oncol.* 2018;44(12):1901-1907. doi:10.1016/j.ejso.2018.08.026
18. de Bree R, Pouw B, Heuveling DA, Castelijns JA. Fusion of freehand SPECT and ultrasound to perform ultrasound-guided fine-needle aspiration cytology of sentinel nodes in head and neck cancer. *AJNR Am J Neuroradiol.* 2015;36(11):2153-2158. doi:10.3174/ajnr.A4426

19. Sieira-Gil R, Paredes P, Martí-Pagés C, et al. SPECT-CT and intraoperative portable gamma-camera detection protocol for sentinel lymph node biopsy in oral cavity squamous cell carcinoma. *J Craniomaxillofac Surg*. 2015;43(10):2205-2213. doi:10.1016/j.jcms.2015.10.006
20. Vidal-Sicart S, Paredes P, Zanón G, et al. Added value of intraoperative real-time imaging in searches for difficult-to-locate sentinel nodes. *J Nucl Med*. 2010;51(8):1219-1225. doi:10.2967/jnumed.110.074880
21. Dietze MMA, Kunnen B, Brontsema F, et al. A compact and mobile hybrid C-arm scanner for simultaneous nuclear and fluoroscopic image guidance. *Eur Radiol*. 2022;32(1):517-523. doi:10.1007/s00330-021-08023-4
22. Ozkan E, Eroglu A. The utility of intraoperative handheld gamma camera for detection of sentinel lymph nodes in melanoma. *Nucl Med Mol Imaging*. 2015;49(4):318-320. doi:10.1007/s13139-015-0341-5
23. Knoll P, Mirzaei S, Schwenkenbecher K, Barthel T. Performance evaluation of a solid-state detector based handheld gamma camera system. *Front. Biomed. Technol*. 2014;1(1):61-67.
24. Barrou J, Cohen M, Brenot-Rossi I et al. Sentinel node detection by Crystal Cam in breast cancer: accuracy and contribution to ambulatory surgery. *Eur J Gynaecol Oncol* 2017: 38.6.
25. Koç ZP, Kara PPÖ, Berkeşoğlu M, Akça T. First experience with a new technique: Portable gamma camera usage for sentinel lymph node identification in a patient with breast cancer. *Turk J Surg*. 2018;34(1):57-59. doi:10.5152/UCD.2016.3654
26. Amin MB, Greene FL, Edge SB, et al. The Eighth Edition AJCC Cancer Staging Manual: Continuing to build a bridge from a population-based to a more “personalized” approach to cancer staging. *CA Cancer J Clin*. 2017;67(2):93-99. doi:10.3322/caac.21388
27. Brierley JD, Gospodarowicz M, Wittekind C. UICC TNM Classification of Malignant Tumours. 8<sup>th</sup> ed. Chichester, United Kingdom: Wiley; 2017.
28. International Consortium for Outcome Research (ICOR) in Head and Neck Cancer, Ebrahimi A, Gil Z, et al. Primary tumor staging for oral cancer and a proposed modification incorporating depth of invasion: an international multicenter retrospective study. *JAMA Otolaryngol Head Neck Surg*. 2014;140(12):1138-1148. doi:10.1001/jamaoto.2014.1548
29. Yoneyama H, Tsushima H, Kobayashi M, Onoguchi M, Nakajima K, Kinuya S. Improved detection of sentinel lymph nodes in SPECT/CT images acquired using a low- to medium-energy general-purpose collimator. *Clin Nucl Med*. 2014;39(1):e1-e6. doi:10.1097/RLU.0b013e31828da362
30. Dhawan I, Sandhu SV, Bhandari R, Sood N, Bhullar RK, Sethi N. Detection of cervical lymph node micrometastasis and isolated tumor cells in oral squamous cell carcinoma using immunohistochemistry and serial sectioning. *J Oral Maxillofac Pathol*. 2016;20(3):436-444. doi:10.4103/0973-029X.190946
31. Alkureishi LW, Burak Z, Alvarez JA, et al. Joint practice guidelines for radionuclide lymphoscintigraphy for sentinel node localization in oral/oropharyngeal squamous cell carcinoma. *Ann Surg Oncol*. 2009;16(11):3190-3210. doi:10.1245/s10434-009-0726-8
32. Valdés Olmos RA, Vidal-Sicart S, Nieweg OE. Technological innovation in the sentinel node procedure: towards 3-D intraoperative imaging. *Eur J Nucl Med Mol Imaging*. 2010;37(8):1449-1451. doi:10.1007/s00259-010-1468-3





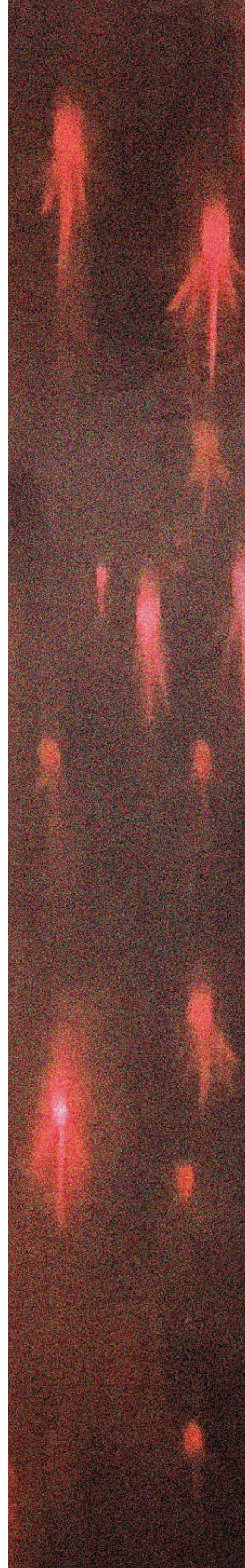
# 5

## Sentinel lymph node detection in oral cancer: a within-patient comparison between [ $^{99m}\text{Tc}$ ]Tc-tilmanocept and [ $^{99m}\text{Tc}$ ]Tc-nanocolloid

---

Inne J. den Toom, Rutger Mahieu, Rob van Rooij, Robert J.J. van Es,  
Monique G.G. Hobbelink, Gerard C. Krijger, Bernard M. Tijink,  
Bart de Keizer, Remco de Bree.

*Eur J Nucl Med Mol Imaging. 2021 Mar;48(3):851-858*



# Abstract

## Purpose

Sentinel lymph node (SLN) biopsy has proven to reliably stage the clinically negative neck in early-stage oral squamous cell carcinoma (OSCC). [<sup>99m</sup>Tc]Tc-tilmanocept may be of benefit in OSCC with complex lymphatic drainage patterns and close spatial relation to SLNs.

## Methods

A prospective within-patient evaluation study was designed to compare [<sup>99m</sup>Tc]Tc-tilmanocept with [<sup>99m</sup>Tc]Tc-nanocolloid for SLN detection. A total of 20 patients with early-stage OSCC were included, who underwent lymphoscintigraphy with both tracers. Both lymphoscintigraphic images of each patient were evaluated for SLN detection and radiotracer distribution at 2-4 hours post-injection.

## Results

The injection site's remaining radioactivity was significantly lower for [<sup>99m</sup>Tc]Tc-tilmanocept (29.9%), compared with [<sup>99m</sup>Tc]Tc-nanocolloid (60.9%;  $p < 0.001$ ). Radioactive uptake in SLNs was significantly lower for [<sup>99m</sup>Tc]Tc-tilmanocept (1.95%) compared with [<sup>99m</sup>Tc]Tc-nanocolloid (3.16%;  $p = 0.010$ ). No significant difference was seen in SLN to injection site ratio in radioactivity between [<sup>99m</sup>Tc]Tc-tilmanocept (0.066) and [<sup>99m</sup>Tc]Tc-nanocolloid (0.054;  $p = 0.232$ ). A median of 3.0 and 2.5 SLNs were identified with [<sup>99m</sup>Tc]Tc-tilmanocept and [<sup>99m</sup>Tc]Tc-nanocolloid, respectively ( $p = 0.297$ ). Radioactive uptake in higher echelon nodes was not significantly different between [<sup>99m</sup>Tc]Tc-tilmanocept (0.57%) and [<sup>99m</sup>Tc]Tc-nanocolloid (0.86%) ( $p = 0.052$ ). A median of 2.0 and 2.5 higher echelon nodes was identified with [<sup>99m</sup>Tc]Tc-tilmanocept and [<sup>99m</sup>Tc]Tc-nanocolloid, respectively ( $p = 0.083$ ).

## Conclusion

[<sup>99m</sup>Tc]Tc-tilmanocept had a higher injection site clearance, but at the same time a lower uptake in the SLN, resulting in an SLN to injection site ratio, which was not significantly different from [<sup>99m</sup>Tc]Tc-nanocolloid. The relatively low radioactive uptake in SLNs of [<sup>99m</sup>Tc]Tc-tilmanocept may limit intraoperative detection of SLNs, but can be overcome by a higher injection dose.

## Introduction

The sentinel lymph node biopsy (SLNB) procedure is a diagnostic staging method that is applied in a variety of tumor types, including oral squamous cell carcinoma (OSCC). The procedure aims to identify the first draining lymph nodes, the “sentinel lymph nodes” (SLN), which are most likely to harbor metastases. The histopathological status of the SLN should reflect the histopathological status of the rest of the nodal basin, and additional treatment of the nodal basin (e.g., surgery or radiotherapy) should only be performed in case of metastatic involvement of the SLN. So far, the routine procedure consists of preoperative peritumoral injection of a  $^{99m}\text{Tc}$ -labeled colloid followed by dynamic and static lymphoscintigraphy using planar and single photon emission computed tomography (SPECT) imaging [1-3]. Intraoperative detection is possible using a portable gamma-probe.

It has been demonstrated that by using this approach, the SLNB procedure reliably stages the clinically negative neck (cN0) in early-stage OSCC with a sensitivity of 87% and a negative predictive value of 94% in the most recent meta-analysis [4]. However, one of the most frequently mentioned difficulties of this procedure occurs when the injection site around the primary tumor produces a large hotspot on lymphoscintigraphy, possibly hiding SLN(s) in close proximity of the primary tumor, usually referred as “shine through” phenomenon (Figure 1). This phenomenon is particularly evident in floor-of-mouth tumors and multiple studies demonstrated a (significantly) lower accuracy of the SLNB procedure in floor-of-mouth tumors compared to other tumor locations in the oral cavity [5-8]. Some authors even advocate adding a superselective level I resection in these cases [9]. Secondly, on lymphoscintigraphy it is often difficult to differentiate hotspots between SLNs and second echelon nodes [10]. As a result, second echelon lymph nodes may erroneously be considered SLNs, resulting in an unnecessary extension of the surgical procedure.

A new radioactive agent,  $^{99m}\text{Tc}$ -tilmanocept (Lymphoseek<sup>®</sup>, Navidea Biopharmaceuticals, Inc.), has been specifically designed for SLN identification and is registered for this purpose in both the USA and Europe.  $^{99m}\text{Tc}$ -tilmanocept is a small-sized receptor-targeted (CD206) sentinel lymph node detection agent (Figure 2) [11]. Due to its proposed rapid clearance from the injection site, rapid uptake and high retention within the SLN, as well as low uptake by the remaining (higher echelon) lymph nodes,  $^{99m}\text{Tc}$ -tilmanocept may particularly be of benefit in floor-of-mouth tumors and other head and neck tumors with complex drainage patterns and close spatial relation to the SLN [12, 13]. A multicenter validation study using  $^{99m}\text{Tc}$ -tilmanocept for SLNB in head and neck squamous cell carcinoma showed an SLN identification rate of 97.6%, a false-negative rate of 2.6% and a negative

predictive value of 97.8% [14]. Of note, these high figures were also obtained in floor-of-mouth cancers, which strengthened the idea that [ $^{99m}\text{Tc}$ ]Tc-tilmanocept may diminish the shine through effect and improve the SLN detection rate for this subsite.

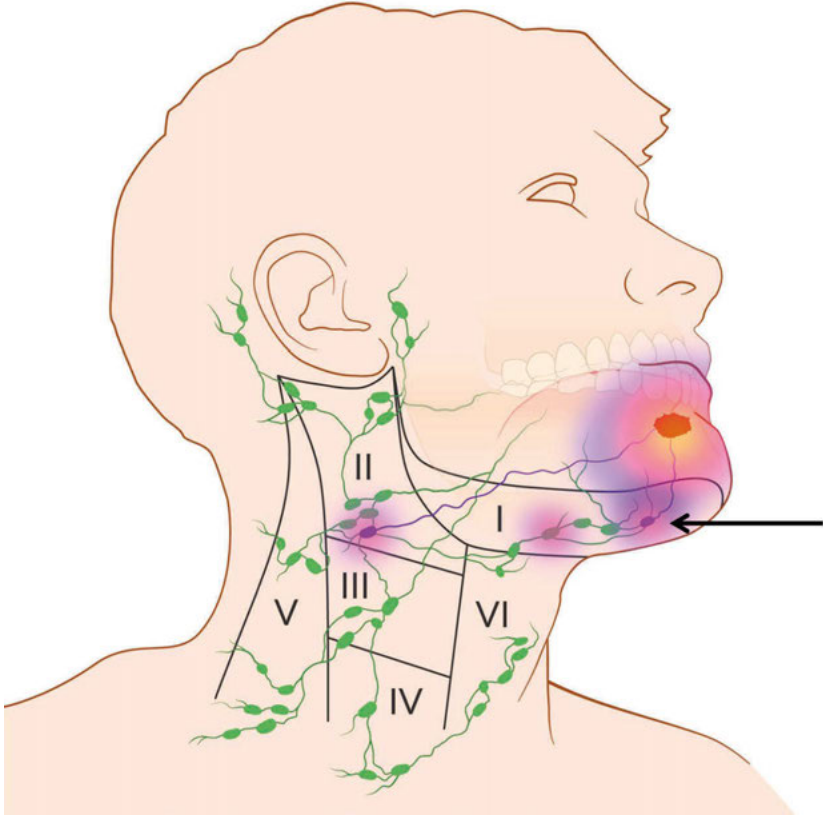


**Figure 1.** Shine through phenomenon. Radiation flare of the primary tumor overshines the hotspot of sentinel lymph node in close proximity to the primary tumor (arrow).

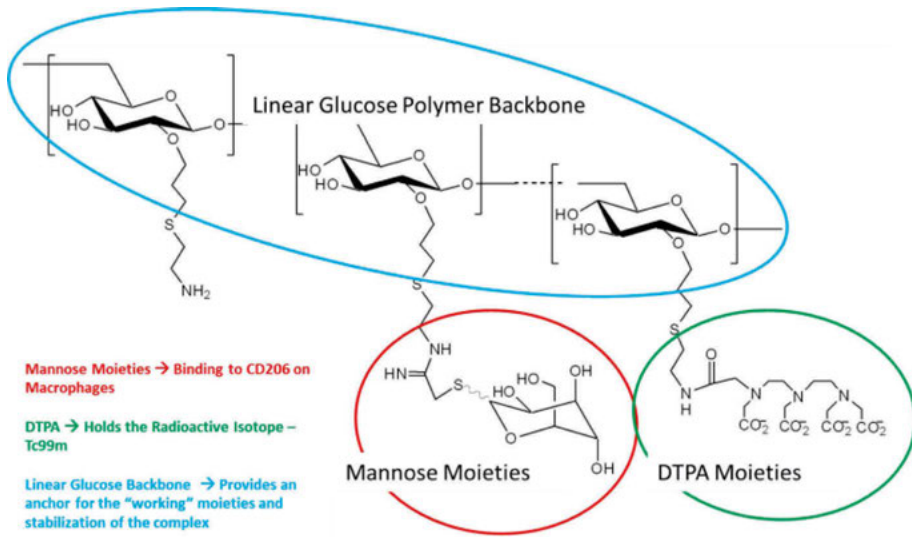


**Figure 2.**  $[^{99m}\text{Tc}]\text{Tc-tilmanocept}$  (Lymphoseek) structure and functional elements.

In Europe  $[^{99m}\text{Tc}]\text{Tc-nanocolloid}$  is the most frequently used radiocolloid for SLN mapping. So far, there are no studies performed comparing head to head  $[^{99m}\text{Tc}]\text{Tc-tilmanocept}$  with  $[^{99m}\text{Tc}]\text{Tc-nanocolloid}$ .

The aim of the present study is to investigate the injection site clearance and uptake in SLN(s) of  $[^{99m}\text{Tc}]\text{Tc-tilmanocept}$  in comparison with a standard  $[^{99m}\text{Tc}]\text{Tc-nanocolloid}$  by means of lymphoscintigraphy in early-stage oral cancer patients.

## Materials and methods

A monocenter prospective within-patient evaluation study was designed in order to compare [<sup>99m</sup>Tc]Tc-tilmanocept with our routinely used [<sup>99m</sup>Tc]Tc-nanocolloid tracer, in terms of SLN visualization, injection site clearance and uptake in SLN(s). This study was approved by the medical ethical review board of the University Medical Center Utrecht (NL58099.041.17).

All patients had an early-stage cT1-2N0M0 OSCC (TNM Staging AJCC UICC 8<sup>th</sup> Edition). Clinical nodal staging was confirmed by at least ultrasound and, in case of suspicious lymph nodes, ultrasound guided fine-needle aspiration cytology. In most cases, MRI was conducted as well, as part of clinical staging.

Patients with a history of neck dissection, neck irradiation or gross injury to the neck, that would hamper surgical dissection of SLNs, were excluded from this study. Besides, patients with a history of head and neck malignancies in the last 5 years were excluded as well.

This study consisted of 2 groups containing 10 patients each (Figure 3). In the first group (cohort 1), 50 µg of [<sup>99m</sup>Tc]Tc-labeled tilmanocept (74 MBq in 0.4 mL) was prepared according to manufacturer's instructions. All tracers were administered in 4 peritumoral injections of 0.1 mL, followed by lymphoscintigraphy. Four to 11 days later, these 10 patients subsequently underwent a [<sup>99m</sup>Tc]Tc-nanocolloid (routine dose 120 MBq) lymphoscintigraphy. After the first cohort, interim analysis was carried out before continuing with the second cohort.

In cohort 2, tracers were administered in opposite order; first 74 MBq [<sup>99m</sup>Tc]Tc-nanocolloid, followed by 74 MBq [<sup>99m</sup>Tc]Tc-tilmanocept. In both cohorts the same imaging protocol was applied. In an effort to administer both tracers at the same injection spots, photographic images were made of the peritumoral injections with consent of patients. Following injection of the second radio-agent, the same imaging protocol was applied. Patients reported their pain scores during the injection procedure for both tracers using the Numeric Pain Rating Scale (NPRS) [15].

### Imaging protocol

Directly post-injection planar images were acquired in dynamic mode (128 × 128 matrix, 20 frames of 1 min) in anterior-posterior projection followed by static mode (256 × 256 matrix, during 4 min) in anterior-posterior and lateral projections (30 min and 2 h post-injection), on a Siemens Symbia T16 SPECT/CT scanner, using “low- and medium energy” (LME) collimators to limit septal penetration (reducing

shine-through) [16]. In addition to the planar imaging 2 h post-injection, SPECT/CT scans were acquired on a  $128 \times 128$  matrix (pixel spacing,  $3.9 \times 3.9$  mm), with 128 angles, 20 s per projection, over a non-circular  $360^\circ$  orbit (CT: 110 kV, 40 mAs eff.,  $16 \times 1.2$  mm). SPECT images were reconstructed using clinical reconstruction software (Siemens Flash3D), with attenuation- and scatter correction (6 iterations, 8 subsets, 5 mm Gaussian filter). Additionally, quantitative SPECT reconstructions were generated using the Utrecht Monte Carlo System (UMCS), a dedicated SPECT reconstructor [17, 18] which includes Monte Carlo modelling of scatter and collimator-detector interactions. During lymphoscintigraphy, a source with known radioactivity was scanned in the same frame as the patient, acting as a verification of quantitative accuracy.

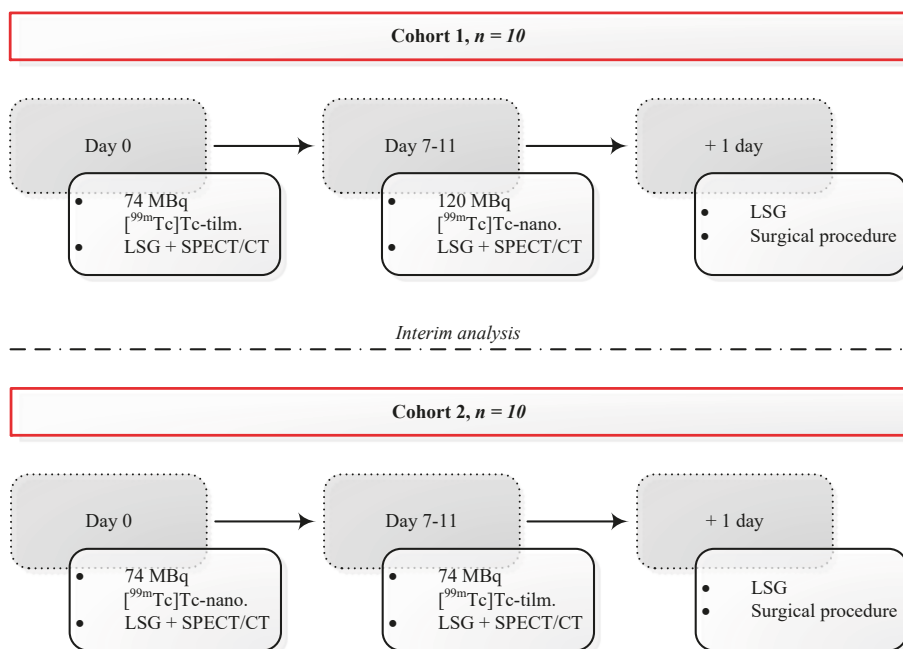


**Figure 3.** Study design.  $[^{99m}\text{Tc}]\text{Tc-tilm.}$ ,  $[^{99m}\text{Tc}]\text{Tc-tilmanocept}$ ;  $[^{99m}\text{Tc}]\text{Tc-nano.}$ ,  $[^{99m}\text{Tc}]\text{Tc-nanocolloid}$ ; LSG, lymphoscintigraphy.

### Intraoperative detection and histology

Intraoperative detection of SLN(s) was performed using a portable gamma-probe, according to standard protocol [3]. The last injected radio-agent was leading to identify SLNs during surgery. In the present study no superselective neck dissection of the preglangular triangle of level I was performed in floor-of-mouth tumors. All harvested nodes were histologically examined for metastasis using step-serial-sectioning (intervals of  $150 \mu\text{m}$ ) with hematoxylin-eosin and pan-cytokeratin

antibody (AE 1/3) staining at each level.

### Evaluation of images

Paired images of both tracers were evaluated regarding similarity of depicted draining lymph node basins, the number and location of SLNs and their histopathology. Furthermore, the amount of radioactivity that resided in the injection site, SLNs, higher echelon nodes, and reference source were measured from quantitative SPECT/CT images, acquired 2 h post-injection.

Volumes of Interest (VOIs) around the injection site, SLNs and the reference source were automatically defined using in-house developed software, adopting a local peak finding algorithm and watershed segmentation [19] (Figure 4a). The VOIs were manually validated with 3D segmentation software ITK-SNAP [20] (Figure 4b). All quantitative results of VOI measurements are presented as percentages of the amount of injected radioactivity. The remaining radioactivity outside of the VOIs but within field of view of the SPECT acquisition was regarded to be  $^{99m}\text{Tc}$  located outside the (S)LNs, injection site or reference source and is further addressed as background radioactivity. Since the measured cumulative background radioactivity is strongly dependent on the volume of the patient within the field of view of SPECT acquisition, the background activity is also presented in terms of standardized uptake value (SUV), analogous to PET (i.e., average measured activity concentration in background, divided by the average activity concentration in the entire patient, based on body mass).

For qualitative evaluation of  $^{99m}\text{Tc}$ -nanocolloid and  $^{99m}\text{Tc}$ -tilmanocept lymphoscintigraphy, images of each subject for both tracers were blinded and scored by 2 head and neck surgeons and 2 nuclear medicine physicians. Per image, every hotspot was classified as SLN using a 3-point scale (yes, potential, no). Afterwards, every “potential” scored SLN was eventually dichotomized into “yes” or “no” by the observers, based on their advice to surgically harvest the concerning lymph node. Besides, all observers rated the difficulty for reviewing the images (i.e., easy, moderate, hard). Interobserver variability regarding the selected SLNs between observers was assessed.

Ultimately, data from qualitative analyses were matched with quantitative results of corresponding VOIs and correlated with intra-operative and pathological findings of the harvested (S)LNs.

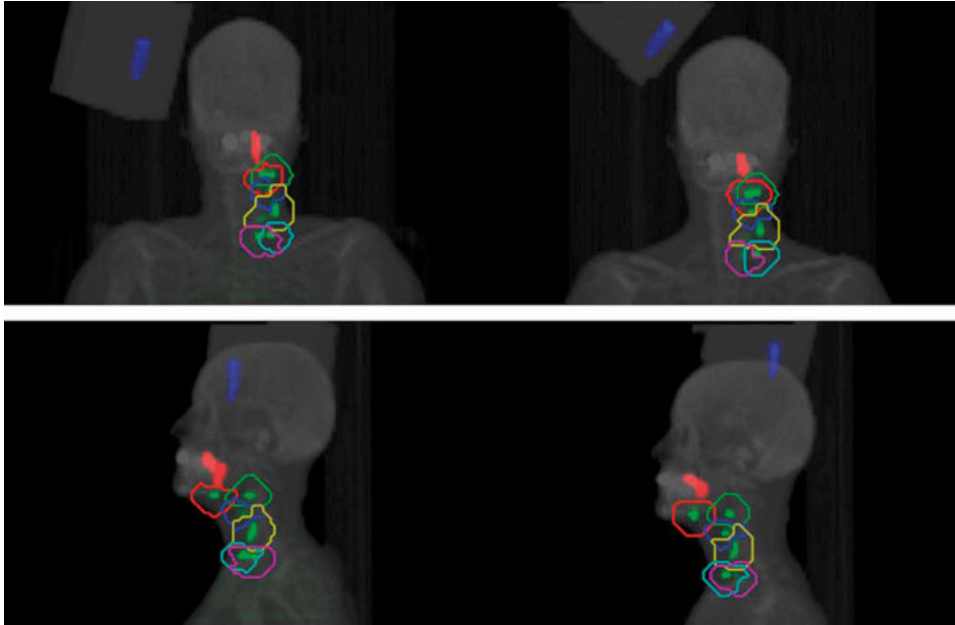


**Figure 4a.** Algorithmic defined VOIs for all hotspots within the scanned area for both  $[^{99m}\text{Tc}]\text{Tc-tilmanocept}$  and  $[^{99m}\text{Tc}]\text{Tc-nanocolloid}$ . Summed intensity projections of SPECT reconstructions of the same patient, injected with either  $[^{99m}\text{Tc}]\text{Tc-tilmanocept}$  (left) or  $[^{99m}\text{Tc}]\text{Tc-nanocolloid}$  (right). Injection site: Red hotspot. Reference source: Blue hotspot. “Hot” lymph nodes: Green hotspots with colored VOIs.

### Statistical analyses

All data was analyzed with professional statistics software (IBM SPSS Statistics Version 25.0). Data is expressed as mean  $\pm$  SD for parametric continuous variables and as median for nonparametric continuous variables. Number of cases and percentages are presented as categorical variables. All quantitative results of VOI measurements are presented as percentages of the amount of injected radioactivity.

To compare the amount of radioactivity in the injection site, SLNs, higher echelon nodes and background between  $[^{99m}\text{Tc}]\text{Tc-tilmanocept}$  and  $[^{99m}\text{Tc}]\text{Tc-nanocolloid}$ , paired Samples T-tests were applied for parametric variables, while Wilcoxon signed-rank tests were applied for nonparametric variables. To compare the “SLN to injection site ratio” in radioactivity between  $[^{99m}\text{Tc}]\text{Tc-nanocolloid}$  and  $[^{99m}\text{Tc}]\text{Tc-tilmanocept}$ , a Wilcoxon signed-rank test was applied.

To determine interobserver variability regarding selected SLNs between observers for both  $[^{99m}\text{Tc}]\text{Tc-nanocolloid}$  and  $[^{99m}\text{Tc}]\text{Tc-tilmanocept}$  lymphoscintigraphic images, Fleiss’ kappa statistics were applied [21]. Finally, to compare the rated difficulty for reviewing  $[^{99m}\text{Tc}]\text{Tc-nanocolloid}$  and  $[^{99m}\text{Tc}]\text{Tc-tilmanocept}$  lymphoscintigraphic

images, McNemar tests were applied. A p-value of  $< 0.05$  was regarded as statistically significant.

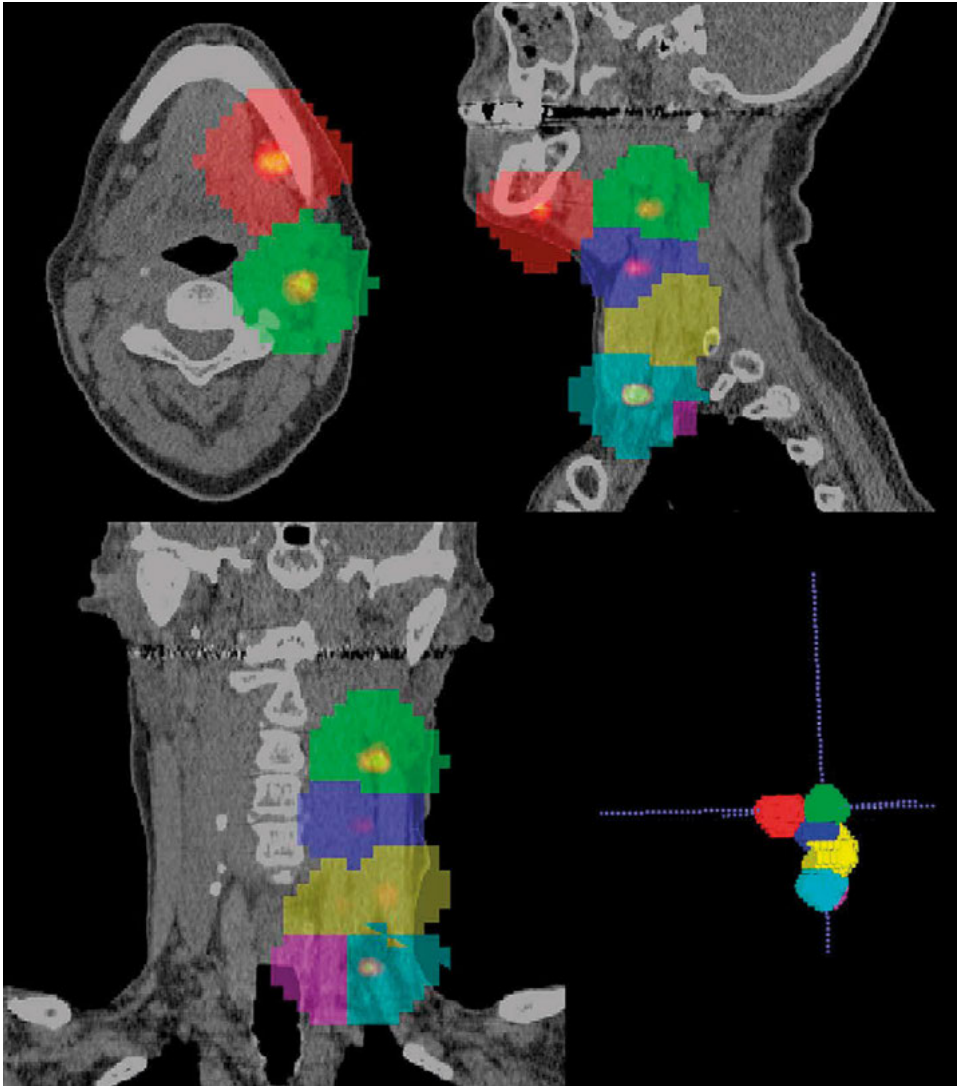


**Figure 4b.** Verification of VOIs containing "hot" lymph nodes using 3D segmentation software (ITK-SNAP). Sentinel lymph nodes: *Red and green VOI*. Higher echelon nodes: *Blue, yellow, turquoise and purple VOI*.

## Results

Characteristics of the 20 patients and tumors are listed in Table 1. The oral tongue was the most affected tumor location. In 5 (25%) cases, the floor-of-mouth was involved. In total, 49 SLNs were harvested (median 2), of which 12 (24%) showed metastasis. These 12 positive SLNs were harvested from 7 patients, making 35% (7 of 20) of our study population positive for lymphatic metastasis. Distribution of hotspots and SLNs per tracer per patient is given in supplementary data 1.

**Table 1.** Patient characteristics.

Characteristics	Overall (%)
<b>Patients, n (%)</b>	20 (100%)
<b>Gender</b>	
Male	13 (75%)
Female	7 (35%)
<b>Median age (y) (range)</b>	63 (39-77)
<b>Tumor location, n (%)</b>	
Tongue	14 (70%)
Floor-of-mouth	5 (25%)
Lower gum	1 (5%)
Retromolar trigone	7 (13%)
Lower gum	3 (6%)
<b>Clinical T-stage, n (%)<sup>a</sup></b>	
T1	9 (45%)
T2	11 (55%)
<b>Pathology primary tumor</b>	3 (0-6)
Diameter (mm) (range)	19 (6-44)
Depth-of-invasion (mm) (range)	6 (1-13)
<b>Pathology sentinel lymph nodes</b>	
Negative	37 (76%)
Positive	12 (24%)
<b>Median harvested SLNs (range)</b>	2 (1-5)
<b>Number of SLN-positive patients (%)</b>	7 (35%)

<sup>a</sup> T-stage according to AJCC TNM classification, 8<sup>th</sup> edition.

### Quantitative analyses (Table 2)

The radioactivity remaining in the injection site was significantly lower for [<sup>99m</sup>Tc]Tc-tilmanocept (29.9%; SD ± 7.6), compared to [<sup>99m</sup>Tc]Tc-nanocolloid (60.9%; SD ± 16.1) (p < 0.001).

The radioactive uptake in SLNs was significantly lower for [<sup>99m</sup>Tc]Tc-tilmanocept compared with [<sup>99m</sup>Tc]Tc-nanocolloid (1.95% vs. 3.16% respectively,  $p = 0.010$ ). The SLN to injection site ratio between [<sup>99m</sup>Tc]Tc-tilmanocept (0.066) and [<sup>99m</sup>Tc]Tc-nanocolloid (0.054) was not statistically different ( $p = 0.232$ ). In 20 patients, a median of 3.0 and 2.5 SLNs were identified with [<sup>99m</sup>Tc]Tc-tilmanocept and [<sup>99m</sup>Tc]Tc-nanocolloid, respectively ( $p = 0.297$ ).

The number of higher echelon nodes did not differ significantly between both tracers with a median of 2.0 in the [<sup>99m</sup>Tc]Tc-tilmanocept cohort and 2.5 in the [<sup>99m</sup>Tc]Tc-nanocolloid group ( $p = 0.083$ ). [<sup>99m</sup>Tc]Tc-tilmanocept showed less radioactive uptake in higher echelon nodes in comparison with the [<sup>99m</sup>Tc]Tc-nanocolloid group, although not statistically significant (0.57% vs 0.86% respectively,  $p = 0.052$ ).

[<sup>99m</sup>Tc]Tc-tilmanocept showed a higher background radioactivity in comparison with [<sup>99m</sup>Tc]Tc-nanocolloid (2.23% vs 0.41% in field of view of the SPECT,  $p < 0.001$ . SUV: 0.132 vs. 0.018,  $p < 0.001$ ).

A median pain score (NPRS) of 3.0 (range 0 – 8) was reported for [<sup>99m</sup>Tc]Tc-tilmanocept compared with 2.0 (range 0 – 8) for [<sup>99m</sup>Tc]Tc-nanocolloid ( $p = 0.041$ ).

**Table 2.** Quantitative analyses.

	[ <sup>99m</sup> Tc]Tc-tilmanocept	[ <sup>99m</sup> Tc]Tc-nanocolloid	p-value
<b>Radioactivity remaining in injection site</b>	29.9%; SD $\pm 7.6$ (range 17.10 – 43.95)	60.9%; SD $\pm 16.1$ (range 30.26 – 89.58)	< 0.001
<b>Uptake in SLNs</b>	1.95%; IQR $\pm 2.6$ (range 0.21 – 6.80)	3.16%; IQR $\pm 3.9$ (range 0.04 – 11.90)	0.010
<b>SLN to injection site ratio</b>	0.066; IQR $\pm 0.1$ (range 0.001 – 0.20)	0.054; IQR $\pm 0.07$ (range 0.001 – 0.22)	0.232
<b>Number of SLNs</b>	3.0; IQR $\pm 2$ (range 0 – 4)	2.5; IQR $\pm 1$ (range 1 – 5)	0.297
<b>Number of higher echelon nodes</b>	2.0; IQR $\pm 2$ (range 0 – 5)	2.5; IQR $\pm 3$ (range 0 – 6)	0.083
<b>Uptake in higher echelon nodes</b>	0.57%; IQR $\pm 1.64$ (range 0.001 – 7.15)	0.86%; IQR $\pm 2.17$ (range 0.001 – 6.95)	0.052
<b>Background activity</b>	2.23%; IQR $\pm 2.01$ (range 0.93 – 5.76)	0.41%; IQR $\pm 0.96$ (range 0.01 – 1.55)	< 0.001
<b>Pain score (NPRS)</b>	3.0; IQR $\pm 3$ (range 0 – 8)	2.0; IQR $\pm 4$ (range 0 – 8)	0.041

SD; standard deviation, IQR; interquartile range, SLN; sentinel lymph node.

### Qualitative analyses

Interobserver agreement regarding selection of SLNs with a 3-point scale using Fleiss' kappa statistics showed substantial agreement for both [<sup>99m</sup>Tc]Tc-tilmanocept and [<sup>99m</sup>Tc]Tc-nanocolloid ( $\kappa=0.677$  [95% CI 0.619-0.735] vs.  $\kappa=0.725$  [95% CI 0.668-0.782] respectively, not significantly different). When dichotomizing, both tracers reached excellent agreement with an equal Fleiss Kappa ( $\kappa=0.885$  [95% CI 0.804-0.966] for [<sup>99m</sup>Tc]Tc-tilmanocept and  $\kappa=0.885$  [95% CI 0.806-0.963] for [<sup>99m</sup>Tc]Tc-nanocolloid).

[<sup>99m</sup>Tc]Tc-tilmanocept scans were categorized scored as easy (6×), moderate (10×) and hard (4×), whereas [<sup>99m</sup>Tc]Tc-nanocolloid was ranked as easy (6×), moderate (9×) and hard (5×) (McNemar test,  $p = 0.80$ ).

No serious adverse events or allergic reactions were reported in our study population.

## Discussion

The present study is the first within-patient evaluation comparing [<sup>99m</sup>Tc]Tc-tilmanocept with [<sup>99m</sup>Tc]Tc-nanocolloid. We showed a significantly higher injection site clearance for [<sup>99m</sup>Tc]Tc-tilmanocept but also a significantly lower uptake in the SLN in comparison with [<sup>99m</sup>Tc]Tc-nanocolloid. No significant difference was seen in SLN to injection site ratio. There was an excellent interobserver agreement for both [<sup>99m</sup>Tc]Tc-tilmanocept and [<sup>99m</sup>Tc]Tc-nanocolloid. Thereby, difficulty of scan interpretation was equal for both tracers.

5  
Currently, there are no other within-patient evaluation studies comparing [<sup>99m</sup>Tc]Tc-tilmanocept to another radioactive tracer. Only one RCT so far has been published by Unkart et al., who presented a trial of 57 breast cancer patients comparing [<sup>99m</sup>Tc]Tc-tilmanocept with [<sup>99m</sup>Tc]Tc-sulfur colloid regarding pain after injection of both tracers [22]. They showed a higher pain sensation in the first 3 minutes after injection of [<sup>99m</sup>Tc]Tc-sulfur colloid compared with [<sup>99m</sup>Tc]Tc-tilmanocept. In contrast, in our study, a higher pain score was found for [<sup>99m</sup>Tc]Tc-tilmanocept as compared with [<sup>99m</sup>Tc]Tc-nanocolloid, regardless whether [<sup>99m</sup>Tc]Tc-tilmanocept was injected as first or second tracer. However, our study size is small and the clinical relevance of a difference of 1 point (median 2.0 vs. 3.0) is questionable.

Additionally, Unkart et al. found no statistical differences in breast cancer patients concerning number of hotspots, number of removed SLNs, time to surgical removal or number of blue nodes for [<sup>99m</sup>Tc]Tc-Tilmanocept compared to [<sup>99m</sup>Tc]Tc-sulfur colloid [23]. However, this study was not especially designed for analyzing differences regarding SLN identification. Randomizing patients for either the one or the other tracer did not clearly clarify discrepancies between both tracers with respect to drainage patterns due to a high variability in lymphatic drainage per patient, especially in complex lymphatic regions. Therefore, it is our opinion that a within-patient study design is superior to reveal characteristics regarding lymphatic drainage patterns of both tracers.

As already mentioned in the introduction, [<sup>99m</sup>Tc]Tc-tilmanocept was specifically designed for SLN identification, providing characteristics that could be of potential value in complex lymphatic regions, as is the case in OSCC. Our data clearly underlines its theoretical effect of a more rapid clearance of the radioactivity from the injection site due to its smaller molecular size. This may benefit SLN detection, particularly in situations with close spatial relation between injection site and SLNs, which is especially the case in floor-of-mouth tumors. Using [<sup>99m</sup>Tc]Tc-tilmanocept, Agrawal et al. supported this theory with an impressively low false-negative rate

of 2.56% for SLNB in OSCC, which was also found in floor-of-mouth tumors [14]. In that study however, a complementary neck dissection in the same session was performed as validation method (reference standard) for the SLNB procedure. However, micrometastases remain undetected in up to 15% of routinely processed neck dissection specimens [24, 25]. Therefore, in case of a negative SLNB, a wait-and-scan approach should be considered the best gold-standard [26]. As a consequence, further studies with long-term follow-up are needed to investigate the efficacy of [<sup>99m</sup>Tc]Tc-tilmanocept for detection of occult metastases.

In our study, a higher percentage of radioactivity in background was seen for [<sup>99m</sup>Tc]Tc-tilmanocept compared with [<sup>99m</sup>Tc]Tc-nanocolloid. One possible explanation could be the smaller molecular diameter of 7 nanometers, which enhances diffusion into lymphatic channels as well as blood capillaries. As stated by Ellner et al., [<sup>99m</sup>Tc]Tc-tilmanocept showed a percentage of injected dose below 2.6% for the liver, kidney, bladder and head [27]. Although the background radioactivity for [<sup>99m</sup>Tc]Tc-tilmanocept was still marginal (2.23%; SUV 0.132), it explains the residual distribution of [<sup>99m</sup>Tc]Tc-tilmanocept in the presence of a lower radioactivity residing in both the injection site, as well as in the lymph nodes.

One of our study limitations is the difference in amount of radioactivity between both tracers in the first 10 patients: 74 MBq [<sup>99m</sup>Tc]Tc-tilmanocept vs 120 MBq [<sup>99m</sup>Tc]Tc-nanocolloid, respectively. [<sup>99m</sup>Tc]Tc-tilmanocept was approved by the FDA (Food and Drug Administration) and EMA (European Medicines Agency) for identification of SLNs using 74 MBq in a two-day protocol. In our institution SLNB is routinely performed with 120 MBq [<sup>99m</sup>Tc]Tc-nanocolloid. Because the first 10 patients were surgically treated based on [<sup>99m</sup>Tc]Tc-nanocolloid, they received this routinely used amount of radioactivity to safely perform SLNB. This difference was corrected during quantitative analysis by correlating measured radioactivity in the VOIs to the radioactive dose injected. In the second 10 patients, [<sup>99m</sup>Tc]Tc-tilmanocept was leading for SLNB procedure and therefore the amount of radioactivity could be equalized for both tracers (74 MBq). Another limitation is the impossibility of comparing hotspots at different time points post-injection. Due to the impossibility of performing attenuation correction on planar lymphoscintigraphy, we unfortunately could not reliably compare SLN visualization at different time points due to different imaging modalities. Intensity of hotspots could easily be under- or overestimated based on physiological structures in near surroundings (e.g., mandible). On planar lymphoscintigraphy, only anterior-posterior or oblique images could be used. This impedes us from differentiating and analyzing hotspots located in the same plane. Therefore, we opted to perform only quantitative analysis based on SPECT/CT.

In some patients for whom [<sup>99m</sup>Tc]Tc-tilmanocept was leading to identify SLNs during surgery, it proved challenging to accurately locate SLNs due to a scarce of activity on the second day, which was considered a drawback by the surgeon. This may be due to the relatively low radioactive uptake in SLNs of [<sup>99m</sup>Tc]Tc-tilmanocept that was seen in our population. As the injected activity was lower than what was used in [<sup>99m</sup>Tc]Tc-nanocolloid SLNB (74 vs. 120 MBq) with also lower uptake in SLNs (3.16% vs. 1.95%) this resulted in less activity in SLNs in SLNB with [<sup>99m</sup>Tc]Tc-tilmanocept, on average 1.4 MBq vs. 3.8 MBq at time of SLN scintigraphy. Vidal-Sicart et al. faced similar challenges during intraoperative localization of SLNs using [<sup>99m</sup>Tc]Tc-tilmanocept , which can probably be overcome by a higher injection dose of [<sup>99m</sup>Tc] Tc-tilmanocept [13].

In conclusion, our results suggest that [<sup>99m</sup>Tc]Tc-tilmanocept had a higher injection site clearance, but at the same time a lower uptake in the SLN, resulting in an SLN to injection site ratio, which was not significantly different from [<sup>99m</sup>Tc]Tc-nanocolloid. The relatively low radioactive uptake in SLNs of [<sup>99m</sup>Tc]Tc-tilmanocept may limit intraoperative detection of SLNs, but might be overcome by a higher injection dose.

## References

1. Alkureishi LW, Burak Z, Alvarez JA, et al. Joint practice guidelines for radionuclide lymphoscintigraphy for sentinel node localization in oral/oropharyngeal squamous cell carcinoma. *Ann Surg Oncol*. 2009;16(11):3190-3210. doi:10.1245/s10434-009-0726-8
2. Giammarile F, Schilling C, Gnanasegaran G, et al. The EANM practical guidelines for sentinel lymph node localisation in oral cavity squamous cell carcinoma. *Eur J Nucl Med Mol Imaging*. 2019;46(3):623-637. doi:10.1007/s00259-018-4235-5
3. Schilling C, Stoeckli SJ, Vigili MG, et al. Surgical consensus guidelines on sentinel node biopsy (SNB) in patients with oral cancer. *Head Neck*. 2019;41(8):2655-2664. doi:10.1002/hed.25739
4. Liu M, Wang SJ, Yang X, Peng H. Diagnostic efficacy of sentinel lymph node biopsy in early oral squamous cell carcinoma: a meta-analysis of 66 studies. *PLoS One*. 2017;12(1):e0170322. doi:10.1371/journal.pone.0170322
5. Alkureishi LW, Ross GL, Shoaib T, et al. Sentinel node biopsy in head and neck squamous cell cancer: 5-year follow-up of a European multicenter trial. *Ann Surg Oncol*. 2010;17(9):2459-2464. doi:10.1245/s10434-010-1111-3
6. Pedersen NJ, Jensen DH, Hedbäck N, et al. Staging of early lymph node metastases with the sentinel lymph node technique and predictive factors in T1/T2 oral cavity cancer: A retrospective single-center study. *Head Neck*. 2016;38 Suppl 1:E1033-E1040. doi:10.1002/hed.24153
7. Den Toom IJ, Heuveling DA, Flach GB, et al. Sentinel node biopsy for early-stage oral cavity cancer: the VU University Medical Center experience. *Head Neck*. 2015;37(4):573-578. doi:10.1002/hed.23632
8. Civantos FJ, Zitsch RP, Schuller DE, et al. Sentinel lymph node biopsy accurately stages the regional lymph nodes for T1-T2 oral squamous cell carcinomas: results of a prospective multi-institutional trial. *J Clin Oncol*. 2010;28(8):1395-1400. doi:10.1200/JCO.2008.20.8777
9. Stoeckli SJ, Huebner T, Huber GF, Broglie MA. Technique for reliable sentinel node biopsy in squamous cell carcinomas of the floor of mouth. *Head Neck*. 2016;38(9):1367-1372. doi:10.1002/hed.24440
10. Flach GB, van Schie A, Witte BI, et al. Practice variation in defining sentinel lymph nodes on lymphoscintigrams in oral cancer patients. *Eur J Nucl Med Mol Imaging*. 2014;41(12):2249-2256. doi:10.1007/s00259-014-2843-2
11. Vera DR, Wallace AM, Hoh CK, Mattrey RF. A synthetic macromolecule for sentinel node detection:  $^{99m}\text{Tc}$ -DTPA-mannosyl-dextran. *J Nucl Med*. 2001;42(6):951-959.
12. Wallace AM, Hoh CK, Vera DR, Darrah DD, Schulteis G. Lymphoseek: a molecular radiopharmaceutical for sentinel node detection. *Ann Surg Oncol*. 2003;10(5):531-538. doi:10.1245/aso.2003.07.012
13. Vidal-Sicart S, Vera DR, Valdés Olmos RA. Next generation of radiotracers for sentinel lymph node biopsy: What is still necessary to establish new imaging paradigms? *Rev Esp Med Nucl Imagen Mol (Engl Ed)*. 2018;37(6):373-379. doi:10.1016/j.remnm.2018.09.001
14. Agrawal A, Civantos FJ, Brumund KT, et al. [ $^{99m}\text{Tc}$ ]Tilmanocept accurately detects sentinel lymph nodes and predicts node pathology status in patients with oral squamous cell carcinoma of the head and neck: results of a phase III multi-institutional trial. *Ann Surg Oncol*. 2015;22(11):3708-3715. doi:10.1245/s10434-015-4382-x
15. Hawker GA, Mian S, Kendzerska T, French M. Measures of adult pain: Visual Analog Scale for Pain (VAS Pain), Numeric Rating Scale for Pain (NRS Pain), McGill Pain Questionnaire (MPQ), Short-Form McGill Pain Questionnaire (SF-MPQ), Chronic Pain Grade Scale (CPGS), Short Form-36 Bodily Pain Scale (SF-36 BPS), and Measure of Intermittent and Constant Osteoarthritis Pain (ICOAP). *Arthritis Care Res (Hoboken)*. 2011;63 Suppl 11:S240-S252. doi:10.1002/acr.20543
16. Yoneyama H, Tsushima H, Kobayashi M, Onoguchi M, Nakajima K, Kinuya S. Improved detection of sentinel lymph nodes in SPECT/CT images acquired using a low- to medium-energy general-purpose collimator. *Clin Nucl Med*. 2014;39(1):e1-e6. doi:10.1097/RLU.0b013e31828da362
17. Beekman FJ, de Jong HW, Slijpen ET. Efficient SPECT scatter calculation in non-uniform media using correlated Monte Carlo simulation. *Phys Med Biol*. 1999;44(8):N183-N192. doi:10.1088/0031-9155/44/8/402
18. Beekman FJ, de Jong HW, van Geloven S. Efficient fully 3-D iterative SPECT reconstruction with Monte Carlo-based scatter compensation. *IEEE Trans Med Imaging*. 2002;21(8):867-877. doi:10.1109/TMI.2002.803130

19. van der Walt S, Schönberger JL, Nunez-Iglesias J, et al. scikit-image: image processing in Python. *PeerJ*. 2014;2:e453. doi:10.7717/peerj.453
20. Yushkevich PA, Piven J, Hazlett HC, et al. User-guided 3D active contour segmentation of anatomical structures: significantly improved efficiency and reliability. *Neuroimage*. 2006;31(3):1116-1128. doi:10.1016/j.neuroimage.2006.01.015
21. Landis JR, Koch GG. The measurement of observer agreement for categorical data. *Biometrics*. 1977;33(1):159-174.
22. Unkart JT, Baker JL, Hosseini A, et al. Comparison of post-injection site pain between technetium sulfur colloid and technetium tilmanocept in breast cancer patients undergoing sentinel lymph node biopsy. *Ann Surg Oncol*. 2015;22 Suppl 3:S559-S565. doi:10.1245/s10434-015-4802-y
23. Unkart JT, Hosseini A, Wallace AM. Tc-99m tilmanocept versus Tc-99m sulfur colloid in breast cancer sentinel lymph node identification: Results from a randomized, blinded clinical trial. *J Surg Oncol*. 2017;116(7):819-823. doi:10.1002/jso.24735
24. Ambrosch P, Kron M, Fischer G, Brinck U. Micrometastases in carcinoma of the upper aerodigestive tract: detection, risk of metastasizing, and prognostic value of depth of invasion. *Head Neck*. 1995;17(6):473-479. doi:10.1002/hed.2880170604
25. Rinaldo A, Devaney KO, Ferlito A. Immunohistochemical studies in the identification of lymph node micrometastases in patients with squamous cell carcinoma of the head and neck. *ORL J Otorhinolaryngol Relat Spec*. 2004;66(1):38-41. doi:10.1159/000077232
26. de Bree R, Hoekstra OS. The potential of FDG-PET in the detection of occult lymph node metastasis: importance of patient selection and reference standard. *Eur Arch Otorhinolaryngol*. 2013;270(8):2173-2174. doi:10.1007/s00405-013-2365-8
27. Ellner SJ, Hoh CK, Vera DR, Darrach DD, Schulteis G, Wallace AM. Dose-dependent biodistribution of [<sup>99m</sup>Tc]DTPA-mannosyl-dextran for breast cancer sentinel lymph node mapping. *Nucl Med Biol*. 2003;30(8):805-810. doi:10.1016/j.nucmedbio.2003.10.001

# Supplementary data

**Supplementary data 1.** Distribution of hotspots and SLNs per tracer per patient.

Patient	cT stage	Tumor location	Side	Hotspots Agent 1	Hotspots Agent 2	Harvested SLNs peroperatively	Pathology
1	T2	Tongue	Left	<u>Ib</u>	Ib	Ib	Positive
				<u>II</u>	II	Ia	Negative
				<u>III</u>	III		
2	T1	Tongue	Left	<u>II</u>	II	Ia	Negative
				<u>II</u>	II	Ia	Negative
						Ib	Negative
3	T2	Tongue	Right	<u>II</u>	II	III	Negative
				<u>Right</u>	Right	Ia	Negative
						Ia	Negative
4	T1	Floor-of-mouth	Right	<u>Ia</u>	Ia	Ia	Negative
				<u>Ib</u>	Ib	Ib	Negative
				<u>Ib</u>	III	III	Negative
5	T1	Floor-of-mouth	Midline	<u>Ib</u>	Ib	Ib	Negative
				<u>Right</u>	Right		
				<u>Left</u>	Left		
6	T2	Tongue	Right	<u>II</u>	II	Ib	Negative
				<u>Right</u>	Right		
				<u>Right</u>	Right		
7	T2	Tongue	Right	<u>II</u>	II	Ib	Negative
				<u>Ib</u>	III	Ib	Positive
				<u>III</u>	IV	IV	Positive

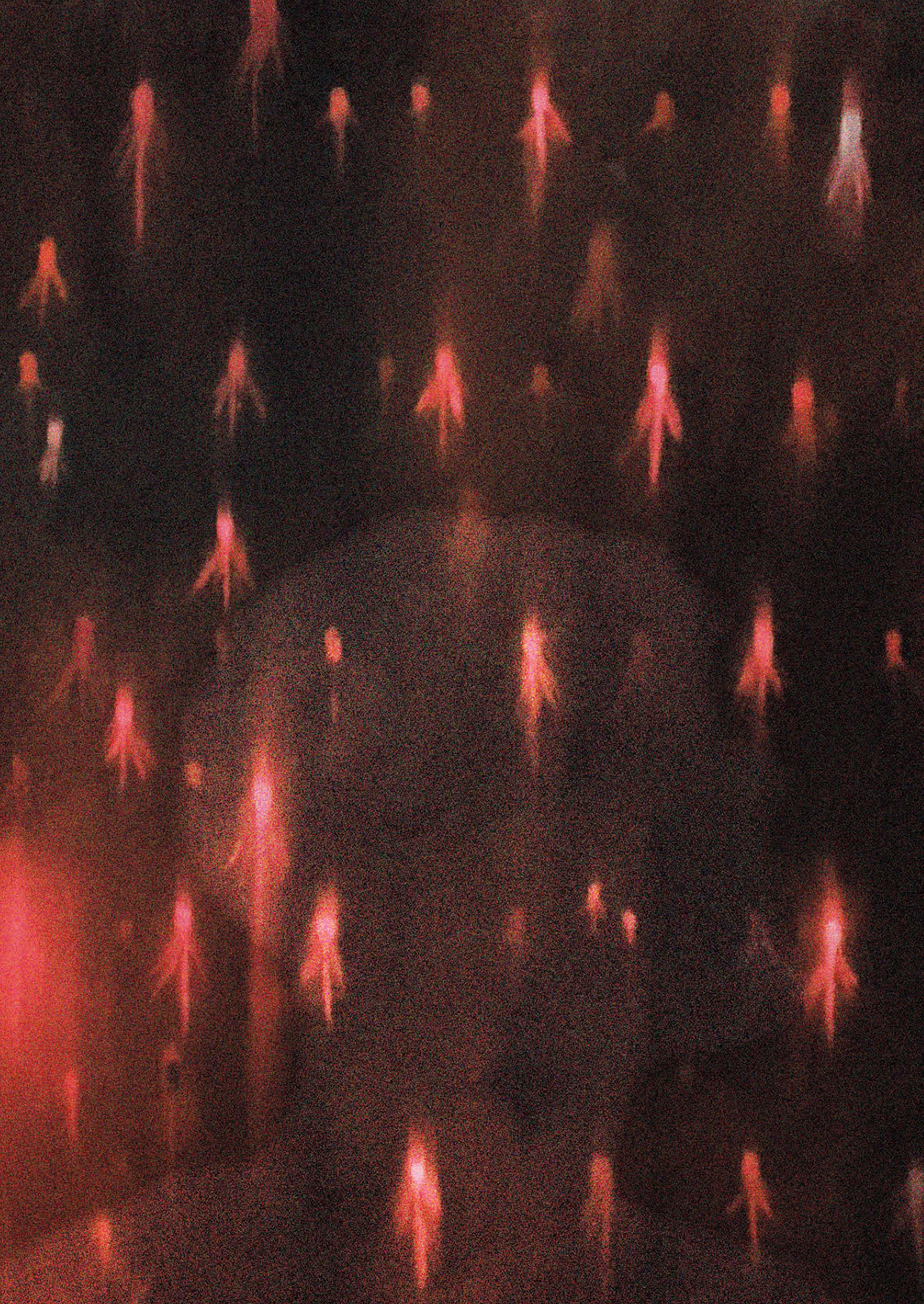
## Supplementary data 1. Continued.

Patient	cT stage	Tumor location	Side	Hotspots Agent 1	Hotspots Agent 2	Harvested SLNs peroperatively	Pathology
8	T1	Tongue	Left	<u>Ib</u> <u>II</u> <u>Left</u>	<u>II</u> <u>Left</u>	<u>III</u> <u>Left</u>	Negative Negative
9	T2	Tongue	Right	<u>I</u> <u>II</u> <u>III</u> <u>II</u>	<u>Right</u> <u>Right</u> <u>Left</u> <u>III</u> <u>Left</u>	<u>Right</u> <u>Ib</u> <u>IIa</u> <u>IIa</u> <u>III</u> <u>Left</u> <u>Left</u>	Positive Negative Negative Negative Negative Negative
10	T1	Floor-of-mouth	Left	<u>Ib</u> <u>II</u> <u>II</u>	<u>II</u> <u>Left</u> <u>II</u>	<u>IIa</u> <u>IIa</u> <u>IIa</u>	Negative Negative Negative
11	T1	Floor-of-mouth	Right	<u>Ia</u> <u>II</u> <u>III</u> <u>II</u> <u>IV</u>	<u>Right</u> <u>Right</u> <u>Right</u> <u>Left</u> <u>Left</u>	<u>Ib</u> <u>IIb</u> <u>IIb</u> <u>IIb</u> <u>Ia</u> <u>IIb</u> <u>IIa</u>	Negative Negative Negative Negative Negative Negative Negative
12	T1	Floor-of-mouth	Left	<u>Ia</u> <u>III</u> <u>III</u>	<u>II</u> <u>III</u> <u>Right</u>	<u>IIa</u> <u>IIa</u> <u>IIa</u>	Negative Negative Negative
13	T2	Tongue	Right	<u>II</u>	<u>II</u>	<u>IIa</u>	Negative
14	T2	Lower alveolus and gingiva	Left	<u>III</u>	<u>II</u>	<u>IIa</u>	Positive
15	T1	Tongue	Left	<u>Ib</u> <u>IV</u>	<u>Ib</u> <u>II</u> <u>III</u> <u>IV</u>	<u>Ib</u> <u>Ib</u> <u>Ib</u> <u>Left</u> <u>Left</u>	Negative Negative Negative Negative

Supplementary data 1. Continued.

Patient	cT stage	Tumor location	Side	Hotspots Agent 1	Hotspots Agent 2	Harvested SLNs peroperatively	Pathology
16	T2	Tongue	Right	II Right	<u>II</u> <u>Right</u>	IIb Right	Positive
17	T2	Tongue	Left	II Left	<u>III</u> <u>Right</u>	III Right	Positive
			Left	II Left	<u>II</u> <u>Left</u>	IIa Left	Positive
			Left	II Left	<u>II</u> <u>Left</u>	IIa Left	Positive
			Left	II Left	<u>II</u> <u>Left</u>	IIa Left	Positive
			Left	II Left	<u>II</u> <u>Left</u>	IIb Left	Negative
			Left	II Left	<u>II</u> <u>Left</u>	IIb Left	Negative
18	T2	Tongue	Left	Ia Left	<u>Ia</u> <u>Left</u>	Ia Left	Negative
			Left	Ib Left	<u>Ib</u> <u>Left</u>	Ia Left	Negative
			Left	II Left	<u>II</u> <u>Left</u>	IIb Left	Negative
19	T1	Tongue	Left	Ia Left	<u>Ia</u> <u>Left</u>	Ia Left	Negative
			Left	II Left	<u>II</u> <u>Left</u>	Ia Left	Negative
			Left	II Left	<u>II</u> <u>Left</u>	IIb Left	Negative
20	T2	Tongue	Left	Ib Right	<u>II</u> <u>Right</u>	Ib Left	Positive
			Left	II Right	<u>III</u> <u>Right</u>	III Left	Negative
			Left	III Right	<u>Ia</u> <u>Left</u>		
			Left	Ib Left	<u>Ib</u> <u>Left</u>		
			Left	III Left	<u>III</u> <u>Left</u>		

Note: All underlined levels are found with [<sup>99m</sup>Tc]Tc-tilmanocept as radioactive agent.



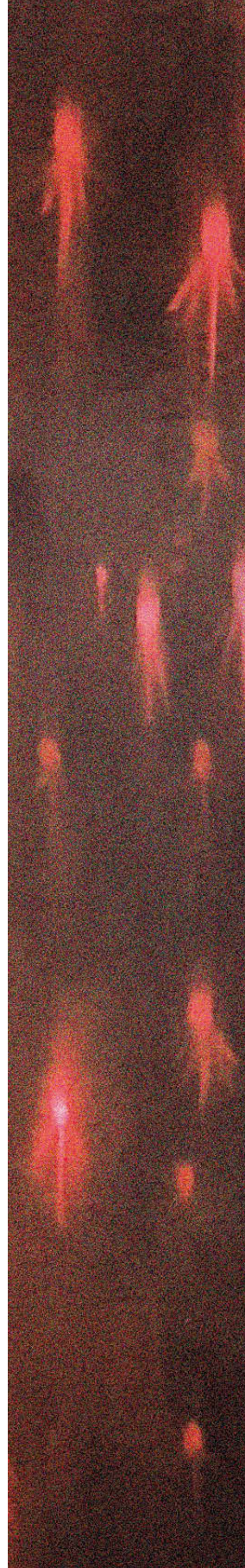
# 6

## Diagnostic accuracy of [<sup>99m</sup>Tc]Tc-tilmanocept compared to [<sup>99m</sup>Tc]Tc-nanocolloid for sentinel lymph node identification in early-stage oral cancer

---

Rutger Mahieu, Inne J. den Toom, Rob van Rooij, Robert J.J. van Es,  
Monique G.G. Hobbelink, Gerard C. Krijger, Bernard M. Tijink,  
Bart de Keizer, Remco de Bree.

*Clin Otolaryngol.* 2021 Nov;46(6):1383-1388



## Introduction

[<sup>99m</sup>Tc]Tc-tilmanocept (Lymphoseek<sup>®</sup>, Navidea Biopharmaceuticals, Inc), a radiotracer specifically designed for sentinel lymph node (SLN) identification, has been registered for sentinel lymph node biopsy (SLNB) in, among others, early-stage oral squamous cell carcinoma (OSCC). On account of its proposed rapid clearance from the injection site, rapid uptake and high retention within SLNs, it is assumed that [<sup>99m</sup>Tc]Tc-tilmanocept enhances SLN identification [1]. These properties may be particularly relevant for patients with SLNs located close to the tumor, as radioactivity residing at the injection site may conceal adjacent SLNs (shine-through phenomenon) [2]. Agrawal et al. achieved a remarkable sensitivity (97.4%) and negative predictive value (NPV; 97.8%) for SLNB with [<sup>99m</sup>Tc]Tc-tilmanocept in early-stage OSCC, including tumors with adjacent SLNs (e.g., floor-of-mouth), supporting the hypothesis that tilmanocept's kinetic properties could improve SLN identification in these patients [1, 3].

6

Our prequel prospective within-patient evaluation study indeed showed higher injection site clearance for [<sup>99m</sup>Tc]Tc-tilmanocept compared to [<sup>99m</sup>Tc]Tc-nanocolloid [4]. However, lower uptake in SLNs was observed for [<sup>99m</sup>Tc]Tc-tilmanocept compared to [<sup>99m</sup>Tc]Tc-nanocolloid. Hence, no difference in the “SLN-to-injection-site-ratio” was seen between both radiotracers. Besides, owing to relatively low activity residing in SLNs for [<sup>99m</sup>Tc]Tc-tilmanocept, intraoperative SLN localization was challenging in some patients when using [<sup>99m</sup>Tc]Tc-tilmanocept for SLNB.

Based on these insights in tilmanocept's biodistribution, it is doubtful whether [<sup>99m</sup>Tc]Tc-tilmanocept is superior to [<sup>99m</sup>Tc]Tc-nanocolloid. Still, the improved injection site clearance of [<sup>99m</sup>Tc]Tc-tilmanocept may benefit SLN identification, particularly when SLNs are located close to the injection site. Therefore, long-term follow-up is required to identify false-negative outcomes and reliably assess [<sup>99m</sup>Tc]Tc-tilmanocept's efficacy for SLN identification.

This study compares SLN identification using [<sup>99m</sup>Tc]Tc-tilmanocept to [<sup>99m</sup>Tc]Tc-nanocolloid and determines both sensitivity and NPV of SLNB using [<sup>99m</sup>Tc]Tc-tilmanocept in our series of early-stage OSCC patients. Histopathological examination of excised SLNs and any complementary neck dissection specimens, as well as follow-up of ≥ 12 months, is used as reference standard.

## Materials and methods

### Patients

This study consisted of two cohorts (Figure 1). The prospective cohort has been described in the prequel study in detail [4]. Patients underwent lymphoscintigraphy including SPECT/CT for both [<sup>99m</sup>Tc]Tc-tilmanocept and [<sup>99m</sup>Tc]Tc-nanocolloid. SLNB (i.e., lymphoscintigraphy and intraoperative SLN localization) was based on the last administered radiotracer.

In the retrospective cohort, corresponding inclusion criteria were applied (i.e., early-stage OSCC, clinical nodal staging confirmed by at least ultrasound, scheduled for SLNB) [4]. Contrary to the prospective cohort, patients with prior head and neck malignancies, neck dissection or neck irradiation were also included. These patients underwent lymphoscintigraphy including SPECT/CT and intraoperative SLN localization (i.e., SLNB) solely with [<sup>99m</sup>Tc]Tc-tilmanocept (74 MBq). The imaging protocol was identical in both cohorts, as previously described [4].

### Intraoperative localization, histopathology and follow-up

Intraoperatively, identified SLNs were localized and extirpated under portable gammaprobe guidance. Harvested SLNs were histopathologically assessed by step-serial-sectioning and immunohistochemistry [5]. Patients with histopathologically negative SLN(s) were assigned to a wait-and-scan approach. In those with at least one SLN containing metastasis, complementary treatment of the affected nodal basin was employed (i.e., neck dissection and/or (chemo)radiotherapy). Complementary neck dissection specimens were histopathologically examined for additional nodal metastases.

Follow-up consultations were scheduled according to standard oncological care. Nodal recurrences that occurred in the neck staged negative for nodal metastasis by lymphoscintigraphy or SLNB (i.e., all SLNs in corresponding side of neck histopathologically negative, no SLNs identified in corresponding side of neck) were regarded false-negative outcomes. Nodal recurrences in presence of local tumor recurrence or second primary tumors were not considered false-negative outcomes, since nodal metastasis might have developed from a reseeding tumor.

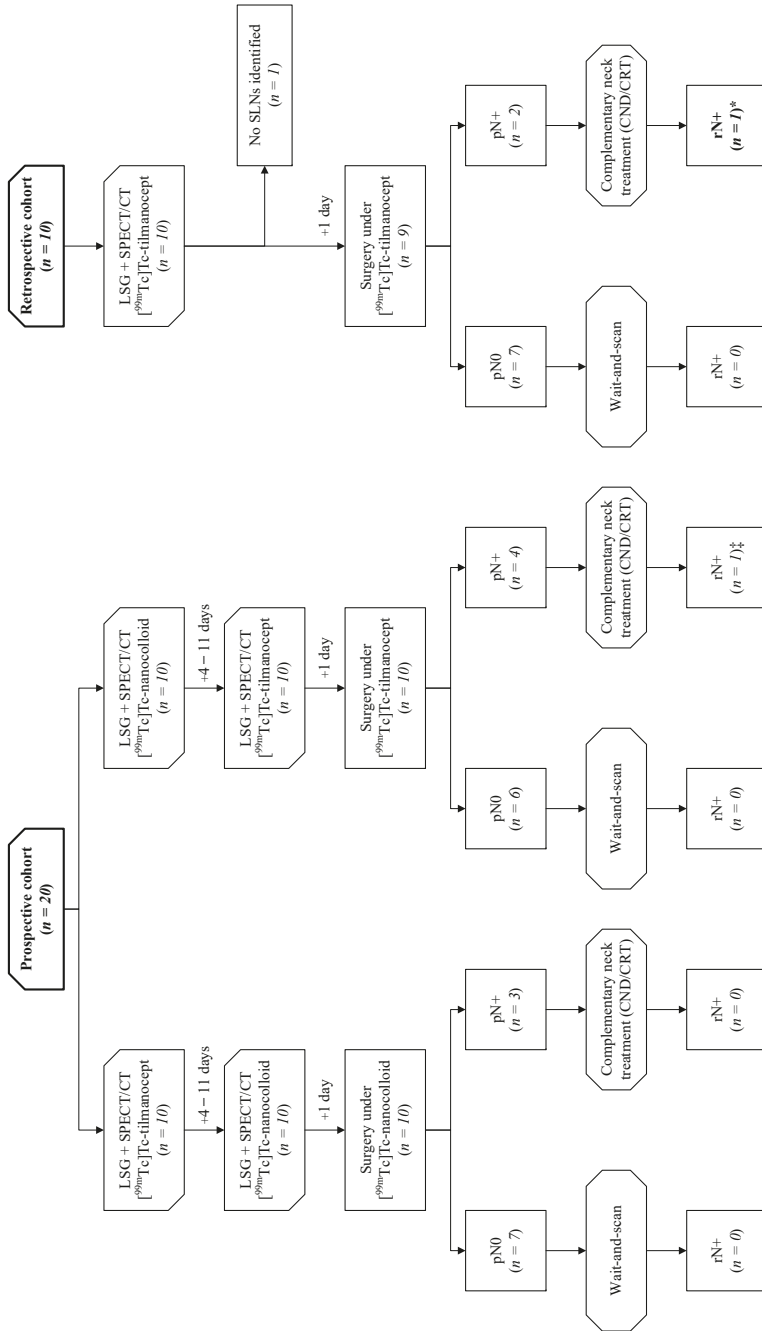


**Figure 1.** Outcome of SLNB for both the prospective and retrospective cohort. LSG, lymphoscintigraphy; SPECT/CT, single photon emission computed tomography/computed tomography; SLN, sentinel lymph node; pN0, patient with histopathologically metastatic involved sentinel lymph node; pN+, patient with at least one histopathologically negative sentinel lymph node(s); rN+, patient with at least one histopathologically metastatic involved sentinel lymph node; CND, complementary neck dissection; CRT, complementary radiotherapy; rN+, patient with nodal recurrence during follow-up. †Nodal recurrence occurred in the ipsilateral neck, which was staged positive by SLNB, and is therefore a consequence of insufficient complementary treatment rather than inadequate SLNB. \*False-negative SLNB outcome, as the nodal recurrence occurred in the contralateral neck in which initially no SLNs were identified by SLNB using  $[^{99m}\text{Tc}]\text{-tilmanocept}$ .

## Analyses

In the prospective cohort, paired images of both radiotracers were evaluated for number, location and histopathological status of identified SLNs. In case of additional nodal metastases in complementary neck dissection specimens or nodal recurrences, their corresponding location was correlated to lymphoscintigraphic images of both radiotracers. Accordingly, false-negative outcomes of lymphoscintigraphy or SLNB for either radiotracer were identified. In the retrospective cohort, false-negative outcomes concerning SLNB with [<sup>99m</sup>Tc]Tc-tilmanocept were analyzed.

Finally, for SLNB with [<sup>99m</sup>Tc]Tc-tilmanocept combined from both cohorts, sensitivity (*true-positives / (true-positives + false-negatives)*) and NPV (*true-negatives / (true-negatives + false-negatives)*) were calculated.

## Results

Characteristics of both cohorts are listed separately in Table 1. Average follow-up duration in patients without any follow-up events (i.e., nodal recurrence, local recurrence, deceased) was 22.6 months (range 13 – 32). Nine patients (30%) were staged positive for nodal metastasis by SLNB and underwent complementary treatment; 20 patients were staged negative for nodal metastasis in whom a wait-and-scan approach was adopted (Figure 1). In one patient, who previously underwent bilateral selective neck dissection, no SLNs were identified. None of the SLNB-negative patients developed nodal recurrence. Three patients (10%) developed local tumor recurrence without evidence of nodal recurrence.

**Table 1.** Patient- and tumor characteristics.

Characteristics	Prospective cohort	Retrospective cohort
<b>Number of patients</b>	20	10
<b>Gender, n (%)</b>		
Male	13 (65%)	9 (90%)
<b>Median age (y) (range)</b>	63 (39-77)	67 (48-84)
<b>Previous treatment of neck</b>		
Neck dissection	N.A.	3 (30%)
Radiotherapy	N.A.	1 (10%)
<b>Tumor location, n (%)</b>		
Tongue	14 (70%)	7 (70%)
Floor-of-mouth	5 (25%)	2 (20%)
Lower gum	1 (5%)	1 (10%)
<b>Clinical T stage, n (%)<sup>a</sup></b>		
T1	9 (45%)	4 (40%)
T2	11 (55%)	6 (60%)
<b>Pathology primary tumor</b>		
Median diameter (mm) (range)	19 (6-44)	19 (10-27)
Median depth-of-invasion (mm) (range)	6 (1-13)	6 (4-11)
<b>Histopathological status SLNs</b>		
Negative	37 (76%)	19 (83%)
Positive	12 (24%)	4 (17%)
Median harvested SLNs (range)	2 (1-5)	2 (0-4)
Number of SLN-positive patients	7 (35%)	2 (20%)

SLN, *sentinel lymph node*; n, *number*; y, *years*; N.A. *not applicable*; mm, *millimeters*. <sup>a</sup>T stage according to 8<sup>th</sup> AJCC TNM classification.

Nodal recurrence occurred in two SLNB-positive patients with no history of head and neck malignancies, neck dissection or neck irradiation (Figure 1, Table 2). In one patient of the prospective cohort (PC16), the nodal recurrence occurred in the ipsilateral neck, which was initially staged positive by SLNB using [<sup>99m</sup>Tc]Tc-tilmanocept and subsequently treated by radiotherapy. The other nodal recurrence occurred in the contralateral neck of a patient from the retrospective cohort (RC7), in which no SLN was identified by SLNB using [<sup>99m</sup>Tc]Tc-tilmanocept (false-negative).

In the prospective cohort, all patients were correctly staged for presence of nodal metastasis by lymphoscintigraphy using either radiotracer. In two patients (PC16, PC17) an additional metastatic SLN was identified by SLNB with [<sup>99m</sup>Tc]Tc-tilmanocept, compared to the designated SLNs by [<sup>99m</sup>Tc]Tc-nanocolloid lymphoscintigraphy. On [<sup>99m</sup>Tc]Tc-nanocolloid lymphoscintigraphy hotspots were visualized corresponding with the location of these additional metastatic SLNs, but were regarded higher echelon nodes due to their position relative to the designated SLNs. As nodal metastasis was already established in these two patients, the additional metastatic SLNs identified by SLNB with [<sup>99m</sup>Tc]Tc-tilmanocept did not have therapeutic consequences.

In the 19 patients who underwent SLNB (lymphoscintigraphy and intraoperative SLN localization) with [<sup>99m</sup>Tc]Tc-tilmanocept, 13 were staged negative and six were staged positive for nodal metastasis; one false-negative outcome was identified (RC7). Consequently, SLNB with [<sup>99m</sup>Tc]Tc-tilmanocept reached a sensitivity of 83.3% and NPV of 93.3%.

**Table 2.** Sentinel lymph node distribution, complementary treatment and follow-up data of patients with histopathologically positive sentinel lymph node(s) or nodal recurrence.

N <sup>o</sup>	Primary tumor	Identified SLNs [ <sup>99m</sup> Tc]-tilmanocept	Identified SLNs [ <sup>99m</sup> Tc]-nanocolloid	Harvested SLNs	PA	Complementary treatment	Additional metastases in CND	Follow-up status
PC1	Tongue (left)	Ib II III	Ib II III	Left Left Left	+	CND (I-IV left)	None	NED
PC7	Tongue (right)	II Ib III	II III III	Right Left Left	+	GRT (Ib-V bilateral)	N.A.	NED
PC9	Tongue (left - midline)	II II III	II II III	Right Right Left Left	+	CND (I-III right)	III & V right	LR
PC14	Lower gum (left)	II	II	Left	+	CND (I-IV left)	None	LR
PC16	Tongue (right)	II III	II	Right Right	+	GRT (Ib-V right)	N.A.	RR (Ib right)
PC17	Tongue (left)	II II II	II II II	Left Left Left	+	GRT (Ib-V left)	N.A.	NED

**Table 2.** Continued.

N°	Primary tumor	Identified SLNs [ <sup>99m</sup> Tc]Tc-tilmanocept	Identified SLNs [ <sup>99m</sup> Tc]Tc-nanocolloid	Harvested SLNs	PA	Complementary treatment	Additional metastases in CND	Follow-up status
PC20	Tongue (right)	Ia	Left	<u>Ib</u>	+	CND	None	NED
		Ib	Left	<u>III</u>	-	(I-III right; I-IV left)		
		III	Left					
RC3	Tongue (right)	II	Right	<u>Ib</u>	+	CND	None	2 <sup>nd</sup>
		III	Right			(I-IV right)		primary (larynx)
		II	Right					RR
RC7	Tongue (right)	Ib	Right	<u>Ib</u>	+	GRT	N.A.	RR
		II	Right	<u>II</u>	-	(I-V right)		(Ib left)*
		III	Right	<u>III</u>	+			

N°, patient number; SLN, sentinel lymph node; PA, pathological assessment; CND, complementary neck dissection; PC, prospective cohort; +, histopathologically positive for metastasis; -, histopathologically negative for metastasis; NED, no evidence of disease; GRT, complementary radiotherapy; N.A., not applicable; LR, local tumor recurrence; RR, regional nodal recurrence; RC, retrospective cohort; 2<sup>nd</sup> primary, second primary tumor. Intraoperative SLN localization was performed with [<sup>99m</sup>Tc]Tc-nanocolloid in patients PC1, PC7 and PC9. In the other patients (PC14, PC16, PC17, PC20, RC3 and RC7) intraoperative SLN localization was performed with [<sup>99m</sup>Tc]Tc-tilmanocept (underlined). \* False-negative SLNB outcome.

## Discussion

In the prospective cohort, nodal recurrence occurred in one patient. Since the corresponding side of the neck was staged positive for metastasis by SLNB, this recurrence is considered a consequence of insufficient complementary treatment rather than inadequate SLNB. Accordingly, in the prospective cohort, the presence of nodal metastasis would have been correctly diagnosed by SLNB using either [<sup>99m</sup>Tc]Tc-tilmanocept or [<sup>99m</sup>Tc]Tc-nanocolloid, assuming that lymphoscintigraphic identified SLNs could be found intraoperatively [4]. Although additional nodal metastases were identified by SLNB with [<sup>99m</sup>Tc]Tc-tilmanocept, these had no therapeutic consequences as the corresponding side of the neck would have been staged positive for nodal metastasis by SLNB with [<sup>99m</sup>Tc]Tc-nanocolloid as well. These patients would have been candidate for complementary treatment, irrespective of these additionally identified nodal metastasis. Moreover, as hotspots were visualized on [<sup>99m</sup>Tc]Tc-nanocolloid lymphoscintigraphy that corresponded with these additional metastatic SLNs, the discrepancy in identified SLNs is most likely the result of variability in lymphoscintigram interpretation [6]. Ergo, in this prospective cohort, [<sup>99m</sup>Tc]Tc-tilmanocept was similar to [<sup>99m</sup>Tc]Tc-nanocolloid for lymphoscintigraphy or SLNB.

In the retrospective cohort, one false-negative outcome was identified for SLNB using [<sup>99m</sup>Tc]Tc-tilmanocept. Thus, for those in whom SLNB was performed with [<sup>99m</sup>Tc]Tc-tilmanocept ( $n = 19$ ), a sensitivity of 83% and NPV of 93% was achieved. These numbers are similar to those reported in a large multicenter study, in which SLNB was performed with [<sup>99m</sup>Tc]Tc-nanocolloid in 488 early-stage OSCC patients (sensitivity 81%, NPV 93%) [2].

Contrary to Agrawal et al., the diagnostic accuracy of SLNB with [<sup>99m</sup>Tc]Tc-tilmanocept does not seem superior when compared to the reported diagnostic accuracy of SLNB with [<sup>99m</sup>Tc]Tc-nanocolloid [2, 3]. The fact that all patients in the study by Agrawal et al. underwent elective neck dissection immediately following SLNB might be underlying to the discrepancy in diagnostic accuracy [3]. Micrometastases remain undetected in ~15% of routinely processed neck dissection specimens, rendering it plausible that actually more nodal metastasis could have been missed by SLNB with [<sup>99m</sup>Tc]Tc-tilmanocept in their population [7]. Hence, long-term observation, following wait-and-scan, is considered a better reference standard [8].

When reevaluating our false-negative case, a lymph node with marginal [<sup>99m</sup>Tc]Tc-tilmanocept uptake was identified at the nodal recurrence's location (Figure 2). This underlines the concern that [<sup>99m</sup>Tc]Tc-tilmanocept's relatively low radioactive uptake in SLNs, as demonstrated by prior quantitative analyses [4], increases the risk to

overlook SLNs and consequently neglect occult nodal metastasis. Unfortunately, as this patient was included in the retrospective cohort, no within-patient comparison could be made with [<sup>99m</sup>Tc]Tc-nanocolloid lymphoscintigraphy. It is therefore uncertain whether the overlooked SLN would have been identified by SLNB with [<sup>99m</sup>Tc]Tc-nanocolloid.

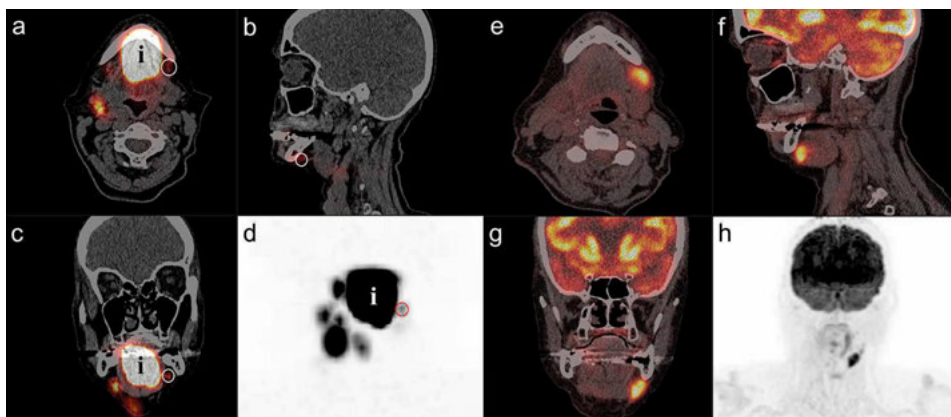


**Figure 2.** (a-d) Overlooked sentinel lymph node on [<sup>99m</sup>Tc]Tc-tilmanocept SPECT/CT in patient with false-negative SLNB outcome. [<sup>99m</sup>Tc]Tc-tilmanocept SPECT/CT images of a 82-year old patient with a cT2N0 tongue carcinoma on the right side, who developed a nodal recurrence in level Ib on the left side 7 months following SLNB (RC7). Re-evaluation of lymphoscintigraphic and SPECT/CT images showed marginal uptake of [<sup>99m</sup>Tc]Tc-tilmanocept in an overlooked SLN on level Ib on the left (*circle*), located adjacent to the injection site (*i*). (e-h) Nodal recurrence on [<sup>18</sup>F]FDG-PET on location corresponding with overlooked sentinel lymph node. [<sup>18</sup>F]FDG-PET images of the same patient (RC7), acquired 7 months following SLNB, showing pathological [<sup>18</sup>F]FDG-uptake in a lymph node in level Ib on the left, which corresponds with the location of the overlooked SLN on [<sup>99m</sup>Tc]Tc-tilmanocept SLN-imaging. Written informed consent has been obtained from this patient.

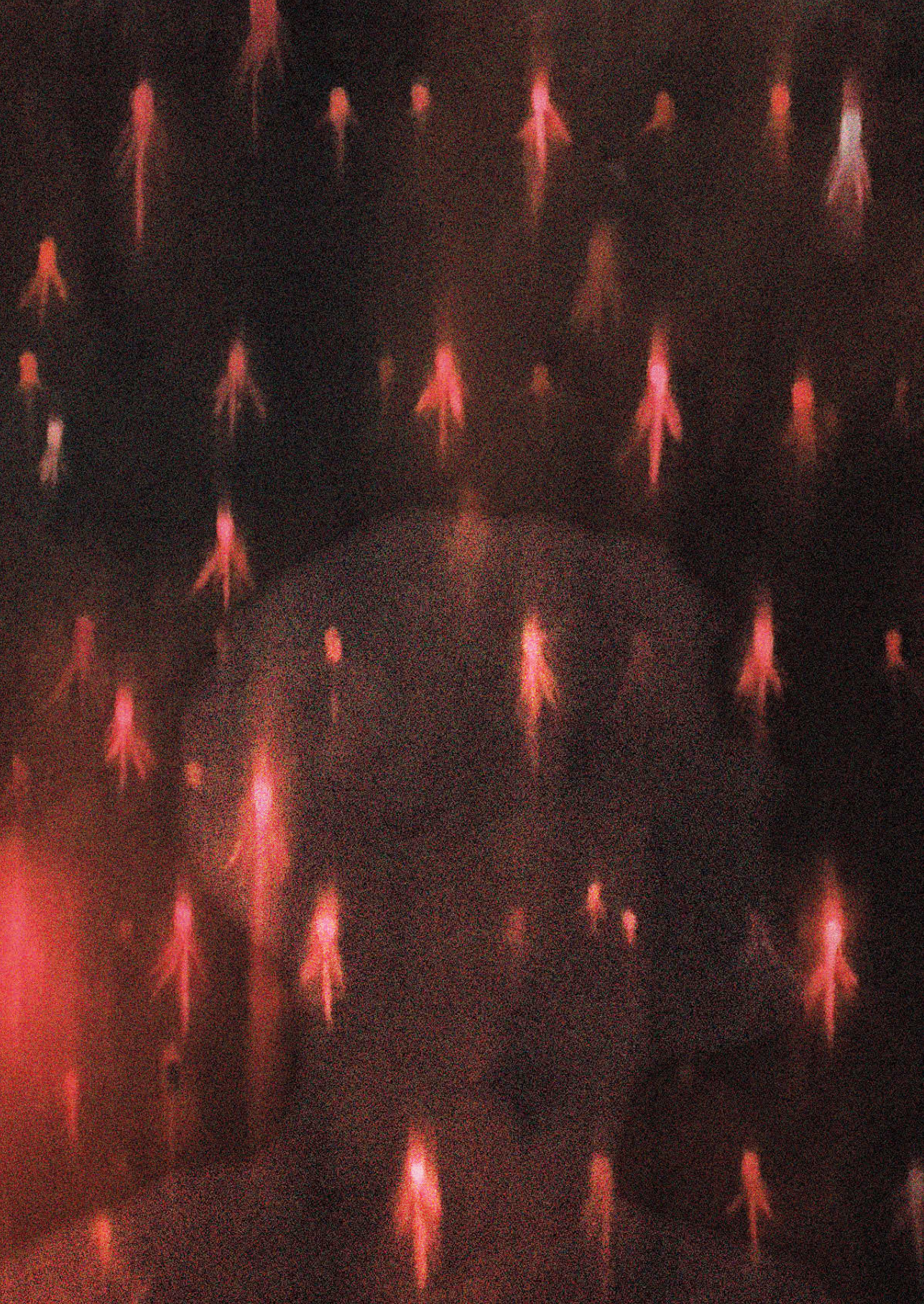
Limitations of this study remain its follow-up duration (on average 23 months) and relatively small sample. Although the majority of nodal recurrences (80%) occur within the first year following SLNB, longer follow-up duration (e.g., ≥ 24 months) may reveal more false-negative outcomes [9, 10].

All considered, the prequel and current study cannot support the propagated potential of [<sup>99m</sup>Tc]Tc-tilmanocept for SLN identification in early-stage OSCC. Since SLNB using [<sup>99m</sup>Tc]Tc-tilmanocept appears to be comparable to SLNB with [<sup>99m</sup>Tc]Tc-nanocolloid, justification of tilmanocept's higher costs seems questionable. Nonetheless, it would be premature to pass a final verdict upon [<sup>99m</sup>Tc]Tc-tilmanocept's value for SLNB in early-stage OSCC.

## References

1. Vidal-Sicart S, Vera DR, Valdés Olmos RA. Next generation of radiotracers for sentinel lymph node biopsy: What is still necessary to establish new imaging paradigms? *Rev Esp Med Nucl Imagen Mol (Engl Ed)*. 2018;37(6):373-379. doi:10.1016/j.remnm.2018.09.001
2. den Toom IJ, Boeve K, Lobeek D, et al. Elective neck dissection or sentinel lymph node biopsy in early stage oral cavity cancer patients: the Dutch experience. *Cancers (Basel)*. 2020;12(7):1783. doi:10.3390/cancers12071783
3. Agrawal A, Civantos FJ, Brumund KT, et al. [<sup>99m</sup>Tc]Tilmanocept accurately detects sentinel lymph nodes and predicts node pathology status in patients with oral squamous cell carcinoma of the head and neck: results of a phase III multi-institutional trial. *Ann Surg Oncol*. 2015;22(11):3708-3715. doi:10.1245/s10434-015-4382-x
4. den Toom IJ, Mahieu R, van Rooij R, et al. Sentinel lymph node detection in oral cancer: a within-patient comparison between [<sup>99m</sup>Tc]Tc-tilmanocept and [<sup>99m</sup>Tc]Tc-nanocolloid. *Eur J Nucl Med Mol Imaging*. 2021;48(3):851-858. doi:10.1007/s00259-020-04984-8
5. Dhawan I, Sandhu SV, Bhandari R, Sood N, Bhullar RK, Sethi N. Detection of cervical lymph node micrometastasis and isolated tumor cells in oral squamous cell carcinoma using immunohistochemistry and serial sectioning. *J Oral Maxillofac Pathol*. 2016;20(3):436-444. doi:10.4103/0973-029X.190946
6. Flach GB, van Schie A, Witte BI, et al. Practice variation in defining sentinel lymph nodes on lymphoscintigrams in oral cancer patients. *Eur J Nucl Med Mol Imaging*. 2014;41(12):2249-2256. doi:10.1007/s00259-014-2843-2
7. Rinaldo A, Devaney KO, Ferlito A. Immunohistochemical studies in the identification of lymph node micrometastases in patients with squamous cell carcinoma of the head and neck. *ORL J Otorhinolaryngol Relat Spec*. 2004;66(1):38-41. doi:10.1159/000077232
8. de Bree R. How to analyze the diagnostic value of sentinel node biopsy in head and neck cancer. *Eur Arch Otorhinolaryngol*. 2013;270(3):789-791. doi:10.1007/s00405-012-2321-z
9. Brands MT, Smeekens EAJ, Takes RP, et al. Time patterns of recurrence and second primary tumors in a large cohort of patients treated for oral cavity cancer. *Cancer Med*. 2019;8(12):5810-5819. doi:10.1002/cam4.2124
10. Garrel R, Poissonnet G, Moyà Plana A, et al. Equivalence randomized trial to compare treatment on the basis of sentinel node biopsy versus neck node dissection in operable T1-T2N0 oral and oropharyngeal cancer. *J Clin Oncol*. 2020;38(34):4010-4018. doi:10.1200/JCO.20.01661





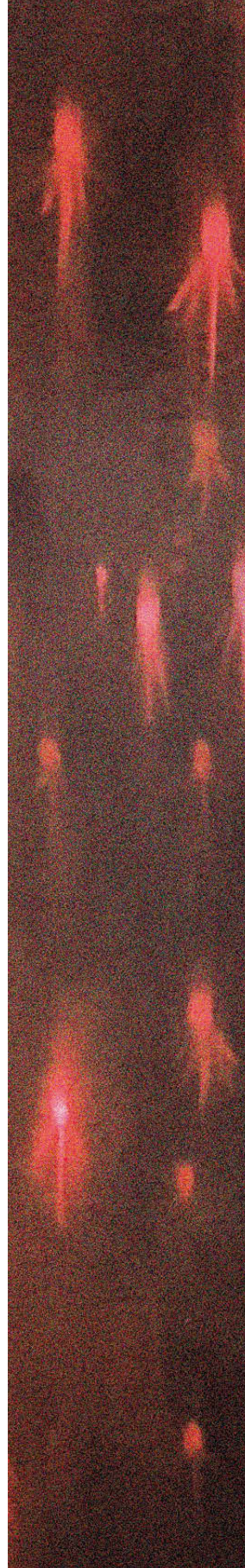
# 7

## New developments in imaging for sentinel lymph node biopsy in early-stage oral cavity squamous cell carcinoma

---

Rutger Mahieu, Josanne S. de Maar, Eliane R. Nieuwenhuis,  
Roel Deckers, Chrit Moonen, Lejla Alic, Bennie ten Haken,  
Bart de Keizer, Remco de Bree.

*Cancers (Basel)*. 2020 Oct 20;12(10):3055



## Abstract

Sentinel lymph node biopsy (SLNB) is a diagnostic staging procedure that aims to identify the first draining lymph node(s) from the primary tumor, the sentinel lymph nodes (SLN), as their histopathological status reflects the histopathological status of the rest of the nodal basin. The routine SLNB procedure consists of peritumoral injections with a technetium-99m ( $^{99m}\text{Tc}$ ) labeled radiotracer followed by lymphoscintigraphy and SPECT/CT imaging. Based on these imaging results, the identified SLNs are marked for surgical extirpation and are subjected to histopathological assessment. The routine SLNB procedure has proven to reliably stage the clinically negative neck in early-stage oral squamous cell carcinoma (OSCC). However, an infamous limitation arises in situations where SLNs are located in close vicinity of the tracer injection site. In these cases, the hotspot of the injection site can hide adjacent SLNs and hamper the discrimination between tracer injection site and SLNs (shine-through phenomenon). Therefore, technical developments are needed to bring the diagnostic accuracy of SLNB for early-stage OSCC to a higher level. This review evaluates novel SLNB imaging techniques for early-stage OSCC: MR lymphography, CT lymphography, PET lymphoscintigraphy and contrast-enhanced lymphosonography. Furthermore, their reported diagnostic accuracy is described and their relative merits, disadvantages and potential applications are outlined.

## Introduction

In early-stage (cT1-2N0) oral squamous cell carcinoma (OSCC), occult lymph node metastases are present in 20–30% of patients, even when the status of the regional lymph nodes has been evaluated using combinations of advanced clinical diagnostic imaging modalities (i.e., ultrasound guided fine-needle aspiration (USgFNA), magnetic resonance imaging (MRI) and/or computed tomography (CT)) [1–3]. As watchful-waiting in these patients has been associated with a poor prognosis, especially when compared to those in whom the clinically negative neck was electively treated [1], two strategies for the clinically negative neck in early-stage OSCC are available: elective neck dissection (END) and sentinel lymph node biopsy (SLNB) [3–6]. Although END is the strategy of choice in the majority of medical centers globally [5], which has the benefit of being a single-stage procedure, SLNB is a less invasive procedure for the 70–80% of patients without metastatic neck involvement and has overall lower morbidity rates, better quality-of-life and lower health-care costs as compared to END [7–10].

The concept of SLNB is based on the premise that lymph flow from the primary tumor travels sequentially to the sentinel lymph node (SLN) and then on to the other regional lymph nodes. Hence, the SLN is the lymph node that has the highest risk of harboring metastasis [11].

The SLNB procedure aims to identify these first draining lymph node(s), as their histopathological status reflects the histopathological status of the rest of the nodal basin. Complementary nodal treatment (e.g., surgery, radiotherapy) should be performed in case of metastatic involvement of SLN(s). A negative SLNB, however, would justify a wait-and-scan policy [12].

In short, the routine SLNB procedure consists of preoperative peritumoral injections with a technetium-99m [<sup>99m</sup>Tc;  $\gamma$ -emitter]-labeled radiotracer followed by planar dynamic and static lymphoscintigraphy including SPECT/CT (single photon emission computed tomography/computed tomography) imaging. Based on preoperative lymphoscintigraphy, the position of the SLN(s) is marked on the skin. The marked SLNs are surgically removed, using a portable  $\gamma$ -probe for intraoperative localization of SLNs. Subsequently, the harvested SLNs are subjected to meticulous histopathological assessment using step-serial-sectioning and immunohistochemistry [12–15].

SLNB has proven to reliably stage the clinically negative neck in early-stage OSCC with a pooled sensitivity and negative predictive value (NPV) of 87% and 94%, respectively [16]. However, an infamous limitation of the routine SLNB procedure arises in

situations where SLNs are located in close vicinity of the tracer injection site. In these cases, the hotspot of the injection site can hide adjacent SLNs, which consequently hampers the discrimination between tracer injection site and SLNs (shine-through phenomenon; Figure 1). This shine-through phenomenon is particularly evident in patients with floor-of-mouth OSCC and sublingual, submental and submandibular SLNs, resulting in a significantly lower accuracy of SLNB in floor-of-mouth tumors (sensitivity 63%; NPV 90%) compared to other oral cavity subsites (sensitivity 86%; NPV 95%) [4, 17–21].

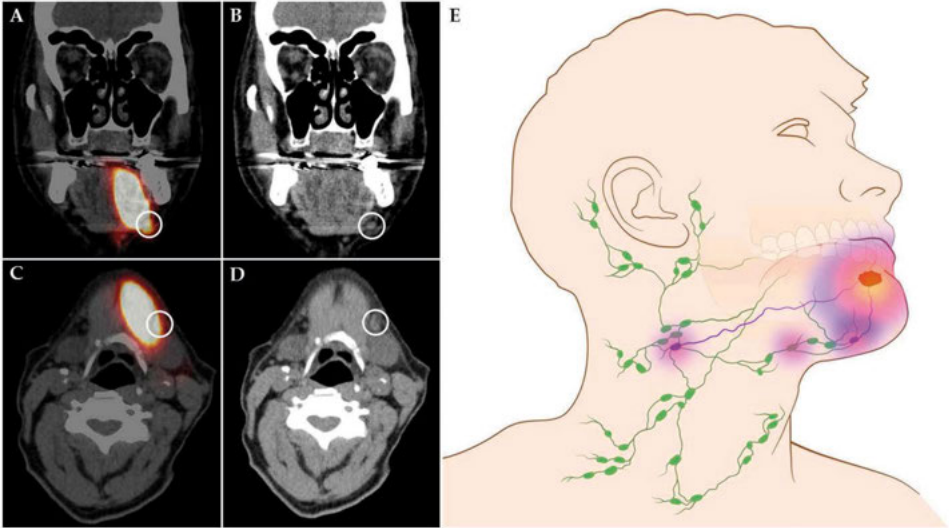


**Figure 1.** Shine-through phenomenon in 72-year-old patient with a cT1N0 floor-of-mouth carcinoma. (a,c) Coronal and axial SPECT/CT images: radiation flare of the tracer injection site over shines a sentinel lymph node located in cervical lymph node level Ib (*white circle*). (b,d) Coronal and axial low-dose CT images of same patient: (sentinel) lymph node located in cervical lymph node level Ib that could not be differentiated from the hotspot originating from tracer injection site on SPECT/CT (*white circle*). (e) Schematic illustration of shine-through phenomenon. (a–d) Informed consent has been obtained from this patient. (e) University Medical Center Groningen©.

Therefore, technical developments are needed to bring the diagnostic accuracy of SLNB for all subsites of OSCC to the same high level. This review evaluates new developments in preoperative SLN imaging techniques for early-stage OSCC: MR lymphography, CT lymphography, PET lymphoscintigraphy and contrast-enhanced lymphosonography. Furthermore, this review describes their diagnostic accuracy as reported in literature and outlines their relative merits, disadvantages and potential applications.

## Materials and methods

A systematic literature search for relevant English written literature published up to 25 May 2020 was conducted in the PubMed database. Search syntaxes combined synonyms and medical subject headings (MeSH) terms for both OSCC and SLNB and was performed for all imaging techniques separately (i.e., MR lymphography, CT lymphography, PET lymphoscintigraphy and contrast-enhanced lymphosonography). Subsequently, title and abstract screening was performed by four authors (R.M, J.S.d.M., E.R.N and R.d.B.). The reference lists of included studies were screened to identify any additional relevant publications. No critical appraisal of the selected literature was performed. This review adheres to the PRISMA guidelines [22].

### MR lymphography

The following keywords and MeSH terms were included for MR lymphography: (“Mouth”[MeSH]) or (“Oral”) or (“Head and Neck”) and (“Sentinel lymph node”[MeSH]) or (“Lymph”) and (“Node”) or (“Sentinel”) and (“Node”) or (“Sentinel node”) and (“Lymphography”[MeSH]) or (“Lymphography”) or (“Lymphangiography”) and (“Magnetic resonance imaging”[MeSH] or (“Magnetic”) and (“Resonance”) and (“Imaging”) or (“Magnetic resonance imaging”) or (“MRI”) or (“MR”).

For magnetic detection of SLNs using superparamagnetic iron oxide, the following keywords and MeSH terms were included: (“Mouth”[MeSH]) or (“Oral”) or (“Head and Neck”) and (“Sentinel lymph node”[MeSH]) or (“Lymph”) and (“Node”) or (“Sentinel”) and (“Node”) or (“Sentinel node”) and (“Iron”[MeSH]) or (“Iron oxide”) or (“SPIO”) or (“SPION”) and (“Magnetics”[MeSH] or (“Magnetic”) or (“Superparamagnetic”) or (“superparamagnetic iron oxide”).

### CT lymphography

The following keywords and MeSH terms were included for CT lymphography: (“Mouth”[MeSH]) or (“Oral”) or (“Head and Neck”) and (“Sentinel lymph node”[MeSH]) or (“Lymph”) and (“Node”) or (“Sentinel”) and (“Node”) or (“Sentinel node”) and (“Lymphography”[MeSH]) or (“Lymphography”) and (“CT”) or (“Computed Tomography”) or (“Computed”) or (“Tomographic”).

### PET lymphoscintigraphy

The following keywords and MeSH terms were included for PET lymphoscintigraphy: (“Mouth”[MeSH]) or (“Oral”) or (“Head and Neck”) and (“Sentinel lymph node”[MeSH]) or (“Sentinel lymph node”) or (“Sentinel”) and (“Node”) or (“Sentinel node”) and (“Positron Emission Tomography Computed Tomography”[MeSH]) or

("Positron-Emission Tomography"[MeSH]) or ("PET") or ("Positron") or ("PET/CT") or ("PET-CT").

### **Contrast-enhanced lymphosonography**

The following keywords and MeSH terms were included for contrast-enhanced ultrasound lymphography: ("Mouth"[MeSH]) or ("Oral") or ("Head and Neck") and ("Sentinel lymph node"[MeSH]) or ("Sentinel lymph node") or ("Sentinel") and ("Node") or ("Sentinel node") and ("Contrast-enhanced") or ("Contrast-assisted") or ("CEUS") or ("Microbubbles") or ("Sonovue") or ("Sonazoid") or ("Optison") or ("Levovist") or ("Imagent") or ("Imavist") or ("Definity") and ("Diagnostic Imaging") or ("Diagnostic") and ("Imaging") or ("Ultrasound") or ("Ultrasonography"[MeSH]) or ("Ultrasonography") or ("Ultrasonics"[MeSH]) or ("Ultrasonics").

## Results

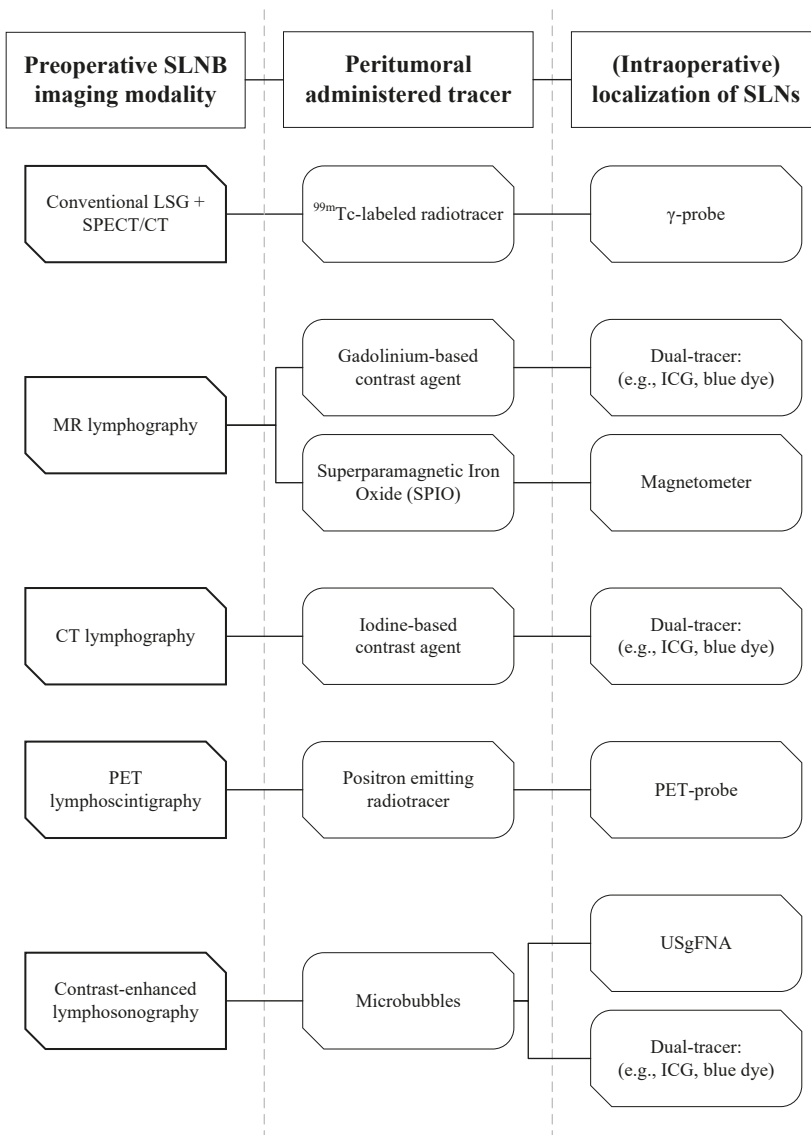
A systematic literature search for new developments in preoperative SLN imaging techniques for early-stage OSCC resulted in a total of 452 PubMed indexed articles, of which 40 were considered relevant. Cross-reference led to 1 additional relevant study with healthy volunteers. Of these 41 articles, 27 were reviews (n = 1), animal or preclinical studies (n = 26). In particular, 20 animal or preclinical studies used similar methods for SLN identification (i.e., imaging modality, tracer) as corresponding clinical studies.

Table 1 shows the range of reported diagnostic accuracy, in terms of sensitivity and NPV, and rate of patients in which SLNs were identified using the reviewed techniques. Figure 2 illustrates how both preoperative detection and intraoperative localization of SLNs was achieved, using the reviewed techniques, as described in literature.

**Table 1.** Reported diagnostic accuracy and detection rate of SLNs per technique.

Technique	Source	Tracer	Number of studies	Sensitivity	NPV	SLN identification in (%) of patients
<u>Conventional lymphoscintigraphy &amp; SPECT/CT</u>	γ-ray	γ-emitting <sup>99m</sup> Tc-labeled radiotracer (e.g., [ <sup>99m</sup> Tc]Tc-nanocolloid)	n = 66	87% <sup>[16]</sup>	94% <sup>[16]</sup>	-
<u>MR Lymphography (Gd<sup>3+</sup>)</u>	Radio-wave	Paramagnetic (Gd <sup>3+</sup> ) contrast agent (e.g., gadobutrol)	n = 1	91% <sup>[23]</sup>	93% <sup>[23]</sup>	100% <sup>[23]</sup>
<u>MR Lymphography (SPIO)</u>	Radio-wave	Superparamagnetic (iron oxide) contrast agent (e.g., Resovist, Magtrace)	n = 2	NR	NR	100% <sup>[24-26]</sup>
<u>CT Lymphography</u>	X-ray	Iodine contrast agent (e.g., iopamidol, lipiodol)	n = 6	56%-80% <sup>[27-30]</sup>	82%-96% <sup>[27-30]</sup>	89-96% <sup>[27-32]</sup>
<u>PET lymphoscintigraphy</u>	β <sup>+</sup> -decay (γ-rays)	Positron emitting isotope ( <sup>89</sup> Zr, <sup>68</sup> Ga, <sup>18</sup> F)-labeled radiotracer (e.g., [ <sup>68</sup> Ga]Ga-tilmanocept)	n = 2	67% <sup>[33]</sup>	67% <sup>[33]</sup>	100% <sup>[33, 34]</sup>
<u>Contrast-enhanced lymphosonography</u>	US-wave	Microbubbles (e.g., SonoVue, Sonazoid)	n = 2	NR	NR	80-92% <sup>[35, 36]</sup>

NPV; negative predictive value, SLN; sentinel lymph node, SPECT/CT; single photon emission computed tomography/computed tomography, <sup>99m</sup>Tc; technetium-99m, MR; magnetic resonance, Gd<sup>3+</sup>; gadolinium, NR; not reported, CT; computed tomography, PET; positron emission tomography, <sup>89</sup>Zr; zirconium-89, <sup>68</sup>Ga; gallium-68, <sup>18</sup>F; fluorine-18, US; ultrasound.



**Figure 2.** Overview of the reviewed preoperative SLN imaging techniques (*column 1*), the administered tracers for the corresponding techniques (*column 2*) and their intraoperative SLN localization techniques (*column 3*) as described in literature. SLNB; *sentinel lymph node biopsy*, LSG; *lymphoscintigraphy*, SPECT/CT; *single photon emission computed tomography/computed tomography*, MR; *magnetic resonance*, CT; *computed tomography*, PET; *positron emission tomography*, ICG; *indocyanine green*, USgFNA; *ultrasound guided fine needle aspiration*.

## MR lymphography

Magnetic resonance (MR) lymphography with peritumoral administration of a paramagnetic gadolinium [Gd<sup>3+</sup>]-based contrast agent has been recently introduced in breast and cervical cancer, as an alternative method for preoperative visualization of SLNs and lymphatics [37–39]. These studies showed that paramagnetic gadolinium [Gd<sup>3+</sup>]-based contrast agents, conventionally administered intravenously for contrast-enhanced MRI or MR angiography [40], are safe and useful for peritumoral administration and SLN mapping in humans.

To review MR lymphography for SLN detection using paramagnetic gadolinium-based contrast agents in early-stage OSCC, a systematic literature search was conducted. This led to retrieval of 53 PubMed indexed articles for MR lymphography; 7 were considered relevant [23, 41–46]. Of these 7 articles, 6 were animal studies [41–46]. Cross-reference led to identification of 1 relevant study with healthy volunteers [47]. In the only study that performed MR lymphography with a gadolinium-based contrast agent (i.e., gadobutrol) in OSCC patients (n = 26) [23], SLNs were consistently visualized in all patients and lymph node vessels were visualized in the majority of patients (81%) (Figure 3). Following MR lymphography, identified SLNs were injected with 1% patent blue dye under sonographic guidance. Subsequently, primary tumor resection and ipsilateral elective neck dissection were performed in all patients. Blue stained SLNs were dissected, marked and sent separately for histopathological assessment.

Among the 11 patients with pathologically positive necks, SLNs containing metastases were accurately identified by MR lymphography in 10 patients. In the remaining patient, MR lymphography depicted SLNs in ipsilateral neck level III. However, in the neck dissection specimen, 3 metastatic lymph nodes in ipsilateral neck level I were found, whereas no metastasis was found in level III. With histopathological assessment of the neck dissection specimen as reference standard, this approach reached a sensitivity of 90.9% with a NPV of 92.8%.

Another type of contrast agent that can be used for MR lymphography are superparamagnetic iron oxide nanoparticles (SPIO), which provide a negative contrast on MR lymphography as opposed to gadolinium-based contrast agents (Figure 4). Following peritumoral administration of SPIOs, transportation through the lymphatic system is mainly facilitated by macrophages, although unbound transport is seen as well [48]. SPIO accumulates primarily in lymph node sinuses and can be detected preoperatively on MRI and intraoperatively with a handheld magnetometer [24, 48–51]. MR lymphography using SPIO has been investigated for several tumor types, including breast and prostate cancer [49, 50].

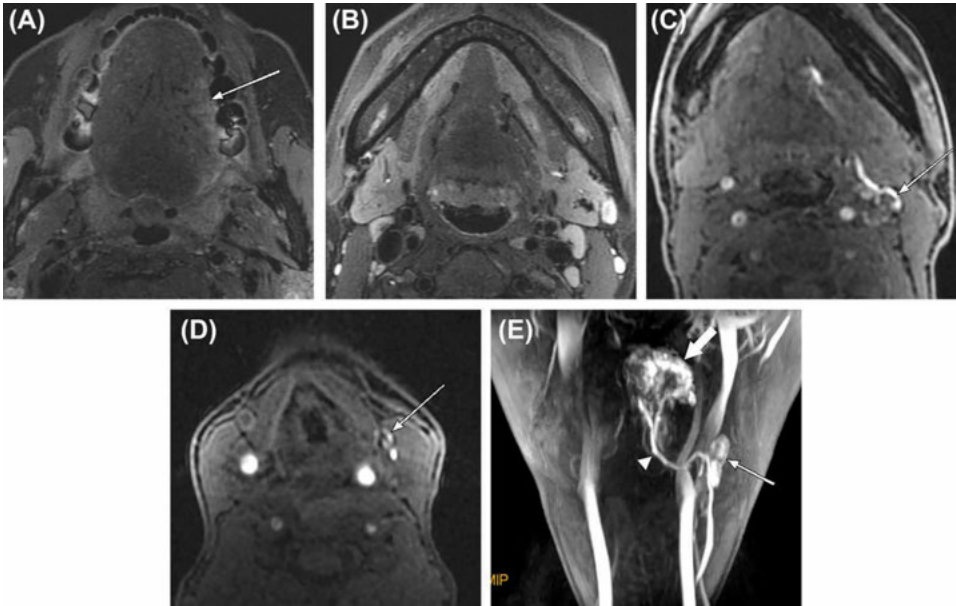


**Figure 3.** A 38-year-old woman with oral tongue cancer and palpably negative neck. (a,b) Fat-saturated T2-weighted MRI scans show a shallow infiltrative tumor on the left lateral surface of oral tongue (*arrow*) and several small lymph nodes in the submandibular areas. (c,d) After peritumoral injection of contrast, MR lymphography revealed two first-enhanced lymph nodes in left level Ib and IIa (*arrows*) on the first phase of the dynamic scan, respectively. (e) The maximum intensity projection reconstruction image of MR lymphography shows the contrast injection site in the tongue (*thick arrow*), the assumed sentinel lymph node (*thin arrow*), and the lymph vessel connecting them (*arrowhead*). After neck dissection, the assumed sentinel lymph nodes observed on MR lymphography revealed no metastasis on histologic examination [23]. Figure used with permission of John Wiley and Sons©, permission license number 4807630108259.

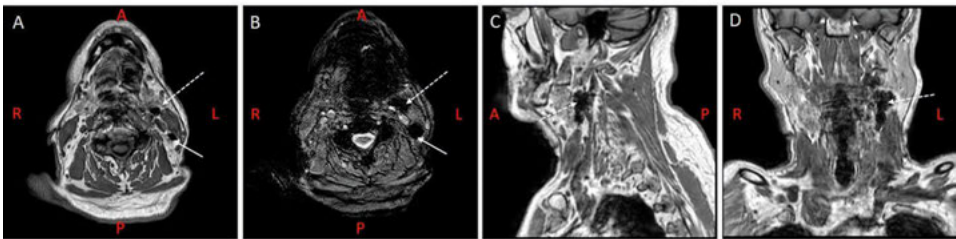


**Figure 4.** MR lymphography using superparamagnetic iron oxide nanoparticles in a 77-year-old man with oral tongue cancer and a clinically negative neck. (a) T1-weighted 3D fast-field echo (FFE) show uptake of SPIO in two SLNs in level IIa (*dotted arrow*) & level IIb (*arrow*) left. (b) T2-weighted FFE shows clear negative contrast in corresponding SLNs, as a result of SPIO uptake. (c,d) Sagittal and coronal reconstruction of (a) shows the SLN in level IIa left (*dotted arrow*). (a-d) Informed consent has been obtained from this patient.

The systematic literature search retrieved 116 PubMed indexed articles, of which 6 were considered relevant [24–26, 45, 50, 51]. Of these 6 articles, 3 were animal studies [46, 51, 52]. Cross-reference did not lead to identification of additional relevant articles, resulting in a total of 3 included human studies [24–26]. One of these studies did not perform preoperative SPIO-enhanced MRI, but was the only study in early-stage OSCC patients that achieved intraoperative localization of SLNs with the magnetometer [24].

Mizokami et al. performed MR lymphography using SPIO in three tongue cancer patients (cT2N0), planned for tumor resection and ipsilateral elective neck dissection [25]. Seven days before surgery, patients received peritumoral injections with Resovist (Bayer Schering Pharma) of 0.1–0.3 mL, corresponding with 2.78–8.37 mg iron. MR lymphographic images were acquired at 10 min, 30 min and 24 h post-injection. On the day before surgery, [<sup>99m</sup>Tc]Tc-phytate was administered peritumorally, followed by planar lymphoscintigraphy. Intraoperatively, SLNs were localized using a conventional  $\gamma$ -probe and were submitted for individual histopathological assessment. All SLNs depicted on 10 min MR lymphography were in accordance with planar lymphoscintigraphy and  $\gamma$ -probe findings. MR lymphography at 30 min and 24 h post-injection showed more uptake of SPIO in SLNs. However, MR lymphography 24 h post-injection also visualized higher echelon nodes (HEN). Besides, on MR lymphography SPIO-induced streak artifacts were seen around the injection site, but did not prevent identification of SLNs in vicinity of the tracer injection site. Histopathological assessment confirmed presence of iron in all harvested SLNs. In one patient nodal metastases were found in a harvested SLN; no additional metastases were seen in the neck dissection specimen. No follow-up results were reported in this study. In two patients, tissue swelling was observed at the injection site after administration of SPIO, which was attributed to the volume of SPIO injected.

Maza et al. evaluated fusion of lymphoscintigraphic SPECT, SPIO MR lymphography and CT, for identification of SLNs in rather complex anatomical regions [26]. Fourteen patients were included of whom two diagnosed with tongue cancer; scheduled for tumor resection and ipsilateral elective neck dissection. A mixture of [<sup>99m</sup>Tc]Tc-nanocolloid and SPIO (Resovist), in total 0.5 mL, was peritumorally injected on the day before surgery. MR lymphography was acquired 2 h post-injection. Lymph nodes were assessed as SLN if they corresponded with SPECT images and exhibited signal loss on T2\*-weighted sequences. SPECT-MRI fusion was successful in both OSCC patients and showed corresponding SLNs. Intraoperatively, SLNs were localized using a  $\gamma$ -probe and were sent for individual histopathological assessment. SLN metastases were found in the contralateral neck of one OSCC patient, leading to a complementary contralateral neck dissection. No (additional) lymph node metastases were found in

the neck dissection specimens of both patients. No follow-up results were reported.

### **CT lymphography**

Another approach for high-resolution lymphography regards computed tomography (CT) lymphography using peritumoral administered iodine-based contrast agents. The use of CT lymphography has been investigated in several tumor types including breast, lung, esophageal, gastric and skin cancer [53–64]. In these studies, CT lymphography provided high-resolution visualization of SLNs, lymphatic vessels and surrounding anatomical structures.

For reviewing the application of CT lymphography in early-stage OSCC, the systematic literature search led to retrieval of 112 PubMed indexed articles for CT lymphography, of which 17 were considered relevant [27–32, 41, 42, 65–73]. Of these 17 articles, 11 were animal studies [41, 42, 65–73]. Cross-reference did not lead to any additional relevant articles.

The case report of Saito et al. [32] was the first article that described the application of CT lymphography in an early-stage OSCC patient. Using CT lymphography with peritumoral injection of iopamidol (2.0 mL), a right lateral lingual lymph node was identified as SLN from a cT2N0 right oral tongue tumor. Following partial glossectomy, without any management of the neck or extirpation of the SLN, the patient showed no evidence of disease after 14 months follow-up. This case-report demonstrated that CT lymphography is suitable for visualization of small SLNs located near the primary tumor, such as lingual lymph nodes.

The first series regarding CT lymphography in early-stage OSCC patients (n = 31; oral tongue) was reported by Honda et al. [30]. In this study, CT images were obtained 1, 3, 5, and 10 min after administration of 1.5 mL iopamidol mixed with 0.5 mL 1% lidocaine hydrochloride. Both contrast-enhanced lymph vessels draining the tumor injection site as well as SLNs were identified in 90.3% of patients. Identified SLNs were marked for biopsy using a lattice marker, combined with intraoperative peritumoral patent blue dye injection. All patients, except for those with T1N0 OSCC and negative frozen-section assessment of SLNs (n = 11), underwent selective neck dissection following tumor resection. Using histopathological examination of the neck dissection specimen and a follow-up of 30 months as reference standard, this approach reached a sensitivity of 80% with a NPV of 95.8%.

In the sequel study of Honda et al., including 18 patients with cT1-2N0 oral tongue carcinoma, similar methods were used for CT lymphography, resulting in a preoperative SLN detection rate of 89% [29]. For intraoperative localization of

SLNs, indocyanine green (ICG) and near-infrared imaging was used, instead of patent blue dye. In contrast to their previous study [30], only patients with advanced cT2N0 disease or positive frozen-section assessment of SLNs underwent selective neck dissection (n = 9). In the 16 patients with at least one detected SLN on CT lymphography, a sensitivity of 71.4% and NPV of 81.8% after 38 months median follow-up was reported.

More recently, Sugiyama et al. [31] performed CT lymphography in 20 early-stage OSCC patients. Following peritumoral administration of 2.0 mL iopamidol, SLNs and lymphatic vessels draining the injection site were detected in 95% and 90% of patients, respectively. Two lingual lymph nodes were identified as SLNs (5.4%). The optimal timing for CT scanning in this study was at both 2 and 5 min post-injection, visualizing all 37 contrast-enhanced SLNs. Intraoperative SLN detection was performed under ICG fluorescence guidance; the authors stated to have localized all CT lymphographic identified SLNs during surgery using intraoperatively administered ICG. Both number of patients with metastatic SLNs as well as follow-up results were not reported.

In the sequel study of Sugiyama et al. [27], preoperative CT lymphographic images were reevaluated in 32 early-stage OSCC patients with an approach similar to their previous study [31]. During follow-up 4 of 27 patients with negative SLNB (14.8%), based on CT lymphography, developed regional recurrence and 1 of 5 patients with SLN metastasis (20%) developed recurrence between primary tumor site and the neck. Accordingly, their approach reached a sensitivity of 55.6% and NPV of 85.2%. Reevaluation of CT lymphographic images showed a subtle increase in Hounsfield units (HU) of overlooked SLNs (n = 5) when compared to non-contrast CT images. Besides, their results showed that HU decreased at 10 min post-injection, indicating that iopamidol is only briefly retained in SLNs.

Figure 5 shows CT lymphographic images from a recent long-term follow-up study with early-stage OSCC patients (n = 27; oral tongue) [28]. In this study, SLNs were detected in 96.3% of patients using CT lymphography after peritumoral administration of 2.0 mL iopamidol. Intraoperatively, SLNs were localized using ICG and near-infrared imaging. In total, 5 patients had metastatic SLNs (18.5%) and 3 patients without SLN metastases developed regional recurrence (13.6%) after median follow-up of 76 months. This resulted in a sensitivity and NPV of 62.5% and 86.3%, respectively.

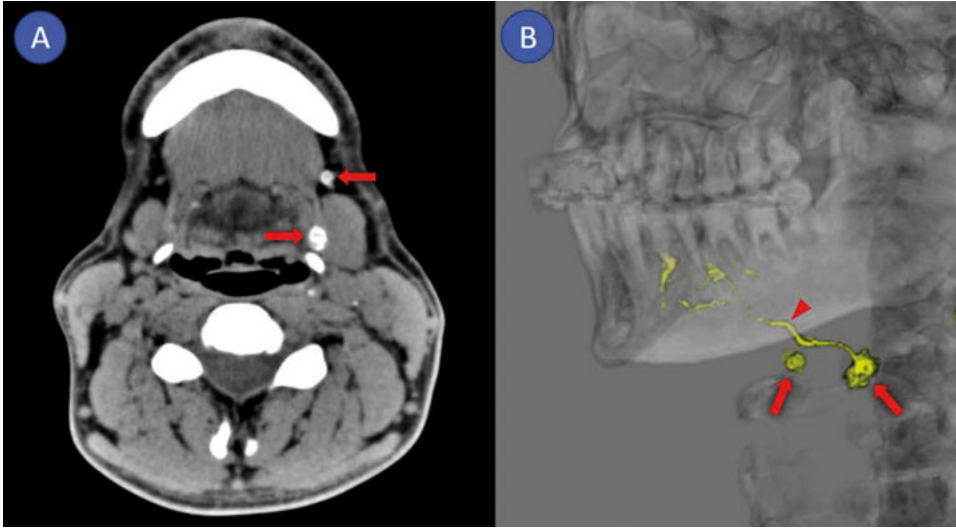


**Figure 5.** Computed tomographic lymphography: (a) axial image, (b) 3D image. Arrows: sentinel lymph node; arrowhead: lymphatics [28]. Figure used with permission of Elsevier©, permission license number: 4807630528815.

### PET lymphoscintigraphy

Alternatively, a potential nuclear imaging modality for improving the diagnostic accuracy of SLNB is positron emission tomography (PET). Since PET is able to detect and record a higher percentage of radioactive emitted events compared to SPECT, PET provides both higher spatial and temporal resolution (i.e., acquires higher number of frames per time unit for dynamic studies) [74]. Consequently, PET could be highly suitable for lymphoscintigraphy and may identify SLNs with higher precision than conventional lymphoscintigraphy with SPECT. Instead of a  $\gamma$ -emitter (e.g.,  $^{99m}\text{Tc}$ ,  $^{60}\text{Co}$ )-labeled radiotracer, generally used for conventional lymphoscintigraphy, PET lymphoscintigraphy requires a positron emitting isotope (e.g.,  $^{89}\text{Zr}$ ,  $^{68}\text{Ga}$ ,  $^{18}\text{F}$ )-labeled radiotracer [75].

A systematic literature search was conducted to review PET lymphoscintigraphy in early-stage OSCC. This led to retrieval of 64 PubMed indexed articles; 4 were considered relevant [33, 34, 76, 77]. Of these 4 studies, 1 regarded an animal study [77] and 1 a review [76] that briefly discusses results from 2 of 3 included studies in our review [34, 77]. Cross-reference did not lead to any additional relevant articles. In 2013, Heuveling et al. were the first to perform dynamic and static PET lymphoscintigraphy in 5 patients with early-stage OSCC, following peritumoral administration of zirconium-89  $^{89}\text{Zr}$ -labeled nanocolloid [34]. Subsequently, 7–9 days after PET lymphoscintigraphy, the routine SLNB procedure with  $^{99m}\text{Tc}$ -labeled nanocolloid was performed. The results of PET and SPECT lymphoscintigraphy were

compared. PET lymphoscintigraphy was able to visualize all foci (n = 22) that were identified on SPECT/CT and even visualized 5 additional foci that were considered to be SLNs; all of which were located near the injection site of the primary tumor (Figure 6). Of these 5 additional foci, considered to be SLNs, 2 regarded lingual lymph nodes. Furthermore, in 4 patients (80%) lymphatic vessels were visualized on dynamic PET lymphoscintigraphy. Intraoperatively, the additionally visualized PET foci close to the injection site could not be localized with the conventional portable  $\gamma$ -probe, due to difficulties in differentiating between SLN and injection site. In two patients metastatic SLNs were found, follow-up results were not reported.

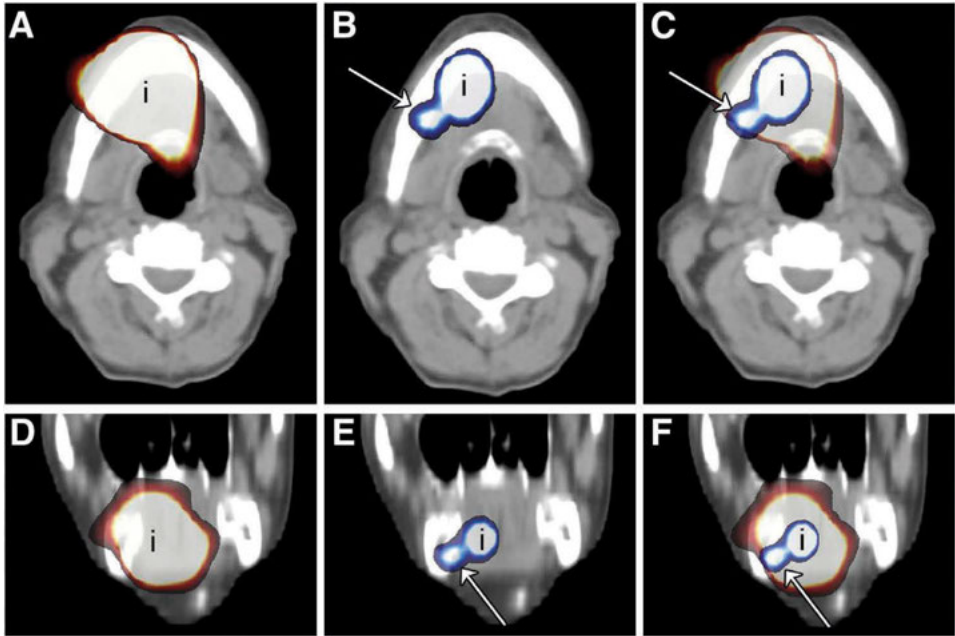


**Figure 6.** (a,d) Axial (a) and coronal (d) SPECT/CT image of injection site (*i*) of patient 1, i.e., floor-of-mouth, in which only a large hot spot from injection site could be visualized. (b,e) PET/CT image of injection site of same patient in which level Ib lymph node (*arrow*) clearly could be identified. (c,f) Fused SPECT and PET/CT images showing that lymph node visualized on PET/CT is hidden behind large hot spot on SPECT/CT images [34]. This research was originally published in JNM [34]. Figure used with permission of original authors. ©SNMMI.

In their sequel study, Heuveling et al. achieved both preoperative SLN detection with PET lymphoscintigraphy, as well as intraoperative SLN localization using a handheld PET-probe, after peritumoral administration of  $^{89}\text{Zr}$ -labeled nanocolloid [33]. This study included 5 OSCC patients who underwent tumor resection including neck dissection (i.e., clinically N1 disease or access of the neck was required for tumor resection or flap reconstruction). Preoperatively 13 SLNs were identified by PET lymphoscintigraphy, whereas the PET-probe detected 10 of 13 SLNs intraoperatively (77%). In this population, 3 patients (60%) had nodal metastases; in 1 patient the histopathologically positive SLN, found in the neck dissection specimen during histopathological assessment, was not localized with the PET-probe, although it was depicted on preoperative PET lymphoscintigraphy. None of the patients developed locoregional recurrence after a median follow-up of 25 months. With histopathological examination of the neck dissection specimen and follow-up as reference standard, this approach reached a sensitivity of 67% with a NPV of 67%. The authors concluded that PET lymphoscintigraphy using  $^{89}\text{Zr}$ -labeled nanocolloid may improve preoperative SLN detection, although it should be combined with other tracers for intraoperative localization.

## Contrast-enhanced lymphosonography

In contrast-enhanced ultrasound (CEUS), echogenic particles such as microbubbles are administered to obtain information on vascularization or delineation of body cavities during ultrasound (US) imaging. FDA and EMA approved microbubbles consist of perfluorocarbons or sulfur hexafluoride ( $\text{SF}_6$ ) gas surrounded by a thin biocompatible shell generally made of phospholipids or proteins [78, 79]. Due to their compressibility and the large difference in acoustic impedance between gas and the surrounding liquid (i.e., blood or lymph) they strongly scatter ultrasound pulses. In addition, due to nonlinear microbubble oscillations, the scattered signal contains higher harmonic frequencies. These higher harmonic frequencies can be distinguished from the fundamental frequency scatter emitted by relatively incompressible tissue surroundings, consequently enhancing microbubble containing structures [78–80] (Figure 7).

Microbubbles are typically administered intravenously, but have more recently been proposed as a radiation-free tracer for lymphosonography. In breast cancer, studies reported SLN localization rates between 60–100%. For CEUS-guided SLNB a pooled sensitivity of 54% (95% CI 47–61%) and a NPV of 83–92%, were reported [81]. Few to no adverse events of the procedure were registered; any minor adverse events consisted of localized redness, pain or bruising at the injection site [81, 82].

To review contrast-enhanced lymphosonography in OSCC, a systematic literature search was conducted, which led to retrieval of 107 PubMed indexed articles. A total of 6 studies were considered relevant (i.e., 2 clinical studies [35, 36] and 4 large animal studies [83–86]). Cross-reference did not lead to identification of additional relevant articles.

Figure 7 illustrates the procedure used in the two clinical studies [35, 36]. Gvetadze et al. [35] used sulfur hexafluoride ( $\text{SF}_6$ ) phospholipid microbubbles (SonoVue; Bracco International B.V.) in 12 patients with T1-2cN0 oral tongue carcinoma and looked for lymph node enhancement after repetitive peritumoral injections. Fifteen SLNs were identified in 11 of 12 patients (91.7%). No attempt was made at intraoperative localization of identified SLNs and therefore the correlation between identified SLNs and histopathological assessment was lacking. In the second clinical study, Wakisaka et al. [36] studied lymphosonography with perfluorobutane phospholipid ( $\text{C}_4\text{F}_8$ ) microbubbles (Sonazoid; GE Healthcare, UK) in 10 patients with T1-4N0 oral or oropharyngeal carcinomas. Sonazoid was injected in four peritumoral locations. In 8 of 10 patients, 12 SLNs were identified. In one patient with a T4 tumor, Sonazoid had to be injected intratumorally and no SLNs were identified. SLN locations were marked on the skin. The next day indigo carmine blue dye was injected intraoperatively at the same injection sites. All lymph nodes marked during lymphosonography, which

were not always dyed blue, were examined with frozen section analysis. Since frozen section analysis was negative in all cases, a less extensive neck dissection was performed. No metastatic lymph nodes were found during histopathological examination of neck dissection specimens. No follow-up results were reported for both studies. Contrast-related adverse events did not occur [35, 36].

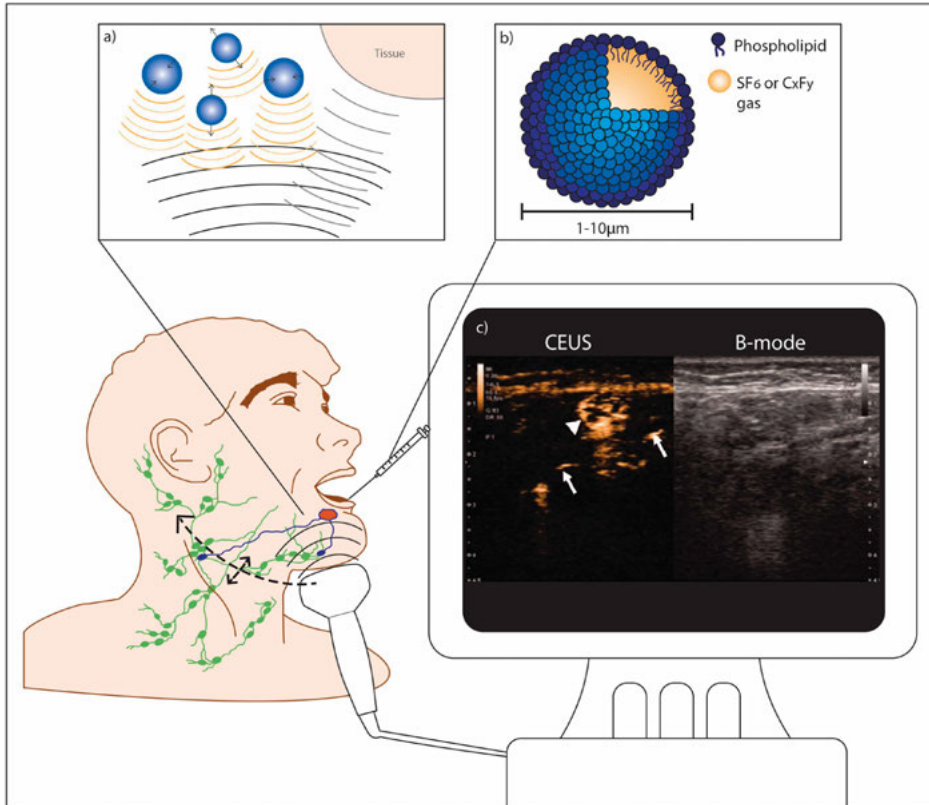


**Figure 7.** Contrast-enhanced lymphosonography in oral cancer. After microbubble injection at one or multiple peritumoral locations, contrast-enhancement of the injection site is visualized in ultrasound contrast mode. Using real-time imaging, the transportation of the microbubbles through lymphatic vessels may be followed until they accumulate in the sentinel lymph nodes. Subsequently, the neck is scanned for additional contrast-enhanced lymph nodes. Contrast-enhanced lymph nodes can be either marked for surgical resection or directly subjected to biopsy or aspiration cytology. Peritumoral injections can be repeated if necessary. (a) Schematic representation of a microbubble; (b) Principle of contrast-enhanced ultrasound (CEUS): oscillating microbubbles produce strong nonlinear scattering which can be distinguished from scattering by the surrounding tissue; (c) Contrast-enhanced ultrasonography with Sonazoid. On the left half is a contrast-enhanced image, and on the right is the B-mode image. Contrast-enhancement of sentinel lymph nodes (SLNs) (arrowheads) was observed concomitant with lymphatic ducts (arrows) draining the nodes. (Adapted with permission from [36], copyright 2019 Taylor & Francis Group; license number: 4810090088685).

## Discussion

This paper reviewed new developments in preoperative SLN imaging techniques in patients with early-stage OSCC. None of the included clinical studies contradicted outcomes or clinical translation predictions from corresponding animal studies, in regard of SLN identification using these novel techniques [23–32, 43–47, 51, 52, 65, 67, 68, 70–73]. The overall reported rate of patients in which SLNs were identified using the presented techniques ranged from 89–100%. The overall reported sensitivity ranged from 56–91%, with a NPV of 67–96% (Table 1).

Although the diagnostic accuracy of most presented techniques appears to be inferior to conventional lymphoscintigraphy including SPECT/CT, there are several promising advantages to the presented preoperative SLN imaging techniques which will be discussed individually in the subsections below. Accordingly, drawbacks of the presented techniques and methodology of the included studies will be discussed as well. While other (head and neck) tumor sites were not included in this review, the discussed strengths and flaws of performing SLNB using these techniques may also be relevant to other (head and neck) tumor sites. A summary of relative merits and disadvantages for each technique is listed in Table 2.

### MR lymphography

Bae et al. showed that MR lymphography using gadobutrol, is a promising technique for SLN detection in early-stage OSCC, with a sensitivity of 90.9%, a NPV of 92.8% and lymphatic vessel visualization in 81% of patients [23]. The high spatial resolution, high signal-to-noise ratio and few artifacts that MR lymphography with gadolinium-based contrast agents provides, even when compared to MR lymphography with SPIO, is the foremost asset of this technique [25, 49, 87–89]. These features result in accurate anatomical detail and facilitate visualization of lymphatic vessels, which is helpful in assessing whether a contrast-enhanced lymph node is a true SLN or a higher echelon node (HEN) [34]. Moreover, the high spatial resolution of MR lymphography eliminates the shine-through phenomenon, allowing identification of SLNs in vicinity of the tracer injection site. Additionally, MR lymphography is free of radiation exposure and does not require radioisotopes, which is of particular benefit if specific nuclear medicine facilities are unavailable [90, 91].

Nevertheless, the low molecular weight of gadolinium-based contrast agents results in rapid lymphatic transportation, little retention in SLNs and rapid washout of the contrast agent [47, 92]. This could increase the risk to overlook SLNs and of contrast-enhanced HEN(s) to erroneously being considered SLN(s). Since Bae et al. performed elective neck dissection in all patients, used only histopathological examination of

the neck dissection specimen as reference standard and did not report any follow-up results (e.g., nodal recurrence), it is uncertain whether SLNs were overlooked with this technique [23]. Therefore, the diagnostic accuracy of SLNB using MR lymphography with gadolinium-based contrast agents in early-stage OSCC patients is yet to be established in larger studies with histopathological examination and follow-up as reference standard.

**Table 2.** Merits and drawbacks per technique

Technique	Advantages	Drawbacks
<u>Conventional lymphoscintigraphy &amp; SPECT/CT</u>	Widely investigated and implemented Allows intraoperative localization of depicted SLNs Differentiation in intensity of radioactive signal Allows (intraoperative) differentiation between SLNs and HENs	Subject to shine-through phenomenon Requires nuclear facilities Low spatial resolution (~5 mm) Poor soft tissue contrast
<u>MR Lymphography (Gd<sup>3+</sup>)</u>	High spatial resolution (~1 mm) High signal-to-noise ratio and few artifacts Accurate anatomical detail Eliminates shine-through phenomenon Visualization lymphatic vessels May facilitate more targeted radiotherapy No nuclear facilities required Free of radiation exposure	Lacks intraoperative localization of depicted SLNs Rapid lymphatic transportation tracer No retention of tracer in SLNs Gd <sup>3+</sup> -based contrast agents not registered for lymphography
<u>MR Lymphography (SPIO)</u>	High spatial resolution (~1 mm) Accurate anatomical detail Allows intraoperative localization of depicted SLNs Eliminates shine-through phenomenon May facilitate more targeted radiotherapy No nuclear facilities required Free of radiation exposure	Limited clinical experience in OSCC Retention in SLNs depends on particle size Excess amounts of iron leads to signal voids Negative contrast may confound effectivity SLN detection Local inflammation following administration Metal elements interfere with magnetometer
<u>CT Lymphography</u>	High spatial resolution (~0.5 mm) High temporal resolution Eliminates shine-through phenomenon Visualization lymphatic vessels Visualization of lingual SLNs May facilitate more targeted radiotherapy No nuclear facilities required Widely available and low costs	Lacks intraoperative localization of depicted SLNs Rapid lymphatic transportation tracer No retention of tracer in SLNs Prone to artifacts Poor soft tissue contrast

SPECT/CT; *single photon emission computed tomography/computed tomography*, SLN; *sentinel lymph node*, HEN; *higher echelon node*, MR; *magnetic resonance*, Gd<sup>3+</sup>; *gadolinium*, SPIO; *superparamagnetic iron oxide*, OSCC; *oral squamous cell carcinoma*, CT; *computed tomography*, PET; *positron emission tomography*, IRD; *infrared dye*, <sup>68</sup>Ga; *gallium-68*, <sup>99m</sup>Tc; *technetium-99m*, USgFNA; *ultrasound guided fine-needle aspiration*.

In addition, MR lymphography with gadolinium-based contrast agents cannot be performed when MRI or administration of these agents is contraindicated [90]. Besides, gadolinium-based contrast agents are not registered for lymphography and clinical trials on MR lymphography using these contrast agents are required before this technique can be implemented in routine clinical care.

Moreover, it is important to note that gadolinium-based contrast agents cannot be detected intraoperatively. The solution offered by Bae et al. [23] (i.e., injection of identified SLNs with blue dye) is probably not reliable enough to assess whether the observed SLNs depicted on MR lymphography exactly matched the same nodes in the neck dissection specimen. A proposed alternative for intraoperative localization of SLNs is fluorescence guided surgery following peritumoral injection of ICG [93, 94]. However, due to limited tissue penetration of the fluorescent signal and rapid flow through lymphatics of unbound ICG, matching of preoperative depicted SLNs and intraoperative fluorescent lymph nodes is challenging [91].

The inability to detect gadolinium intraoperatively, may be overcome by using SPIO for MR lymphography, as SPIO can be detected by both MRI and a handheld magnetometer [24, 25]. Accordingly, SPIO may facilitate intraoperative localization of preoperative depicted SLNs, while maintaining benefits of MR lymphography over other imaging modalities (Table 2). Still, a correlation between preoperatively identified SLNs on MR lymphography and intraoperative localized SLNs with the handheld magnetometer has not yet been reported for early-stage OSCC patients.

The first results of MR lymphography using SPIO are auspicious, as all identified SLNs by MR lymphography corresponded with those identified by conventional lymphoscintigraphy [25, 26]. Besides, adequate differentiation of SLN from injection site was seen [25] and precise anatomical information on SLN location was acquired when fused with SPECT [26].

However, some challenges for MR lymphography with SPIO remain. First of all, both ideal SPIO particle size and amount of iron administered are still under consideration. A hydrodynamic diameter of 59 nm was considered most suitable due to its fast uptake in lymphatics, retention in SLNs and its high accumulation when compared to SPIOs with a hydrodynamic diameter of 32 nm and 111 nm [51]. Hence, Resovist (45–60 nm) and Magtrace (59 nm) may be fitting candidates [24–26]. With respect to the volume of SPIO administered with corresponding iron quantity, a considerable difference is seen among reports [24–26]. While a higher concentration may assist intraoperative localization of SLNs [24], excessive concentrations of SPIO can lead to disproportionate signal voids on MR lymphography and may hamper

preoperative SLN identification [88]. Vice versa, a lower concentration may benefit preoperative SLN identification [25], but may impede intraoperative localization [49]. Furthermore, the negative contrast that SPIO provides on MR lymphography, which can be induced by other factors as well (i.e., dental implants, tissue interfaces, background noise, air), may confound the efficiency of detecting SLNs [26, 88, 89]. Moreover, in regard of intraoperative localization of SPIO-enhanced SLNs using the magnetometer, magnetic signals deriving from metal elements (e.g., pacemakers, prosthetics, surgical instruments) interfere with the magnetometer. This can instigate some logistical issues, such as requiring plastic surgical instruments, and can even lead to a contraindication for using the magnetometer in some cases (e.g., patients with pacemakers or prosthetics) [24]. Finally, concerns were addressed concerning swelling, local inflammation and pain of the injection site following administration of SPIO, which may depend on the volume of SPIO administered [24, 25].

Some reports mention a higher number of identified SLNs on MR lymphography with SPIO when compared to conventional lymphoscintigraphy and SPECT/CT, due to the better resolution of MR lymphography [49, 50]. It can be debated if the higher number of identified SLNs by MR lymphography with SPIO includes not only true SLNs, but HENs as well. Since Mizokami et al. showed more enhanced lymph nodes at 24 h post-injection, which were considered HENs, the timing of MR lymphography following SPIO administration seems to be pertinent in selecting the right contrast-enhanced lymph nodes for SLNB [25]. To distinguish true SLNs from HENs, visualization of lymphatic vessels may provide a solution. However, visualization of contrast-enhanced lymphatic vessels was not reported in any of the included studies [25, 26]. To enable visualization of contrast-enhanced lymphatic vessels administration of smaller SPIOs is suggested, but is criticized by their faster migration through the lymphatic system [25].

Currently, the limited number of early-stage OSCC patients who underwent MR lymphography with SPIO prevents assessment of its diagnostic accuracy. Larger studies with adequate reference standards (i.e., histopathological assessment including follow-up) should be conducted to establish the diagnostic accuracy of MR lymphography with SPIO in OSCC patients.

In conclusion, MR lymphography using gadolinium-based contrast agents may currently not offer an alternative for conventional SLNB using radiotracers, mainly due to the lack of reliable intraoperative localization of preoperatively depicted SLNs. MR lymphography with SPIO may provide a solution, as it allows for intraoperative localization of SLNs with a magnetometer. However, MR lymphography with SPIO is subject to other limitations that may confound the efficiency of preoperative detection

and intraoperative localization of SLNs. Nonetheless, MR lymphography using either contrast agent can provide precise preoperative anatomical localization and identification of SLNs, particularly in situations with close spatial relation between injection site and SLN(s). Accordingly, MR lymphography might be a valuable addition to radiotherapy planning (e.g., higher radiation dose on SLNs), by performing MR lymphography as part of MRI that is increasingly used for radiotherapy planning in head and neck cancer [95]. MR lymphography-guided nodal irradiation may improve regional control, reduce acute and late radiation-related toxicity and enhance health-related quality-of-life [96].

### **CT lymphography**

CT lymphography has been proposed as a high potential alternative for conventional lymphoscintigraphy, with a sensitivity ranging from 56–80% and a NPV ranging from 82–96% [27–30]. Two series reported enhanced lymphatic vessel visualization in 90% of their patients [30, 31]; in two studies lingual lymph nodes were identified as SLNs using CT lymphography [31, 32].

CT lymphography shares several beneficial properties with MR lymphography: high spatial resolution, visualization of lymphatic vessels and elimination of shine-through phenomenon. The latter has been demonstrated by the identification of lingual lymph nodes as SLNs using CT lymphography [31, 32]. Besides, CT lymphography does not require specific nuclear facilities and is easily implemented due to the wide availability of CT and iodine-based contrast agents [29, 90]. Compared to MRI, CT has lower costs and is considered more comfortable for patients [90].

Yet, challenges for CT lymphography are similar to those in MR lymphography using gadolinium-based contrast agents. First of all, iodine-based contrast agents cannot be detected intraoperatively. Most authors used fluorescence guidance with intraoperatively administered ICG for SLN localization of preoperatively depicted SLNs by CT lymphography [27–29, 31]. As previously mentioned, matching of preoperative depicted SLNs and intraoperative fluorescent lymph nodes is challenging [91]. Secondly, the rapid lymphatic transportation, limited retention in SLNs and rapid washout of iopamidol increases the risk to overlook SLNs and of contrast-enhanced HEN(s) to erroneously being considered SLN(s). This risk has been especially emphasized by Sugiyama et al., who showed that overlooked SLNs were only marginally contrast-enhanced on CT lymphography and that iopamidol was only briefly retained in SLNs [27].

Additional challenges arise for CT lymphography, especially when compared to MR lymphography, since CT has poor soft tissue contrast and is prone to artefacts from

dental amalgam or orthopedic material, if present, which may hamper adequate visualization of SLNs. Besides, CT implies radiation exposure and, although only a low volume (2 mL) is used compared to regular intravenous use, iodine-based contrast agents may induce anaphylactic reactions, contrast-induced nephropathy or thyroid dysfunction [90]. However, contrast-related adverse events did not occur in any of the included studies [27–32].

Further developments regarding CT lymphography should address these limitations (i.e., dual-tracer methods, high velocity lymphatic drainage tracer, limited retention of tracer in SLNs) to improve its diagnostic accuracy for SLNB.

As an alternative for iopamidol as CT lymphographic tracer, lipiodol might be worth considering. In contrast to iopamidol, lipiodol is oil-based with higher viscosity and is registered and widely used for lymphographic purposes [97]. The higher viscosity of lipiodol might result in increased retention in SLNs and delayed tracer wash-out, possibly improving preoperative SLN detection on CT lymphography. Moreover, lipiodol has been combined with ICG as a single emulsion, which could overcome the limitations of dual tracer methods, potentially enabling reliable intraoperative localization of preoperative depicted SLNs [98]. This has yet to be investigated in a clinical trial with an adequate reference standard (i.e., histopathological examination and follow-up).

Although CT lymphography requires some further developments, it has the potential for highly accurate identification of SLNs in early-stage OSCC patients. Especially in cases where SLNs are in close vicinity to the tracer injection site. Besides, analogous to MR lymphography, CT lymphography, performed concomitantly with conventional CT imaging for radiotherapy planning, may facilitate more targeted radiotherapy and consequently improve regional control, reduce acute and late radiation-related toxicity and enhance health-related quality-of-life [95, 96].

### **PET lymphoscintigraphy**

Heuveling et al. demonstrated the high potential of preoperative PET lymphoscintigraphy using  $^{89}\text{Zr}$ -labeled nanocolloid for SLN detection in OSCC patients, by visualizing all foci identified on SPECT/CT and even detecting 5 additional SLNs in vicinity of the tracer injection site. Additionally, in 80% of patients, lymphatic vessels were visualized and 2 lingual lymph nodes (7%) were identified as SLNs [34]. In correspondence with MR- and CT lymphography, the high spatial resolution of PET lymphoscintigraphy enables identification of SLNs located close to the tracer injection site, which was demonstrated by detection of 2 lingual SLNs using PET lymphoscintigraphy. Moreover, PET lymphoscintigraphy provides both high temporal

resolution as well as visualization of lymphatic vessels, contributing to better differentiation between true SLNs and HENs [34].

In contrast to the other presented techniques in this review, PET lymphoscintigraphy permits the use of commonly administered tracers for SLNB (e.g., nanocolloids, tilmanocept), whose kinetics have proven to be particularly suitable for SLNB [14, 99]. Moreover, Heuveling et al. achieved reliable intraoperative localization of SLNs that were preoperatively identified by PET lymphoscintigraphy, using a handheld PET-probe [33]. Consequently, this method is unaffected by limitations of dual tracer methods.

Although intraoperative localization of SLNs using a handheld PET-probe was considered feasible, some concerns were addressed [33]. First of all, the PET-probe detected only 12 of 15 SLNs as identified by PET lymphoscintigraphy, which was attributed to the PET-probe's limited sensitivity, resulting in a relatively low accuracy of the procedure (i.e., sensitivity 67%; NPV 67%). Secondly, a handheld PET-probe is relatively large in size because of features necessary for detection of high-energy photons from positron emitting isotopes [33, 100]. Due to the limited sensitivity and large size of the PET-probe, wider skin incisions and exploration of the neck were required for SLN localization [33].

To overcome the problems with the use of a PET-probe, a radiotracer labeled with both  $^{89}\text{Zr}$  and a  $\gamma$ -emitter (e.g.,  $^{99\text{m}}\text{Tc}$ ) could allow high-resolution preoperative PET lymphoscintigraphy and intraoperative localization of SLNs using the conventional portable  $\gamma$ -probe. However, due to its half-life of 78.4 h,  $^{89}\text{Zr}$  will interfere with the  $^{99\text{m}}\text{Tc}$ -signal [101]. Therefore, a positron emitting isotope with a shorter half-life is required to enable detection of the  $^{99\text{m}}\text{Tc}$ -signal for intraoperative localization of SLNs using the conventional portable  $\gamma$ -probe.

Fluorine-18 ( $^{18}\text{F}$ ) is considered the ideal radioisotope for PET imaging owing to the low positron energy (0.64 MeV), providing high-resolution images. Furthermore,  $^{18}\text{F}$  has a half-life of only 110 min [102]. However,  $^{18}\text{F}$  relies on C–F bond formation and is therefore difficult to label to currently used radiotracers for SLNB (e.g., nanocolloids or tilmanocept) [103]. Recently, PET lymphoscintigraphy with interstitially injected [ $^{18}\text{F}$ ]FDG has been investigated in patients with cervical or endometrial cancer and in healthy subjects [104, 105]. Hypothesized was that the small size of the tracer allows passage through channels infiltrated with tumor cells, and that its molecular function allows uptake by tumor cells, which is not achieved by any of the currently used radiotracers for SLNB [104]. In the study with cervical or uterine cancer patients, SLN mapping was successful in 80% of patients [104]. In the study with healthy

subjects however, PET lymphoscintigraphy using [ $^{18}\text{F}$ ]FDG was not considered feasible due to significant tracer washout to systemic capillaries [105]. Alternatively, gallium-68 ( $^{68}\text{Ga}$ ) is a good candidate due to its half-life of only 68 min and its production with a  $^{68}\text{Ge}/^{68}\text{Ga}$ -generator, which provides an opportunity to prepare PET-radiopharmaceuticals on site when needed [101, 106]. Moreover, its chemical properties allow labelling to various diagnostic molecules [107].

Whereas labelling of nanocolloids with  $^{68}\text{Ga}$  is complicated, mainly due to instability of the bond between  $^{68}\text{Ga}$  and nanocolloids [107],  $^{68}\text{Ga}$  has been successfully labeled to tilmanocept [107]. Moreover, fluorescent (IRD-800CW)-labeled tilmanocept can be radiolabeled with both  $^{68}\text{Ga}$  and  $^{99\text{m}}\text{Tc}$ . The resulting tri-modal agent provides high-resolution preoperative PET-images for SLN mapping and intraoperative localization of SLNs with both a conventional portable  $\gamma$ -probe and fluorescence imaging [109]. This tri-model agent has been successfully tested with reliable SLN identification in animal models [110, 111]. Although PET lymphoscintigraphy using this tri-model agent might provide a solution to the issues addressed for SLNB in early-stage OSCC, it is indisputable that first it has to be investigated in a clinical trial with adequate reference standards.

### **Contrast-enhanced lymphosonography**

Compared to conventional lymphoscintigraphy, lymphosonography has many advantages (Table 2). Importantly, microbubbles are free of ionizing radiation and have a good safety profile, which was extensively documented for intravenous administration [112–114]. Secondly, lymphosonography is not affected by the shine-through phenomenon. Furthermore, none of the studies in humans or large animals found HEN enhancement [35, 36, 83–86]. It is possible that this is prevented by phagocytosis of microbubbles (which was histologically confirmed in animals for Sonazoid [86]) and the size of microbubbles compared to small-molecule dyes. Another advantage is the possibility to use lymphosonography preoperatively to improve lymph node selection for USgFNA. The sensitivity of USgFNA alone ranges from 45 up to 90% [115, 116]. Adding lymphosonography could lead to more true positive patients, in whom the complex SLNB procedure may be omitted. A clinical trial using the combination of lymphosonography and USgFNA preceding SLNB will have to determine the value of this technique in head and neck oncological practice. Finally, ultrasound equipment is globally widely available and its mobility provides the option to use it in the operating room. Accordingly, lymphosonography may extend the application of SLNB from OSCC to less reachable sites of the head and neck (i.e., nasopharynx, oropharynx, larynx and hypopharynx), by allowing both peritumoral injection as well as SLN identification under general anesthesia.

However, lymphosonography has some disadvantages (Table 2). Foremost, the procedure is highly operator dependent and fast (a few seconds to minutes) transportation of microbubbles through the lymphatic system can make SLN identification challenging. Therefore, experienced staff will have to be appointed and trained. Future research will need to determine interobserver variability. Furthermore, if used without FNA it might be challenging to intraoperatively localize SLNs identified with preoperative lymphosonography; a reliable system to mark the exact location of SLNs is necessary. This drawback however is valid for several preoperative SLNB imaging techniques (i.e., CT lymphography, MR lymphography), and can be circumvented by combining lymphosonography with USgFNA or by performing lymphosonography intraoperatively.

Besides, further research is needed to find out which CEUS imaging method and which microbubble are most suitable. The two clinical studies report a specific contrast imaging mode at a low mechanical index (MI), thus leaving the microbubbles intact [35, 36, 83, 84, 86]. Four animal studies performed lymphosonography in the head and neck region using Sonazoid, combined with either blue dye or ICG, in swine and rabbits without tumors [83, 84, 86] and with Definity in dogs with spontaneously arisen tumors [85]. The studies in swine added color flow Doppler at a high (microbubble destructing) mechanical index of 1.0 to confirm the presence of microbubbles [83, 84]. In dogs power Doppler with a mechanical index of 1.3 was used primarily, which produces a color flair upon microbubble destruction [85]. To select the most suitable microbubble, it is necessary to consider practicalities: using a microbubble that quickly reaches SLNs and is retained and detectable in the SLN for a long time might increase reproducibility. SonoVue consists of SF<sub>6</sub> phospholipid microbubbles with a mean bubble diameter of ~2.5 μm [80], while Sonazoid consists of perfluorobutane phospholipid (C<sub>x</sub>F<sub>y</sub>) microbubbles with a mean bubble diameter ~2.1 μm [117]. In most studies the time between peritumoral administration and lymph node enhancement (transit time) was described. Although no within-study comparisons have been made and clinical studies cannot be compared directly to preclinical studies, the transit time appears to be shorter for SonoVue (10–50 s post-injection [35]), than for Sonazoid (1–11 min post-injection [83, 84, 86]). Sonazoid enhancement seems to persist longer, namely ≥ 90 min [86], versus 2–4 min with SonoVue [35]. This could explain why multiple injections were necessary to identify SLNs in the clinical study using SonoVue [35]. However, Sonazoid has not yet been approved by FDA and EMA as a US contrast agent, which could complicate its application in clinical lymphosonography trials.

To conclude, lymphosonography is a promising method, but current clinical experience in OSCC is sparse. The two published clinical studies indicate that this

technique is feasible, with SLN detection rates of 80 and 92% [35, 36]. Unfortunately, correlation with histopathology is still lacking. In the only study that attempted this, no metastatic lymph nodes were detected [36]. Larger studies, preferably with histopathological examination and follow-up as reference standard, are needed to determine the diagnostic accuracy (i.e., sensitivity and NPV) of this technique for SLNB in OSCC and its place in the diagnostic workflow.

## References

1. D'Cruz AK, Vaish R, Kapre N, et al. Elective versus therapeutic neck dissection in node-negative oral cancer. *N Engl J Med*. 2015;373(6):521-529. doi:10.1056/NEJMoa1506007
2. Abu-Ghanem S, Yehuda M, Carmel NN, et al. Elective neck dissection vs observation in early-stage squamous cell carcinoma of the oral tongue with no clinically apparent lymph node metastasis in the neck: a systematic review and meta-analysis. *JAMA Otolaryngol Head Neck Surg*. 2016;142(9):857-865. doi:10.1001/jamaoto.2016.1281
3. de Bree R, Takes RP, Shah JP, et al. Elective neck dissection in oral squamous cell carcinoma: Past, present and future. *Oral Oncol*. 2019;90:87-93. doi:10.1016/j.oraloncology.2019.01.016
4. den Toom IJ, Boeve K, Lobeek D, et al. Elective neck dissection or sentinel lymph node biopsy in early stage oral cavity cancer patients: the Dutch experience. *Cancers (Basel)*. 2020;12(7):1783. doi:10.3390/cancers12071783
5. Schilling C, Shaw R, Schache A, et al. Sentinel lymph node biopsy for oral squamous cell carcinoma. Where are we now? *Br J Oral Maxillofac Surg*. 2017;55(8):757-762. doi:10.1016/j.bjoms.2017.07.007
6. Cramer JD, Sridharan S, Ferris RL, Duvvuri U, Samant S. Sentinel lymph node biopsy versus elective neck dissection for stage I to II oral cavity cancer. *Laryngoscope*. 2019;129(1):162-169. doi:10.1002/lary.27323
7. Schiefke F, Akdemir M, Weber A, Akdemir D, Singer S, Frerich B. Function, postoperative morbidity, and quality of life after cervical sentinel node biopsy and after selective neck dissection. *Head Neck*. 2009;31(4):503-512. doi:10.1002/hed.21001
8. Murer K, Huber GF, Haile SR, Stoeckli SJ. Comparison of morbidity between sentinel node biopsy and elective neck dissection for treatment of the n0 neck in patients with oral squamous cell carcinoma. *Head Neck*. 2011;33(9):1260-1264. doi:10.1002/hed.21622
9. Govers TM, Schreuder WH, Klop WM, et al. Quality of life after different procedures for regional control in oral cancer patients: cross-sectional survey. *Clin Otolaryngol*. 2016;41(3):228-233. doi:10.1111/coa.12502
10. Govers TM, Takes RP, Baris Karakullukcu M, et al. Management of the N0 neck in early stage oral squamous cell cancer: a modeling study of the cost-effectiveness. *Oral Oncol*. 2013;49(8):771-777. doi:10.1016/j.oraloncology.2013.05.001
11. de Bree R, Nieweg OE. The history of sentinel node biopsy in head and neck cancer: From visualization of lymphatic vessels to sentinel nodes. *Oral Oncol*. 2015;51(9):819-823. doi:10.1016/j.oraloncology.2015.06.006
12. Schilling C, Stoeckli SJ, Vigili MG, et al. Surgical consensus guidelines on sentinel node biopsy (SNB) in patients with oral cancer. *Head Neck*. 2019;41(8):2655-2664. doi:10.1002/hed.25739
13. Alkureishi LW, Burak Z, Alvarez JA, et al. Joint practice guidelines for radionuclide lymphoscintigraphy for sentinel node localization in oral/oropharyngeal squamous cell carcinoma. *Ann Surg Oncol*. 2009;16(11):3190-3210. doi:10.1245/s10434-009-0726-8
14. Giammarile F, Schilling C, Gnanasegaran G, et al. The EANM practical guidelines for sentinel lymph node localisation in oral cavity squamous cell carcinoma. *Eur J Nucl Med Mol Imaging*. 2019;46(3):623-637. doi:10.1007/s00259-018-4235-5
15. Dhawan I, Sandhu SV, Bhandari R, Sood N, Bhullar RK, Sethi N. Detection of cervical lymph node micrometastasis and isolated tumor cells in oral squamous cell carcinoma using immunohistochemistry and serial sectioning. *J Oral Maxillofac Pathol*. 2016;20(3):436-444. doi:10.4103/0973-029X.190946
16. Liu M, Wang SJ, Yang X, Peng H. Diagnostic efficacy of sentinel lymph node biopsy in early oral squamous cell carcinoma: a meta-analysis of 66 studies. *PLoS One*. 2017;12(1):e0170322. doi:10.1371/journal.pone.0170322
17. Boeve K, Schepman KP, Schuurings E, et al. High sensitivity and negative predictive value of sentinel lymph node biopsy in a retrospective early stage oral cavity cancer cohort in the Northern Netherlands. *Clin Otolaryngol*. 2018;43(4):1080-1087. doi:10.1111/coa.13107
18. Den Toom IJ, Heuveling DA, Flach GB, et al. Sentinel node biopsy for early-stage oral cavity cancer: the VU University Medical Center experience. *Head Neck*. 2015;37(4):573-578. doi:10.1002/hed.23632
19. Alkureishi LW, Ross GL, Shoaib T, et al. Sentinel node biopsy in head and neck squamous cell cancer: 5-year follow-up of a European multicenter trial. *Ann Surg Oncol*. 2010;17(9):2459-2464. doi:10.1245/s10434-010-1111-3

20. Pedersen NJ, Jensen DH, Hedbäck N, et al. Staging of early lymph node metastases with the sentinel lymph node technique and predictive factors in T1/T2 oral cavity cancer: A retrospective single-center study. *Head Neck*. 2016;38 Suppl 1:E1033-E1040. doi:10.1002/hed.24153
21. Stoeckli SJ, Huebner T, Huber GF, Broglie MA. Technique for reliable sentinel node biopsy in squamous cell carcinomas of the floor of mouth. *Head Neck*. 2016;38(9):1367-1372. doi:10.1002/hed.24440
22. Moher D, Liberati A, Tetzlaff J, Altman DG; PRISMA Group. Preferred reporting items for systematic reviews and meta-analyses: the PRISMA Statement. *Open Med*. 2009;3(3):e123-e130.
23. Bae S, Lee HJ, Nam W, Koh YW, Choi EC, Kim J. MR lymphography for sentinel lymph node detection in patients with oral cavity cancer: Preliminary clinical study. *Head Neck*. 2018;40(7):1483-1488. doi:10.1002/hed.25167
24. Hernando J, Aguirre P, Aguilar-Salvatierra A, Leizaola-Cardesa IO, Bidaguren A, Gómez-Moreno G. Magnetic detection of sentinel nodes in oral squamous cell carcinoma by means of superparamagnetic iron oxide contrast. *J Surg Oncol*. 2020;121(2):244-248. doi:10.1002/jso.25810
25. Mizokami D, Kosuda S, Tomifuji M, et al. Superparamagnetic iron oxide-enhanced interstitial magnetic resonance lymphography to detect a sentinel lymph node in tongue cancer patients. *Acta Otolaryngol*. 2013;133(4):418-423. doi:10.3109/00016489.2012.744143
26. Maza S, Taupitz M, Taymoorian K, et al. Multimodal fusion imaging ensemble for targeted sentinel lymph node management: initial results of an innovative promising approach for anatomically difficult lymphatic drainage in different tumour entities. *Eur J Nucl Med Mol Imaging*. 2007;34(3):378-383. doi:10.1007/s00259-006-0223-2
27. Sugiyama S, Iwai T, Izumi T, et al. Sentinel lymph node mapping of clinically N0 early oral cancer: a diagnostic pitfall on CT lymphography. *Oral Radiol*. 2021;37(2):251-255. doi:10.1007/s11282-020-00442-1
28. Ishiguro K, Iwai T, Izumi T, et al. Sentinel lymph node biopsy with preoperative CT lymphography and intraoperative indocyanine green fluorescence imaging for N0 early tongue cancer: A long-term follow-up study. *J Craniomaxillofac Surg*. 2020;48(3):217-222. doi:10.1016/j.jcms.2020.01.007
29. Honda K, Ishiyama K, Suzuki S, Kawasaki Y, Saito H, Horii A. Sentinel lymph node biopsy using preoperative computed tomographic lymphography and intraoperative indocyanine green fluorescence imaging in patients with localized tongue cancer. *JAMA Otolaryngol Head Neck Surg*. 2019;145(8):735-740. doi:10.1001/jamaoto.2019.1243
30. Honda K, Ishiyama K, Suzuki S, et al. Sentinel lymph node biopsy using computed tomographic lymphography in patients with early tongue cancer. *Acta Otolaryngol*. 2015;135(5):507-512. doi:10.3109/00016489.2015.1010126
31. Sugiyama S, Iwai T, Izumi T, et al. CT lymphography for sentinel lymph node mapping of clinically N0 early oral cancer. *Cancer Imaging*. 2019;19(1):72. doi:10.1186/s40644-019-0258-9
32. Saito M, Nishiyama H, Oda Y, Shingaki S, Hayashi T. The lingual lymph node identified as a sentinel node on CT lymphography in a patient with cN0 squamous cell carcinoma of the tongue. *Dentomaxillofac Radiol*. 2012;41(3):254-258. doi:10.1259/dmfr/61883763
33. Heuveling DA, Karagozoglu KH, Van Lingen A, Hoekstra OS, Van Dongen GAMS, De Bree R. Feasibility of intraoperative detection of sentinel lymph nodes with 89-zirconium-labelled nanocolloidal albumin PET-CT and a handheld high-energy gamma probe. *EJNMMI Res*. 2018;8(1):15. doi:10.1186/s13550-018-0368-6
34. Heuveling DA, van Schie A, Vugts DJ, et al. Pilot study on the feasibility of PET/CT lymphoscintigraphy with <sup>89</sup>Zr-nanocolloidal albumin for sentinel node identification in oral cancer patients. *J Nucl Med*. 2013;54(4):585-589. doi:10.2967/jnumed.112.115188
35. Gvetadze SR, Xiong P, Lv M, et al. Contrast-enhanced ultrasound mapping of sentinel lymph nodes in oral tongue cancer-a pilot study. *Dentomaxillofac Radiol*. 2017;46(3):20160345. doi:10.1259/dmfr.20160345
36. Wakisaka N, Endo K, Kitazawa T, et al. Detection of sentinel lymph node using contrast-enhanced agent, Sonazoid™, and evaluation of its metastasis with superb microvascular imaging in oral and oropharyngeal cancers: a preliminary clinical study. *Acta Otolaryngol*. 2019;139(1):94-99. doi:10.1080/00016489.2018.1535193
37. Li C, Meng S, Yang X, Zhou D, Wang J, Hu J. Sentinel lymph node detection using magnetic resonance lymphography with conventional gadolinium contrast agent in breast cancer: a preliminary clinical study. *BMC Cancer*. 2015;15:213. doi:10.1186/s12885-015-1255-4

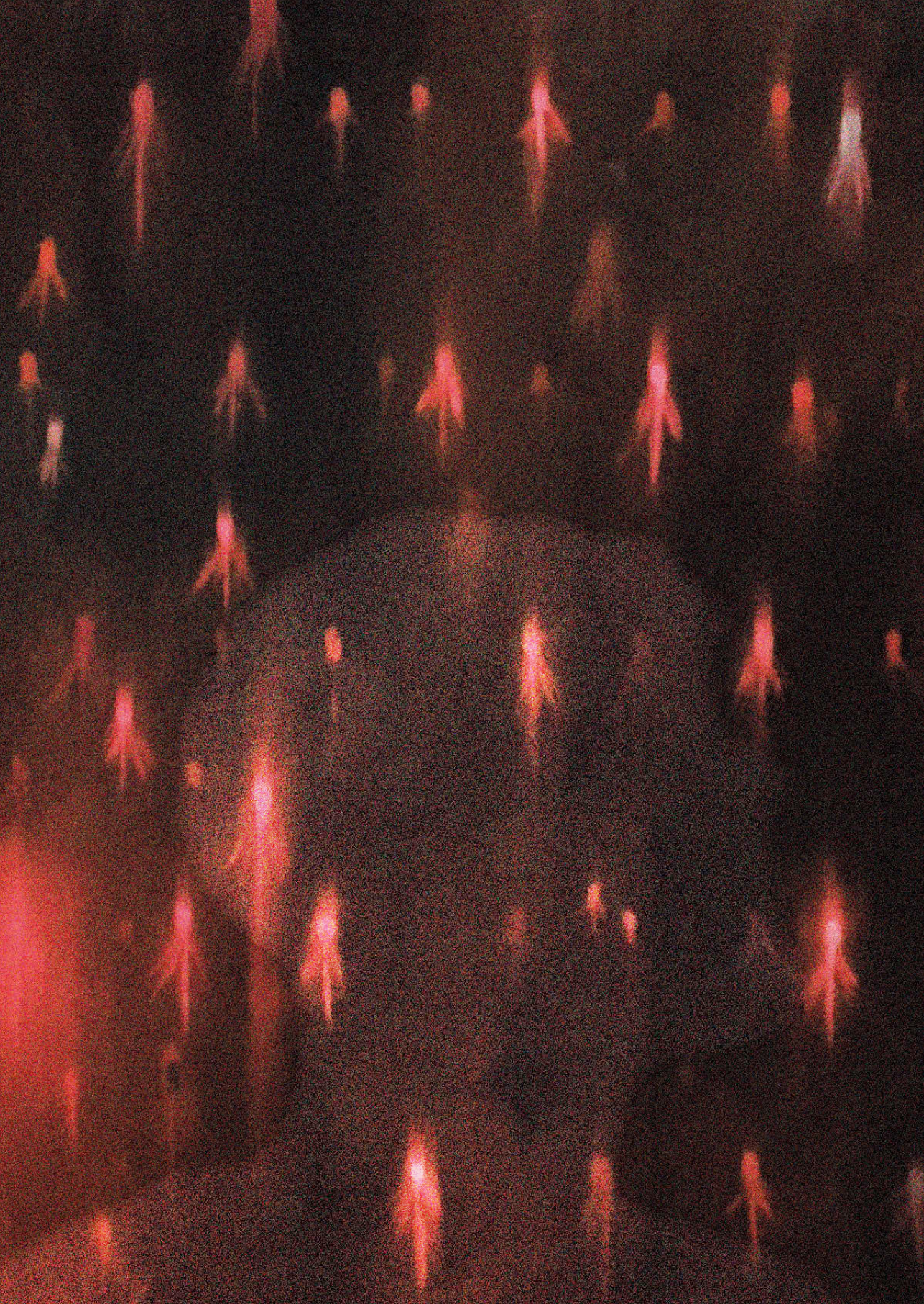
38. Lu Q, Hua J, Kassir MM, et al. Imaging lymphatic system in breast cancer patients with magnetic resonance lymphangiography. *PLoS One*. 2013;8(7):e69701. doi:10.1371/journal.pone.0069701
39. Hong Y, Xiang L, Hu Y, Zhou Z, Yu H, Zhu B. Interstitial magnetic resonance lymphography is an effective diagnostic tool for the detection of lymph node metastases in patients with cervical cancer. *BMC Cancer*. 2012;12:360. doi:10.1186/1471-2407-12-360
40. Scott LJ. Gadobutrol: A review in contrast-enhanced MRI and MRA *Clin Drug Investig*. 2018;38(8):773-784. doi:10.1007/s40261-018-0674-9
41. Yang Y, Zhou B, Zhou J, Shi X, Sha Y, Wu H. Assessment of lingual sentinel lymph nodes metastases using dual-modal indirect CT/MR lymphography with gold-gadolinium-based nanoprobe in a tongue VX<sub>2</sub> carcinoma model. *Acta Otolaryngol*. 2018;138(8):727-733. doi:10.1080/00016489.2018.1441544
42. Yang Y, Zhou J, Shi X, Sha Y, Wu H. Long-term observation of indirect lymphography using gadolinium-loaded polyethylenimine-entrapped gold nanoparticles as a dual mode CT/MR contrast agent for rabbit lingual sentinel lymph node identification. *Acta Otolaryngol*. 2017;137(2):207-214. doi:10.1080/00016489.2016.1222550
43. Mayer MN, Kraft SL, Bucy DS, Waldner CL, Elliot KM, Wiebe S. Indirect magnetic resonance lymphography of the head and neck of dogs using Gadofluorine M and a conventional gadolinium contrast agent: a pilot study. *Can Vet J*. 2012;53(10):1085-1090.
44. Nason RW, Torchia MG, Morales CM, Thliveris J. Dynamic MR lymphangiography and carbon dye for sentinel lymph node detection: a solution for sentinel lymph node biopsy in mucosal head and neck cancer. *Head Neck*. 2005;27(4):333-338. doi:10.1002/hed.20173
45. Torchia MG, Misselwitz B. Combined MR lymphangiography and MR imaging-guided needle localization of sentinel lymph nodes using Gadomer-17. *AJR Am J Roentgenol*. 2002;179(6):1561-1565. doi:10.2214/ajr.179.6.1791561
46. Kitamura N, Kosuda S, Araki K, et al. Comparison of animal studies between interstitial magnetic resonance lymphography and radiocolloid SPECT/CT lymphoscintigraphy in the head and neck region. *Ann Nucl Med*. 2012;26(3):281-285. doi:10.1007/s12149-011-0565-0
47. Loo BW Jr, Draney MT, Sivanandan R, et al. Indirect MR lymphangiography of the head and neck using conventional gadolinium contrast: a pilot study in humans. *Int J Radiat Oncol Biol Phys*. 2006;66(2):462-468. doi:10.1016/j.ijrobp.2006.05.045
48. Johnson L, Pinder SE, Douek M. Deposition of superparamagnetic iron-oxide nanoparticles in axillary sentinel lymph nodes following subcutaneous injection. *Histopathology*. 2013;62(3):481-486. doi:10.1111/his.12019
49. Pouw JJ, Grootendorst MR, Bezooijen R, et al. Pre-operative sentinel lymph node localization in breast cancer with superparamagnetic iron oxide MRI: the SentiMAG Multicentre Trial imaging subprotocol. *Br J Radiol*. 2015;88(1056):20150634. doi:10.1259/bjr.20150634
50. Winter A, Kowald T, Paulo TS, et al. Magnetic resonance sentinel lymph node imaging and magnetometer-guided intraoperative detection in prostate cancer using superparamagnetic iron oxide nanoparticles. *Int J Nanomedicine*. 2018;13:6689-6698. doi:10.2147/IJN.S173182
51. Pouw JJ, Ahmed M, Anninga B, et al. Comparison of three magnetic nanoparticle tracers for sentinel lymph node biopsy in an in vivo porcine model. *Int J Nanomedicine*. 2015;10:1235-1243. doi:10.2147/IJN.S76962
52. Torchia MG, Nason R, Danzinger R, Lewis JM, Thliveris JA. Interstitial MR lymphangiography for the detection of sentinel lymph nodes. *J Surg Oncol*. 2001;78(3):151-157. doi:10.1002/jso.1139
53. Suga K, Ogasawara N, Okada M, Matsunaga N. Interstitial CT lymphography-guided localization of breast sentinel lymph node: preliminary results. *Surgery*. 2003;133(2):170-179. doi:10.1067/msy.2003.17
54. Tangoku A, Yamamoto S, Suga K, et al. Sentinel lymph node biopsy using computed tomography-lymphography in patients with breast cancer. *Surgery*. 2004;135(3):258-265. doi:10.1016/j.surg.2003.07.003
55. Yamamoto S, Suga K, Maeda K, Maeda N, Yoshimura K, Oka M. Breast sentinel lymph node navigation with three-dimensional computed tomography-lymphography: a 12-year study. *Breast Cancer*. 2016;23(3):456-462. doi:10.1007/s12282-015-0584-0
56. Nakagawa M, Morimoto M, Takechi H, Tadokoro Y, Tangoku A. Preoperative diagnosis of sentinel lymph node (SLN) metastasis using 3D CT lymphography (CTLG). *Breast Cancer*. 2016;23(3):519-524. doi:10.1007/s12282-015-0597-8

57. Sugi K, Kitada K, Yoshino M, et al. New method of visualizing lymphatics in lung cancer patients by multidetector computed tomography. *J Comput Assist Tomogr.* 2005;29(2):210-214. doi:10.1097/01.rct.0000154241.22519.2f
58. Takizawa H, Kondo K, Toba H, et al. Computed tomography lymphography by transbronchial injection of iopamidol to identify sentinel nodes in preoperative patients with non-small cell lung cancer: a pilot study. *J Thorac Cardiovasc Surg.* 2012;144(1):94-99. doi:10.1016/j.jtcvs.2012.03.040
59. Hayashi H, Tangoku A, Suga K, et al. CT lymphography-navigated sentinel lymph node biopsy in patients with superficial esophageal cancer. *Surgery.* 2006;139(2):224-235. doi:10.1016/j.surg.2005.07.027
60. Yuasa Y, Seike J, Yoshida T, et al. Sentinel lymph node biopsy using intraoperative indocyanine green fluorescence imaging navigated with preoperative CT lymphography for superficial esophageal cancer. *Ann Surg Oncol.* 2012;19(2):486-493. doi:10.1245/s10434-011-1922-x
61. Filip B, Scarpa M, Cavallin F, Alfieri R, Cagol M, Castoro C. Minimally invasive surgery for esophageal cancer: a review on sentinel node concept. *Surg Endosc.* 2014;28(4):1238-1249. doi:10.1007/s00464-013-3314-8
62. Lee JH, Park DJ, Kim YH, Shin CM, Lee HS, Kim HH. Clinical implementations of preoperative computed tomography lymphography in gastric cancer: a comparison with dual tracer methods in sentinel node navigation surgery. *Ann Surg Oncol.* 2013;20(7):2296-2303. doi:10.1245/s10434-012-2855-8
63. Kim YH, Lee YJ, Park JH, et al. Early gastric cancer: feasibility of CT lymphography with ethiodized oil for sentinel node mapping. *Radiology.* 2013;267(2):414-421. doi:10.1148/radiol.12121527
64. Yasuta M, Sato S, Ishida T, Kiyohara T. Usefulness of CT-lymphography in sentinel lymph node navigation. *Int J Clin Oncol.* 2014;19(3):557-562. doi:10.1007/s10147-013-0582-1
65. Randall EK, Jones MD, Kraft SL, Worley DR. The development of an indirect computed tomography lymphography protocol for sentinel lymph node detection in head and neck cancer and comparison to other sentinel lymph node mapping techniques. *Vet Comp Oncol.* 2020;18(4):634-644. doi:10.1111/vco.12585
66. Shi F, Yang Y, Chen J, Sha Y, Shu Y, Wu H. Dendrimer-entrapped gold nanoparticles as potential CT contrast agents for localizing sentinel lymph node via indirect CT lymphography on rabbit model. *Biomed Res Int.* 2018;2018:1230151. doi:10.1155/2018/1230151
67. Rossi F, Körner M, Suárez J, et al. Computed tomographic-lymphography as a complementary technique for lymph node staging in dogs with malignant tumors of various sites. *Vet Radiol Ultrasound.* 2018;59(2):155-162. doi:10.1111/vru.12569S
68. Grimes JA, Secrest SA, Northrup NC, Saba CE, Schmiedt CW. Indirect computed tomography lymphangiography with aqueous contrast for evaluation of sentinel lymph nodes in dogs with tumors of the head. *Vet Radiol Ultrasound.* 2017;58(5):559-564. doi:10.1111/vru.12514
69. Yang Y, Shi F, Zhou J, Shi X, Sha Y, Wu H. Short-term dynamic observation of the color change and enhancement effect of polyethylenimine-entrapped gold nanoparticles used for indirect lymphography. *ORL J Otorhinolaryngol Relat Spec.* 2016;78(3):136-143. doi:10.1159/000446190
70. Shu Y, Xu X, Wang Z, et al. Assessment of cervical lymph node metastases using indirect computed tomography lymphography with iopamidol in a tongue VX2 carcinoma model. *J Laryngol Otol.* 2011;125(8):820-828. doi:10.1017/S0022215111000958
71. Shu Y, Xu X, Chodara AM, et al. Correlative study of indirect computed tomography lymphography using iopamidol and histopathology in a cervical lymph node metastasis model. *Laryngoscope.* 2011;121(4):724-731. doi:10.1002/lary.21404
72. Wu H, Ying H, Xi X, et al. Localization of the sentinel lymph node in tongue VX2 carcinoma via indirect CT lymphography combined with methylene blue dye injection. *Acta Otolaryngol.* 2010;130(4):503-510. doi:10.3109/00016480903253595
73. Wu H, Xu X, Ying H, et al. Preliminary study of indirect CT lymphography-guided sentinel lymph node biopsy in a tongue VX2 carcinoma model. *Int J Oral Maxillofac Surg.* 2009;38(12):1268-1272. doi:10.1016/j.ijom.2009.07.009
74. Rahmim A, Zaidi H. PET versus SPECT: strengths, limitations and challenges. *Nucl Med Commun.* 2008;29(3):193-207. doi:10.1097/MNM.0b013e3282f3a515
75. Wadsak W, Mitterhauser M. Basics and principles of radiopharmaceuticals for PET/CT. *Eur J Radiol.* 2010;73(3):461-469. doi:10.1016/j.ejrad.2009.12.022
76. Bluemel C, Rubello D, Colletti PM, de Bree R, Herrmann K. Sentinel lymph node biopsy in oral and oropharyngeal squamous cell carcinoma: current status and unresolved challenges. *Eur J Nucl Med Mol Imaging.* 2015;42(9):1469-1480. doi:10.1007/s00259-015-3049-y

77. Heuveling DA, Visser GW, Baclayon M, et al. <sup>89</sup>Zr-nanocolloidal albumin-based PET/CT lymphoscintigraphy for sentinel node detection in head and neck cancer: preclinical results. *J Nucl Med.* 2011;52(10):1580-1584. doi:10.2967/jnumed.111.089557
78. Chong WK, Papadopoulou V, Dayton PA. Imaging with ultrasound contrast agents: current status and future. *Abdom Radiol (NY).* 2018;43(4):762-772. doi:10.1007/s00261-018-1516-1
79. Frinking P, Segers T, Luan Y, Tranquart F. Three Decades of Ultrasound Contrast Agents: A Review of the Past, Present and Future Improvements. *Ultrasound Med Biol.* 2020;46(4):892-908. doi:10.1016/j.ultrasmedbio.2019.12.008
80. Greis C. Technology overview: SonoVue (Bracco, Milan). *Eur Radiol.* 2004;14 Suppl 8:P11-P15.
81. Nielsen Moody A, Bull J, Culpán AM, et al. Preoperative sentinel lymph node identification, biopsy and localisation using contrast enhanced ultrasound (CEUS) in patients with breast cancer: a systematic review and meta-analysis. *Clin Radiol.* 2017;72(11):959-971. doi:10.1016/j.crad.2017.06.121
82. Machado P, Stanczak M, Liu JB, et al. Subdermal ultrasound contrast agent injection for sentinel lymph node identification: an analysis of safety and contrast agent dose in healthy volunteers. *J Ultrasound Med.* 2018;37(7):1611-1620. doi:10.1002/jum.14502
83. Curry JM, Bloedon E, Malloy KM, et al. Ultrasound-guided contrast-enhanced sentinel node biopsy of the head and neck in a porcine model. *Otolaryngol Head Neck Surg.* 2007;137(5):735-741. doi:10.1016/j.otohns.2007.07.019
84. Curry JM, Grindle CR, Merton DA, Goldberg BB, Rosen D, Pribitkin EA. Lymphosonographic sentinel node biopsy of the supraglottis in a swine model. *Otolaryngol Head Neck Surg.* 2008;139(6):798-804. doi:10.1016/j.otohns.2008.08.029
85. Lurie DM, Seguin B, Schneider PD, Verstraete FJ, Wisner ER. Contrast-assisted ultrasound for sentinel lymph node detection in spontaneously arising canine head and neck tumors. *Invest Radiol.* 2006;41(4):415-421. doi:10.1097/01.rli.0000201230.29925.95
86. Kogashiwa Y, Sakurai H, Akimoto Y, et al. Sentinel node biopsy for the head and neck using contrast-enhanced ultrasonography combined with indocyanine green fluorescence in animal models: a feasibility study. *PLoS One.* 2015;10(7):e0132511. doi:10.1371/journal.pone.0132511
87. Choi SH, Moon WK. Contrast-enhanced MR imaging of lymph nodes in cancer patients. *Korean J Radiol.* 2010;11(4):383-394. doi:10.3348/kjr.2010.11.4.383
88. Liu T, Spincemaille P, de Rochefort L, Wong R, Prince M, Wang Y. Unambiguous identification of superparamagnetic iron oxide particles through quantitative susceptibility mapping of the nonlinear response to magnetic fields. *Magn Reson Imaging.* 2010;28(9):1383-1389. doi:10.1016/j.mri.2010.06.011
89. Lin C, Cai S, Feng J. Positive contrast imaging of SPIO nanoparticles. *J Nanomater.* 2012;2012. doi: <https://doi.org/10.1155/2012/734842>
90. Tshering Vogel DW, Thoeny HC. Cross-sectional imaging in cancers of the head and neck: how we review and report. *Cancer Imaging.* 2016;16(1):20. doi:10.1186/s40644-016-0075-3
91. de Bree R, Dankbaar JW, de Keizer B. New developments in sentinel lymph node biopsy procedure in localized oral cancer. *JAMA Otolaryngol Head Neck Surg.* 2019;145(8):741-742. doi:10.1001/jamaoto.2019.1342
92. Bisso S, Degrassi A, Brambilla D, Leroux JC. Poly(ethylene glycol)-alendronate coated nanoparticles for magnetic resonance imaging of lymph nodes. *J Drug Target.* 2019;27(5-6):659-669. doi:10.1080/1061186X.2018.1545235
93. Nakamura T, Kogashiwa Y, Nagafuji H, Yamauchi K, Kohno N. Validity of sentinel lymph node biopsy by ICG fluorescence for early head and neck cancer. *Anticancer Res.* 2015;35(3):1669-1674.
94. Peng H, Wang SJ, Niu X, Yang X, Chi C, Zhang G. Sentinel node biopsy using indocyanine green in oral/oropharyngeal cancer. *World J Surg Oncol.* 2015;13:278. doi:10.1186/s12957-015-0691-6
95. Wong KH, Panek R, Bhide SA, Nutting CM, Harrington KJ, Newbold KL. The emerging potential of magnetic resonance imaging in personalizing radiotherapy for head and neck cancer: an oncologist's perspective. *Br J Radiol.* 2017;90(1071):20160768. doi:10.1259/bjr.20160768
96. de Veij Mestdagh PD, Walraven I, Vogel WV, et al. SPECT/CT-guided elective nodal irradiation for head and neck cancer is oncologically safe and less toxic: A potentially practice-changing approach. *Radiother Oncol.* 2020;147:56-63. doi:10.1016/j.radonc.2020.03.012
97. Pieper CC, Hur S, Sommer CM, et al. Back to the future: Lipiodol in lymphography-from diagnostics to theranostics. *Invest Radiol.* 2019;54(9):600-615. doi:10.1097/RLI.0000000000000578

98. Kim H, Lee SK, Kim YM, et al. Fluorescent iodized emulsion for pre- and intraoperative sentinel lymph node imaging: validation in a preclinical model. *Radiology*. 2015;275(1):196-204. doi:10.1148/radiol.14141159
99. Wallace AM, Hoh CK, Ellner SJ, Darrah DD, Schulteis G, Vera DR. Lymphoseek: a molecular imaging agent for melanoma sentinel lymph node mapping. *Ann Surg Oncol*. 2007;14(2):913-921. doi:10.1245/s10434-006-9099-4
100. Gulec SA. PET probe-guided surgery. *J Surg Oncol*. 2007;96(4):353-357. doi:10.1002/jso.20862
101. Kasbollah A, Eu P, Cowell S, Deb P. Review on production of <sup>89</sup>Zr in a medical cyclotron for PET radiopharmaceuticals. *J Nucl Med Technol*. 2013;41(1):35-41. doi:10.2967/jnmt.112.111377
102. Couturier O, Luxen A, Chatal JF, Vuillez JF, Rigo P, Hustinx R. Fluorinated tracers for imaging cancer with positron emission tomography. *Eur J Nucl Med Mol Imaging*. 2004;31(8):1182-1206. doi:10.1007/s00259-004-1607-9
103. Ting R, Aguilera TA, Crisp JL, et al. Fast <sup>18</sup>F labeling of a near-infrared fluorophore enables positron emission tomography and optical imaging of sentinel lymph nodes. *Bioconjug Chem*. 2010;21(10):1811-1819. doi:10.1021/bc1001328
104. Mueller JJ, Dauer LT, Murali R, et al. Positron lymphography via intracervical <sup>18</sup>F-FDG injection for presurgical lymphatic mapping in cervical and endometrial malignancies. *J Nucl Med*. 2020;61(8):1123-1130. doi:10.2967/jnumed.119.230714
105. Jensen MR, Simonsen L, Lonsdale M, Bülow JB. Foot skin depots of <sup>18</sup>F-fluorodeoxyglucose do not enable PET/CT lymphography of the lower extremity lymphatic system in man. *EJNMMI Res*. 2013;3(1):17. doi:10.1186/2191-219X-3-17
106. Martiniova L, Palatis L, Etchebehere E, Ravizzini G. Gallium-68 in medical imaging. *Curr Radiopharm*. 2016;9(3):187-207. doi:10.2174/1874471009666161028150654
107. Persico MG, Marengo M, De Matteis G, et al. <sup>99m</sup>Tc-<sup>68</sup>Ga-ICG-labelled macroaggregates and nanocolloids of human serum albumin: synthesis procedures of a trimodal imaging agent using commercial kits. *Contrast Media Mol Imaging*. 2020;2020:3629705. doi:10.1155/2020/3629705
108. Stroup SP, Kane CJ, Farchshchi-Heydari S, et al. Preoperative sentinel lymph node mapping of the prostate using PET/CT fusion imaging and Ga-68-labeled tilmanocept in an animal model. *Clin Exp Metastasis*. 2012;29(7):673-680. doi:10.1007/s10585-012-9498-9
109. Qin Z, Hoh CK, Hall DJ, Vera DR. A tri-modal molecular imaging agent for sentinel lymph node mapping. *Nucl Med Biol*. 2015;42(12):917-922. doi:10.1016/j.nucmedbio.2015.07.011
110. Lee HJ, Barback CV, Hoh CK, et al. Fluorescence-based molecular imaging of porcine urinary bladder sentinel lymph nodes. *J Nucl Med*. 2017;58(4):547-553. doi:10.2967/jnumed.116.178582
111. Anderson KM, Barback CV, Qin Z, et al. Molecular imaging of endometrial sentinel lymph nodes utilizing fluorescent-labeled Tilmanocept during robotic-assisted surgery in a porcine model. *PLoS One*. 2018;13(7):e0197842. doi:10.1371/journal.pone.0197842
112. Wei K, Mulvagh SL, Carson L, et al. The safety of deFinity and Optison for ultrasound image enhancement: a retrospective analysis of 78,383 administered contrast doses. *J Am Soc Echocardiogr*. 2008;21(11):1202-1206. doi:10.1016/j.echo.2008.07.019
113. Tang C, Fang K, Guo Y, et al. Safety of sulfur hexafluoride microbubbles in sonography of abdominal and superficial organs: retrospective analysis of 30,222 cases. *J Ultrasound Med*. 2017;36(3):531-538. doi:10.7863/ultra.15.11075
114. Miyamoto Y, Ito T, Takada E, Omoto K, Hirai T, Moriyasu F. Efficacy of sonazoid (perflubutane) for contrast-enhanced ultrasound in the differentiation of focal breast lesions: phase 3 multicenter clinical trial. *AJR Am J Roentgenol*. 2014;202(4):W400-W407. doi:10.2214/AJR.12.10518
115. de Bondt RB, Nelemans PJ, Hofman PA, et al. Detection of lymph node metastases in head and neck cancer: a meta-analysis comparing US, USgFNAC, CT and MR imaging. *Eur J Radiol*. 2007;64(2):266-272. doi:10.1016/j.ejrad.2007.02.037
116. Liao LJ, Hsu WL, Wang CT, Lo WC, Lai MS. Analysis of sentinel node biopsy combined with other diagnostic tools in staging cN0 head and neck cancer: A diagnostic meta-analysis. *Head Neck*. 2016;38(4):628-634. doi:10.1002/hed.23945
117. Sontum PC. Physicochemical characteristics of Sonazoid, a new contrast agent for ultrasound imaging. *Ultrasound Med Biol*. 2008;34(5):824-833. doi:10.1016/j.ultrasmedbio.2007.11.006





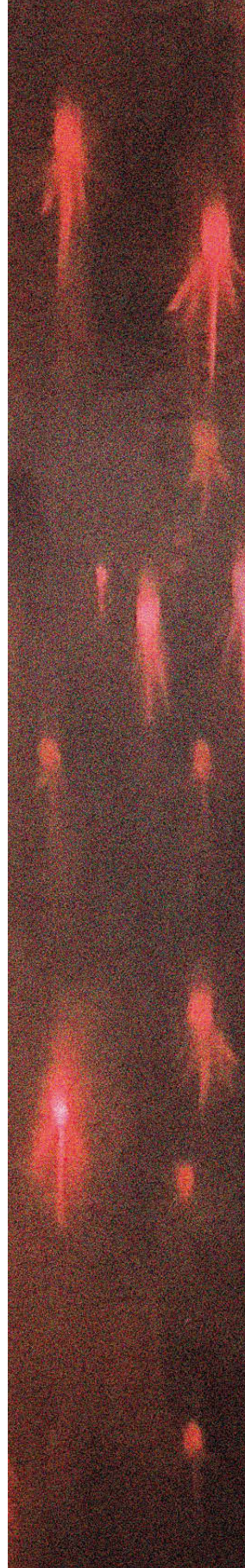
# 8

## Sentinel lymph node detection in early-stage oral squamous cell carcinoma using magnetic resonance lymphography: a pilot study

---

Dominique N.V. Donders, Rutger Mahieu, Roosmarijn S. Tellman,  
Marielle E.P. Philippens, Robert J.J. van Es, Ellen M. van Cann,  
Gerben E. Breimer, Remco de Bree, Bart de Keizer.

*J Clin Med. 2024 Nov 22;13(23):7052*



# Abstract

## Objective

To evaluate MR lymphography following peritumoral administration of a gadolinium-based contrast agent for sentinel lymph node (SLN) mapping in early-stage (cT1-2N0) oral squamous cell carcinoma (OSCC).

## Methods

This pilot study compared the identification of SLNs by MR lymphography using a gadolinium-based contrast agent (gadobutrol) to conventional [ $^{99m}\text{Tc}$ ]Tc-nanocolloid lymphoscintigraphy (including SPECT/CT) in 10 early-stage OSCC patients undergoing sentinel lymph node biopsy (SLNB). Patients initially underwent conventional lymphoscintigraphy following peritumoral administration of indocyanine green- $^{99m}\text{Tc}$ ]Tc-nanocolloid (120 megabecquerel;  $\sim 0.5$  mL). Subsequently, 0.5-1.0 mL gadobutrol was peritumorally injected, and MR imaging was acquired for 30 minutes. The following day, the identified SLNs were harvested and subjected to histopathological assessment. MR lymphography and [ $^{99m}\text{Tc}$ ]Tc-nanocolloid lymphoscintigraphy were evaluated and compared with respect to SLN identification. The reference standard consisted of histopathological evaluation of the harvested SLNs, specimens from complementary neck dissection, and follow-up data.

## Results

MR lymphography detected 16 out of 27 SLNs identified by [ $^{99m}\text{Tc}$ ]Tc-nanocolloid lymphoscintigraphy, revealing an additional SLN that did not harbor metastasis. MR lymphography failed to identify any SLNs in one patient. Of 7 histopathologically positive SLNs detected by [ $^{99m}\text{Tc}$ ]Tc-nanocolloid lymphoscintigraphy, 3 were identified by MR lymphography. All patients remained disease-free after a median follow-up of 16 months. Compared to [ $^{99m}\text{Tc}$ ]Tc-nanocolloid lymphoscintigraphy, MR lymphography using gadobutrol achieved an SLN identification rate of 59%, a sensitivity of 75%, and a negative predictive value of 86%.

## Conclusion

The study suggests that MR lymphography using gadobutrol is unreliable for SLN mapping in early-stage OSCC.

## Introduction

Sentinel lymph node biopsy (SLNB) is a well-established staging procedure for patients with clinically negative necks in early-stage oral squamous cell carcinoma (OSCC). Compared to elective neck dissection, SLNB provides similar survival outcomes while significantly reducing functional morbidity [1–3]. Despite advances in sentinel lymph node (SLN) imaging techniques, such as single-photon emission computed tomography/computed tomography (SPECT/CT) [4], the utilization of conventional technetium-99m ( $^{99m}\text{Tc}$ ) labeled radiotracers in SLNB still presents technical and logistical challenges. Moreover, it emits gamma radiation, and is potentially harmful for both patients and healthcare workers. Therefore, ongoing investigations are being conducted to examine alternative high-resolution imaging techniques for SLN imaging [5–7].

A major challenge in SLNB for OSCC is the shine-through phenomenon, where radioactivity from the injection site overshadows nearby SLNs, particularly in tumors located in the floor-of-mouth. This phenomenon reduces the sensitivity of SLN detection. Magnetic resonance (MR) lymphography, using gadolinium-based contrast agents, offers high spatial resolution and a superior signal-to-noise ratio compared to conventional lymphoscintigraphy. This technique can potentially eliminate the shine-through effect by providing detailed anatomical images that allow for the reliable identification of SLNs located close to the injection site. Moreover, MR lymphography does not involve radiation exposure or require radioisotopes, making it a safer and more accessible option, especially in settings where nuclear medicine facilities are limited [8–10]. Recent studies have demonstrated the potential of interstitial contrast-enhanced magnetic resonance imaging (MRI) with extracellular gadolinium-based contrast agents for SLN mapping in patients with breast cancer and OSCC [11–13]. In a pioneering study involving OSCC patients, MR lymphography using a small volume (1 mL) of peritumorally administered gadobutrol consistently identified SLNs in all 26 patients, with the majority (81%) also visualizing draining lymphatic vessels. Among the 11 patients with pathologically positive necks, 10 were correctly staged using MR lymphography. However, in one case, MR lymphography identified SLNs in ipsilateral level III, while final histopathology revealed metastases in ipsilateral level I without level III involvement [11].

Despite these promising findings, significant concerns remain due to methodological limitations. These include patient selection bias, reliance on inferior reference standards, and the lack of follow-up data. For instance, SLNs identified by MR lymphography were injected with blue dye under ultrasound guidance the day before surgery; the blue stained SLN were dissected from the elective neck dissection

specimen one to two weeks following MR lymphography. Additionally, the inclusion of larger tumors, which inherently have a higher risk of cervical metastases, may have skewed results. Furthermore, the absence of follow-up data limits the assessment of the true accuracy of MR lymphography using gadolinium-based contrast agents. The histopathological examination in this study did not employ step-serial-sectioning or immunohistochemistry, increasing the risk of missing micrometastases.

The present study aims to provide a more rigorous comparison of the SLN identification rate and accuracy of MR lymphography using gadobutrol versus conventional lymphoscintigraphy in early-stage OSCC patients. By utilizing detailed histopathological assessment and follow-up, particularly in cases with negative SLNB results, this study seeks to offer a clearer understanding of the true accuracy of MR lymphography with gadobutrol for SLN mapping.

## Materials and methods

### Patients

This study received approval from the Ethics Committee of the University Medical Center Utrecht (no. 21/722). Between April 2022 and June 2023, a total of 10 patients diagnosed with early-stage OSCC (cT1-2N0; TNM Staging Union for International Cancer Control (UICC) 8<sup>th</sup> Edition [14]) and scheduled for SLNB were prospectively included in this study.

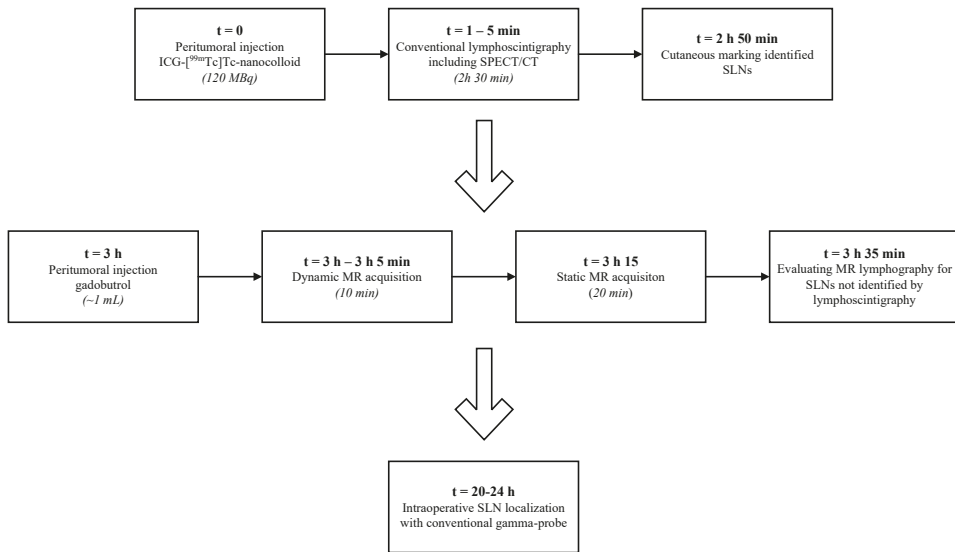
A clinical negative nodal staging was determined by palpation and ultrasound of the neck in all patients; ultrasound-guided fine-needle aspiration cytology (USgFNAC) was performed in those with enlarged and suspicious lymph nodes [15]. Additional diagnostic MRIs of the head and neck were performed on 4 out of 10 patients.

Patients with previous head and neck malignancies in the past five years were excluded from participation in this study, as well as those with a history of significant neck injury that would hinder surgical dissection of SLNs, previous neck dissection, or radiotherapy to the neck. Furthermore, patients with a documented allergic reaction to gadolinium-based contrast agents, known claustrophobia, or severe renal impairment (eGFR <30) were ineligible for enrollment in this study.

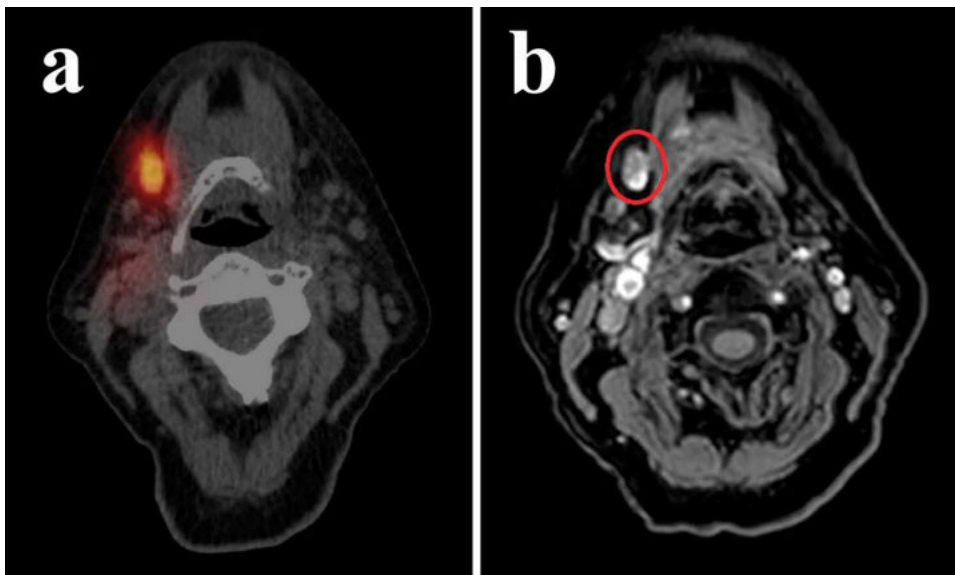
### Study design

Figure 1 presents an overview of the study procedures. On the day before surgery, enrolled patients first received peritumoral injections of 120 megabecquerel (MBq) and 0.05 mg indocyanine green (ICG-)[<sup>99m</sup>Tc]Tc-nanocolloid in a volume of ~0.5 mL, followed by lymphoscintigraphy, including SPECT/CT. Following lymphoscintigraphy, the location of identified SLNs was marked on the overlying skin using a <sup>57</sup>Co-penpoint marker and handheld gamma-camera (Crystal Cam, Crystal Photonics GmbH, Berlin, Germany) [16].

After conventional lymphoscintigraphy, a total of ~1.0 mL undiluted gadobutrol was injected peritumorally, which was immediately followed by MRI acquisition with a total duration of 30 minutes (Figure 2).



**Figure 1.** Time schedule of study procedures. ICG, indocyanine green;  $^{99m}\text{Tc}$ , technetium-99m; MBq, megabecquerel; SPECT/CT, single-photon emission computed tomography/computed tomography; SLNs, sentinel lymph nodes; mL, milliliter; MR, magnetic resonance.



**Figure 2.** (a) Conventional [ $^{99m}\text{Tc}$ ]Tc-nanocolloid lymphoscintigraphy of a patient diagnosed with cT1N0 OSCC on the right side of the oral tongue (*patient 2*), sentinel lymph node in level Ib on the right side with uptake of [ $^{99m}\text{Tc}$ ]Tc-nanocolloid. (b) Gadobutrol-enhanced MR lymphography for the same patient depicting the sentinel lymph node in level Ib on the right side (*red circle*).

The following day, the marked SLNs were harvested under conventional gamma-probe (Europrobe 3; Eurorad S.A., Eckbolsheim, France) and fluorescence guidance (PDE NEO II near-infrared camera; Hamamatsu, Herrsching, Germany). Any additional SLNs identified by MR lymphography were harvested based on their anatomical localization. The location of excised SLNs and their counts per second as well as ICG uptake, as measured by the portable gamma-probe and PDE NEO II near-infrared camera, were registered.

Harvested SLNs underwent histopathological examination utilizing step-serial-sectioning (~150 µm section thickness) and staining with hematoxylin-eosin (HE), and, if no metastasis was identified on the HE slides, pan-cytokeratin antibody (AE 1/3) [17, 18]. Histopathologically positive lymph nodes were classified according to Hermanek et al. [19]: isolated tumor cells (ITC) if their diameter was less than 0.2 mm, micrometastases if the diameter measured between 0.2 mm and 2.0 mm, and macro-metastases if the metastatic tumor tissue exceeded 2.0 mm in diameter.

Patients with histopathologically negative SLN(s) were managed with a wait-and-scan approach during follow-up. For those with at least one histopathologically positive SLN, complementary treatment of the affected and adjacent nodal basins was applied (i.e., neck dissection). Complementary neck dissection specimens underwent histopathological assessment to detect additional (non-sentinel) nodal metastases.

### **Gadolinium-based contrast agent (gadobutrol) for peritumoral injection**

The gadolinium-based contrast agent (gadobutrol/Gadovist™) was procured from Bayer Healthcare Pharmaceuticals, Berlin, Germany. A total volume of 0.5 – 1.0 mL of undiluted gadobutrol was injected peritumorally at room temperature using a compatible 1 mL syringe.

### **MR lymphography**

MRI scanning was conducted using a 3 Tesla (3T) MRI scanner (Philips Healthcare, Best, the Netherlands), using a head receive coil and an anterior receive coil. MR lymphography consisted of water-only images of 3D dynamic multiple Dixon T1-weighted spoiled gradient echo (T1 mDixon SPGR) scan (TE: 1.52 / 3.0 ms, TR: 4.7 ms, flip angle: 10°, SENSE: 1.4, resolution: 1.2 × 1.2 × 2.0 mm<sup>3</sup>) for 10 minutes. Followed by water-only images of 3D multiple Dixon T1-weighted spoiled gradient echo (T1 mDixon SPGR), scan (TE: 1.94 / 3.4 ms, TR: 5.6 ms, flip angle: 10°, SENSE: 1.1, resolution: 1 × 1 × 1 mm<sup>3</sup>), water-only images of coronal T1 turbo spin echo (c T1 TSE) scan (TE: 14 / 15 ms, TR: 584 ms, SENSE: 2, resolution: 0.9 × 1.0 mm<sup>2</sup>, slice thickness: 3 mm) and water-only images of multiple Dixon T2-weighted turbo spin

echo (T2 mDixon TSE) scan (TE: 100 / 101 ms, TR: 3000 ms, SENSE: 2, resolution:  $1.3 \times 1.2 \text{ mm}^2$ , slice thickness: 3 mm). All MR sequences for anatomical imaging were correlated with MR lymphography.

### **Scintigraphy and SPECT/CT**

Conventional lymphoscintigraphy consisted of early dynamic and static scintigraphy, followed by late static scintigraphy and SPECT/CT acquisition two hours post injection, according to European Association of Nuclear Medicine (EANM) guidelines [20]. Dynamic planar scintigraphic images were obtained with a  $128 \times 128$  matrix: 60 frames of 30 seconds each in anterior-posterior projection, followed by static mode ( $256 \times 256$  matrix) for 4 minutes in both anterior-posterior and lateral projections. Static images were acquired at 30 minutes and 2 hours post-injection. Additionally, a 30-second flood field images were acquired to supplement dynamic and static scintigraphic imaging. SPECT/CT imaging was performed using a  $128 \times 128$  matrix with a pixel spacing of,  $4.8 \times 4.8 \text{ mm}^2$ , encompassing 128 angles with 20 seconds per projection, over a non-circular  $360^\circ$  orbit. CT parameters were set at 110 kV, 40 mAs effective, and a slice thickness of 1.2 mm.

Lymphoscintigraphy was conducted with a Symbia™ T16 SPECT/CT scanner (Siemens Healthineers, Erlangen, Germany) with “low- and medium energy” collimators, aimed at limiting septal penetration and minimizing shine-through artifacts [21]. SPECT/CT images were reconstructed using clinical reconstruction software (Siemens Flash3D), incorporating attenuation and scatter correction with parameters set at 6 iterations, 8 subsets, and a 5 mm Gaussian filter.

### **Evaluation and analyses**

Each patient’s MR lymphographic images and conventional [ $^{99\text{m}}\text{Tc}$ ]Tc-nanocolloid lymphoscintigraphy images were assessed to determine the similarity of the depicted draining lymph node basins, as well as the number and location of SLNs. Additionally, comparisons were made between MR lymphography and conventional lymphoscintigraphy regarding the visualization of draining lymphatic vessels transporting the (radio)tracer.

SLNs identified by either MR lymphography or conventional lymphoscintigraphy were correlated with findings from histopathological examination of excised SLNs and any complementary neck dissection specimens, as well as follow-up results, in particular regional recurrences in absence of local recurrence. All images were reviewed by a radiologist/nuclear medicine physician (B.K.) and a second observer (D.N.V.D.).

The diagnostic accuracy of MR lymphography was assessed using histopathological examination of harvested SLNs and complementary neck dissection specimens, along with follow-up data as the reference standard. Sensitivity ( $\text{true positives} / (\text{true positives} + \text{false negatives})$ ) and negative predictive value (NPV) ( $\text{true negatives} / (\text{true negatives} + \text{false negatives})$ ) were calculated.

Adverse reactions were scored and graded according to the Common Terminology Criteria for Adverse Events (CTCAE) [22].

All data were analyzed using IBM SPSS Statistics Version 29.0.1. Categorical variables are presented as the number of cases and percentages. Continuous parametric variables are presented as mean ( $\pm$  standard deviation (SD)), while non-parametric variables are presented as median. Statistical tests were not performed due to the small number of patients in this study.

## Results

Patient- and tumor characteristics of included patients are summarized in Table 1. The majority of patients presented with an OSCC of the oral tongue (60%). Most tumors were classified as cT1 (70%). A total of 41 SLNs were harvested, with a median of 4 SLNs per patient, among which 7 contained metastasis (17%). Out of 7 SLNs, 4 histopathologically positive lymph nodes contained macro-metastases, 2 contained micrometastases, and one contained ITC only. These occult lymph node metastases were detected in 4 out of 10 patients by SLNB. Among those with histopathologically positive SLNs, 3 underwent complementary neck dissection (75%), two of whom also underwent postoperative radiotherapy following complementary neck dissection, due to pN2 staging, and one patient refused postoperative radiotherapy. The remaining patient adopted a wait-and-scan approach due to ITC. Subsequent histopathological examination of complementary neck dissection specimens revealed no additional nodal metastases. All included patients remained disease-free after a median follow-up of 16 months (range 7 – 21 months).

**Table 1.** Patient- and tumor characteristics.

Characteristics	<i>n = 10</i>
<b>Gender, n (%)</b>	
Female	6 (60%)
<b>Median age (y) (range)</b>	62.3 (51–80)
<b>Tumor location, n (%)</b>	
Tongue	6 (60%)
Floor-of-mouth	2 (20%)
Buccal mucosa	1 (10%)
Retromolar trigone	1 (10%)
<b>Side primary tumor, n (%)</b>	
Left	4 (40%)
Right	6 (60%)
<b>Clinical T-stage, n (%)*</b>	
T1	7 (70%)
T2	3 (30%)
<b>Pathology primary tumor</b>	
Mean diameter (mm) (SD)	14.7 ( $\pm$ 7.4)
Mean depth-of-invasion (mm) (SD)	4.1 ( $\pm$ 2.2)
Median harvested SLNs (range)	4 (1–7)

**Table 1.** Continued.

Characteristics	<i>n</i> = 10
<b>Histopathological status SLNs, n (%)</b>	
Negative	34 (83%)
Positive	7 (17%)
<b>Pathological N-stage after SLNB, n (%)*</b>	
pN0(sn)	6 (60%)
pN0(i <sup>+</sup> sn)	1 (10%)
pN2b(sn)	2 (20%)
pN2c(sn)	1 (10%)
<b>Complementary neck treatment, n (%)</b>	
Complementary ND	3 (30%)
Complementary RT	2 (20%)
<b>Follow-up in months (range)</b>	16 (7–21)

*n*, number; *y*, years; *mm*, millimeters; *SD*, standard deviation; *SLNs*, sentinel lymph nodes; *SLNB*, sentinel lymph node biopsy; *i<sup>+</sup>*, isolated tumor cells; *ND*, neck dissection; *RT*, radiotherapy.

\*According to AJCC TNM classification, 8<sup>th</sup> edition.

### Sentinel lymph node identification on MR lymphography

The results of MR lymphography and [<sup>99m</sup>Tc]Tc-nanocolloid lymphoscintigraphy for all enrolled patients are presented in Table 2. Most of the detected SLNs on MR lymphography were found in level II (10 out of 17 detected SLNs). [<sup>99m</sup>Tc]Tc-nanocolloid lymphoscintigraphy detected a total of 27 SLNs, of which 16 SLNs (59%) were also identified by MR lymphography (Figure 2). Additionally, MR lymphography identified one extra SLN (*patient 8*, level IIa), which was harvested intra-operatively based on its anatomical location. This SLN exhibited no histopathological evidence of metastasis. In one patient, MR lymphography failed to detect any SLNs (10%).



**Table 2.** Continued.

N°	Primary tumor	Identified SLNs LSG	Identified SLNs MRL	Harvested SLNs (cps)	PA	Comp. treatment	pTNM*	Follow-up (months)
6	Retromolar trigone (right)	Ib Right II/III Right	Ib Right	Ib Right (55) Right (129) Right (88)	- + +	MRND right	pT2N2b	NED (17)
7	Tongue (left)	II Left IV Left	II Left IV Left	Left (1050) Left (9200)	- -	N.A.	pT2N0(sn)	NED (16)
8	FOM (right)	Ib Right II Right II Left	II Right	Right (20) Right (799) Left (274)	- - -	N.A.	pT1N0(sn)	NED (15)
9	Tongue (left)	IIa Left	IIa Left	Right (729) Right (63) Left (3740)	- - -	N.A.	pT1N0(sn)	NED (9)
10	Tongue (right)	IIa Right IIa Right IIb Right	IIa Right IIb Right	Right (1683) Right (2168) Right (1520) Right (1800) Right (443) Right (242) Right (338)	+ + - - - - -	SND I-IV right	pT1N2b	NED (7)

N°, patient number; SLN, sentinel lymph node; LSG, lymphoscintigraphy; MRL, gadolinium-enhanced magnetic resonance lymphography; cps, counts per second as measured by conventional gamma-probe; PA, pathological assessment; comp., complementary; +, histopathologically positive for metastasis; -, histopathologically negative for metastasis; (I), isolated tumor cells; N.A., not applicable; FOM, floor-of-mouth; MRND, modified radical neck dissection; SND, selective neck dissection.

\*According to AJCC TNM classification, 8<sup>th</sup> edition.

Among the 7 histopathologically positive SLNs detected by conventional lymphoscintigraphy in 4 patients, 3 SLNs were identified by MR lymphography (43%) in 3 patients.

Overall, MR lymphography using gadobutrol reached a sensitivity of 75% (3/4) and an NPV of 85.7% (6/7) when histopathological assessment of the harvested SLNs and specimen of the complementary neck dissection, along with follow-up data, were used as reference standards.

Contrast-enhanced lymphatic vessels were visualized in 2 patients with MR lymphography (20%), whereas conventional lymphoscintigraphy successfully visualized lymphatic vessels draining [ $^{99m}\text{Tc}$ ]Tc-nanocolloid in 4 patients (40%) (Figure 3).

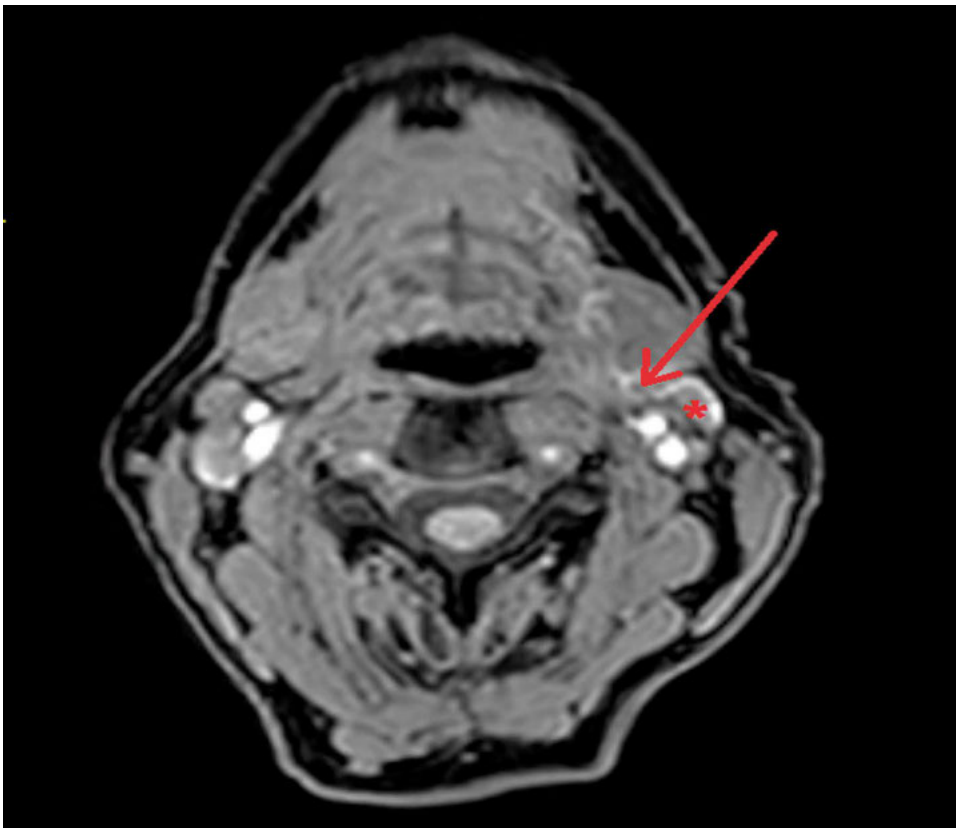


**Figure 3.** Gadobutrol-enhanced MR lymphography of a patient diagnosed with cT1N0 OSCC on the left side of the oral tongue (*patient 9*) depicting the sentinel lymph node in level IIa on the left side (\*) and lymphatic drainage with uptake of gadobutrol (*red arrow*).

On dynamic imaging, brief SLN contrast-enhancement with fast tracer washout was observed in 5 of the 17 detected SLNs by MR lymphography, as depicted in Figure 4.

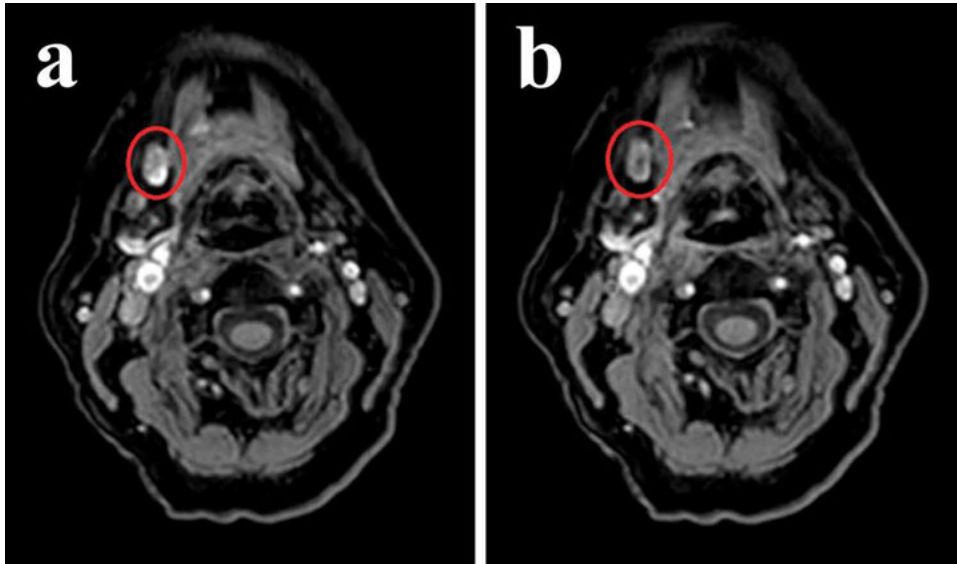


**Figure 4.** Contrast-enhanced dynamic MR images acquired for 10 minutes after peritumoral injection of undiluted gadobutrol in the same patient as in Figure 2 (*patient 2*). Rapid lymphatic drainage of gadobutrol was observed through dynamic MR lymphography, with gadobutrol washed out from the SLN within 7 minutes. (a) Initial dynamic MR depicting the sentinel lymph node in level Ib on the right side (*red circle*). (b) MR imaging acquired 6 minutes and 23 seconds following (a), showing the same SLN in level Ib on the right side (*red circle*).

In one patient with a tumor located in the retromolar trigone, an injection volume of  $\sim 1.0$  mL was not feasible, and  $\sim 0.5$  mL gadobutrol was injected. Mild swelling and some discomfort from the peritumoral injection with gadobutrol was observed in 8 patients, corresponding with CTCAE grade 1. No severe adverse reactions were reported following peritumoral injection of gadobutrol or MR lymphography.

In all patients, paramagnetic artifacts from previous [ $^{99m}\text{Tc}$ ]Tc-nanocolloid injections were observed in proximity to the injection site (Figure 5).

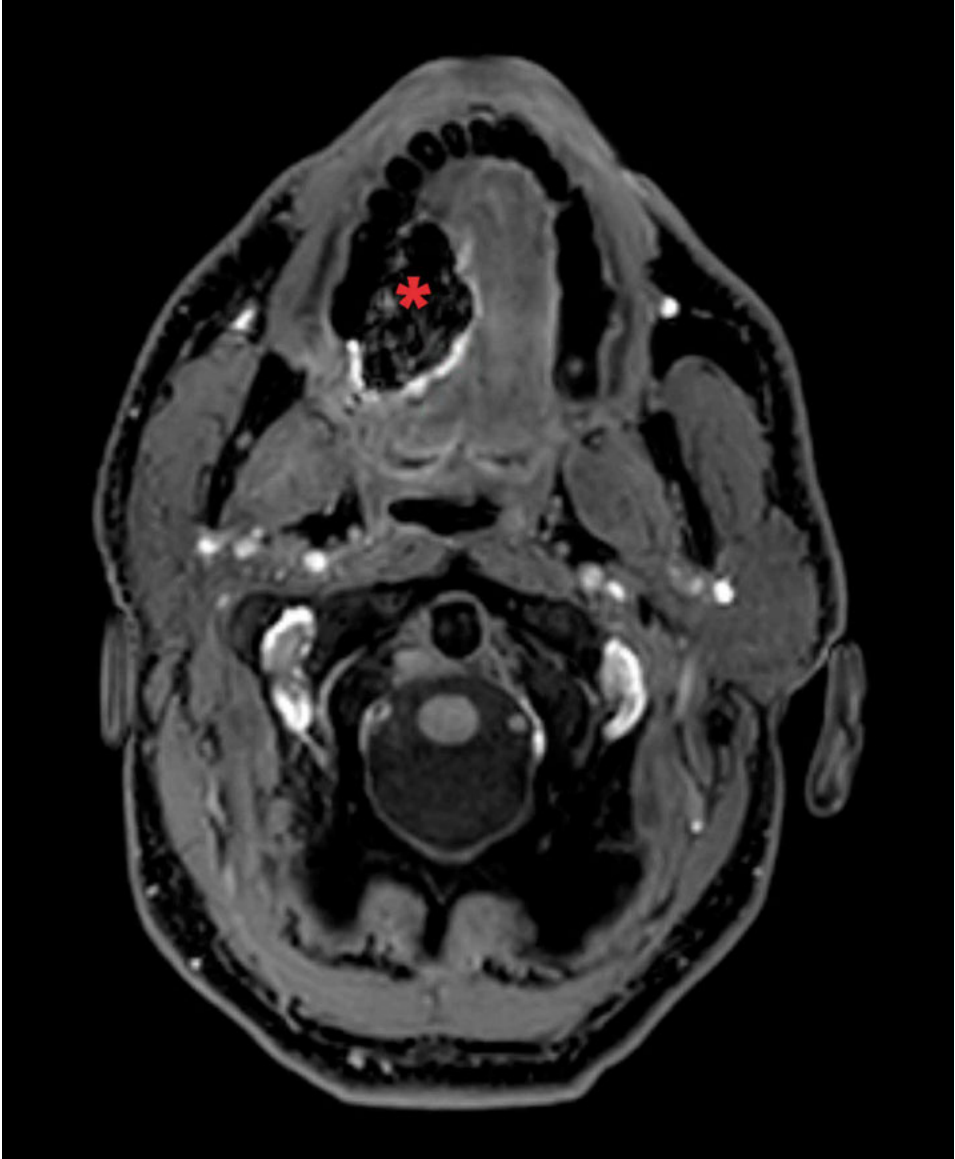


**Figure 5.** Gadobutrol-enhanced MR lymphography in a patient diagnosed with cT1N0 OSCC on the right side of the oral tongue (*patient 4*), showing an artifact of [<sup>99m</sup>Tc]Tc-nanocolloid radiotracer at the injection site (\*).

## Discussion

In this pilot study, the efficacy of magnetic resonance (MR) lymphography using a gadolinium-based contrast agent for sentinel lymph node (SLN) mapping in patients with early-stage oral squamous cell carcinoma (OSCC) was evaluated. Our findings revealed that MR lymphography achieved a relatively low SLN identification rate of only 59%, and it failed to detect 4 out of 7 histopathologically positive SLNs (57%). Notably, in one patient (10%), no contrast-enhanced SLN was detected, and in another patient both histopathologically positive SLNs were missed, which would have led to false-negative staging if MR lymphography had been the sole diagnostic modality.

These results are in contrast to those reported by Bae et al., who achieved a higher SLN detection rate and a 91% success rate in identifying patients with pathologically positive necks using gadolinium-enhanced MR lymphography [11]. The discrepancies between our findings and those of Bae et al. may be attributed to several key differences in study design and methodology. Bae et al. included larger tumors (median size of 2.2 cm, ranging from 1.0 to 4.6 cm), specifically cT3 and cT4 OSCC, which inherently have a higher likelihood of cervical metastases. This difference in tumor size and stage could introduce a selection bias that may have inflated the detection rates reported in their study. Additionally, Bae et al. relied on elective neck dissection as the reference standard, which, while effective, does not utilize step-serial-sectioning or immunohistochemistry—techniques that significantly improve the detection accuracy of micrometastases and reduce the risk of false negatives. Our study employed a more rigorous reference standard, utilizing step-serial-sectioning and immunohistochemistry for detailed histopathological assessment. This method is known to improve the detection of micrometastases, and upstage the nodal status in up to 15.2 – 19.5% of patients [23, 24]. Additionally, the study by Bae et al. also does not provide follow-up results, resulting in the inability to identify false-negative cases over time.

Several drawbacks of MR lymphography with gadobutrol were encountered in this study. In particular, rapid lymphatic transportation of gadobutrol was observed with minimal retention in SLNs and rapid tracer washout (Figure 4). This is considered to be due to the low molecular weight of gadolinium-based contrast agents [25, 26] and could increase the risk of overlooking SLNs and erroneously designating contrast-enhanced higher echelon nodes as SLNs [27]. Rapid drainage was observed even when gadobutrol was administered without dilution, as in our study, which differs from the methodology employed by Bae et al. [11]. We anticipated that drainage would be slower with the undiluted contrast agent compared to their diluted mixture, yet even with undiluted gadobutrol the lymphatic drainage may be too fast to allow

for reliable SLN identification.

In addition, it must be emphasized that there is currently no method to detect gadolinium-based contrast agents during surgery. As a consequence, MR lymphography using gadobutrol is dependent on less reliable dual-tracer methods [28]. The challenge of detecting SLNs by MR lymphography and localizing them intraoperatively may be solved by using superparamagnetic iron oxide (SPIO). SPIO can be detected by both MRI and a handheld magnetometer, offering a potential method for intraoperative localization of SLNs [29, 30]. The initial results of MR lymphography using SPIO are promising, as all SLNs identified by MR lymphography corresponded with those identified by conventional lymphoscintigraphy [30, 31]. Currently, the limited number of early-stage OSCC patients who underwent MR lymphography with SPIO in our center yet prevents assessment of its diagnostic accuracy. Larger studies with adequate reference standards (i.e., a combination of detailed histopathological assessment and follow-up) should be conducted.

Another drawback of MR lymphography using gadobutrol is the swelling and painful discomfort following peritumoral injection of gadobutrol. This reaction is likely attributable to the lower osmolarity of gadobutrol compared to [<sup>99m</sup>Tc]Tc-nanocolloid [32]. Osmolarity plays a significant role in determining the tolerability of contrast agents, with lower osmolar agents generally associated with a reduced risk of adverse reactions [15, 33, 34]. Nonetheless, the observed swelling and discomfort were transient and resolved spontaneously without the need for intervention, affirming the safety profile of gadobutrol in peritumoral administration.

Still, if the current shortcomings of MR lymphography can be overcome, it could further benefit oncological practice. For instance, in patients in whom MRI of the head and neck is already acquired as part of clinical staging, the addition of a viable peritumoral injected MR-contrast agent could facilitate the selection of lymph nodes with the highest risk of (occult) metastases (i.e., SLNs) for USgFNAC, thus enhancing the accuracy of USgFNAC and improving the selection of patients for either SLNB in case of cN0, or a therapeutic neck dissection in case of cN+. Similarly, since MRI is already increasingly used for radiotherapy planning [7], MR lymphography could be used to adapt radiotherapy planning: a higher radiation dose targeted to lymph nodes (areas) with the highest risk of harboring occult metastases [35–38]. These potential applications underscore the importance of further research into MR lymphography, as it promises to enhance diagnostic and therapeutic approaches in early-stage OSCC. There are several limitations of this study. First, due to the small number of included patients in this pilot study, our results should be interpreted with caution. Besides, it should be realized that the results of this study cannot be fully compared to those

achieved by Bae et al. on account of some discrepancies in methods [11]. Furthermore, to ensure that the standard of care for our patients was not compromised, MR lymphography was conducted after conventional lymphoscintigraphy. As a result, artifacts were observed on MR lymphography, presumably induced by [<sup>99m</sup>Tc]Tc-nanocolloid (Figure 5). Artifacts related to [<sup>99m</sup>Tc]Tc-nanocolloid on MRI scans have not been previously documented in the literature, but may have hindered the detection of SLNs by MR lymphography in this study.

Noteworthy, the average number of harvested SLNs in this study was relatively high [39]. This could be attributed to the supplementation of ICG to [<sup>99m</sup>Tc]Tc-nanocolloid and the use of intraoperative near-infrared imaging. As previously demonstrated by Berger et al. [40], the use of intraoperative near-infrared imaging, in melanomas of the head and neck region, resulted in an increased number of harvested lymph nodes. Yet, in the cohort of Berger et al. where ICG was available, no significant decline in false-negative cases was seen, irrespective of the higher yield, raising questions about whether these additionally harvested lymph nodes based on a fluorescent signal were true SLNs. During surgery, many lymph nodes turn out to be fluorescent, sometimes without the presence of radioactive deposition. Consequently, in our study, surgeons may have excised more lymph nodes based on this visual signal. The relatively high number of harvested SLNs based on the conventional procedure in this study may negatively affect the SLN identification rate by MR lymphography. If many lymph nodes are excised and considered as SLNs, the SLN detection level of MR lymphography (relative to harvested SLNs) naturally shifts to the disadvantage of MR lymphography.

Strengths of our study include the homogeneous early-stage OSCC patient group, the within-patient comparison with conventional lymphoscintigraphy, and the use of an adequate reference standard (i.e., detailed histopathological assessment after SLN biopsy, complementary treatment, and follow-up data).

## Conclusion

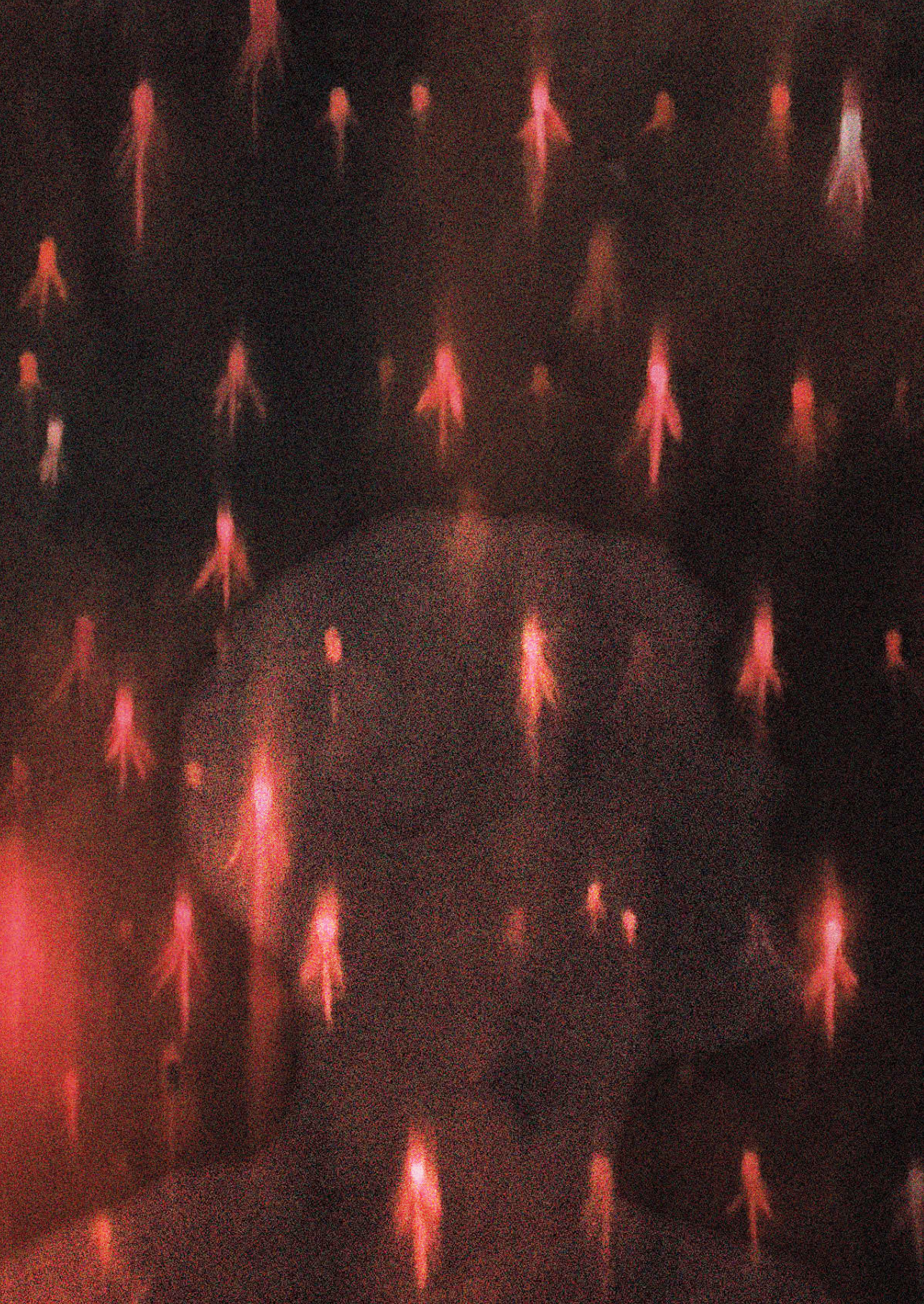
In conclusion, the findings of this study show that MR lymphography subsequent to peritumoral injection of gadobutrol yet lacks reliability as a technique for SLN mapping in early-stage OSCC.

## References

1. Garrel R, Poissonnet G, Moyà Plana A, et al. Equivalence randomized trial to compare treatment on the basis of sentinel node biopsy versus neck node dissection in operable T1-T2N0 oral and oropharyngeal cancer. *J Clin Oncol*. 2020;38(34):4010-4018. doi:10.1200/JCO.20.01661
2. Hasegawa Y, Tsukahara K, Yoshimoto S, et al. Neck dissections based on sentinel lymph node navigation versus elective neck dissections in early oral cancers: a randomized, multicenter, and noninferiority trial. *J Clin Oncol*. 2021;39(18):2025-2036. doi:10.1200/JCO.20.03637
3. Gupta T, Maheshwari G, Kannan S, Nair S, Chaturvedi P, Agarwal JP. Systematic review and meta-analysis of randomized controlled trials comparing elective neck dissection versus sentinel lymph node biopsy in early-stage clinically node-negative oral and/or oropharyngeal squamous cell carcinoma: Evidence-base for practice and implications for research. *Oral Oncol*. 2022;124:105642. doi:10.1016/j.oraloncology.2021.105642
4. den Toom IJ, van Schie A, van Weert S, et al. The added value of SPECT-CT for the identification of sentinel lymph nodes in early stage oral cancer. *Eur J Nucl Med Mol Imaging*. 2017;44(6):998-1004. doi:10.1007/s00259-017-3613-8
5. den Toom IJ, Boeve K, Lobeek D, et al. Elective Neck Dissection or Sentinel Lymph Node Biopsy in Early Stage Oral Cavity Cancer Patients: The Dutch Experience. *Cancers (Basel)*. 2020;12(7):1783. doi:10.3390/cancers12071783
6. Bowe CM, Shastri M, Gulati A, et al. Challenges and outcomes in establishing a sentinel lymph node biopsy service for oral squamous cell carcinoma in a regional district specialist hospital. *Br J Oral Maxillofac Surg*. 2021;59(2):217-221. doi:10.1016/j.bjoms.2020.08.057
7. Mahieu R, de Maar JS, Nieuwenhuis ER, et al. New Developments in Imaging for Sentinel Lymph Node Biopsy in Early-Stage Oral Cavity Squamous Cell Carcinoma. *Cancers (Basel)*. 2020;12(10):3055. doi:10.3390/cancers12103055
8. Wallace AM, Hoh CK, Ellner SJ, Darrach DD, Schulteis G, Vera DR. Lymphoseek: a molecular imaging agent for melanoma sentinel lymph node mapping. *Ann Surg Oncol*. 2007;14(2):913-921. doi:10.1245/s10434-006-9099-4
9. Gulec SA. PET probe-guided surgery. *J Surg Oncol*. 2007;96(4):353-357. doi:10.1002/jso.20862
10. Honda K, Ishiyama K, Suzuki S, et al. Sentinel lymph node biopsy using computed tomographic lymphography in patients with early tongue cancer. *Acta Otolaryngol*. 2015;135(5):507-512. doi:10.3109/00016489.2015.1010126
11. Bae S, Lee HJ, Nam W, Koh YW, Choi EC, Kim J. MR lymphography for sentinel lymph node detection in patients with oral cavity cancer: Preliminary clinical study. *Head Neck*. 2018;40(7):1483-1488. doi:10.1002/hed.25167
12. Li C, Meng S, Yang X, Zhou D, Wang J, Hu J. Sentinel lymph node detection using magnetic resonance lymphography with conventional gadolinium contrast agent in breast cancer: a preliminary clinical study. *BMC Cancer*. 2015;15:213. doi:10.1186/s12885-015-1255-4
13. Lu Q, Hua J, Kassir MM, et al. Imaging lymphatic system in breast cancer patients with magnetic resonance lymphangiography. *PLoS One*. 2013;8(7):e69701. doi:10.1371/journal.pone.0069701
14. Brierley JD, Gospodarowicz M, Wittekind C. UICC TNM Classification of Malignant Tumours. 8<sup>th</sup> ed. Chichester, United Kingdom: Wiley; 2017.
15. Ahuja AT, Ying M, Ho SY, et al. Ultrasound of malignant cervical lymph nodes. *Cancer Imaging*. 2008;8(1):48-56. doi:10.1102/1470-7330.2008.0006
16. Mahieu R, Tijink BM, van Es RJJ, et al. The potential of the Crystal Cam handheld gamma-camera for preoperative and intraoperative sentinel lymph node localization in early-stage oral cancer. *Eur Arch Otorhinolaryngol*. 2023;280(12):5519-5529. doi:10.1007/s00405-023-08138-y
17. Alkureishi LW, Burak Z, Alvarez JA, et al. Joint practice guidelines for radionuclide lymphoscintigraphy for sentinel node localization in oral/oropharyngeal squamous cell carcinoma. *Ann Surg Oncol*. 2009;16(11):3190-3210. doi:10.1245/s10434-009-0726-8
18. Dhawan I, Sandhu SV, Bhandari R, Sood N, Bhullar RK, Sethi N. Detection of cervical lymph node micrometastasis and isolated tumor cells in oral squamous cell carcinoma using immunohistochemistry and serial sectioning. *J Oral Maxillofac Pathol*. 2016;20(3):436-444. doi:10.4103/0973-029X.190946
19. Hermanek P, Hutter RV, Sobin LH, Wittekind C. International Union Against Cancer. Classification of isolated tumor cells and micrometastasis. *Cancer*. 1999;86(12):2668-2673.

20. Giammarile F, Schilling C, Gnanasegaran G, et al. The EANM practical guidelines for sentinel lymph node localisation in oral cavity squamous cell carcinoma. *Eur J Nucl Med Mol Imaging*. 2019;46(3):623-637. doi:10.1007/s00259-018-4235-5
21. Yoneyama H, Tsushima H, Kobayashi M, Onoguchi M, Nakajima K, Kinuya S. Improved detection of sentinel lymph nodes in SPECT/CT images acquired using a low- to medium-energy general-purpose collimator. *Clin Nucl Med*. 2014;39(1):e1-e6. doi:10.1097/RLU.0b013e31828da362
22. Freites-Martinez A, Santana N, Arias-Santiago S, Viera A. Using the Common Terminology Criteria for Adverse Events (CTCAE - Version 5.0) to Evaluate the Severity of Adverse Events of Anticancer Therapies. CTCAE versión 5.0. Evaluación de la gravedad de los eventos adversos dermatológicos de las terapias antineoplásicas. *Actas Dermosifiliogr (Engl Ed)*. 2021;112(1):90-92. doi:10.1016/j.ad.2019.05.009
23. Rinaldo A, Devaney KO, Ferlito A. Immunohistochemical studies in the identification of lymph node micrometastases in patients with squamous cell carcinoma of the head and neck. *ORL J Otorhinolaryngol Relat Spec*. 2004;66(1):38-41. doi:10.1159/000077232
24. King C, Elsherif N, Kirwan R, et al. Serial step sections at narrow intervals with immunohistochemistry are required for accurate histological assessment of sentinel lymph node biopsy in oral squamous cell carcinoma. *Head Neck*. 2021;43(10):2985-2993. doi:10.1002/hed.26784
25. Loo BW Jr, Draney MT, Sivanandan R, et al. Indirect MR lymphangiography of the head and neck using conventional gadolinium contrast: a pilot study in humans. *Int J Radiat Oncol Biol Phys*. 2006;66(2):462-468. doi:10.1016/j.ijrobp.2006.05.045
26. Bisso S, Degrassi A, Brambilla D, Leroux JC. Poly(ethylene glycol)-alendronate coated nanoparticles for magnetic resonance imaging of lymph nodes. *J Drug Target*. 2019;27(5-6):659-669. doi:10.1080/1061186X.2018.1545235
27. Sugiyama S, Iwai T, Izumi T, et al. Sentinel lymph node mapping of clinically N0 early oral cancer: a diagnostic pitfall on CT lymphography. *Oral Radiol*. 2021;37(2):251-255. doi:10.1007/s11282-020-00442-1
28. KleinJan GH, van Werkhoven E, van den Berg NS, et al. The best of both worlds: a hybrid approach for optimal pre- and intraoperative identification of sentinel lymph nodes. *Eur J Nucl Med Mol Imaging*. 2018;45(11):1915-1925. doi:10.1007/s00259-018-4028-x
29. Hernando J, Aguirre P, Aguilar-Salvatierra A, Leizaola-Cardesa IO, Bidaguren A, Gómez-Moreno G. Magnetic detection of sentinel nodes in oral squamous cell carcinoma by means of superparamagnetic iron oxide contrast. *J Surg Oncol*. 2020;121(2):244-248. doi:10.1002/jso.25810
30. Mizokami D, Kosuda S, Tomifuji M, et al. Superparamagnetic iron oxide-enhanced interstitial magnetic resonance lymphography to detect a sentinel lymph node in tongue cancer patients. *Acta Otolaryngol*. 2013;133(4):418-423. doi:10.3109/00016489.2012.744143
31. Maza S, Taupitz M, Taymoorian K, et al. Multimodal fusion imaging ensemble for targeted sentinel lymph node management: initial results of an innovative promising approach for anatomically difficult lymphatic drainage in different tumour entities. *Eur J Nucl Med Mol Imaging*. 2007;34(3):378-383. doi:10.1007/s00259-006-0223-2
32. Glutig K, Bhargava R, Hahn G, et al. Safety of gadobutrol in more than 1,000 pediatric patients: subanalysis of the GARDIAN study, a global multicenter prospective non-interventional study. *Pediatr Radiol*. 2016;46(9):1317-1323. doi:10.1007/s00247-016-3599-6
33. McClellan BL. Low-osmolality contrast media: premises and promises. *Radiology*. 1987;162(1 Pt 1):1-8. doi:10.1148/radiology.162.1.3786748
34. Almén T. Contrast agent design. Some aspects on the synthesis of water soluble contrast agents of low osmolality. *J Theor Biol*. 1969;24(2):216-226. doi:10.1016/s0022-5193(69)80047-0
35. van den Bosch S, Takes RP, de Ridder M, et al. Personalized neck irradiation guided by sentinel lymph node biopsy in patients with squamous cell carcinoma of the oropharynx, larynx or hypopharynx with a clinically negative neck: (Chemo)radiotherapy to the PRIMary tumor only. Protocol of the PRIMO study. *Clin Transl Radiat Oncol*. 2023;44:100696. doi:10.1016/j.ctro.2023.100696
36. de Veij Mestdagh PD, Jonker MCJ, Vogel WV, et al. SPECT/CT-guided lymph drainage mapping for the planning of unilateral elective nodal irradiation in head and neck squamous cell carcinoma. *Eur Arch Otorhinolaryngol*. 2018;275(8):2135-2144. doi:10.1007/s00405-018-5050-0
37. de Veij Mestdagh PD, Schreuder WH, Vogel WV, et al. Mapping of sentinel lymph node drainage using SPECT/CT to tailor elective nodal irradiation in head and neck cancer patients (SUSPECT-2): a single-center prospective trial. *BMC Cancer*. 2019;19(1):1110. doi:10.1186/s12885-019-6331-8

38. de Veij Mestdagh PD, Walraven I, Vogel WV, et al. SPECT/CT-guided elective nodal irradiation for head and neck cancer is oncologically safe and less toxic: A potentially practice-changing approach. *Radiother Oncol.* 2020;147:56-63. doi:10.1016/j.radonc.2020.03.012
39. Schilling C, Stoeckli SJ, Haerle SK, et al. Sentinel European Node Trial (SENT): 3-year results of sentinel node biopsy in oral cancer. *Eur J Cancer.* 2015;51(18):2777-2784. doi:10.1016/j.ejca.2015.08.023
40. Berger DMS, van den Berg NS, van der Noort V, et al. Technologic (R)Evolution Leads to Detection of More Sentinel Nodes in Patients with Melanoma in the Head and Neck Region. *J Nucl Med.* 2021;62(10):1357-1362. doi:10.2967/jnumed.120.246819



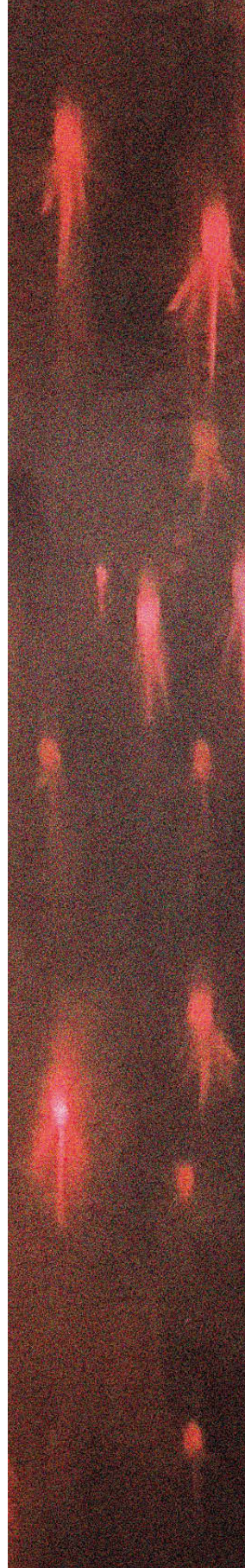
# 9

## CT lymphography using Lipiodol® for sentinel lymph node biopsy in early-stage oral cancer

---

Rutger Mahieu, Dominique N.V. Donders, Jan Willem Dankbaar,  
Remco de Bree, Bart de Keizer.

*J Clin Med.* 2022 Aug 31;11(17):5129



## Abstract

This study evaluated sentinel lymph node (SLN) identification with CT lymphography (CTL) following peritumoral administration of Lipiodol® relative to conventional [<sup>99m</sup>Tc]Tc-nanocolloid lymphoscintigraphy (including SPECT/CT) in 10 early-stage oral cancer patients undergoing SLN biopsy. Patients first underwent early dynamic and static scintigraphy after peritumoral administration of [<sup>99m</sup>Tc]Tc-nanocolloid. Subsequently, Lipiodol® was administered at the same injection sites, followed by fluoroscopy and CT acquisition. Finally, late scintigraphy and SPECT/CT were conducted, enabling the fusion of late CTL and SPECT imaging. The next day, designated SLNs were harvested, radiographically examined for Lipiodol® uptake and histopathologically assessed. Corresponding images of CT, [<sup>99m</sup>Tc]Tc-nanocolloid lymphoscintigraphy and SPECT/late CTL fusion were evaluated. [<sup>99m</sup>Tc]Tc-nanocolloid lymphoscintigraphy identified 21 SLNs, of which 7 were identified with CTL (33%). CTL identified no additional SLNs and failed to identify any SLNs in four patients (40%). Out of six histopathologically positive SLNs, two were identified with CTL (33%). Radiographic examination confirmed Lipiodol® uptake in seven harvested SLNs (24%), of which five were depicted with CTL. CTL using Lipiodol® reached a sensitivity of 50% and a negative predictive value (NPV) of 75% (median follow-up: 12.3 months). These results suggest that CTL using Lipiodol® is not a reliable technique for SLN mapping in early-stage oral cancer.

## Introduction

In early-stage oral squamous cell carcinoma (OSCC), sentinel lymph node biopsy (SLNB) has proven to be a reliable staging procedure for the clinically negative neck (cN0), with similar locoregional-free, disease-specific and overall survival rates as well as significantly lower functional morbidity compared to its alternative, elective neck dissection (END) [1–3].

Since the introduction of SLNB, sentinel lymph node (SLN) imaging has undergone several technologic refinements, including the introduction of single-photon emission computed tomography/computed tomography (SPECT/CT) [4]. Yet, both technical and logistical challenges remain for SLNB using conventional technetium-99m ( $^{99m}\text{Tc}$ ) labeled radiotracers, which instigate the ongoing investigation for alternative high-resolution SLN imaging techniques [5–7].

Among others, CT lymphography (CTL) using peritumorally administered water-soluble iodine-based contrast agents (e.g., iopamidol) has been put forward as a high-resolution alternative for conventional lymphoscintigraphy and has been studied in several tumor types, including early-stage OSCC [8–12].

However, owing to the high velocity of lymphatic transportation, limited retention and rapid washout of water-soluble iodine-based contrast agents [13], true SLNs may be overlooked, and contrast-enhanced higher-echelon nodes may be erroneously designated as SLNs. Sugiyama et al. found that 4 of 27 SLNB-negative patients by CTL using iopamidol actually had occult cervical lymph node metastases. In these patients, overlooked SLNs were only marginally contrast-enhanced on CTL, resulting in a poor accuracy of the procedure (sensitivity: 56%, negative predictive value (NPV): 85%). Furthermore, re-evaluation of the CTL images showed that iopamidol was only briefly retained in SLNs, with Hounsfield units (HU) of the contrast-enhanced SLNs already decreasing after 10 min post-injection [14].

Lipiodol<sup>®</sup>, an oil-based iodinated contrast agent with a higher viscosity, may provide increased retention of SLNs as well as delayed tracer wash-out and, thus, might improve SLN identification on CTL in early-stage OSCC patients [13, 15]. Kim et al. already demonstrated the feasibility of CTL using Lipiodol<sup>®</sup> for SLN mapping in patients with early gastric cancer [13]. In their study, CTL successfully visualized contrast-enhanced SLNs at 1 h following the peritumoral submucosal injection of Lipiodol<sup>®</sup> in all patients.

Furthermore, Lipiodol® has been combined with indocyanine green (ICG) as a single emulsion, which could overcome the limitations of injecting two individual tracers consecutively (i.e., dual-tracer methods), potentially enabling the reliable intra-operative localization of pre-operative depicted SLNs [7, 16].

Therefore, this study evaluated SLN identification with CTL following the peritumoral administration of Lipiodol® compared to SLN identification using conventional lymphoscintigraphy, including SPECT/CT with [<sup>99m</sup>Tc]Tc-nanocolloid in early-stage OSCC patients.

# Materials and methods

## Patients

This study was approved by the Ethics Committee of the University Medical Center Utrecht (no. 20/079) and was registered in the Netherlands Trial Register (accessible via <https://www.trialregister.nl/>, registration number NL9005).

Between November 2020 and June 2021, a total of 10 patients with newly diagnosed early-stage OSCC (cT1-2N0; TNM Staging AJCC UICC 8<sup>th</sup> Edition [17, 18]), scheduled for SLNB, were prospectively included in this study.

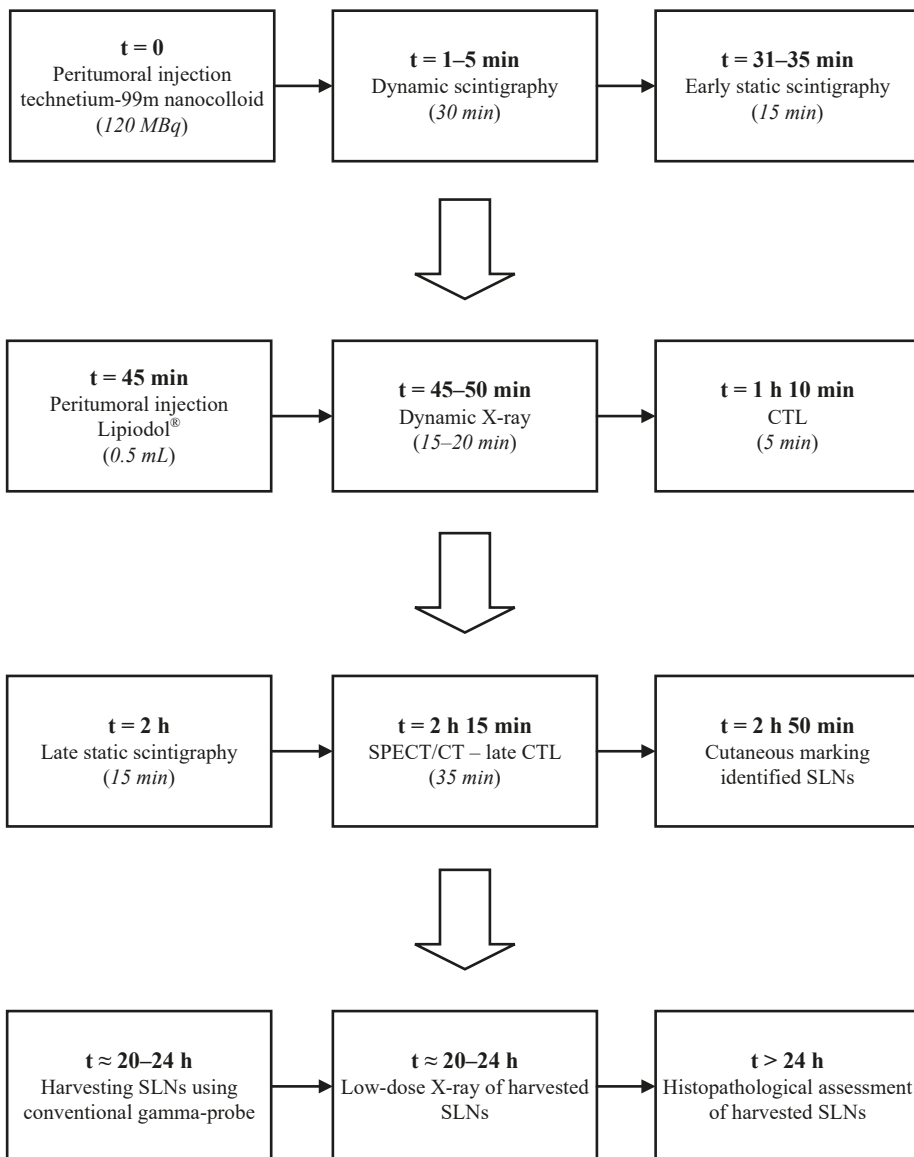
In all patients, cN0 status was confirmed by palpation and ultrasound of the neck. In those with suspect lymph nodes on ultrasound, ultrasound-guided fine-needle aspiration cytology was performed. In most patients (80%), magnetic resonance images of the head and neck were acquired as part of clinical staging.

Patients with prior head and neck malignancies in the past 5 years were excluded from this study. In addition, patients with a history of gross injury to the neck that precluded the reasonable surgical dissection of SLNs for this trial, neck dissection or radiotherapy to the neck were excluded from this study as well. Finally, patients who previously had an allergic reaction after the administration of an iodine-based contrast agent or those who manifest hyperthyroidism could not participate in this study.

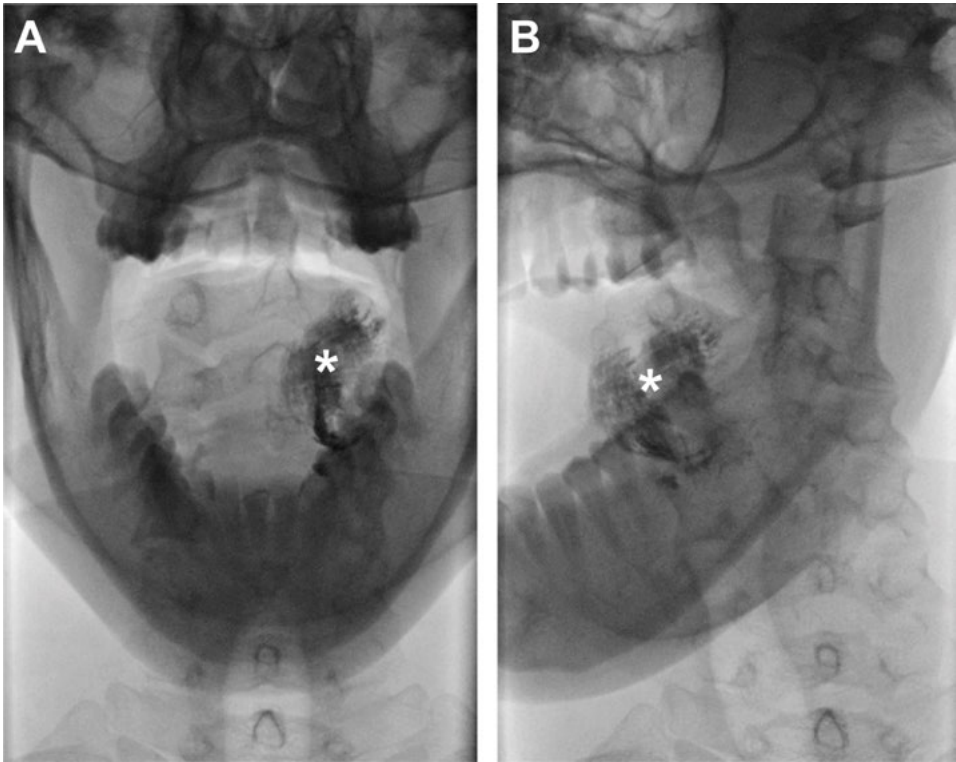
## Study design

Figure 1 provides an overview of the study's procedures. The day before surgery, included patients first underwent conventional early scintigraphy (i.e., dynamic and early static) following the peritumoral administration of 120 megabecquerel (MBq) [<sup>99m</sup>Tc]Tc-nanocolloid in a volume of ~0.5 mL by an experienced radiologist and nuclear medicine physician (B.d.K.).

Then, a total volume of 0.5 mL Lipiodol<sup>®</sup> was administered peritumorally at the same injection site by the same physician (B.d.K.) in the presence of a second observer (R.M.; D.N.V.D.). In order to record the early lymphatic drainage of Lipiodol<sup>®</sup>, peritumoral administration of Lipiodol<sup>®</sup> was immediately followed by a dynamic X-ray in odontoid view (projections, anterior–posterior and anterior–oblique; 75 kV, 220 mA, small focus, filter: 0.1 mm Cu + 1 mm Al) until 20 min post-injection (Figure 2). Subsequently, CTL images were acquired using IQon Spectral CT (Philips Healthcare, the Netherlands) (Figure 3). CT acquisition was conducted using the following settings: 120 kV; 62 mAs; rotation time: 0.27 s; slice thickness: 0.9 mm.



**Figure 1.** Time schedule of study events. MBq, megabecquerel; mL, milliliter; CTL, computed tomography lymphography; SPECT/CT, single-photon emission computed tomography/computed tomography; SLNs, sentinel lymph nodes.



**Figure 2.** Contrast-inverted dynamic X-ray images acquired 10 min following peritumoral injection of Lipiodol® in a patient with cT1N0 OSCC on the left side of the oral tongue (*patient 6*). No lymphatic drainage of Lipiodol® was observed with dynamic X-ray. (a) Anterior–posterior odontoid projection; (b) anterior–oblique odontoid projection; (\*) injection site.



**Figure 3.** CT lymphographic images acquired 25 min post-injection of Lipiodol® in the same patient (*patient 6*). (a) Axial plane, (b) coronal plane, and (c) sagittal plane; (\*) injection site. Lymphatic drainage was observed (*white arrows*), yet no SLNs were identified on CTL in this patient.

After CTL, late scintigraphy and SPECT acquisition were initiated 2 h post-injection of [ $^{99m}\text{Tc}$ ]Tc-nanocolloid and were followed by low-dose CT acquisition as part of SPECT/CT, according to the EANM guidelines [19]. Since the low-dose CT, as part of SPECT/CT, was conducted after the injection of Lipiodol<sup>®</sup> (120–125 min post-injection), SPECT/CT acquisition inherently allowed for the fusion of late CTL and SPECT imaging (Figure 4).

SLNs identified by [ $^{99m}\text{Tc}$ ]Tc-nanocolloid lymphoscintigraphy (including SPECT/CT) were marked on the overlying skin. Any additional SLNs identified in vicinity of the primary tumor by CTL were marked for surgical extirpation as well on the basis of their anatomical location.

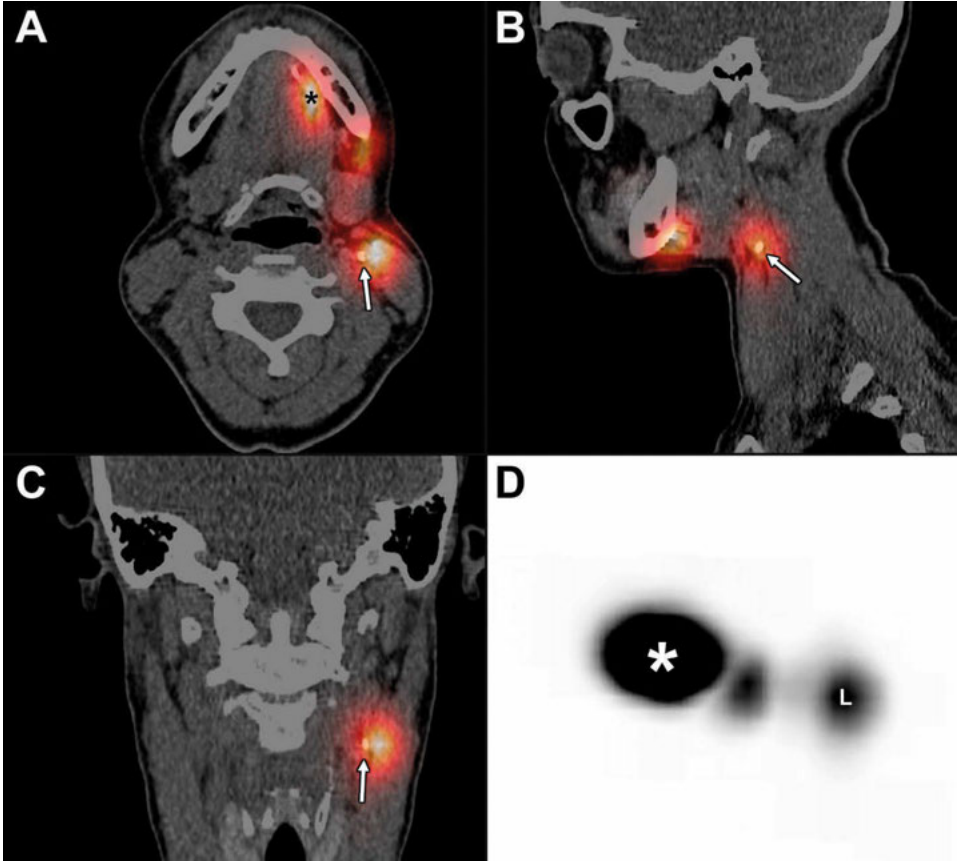


**Figure 4.** Fusion of SPECT and late CTL at 120 min post-injection of Lipiodol<sup>®</sup> in the same patient (*patient 6*). (a) Axial plane, (b) sagittal plane, (c) coronal plane, and (d) maximum intensity projection (MIP); (\*) injection site. The presence of Lipiodol<sup>®</sup> was seen in a SLN located in cervical lymph node level IIa on the left side (*white arrows*), as identified with SPECT, corresponding with the hotspot (*L*) on MIP. Conventional [ $^{99m}\text{Tc}$ ]Tc-nanocolloid lymphoscintigraphy (including SPECT/CT) identified another SLN in cervical lymph node level Ib on the left side, in which no uptake of Lipiodol<sup>®</sup> could be seen on late CTL.

The next day, the marked SLNs were harvested under conventional portable gamma-probe guidance. The location of the extirpated SLNs, including their counts per second, as measured with the portable gamma-probe, were registered. In those with tumors involving the floor-of-mouth, super-selective neck dissections of cervical lymph node level I were performed [20]. Any SLNs in the super-selective neck dissection specimen were extirpated by gamma-probe guidance ex vivo.

All extirpated SLNs were subjected to a low-dose X-ray using a mammography system (Hologic 3Dimension™; target-filter rhodium, 30 kV, 10 mAs, small focus) to assess whether those SLNs contained Lipiodol® (Figure 5).

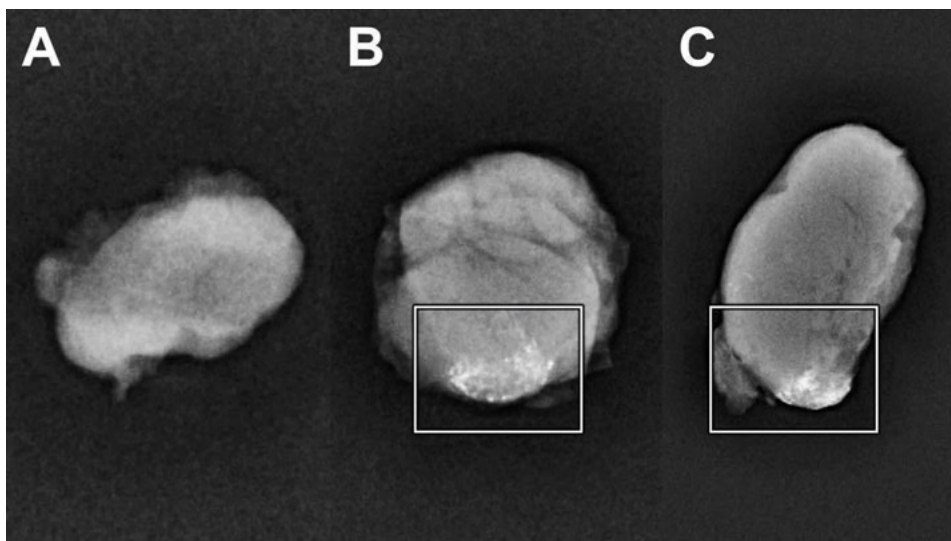


**Figure 5.** Low-dose X-ray of extirpated SLNs from patient 6. (a) SLN level Ib left (750 counts per second), which proved histopathologically positive for metastasis, showed no traces of Lipiodol®. (b,c) SLN level Ib left (5387 counts per second; histopathologically negative) and SLN level Iia left (9194 counts per second; histopathologically positive) with the uptake of Lipiodol® as confirmed by low-dose X-ray (*white squares*).

Finally, harvested SLNs were sent for histopathological examination using step-serial-sectioning (section thickness 150  $\mu\text{m}$ ) with hematoxylin-eosin and pan-cytokeratin antibody (AE 1/3) staining [21, 22]. Patients with histopathologically negative SLNs were assigned to a wait-and-scan approach. In those with at least one histopathologically positive SLN, complementary treatment of the affected and adjacent nodal basins was employed (i.e., neck dissection or (chemo)radiotherapy). Complementary neck dissection specimens were histopathologically assessed for additional (non-SLN) nodal metastases. The follow-up of patients was in compliance with standard oncological care.

## Preparation of Lipiodol® for peritumoral injection

Lipiodol® was obtained from Guerbet, Roissy, France. Before peritumoral administration, Lipiodol® was pre-heated at 37 °C using a contrast media warming cabinet, having a viscosity of approximately 25 mPa·s [15]. A total volume of 0.5 mL Lipiodol® was peritumorally injected using a 1 mL compatible syringe.

## Scintigraphy and SPECT/CT

Planar scintigraphic images were acquired in the dynamic mode (128 × 128 matrix; 60 frames of 30 s) in anterior–posterior projection, followed by a static mode (256 × 256 matrix; 4 m) in anterior–posterior and lateral projections (30 m and 2 h post-injection). Dynamic and static scintigraphic imaging was supplemented with 30 s flood field images. SPECT/CT was acquired on a 128 × 128 matrix (pixel spacing, 4.8 × 4.8 mm), with 128 angles, 20 s per projection, over a non-circular 360° orbit (CT: 110 kV, 40 mAs eff., slice thickness 1.2 mm). Both scintigraphic and SPECT/CT images were acquired using a Siemens Symbia T16 SPECT/CT scanner with “low- and medium energy” (LME) collimators to limit septal penetration and reduce shine-through [23]. SPECT/CT images were reconstructed using clinical reconstruction software (Siemens Flash3D, Siemens Healthineers, Erlangen, Germany), with attenuation and scatter correction (6 iterations, 8 subsets, and a 5 mm Gaussian filter).

## Evaluation and analyses

For each patient, corresponding images of CTL and conventional [<sup>99m</sup>Tc]Tc-nanocolloid lymphoscintigraphy (including SPECT/CT), as well as fusion images of late CTL and SPECT, were evaluated for the similarity of depicted draining lymph node basins, and the number and location of identified SLNs. Furthermore, CTL and [<sup>99m</sup>Tc]Tc-nanocolloid lymphoscintigraphy were compared with respect to the visualization of lymphatic vessels transporting the radiotracer. SLNs identified with either CTL or [<sup>99m</sup>Tc]Tc-nanocolloid lymphoscintigraphy, as well as outcomes of low-dose X-ray of harvested SLNs, were related to the outcomes from histopathological assessment of extirpated SLNs and any complementary neck dissection specimens. All images were simultaneously reviewed by a radiologist/nuclear medicine physician (B.K.) and a second observer (R.M.).

All data were analyzed with IBM SPSS Statistics Version 28.0 (IBM Corp., released 2021, Armonk, NY, USA). For categorical variables, the number of cases and percentages are presented. Continuous parametric variables are presented as mean (±SD); non-parametric variables are presented as median. With histopathological examination of extirpated SLNs as well as any complementary neck dissection specimens and follow-up as reference standard, both sensitivity and NPV were calculated for CTL. Statistical tests were considered unfeasible, due to the small number of patients included in this study.

## Results

Patient- and tumor characteristics of included patients are listed in Table 1. The most frequently involved tumor subsite was the oral tongue (40%). Tumors were clinically classified as T2 in the majority of patients (80%). A total of 32 SLNs were harvested (a median of 3 per patient), of which 6 contained metastases. In this population, 40% of patients had occult lymph node metastasis as detected by SLNB. Of those with histopathologically positive SLNs, three underwent complementary neck dissection (75%), while the remaining patients underwent complementary radiotherapy. No additional nodal metastases were found by the histopathological examination of complementary neck dissection specimens. Adverse reactions following the peritumoral injection of Lipiodol® did not occur. The median follow-up time was 12.3 months (ranging between 5.6 and 15.6 months).

**Table 1.** Patient- and tumor characteristics.

Characteristics	<i>n</i> = 10
<b>Gender, n (%)</b>	
Female	6 (60%)
<b>Median age (y) (range)</b>	67.0 (20-81)
<b>History of head and neck cancer, n (%)</b>	0 (0%)
<b>Tumor location, n (%)</b>	
Tongue	4 (40%)
Floor-of-mouth	2 (20%)
Buccal mucosa	3 (30%)
Vestibule of mouth	1 (10%)
<b>Side primary tumor, n (%)</b>	
Left	3 (30%)
Right	6 (60%)
Midline	1 (10%)
<b>Clinical T-stage, n (%)*</b>	
T1	2 (20%)
T2	8 (80%)
<b>Pathology primary tumor</b>	
Mean diameter (mm) (SD)	14.8 (±8.7)
Mean depth-of-invasion (mm) (SD)	4.0 (±2.6)
Median harvested SLNs (range)	3 (2-5)
<b>Histopathological status SLNs, n (%)</b>	
Negative	26 (81%)
Positive	6 (19%)

**Table 1.** Continued.

Characteristics	<i>n</i> = 10
<b>Pathological N-stage after SLNB, n (%)*</b>	
pN0(sn)	6 (60%)
pN1(sn)	2 (20%)
pN2b(sn)	2 (20%)
<b>Complementary neck treatment, n (%)</b>	
Complementary ND	3 (30%)
Complementary RT	1 (10%)
<b>Follow-up in months (range)</b>	12.3 (6 – 16)

*n*, number; *y*, years; *mm*, millimeters; *SD*, standard deviation; *SLNs*, sentinel lymph nodes; *SLNB*, sentinel lymph node biopsy; *ND*, neck dissection; *RT*, radiotherapy.

\*According to AJCC TNM classification, 8<sup>th</sup> edition.

### Sentinel lymph node identification

The outcomes of CTL and [<sup>99m</sup>Tc]Tc-nanocolloid lymphoscintigraphy for all included patients are presented in Table 2. [<sup>99m</sup>Tc]Tc-nanocolloid lymphoscintigraphy identified a total of 21 SLNs, of which 7 were identified by CTL as well (33%). No additional SLNs were identified by CTL. In four patients, CTL failed to identify any SLN (40%). Out of the six histopathologically positive SLNs, two were identified by CTL (33%). Low dose X-ray confirmed the uptake of Lipiodol® in seven harvested SLNs (24%), in a total of five patients, of which five SLNs were also depicted by CTL. Due to logistical issues, the extirpated SLNs of patient four were not assessed for the presence of Lipiodol® using low-dose X-ray.

Lymphatic vessels draining [<sup>99m</sup>Tc]Tc-nanocolloid towards SLNs were visualized in four patients with early dynamic and static scintigraphy (patients 2, 3, 5 and 6; 40%). In regard to CTL, lymphatic vessels draining Lipiodol® were identified in three patients (patients 3, 6 and 9; 30%).

**Table 2.** Comparison of sentinel lymph node distribution between CT lymphography and [<sup>99m</sup>Tc]Tc-nanocolloid lymphoscintigraphy.

N°	Primary tumor	Identified SLNs SG & SPECT/CT	Identified SLNs CTL	Harvested SLNs (cps)	PA	Lipiodol® in harvested SLN	Comp. treatment	pTNM*	
1	Lower gum (right)	Ib Ila	Right Right	None	Ib Ib	Right (360) Right (259)	+	No No	RT I-V right pT4aN2b(sn)
2	Tongue (right)	III III III	Right Right Left	II III III	III III III	Right (198) Right (2347) Right (2004)	-	No Yes Yes	N.A. pT2N0(sn)
3	FOM (midline)	Ib III III	Right Right Left	III III III	Ib III III	Right (171) Right (429) Left (411)	-	No Yes No	N.A. pT1N0(sn)
4	FOM (midline)	Ib IIa III	Right Right Left	Ib IIa III	Ib IIa III	Right (701) Right (174) Left (276)	+	N.S. N.S. N.S.	SND I-III right pT1N1
5	Tongue (left)	III III IV	Left Left Left	None	III III III	Left (447) Left (441) Left (927)	-	No No No	N.A. pT1N0(sn)
6	Tongue (left)	Ib IIa	Left Left	IIa Ib	Ib Ib	Left (750) Left (5387)	+	Yes No	MRND I-V left pT1N2b
7	Buccal mucosa (right)	Ib II	Right Right	Right Right	Ib Ib	Right (97) Right (13) Right (411) Right (432) Right (310)	-	No No No No Yes	N.A. pT1N0(sn)

Table 2. Continued.

N <sup>o</sup>	Primary tumor	Identified SLNs SG & SPECT/CT	Identified SLNs CTL	Harvested SLNs (cps)	PA	Lipiodol <sup>®</sup> in harvested SLN	Comp. treatment	pTNM*
8	Buccal mucosa (left)	Ila Left	None	Ila Left (184) Ila Left (228) II Left (73)	-	No No No	N.A.	pT2N0(sn)
9	Tongue (right)	II Right III Right	II Right	IIb Right (963) III Right (363) V Right (648)	- +	Yes No No	MRND I-V right	pT2N1
10	Buccal mucosa (right)	III Right	None	III Right (23) III Right (158)	-	No No	N.A.	pT1N0(sn)

N<sup>o</sup>: patient number; SLN, sentinel lymph node; SG, scintigraphy; SPECT/CT, single-photon emission computed tomography/computed tomography; CTL, computed tomography lymphography; cps, counts per second as measured by conventional gamma-probe; PA, pathological assessment; comp., complementary; +, histopathologically positive for metastasis; -, histopathologically negative for metastasis; RT, radiotherapy; N.A., not applicable; FOM, floor-of-mouth; MRND, modified radical neck dissection; SND, selective neck dissection.

\*According to AJCC TNM classification, 8<sup>th</sup> edition.

## Follow-up

During follow-up, one patient developed nodal recurrence 11 months following SLNB (patient 1). Since the nodal recurrence occurred in the nodal basin that was initially staged positive by SLNB and subsequently treated with complementary radiotherapy, it was considered to be a consequence of inadequate complementary treatment rather than SLNB failure. All other included patients remained free of disease after a median follow-up duration of 11.9 months. With a median follow-up of 12.3 months, CTL using Lipiodol<sup>®</sup> reached a sensitivity of 50% and a NPV of 75% in this population.

Follow-up cross-sectional imaging was performed in two patients, according to the standard of oncological care, on account of a suspected recurrence (patient 1) or for further oncological staging after a positive SLNB (patient 6) at 331 days and 13 days following SLNB, respectively. In both patients, remains of Lipiodol<sup>®</sup> were still seen surrounding the initial primary tumor site on [<sup>18</sup>F]FDG-PET/CT (Figure 6). However, no further lymphatic drainage of Lipiodol<sup>®</sup> nor depositions of Lipiodol<sup>®</sup> in lymph nodes were observed in either patient on follow-up imaging.

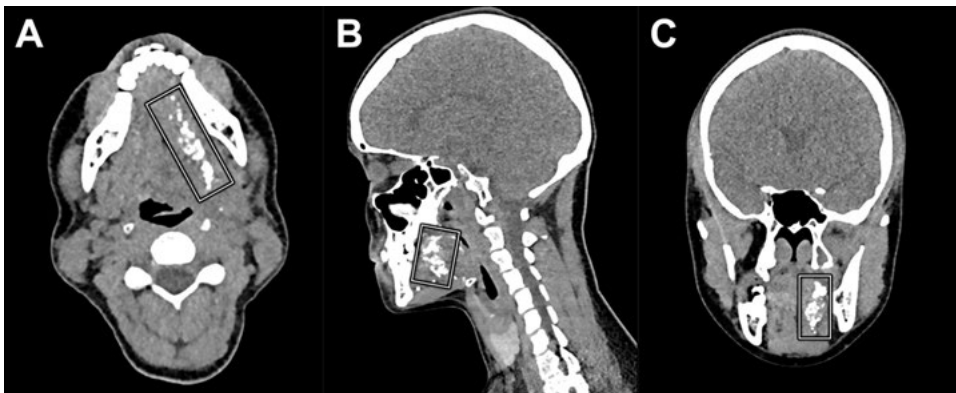


**Figure 6.** CT images as part of the [<sup>18</sup>F]FDG-PET/CT acquired 13 days following peritumoral administration of Lipiodol<sup>®</sup> (patient 6) clearly depicts remains of Lipiodol<sup>®</sup> located around the initial primary tumor site (white squares). (a) Axial plane, (b) coronal plane, and (c) sagittal plane.

## Discussion

In this within-patient comparison study aimed at evaluating SLN mapping using CTL with Lipiodol® in early-stage OSCC, a disappointing SLN identification rate of only 33% was found for CTL. Contrast-enhanced lymphatic vessels were identified in three patients by CTL (30%), while conventional early dynamic and static scintigraphy managed to visualize lymphatic vessels draining [<sup>99m</sup>Tc]Tc-nanocolloid in four patients (40%). Moreover, in 40% of patients, neither lymphatic drainage of Lipiodol® nor contrast-enhanced lymph nodes were observed at all on CTL. In this population, CTL using Lipiodol® would have falsely staged two patients as negative for nodal metastatic disease (patients 1 and 9), corresponding with a sensitivity of 50% and an NPV of 75%.

Hence, our results contradict those of Kim et al. [13], who identified at least one contrast-enhanced lymph node in all 10 early gastric adenocarcinoma patients by CTL one hour following the peritumoral injection of 1 mL Lipiodol®. Furthermore, in their study, all metastatic lymph nodes (n = 3) retained Lipiodol® as confirmed by histopathological examination of the sentinel nodal basin including immunohistochemistry and Oil-Red-O staining [13]. Given that elective lymphadenectomy was performed in all patients, no step-serial-sectioning of ex vivo-dissected (S)LN was performed (sectioning thickness 2 mm), non-sentinel basins were subjected to routine histopathological examination and no follow-up results were reported, the accuracy of CTL using Lipiodol® as described by Kim et al. may actually be lower. Especially when considering that micro-metastases and isolated tumor cells are easily missed by routine histopathological examination of lymphadenectomy specimens or by sectioning SLNs at larger intervals than 150 μm [24–27]. Still, this does not entirely clarify the discrepancy in the rate of identified contrast-enhanced lymph nodes by CTL using Lipiodol® between both studies. Although larger volumes of Lipiodol® were administered by Kim et al., the effect of larger volumes (> 0.5 mL) on SLN identification is dubious and has not been recommended by EANM guidelines, as it may lead to a collapse of lymphatics and an increase in patient discomfort [19, 28, 29]. Presumably, differences in characteristics of the lymphatic system between tumor sites contribute to these contrasting results. Despite the fact that peritumorally administered Lipiodol® exhibited poor lymphatic drainage in our population, its capabilities in terms of long-term retention and delayed tracer wash-out were demonstrated by the results of both late CTL and low-dose X-ray of harvested SLNs. In fact, follow-up cross-sectional imaging in two patients showed retention of Lipiodol® at 13 days and 11 months post-injection. However, it should be pointed out that these remains of Lipiodol® were only seen surrounding the initial primary tumor site and that no further lymphatic drainage nor depositions of

Lipiodol® in lymph nodes were observed. These findings on the long-term retention of Lipiodol® are in line with Kim et al., which revealed that extirpated lymph nodes still contained Lipiodol® one day following CTL [13].

Overall, our results suggest that CTL using Lipiodol® is inferior to CTL using water-soluble iodine-based contrast agents. In previous studies investigating CTL using a water-soluble iodine-based contrast agent (i.e., iopamidol), at least one SLN could be identified by CTL in 89–96% of patients [7–12, 14]. In addition, two series reported contrast-enhanced lymphatic vessel visualization in 90% of their patients [9, 11]. Their approach for SLNB using CTL led to a reported sensitivity ranging from 56 to 80% and a NPV ranging from 82 to 96% [7, 9, 10, 12, 14]. Nonetheless, it should be mentioned that in some of these studies, SLNB was immediately followed by END, irrespective of the histopathological status of harvested SLNs [9, 10]. As aforementioned, micrometastases are easily missed by routine histopathological examination of neck dissection specimens; therefore, the reported false-negative rate of SLN mapping by CTL in these studies may be underestimated [24–26]. In those studies with more reliable reference standards (i.e., observation of the untreated neck during follow-up after a negative SLNB), the reported diagnostic accuracy of SLNB on the basis of CTL using iopamidol was significantly worse (sensitivity 56–63%, NPV 85–86%) [12, 14]. For now, both our data as well as results from previous studies suggest that the strategy of SLNB with CTL, using either Lipiodol® or water-soluble iodine-based contrast agents (e.g., iopamidol), is inferior to SLNB with conventional <sup>99m</sup>Tc-labeled radiotracers [30].

Even so, modifications of oil-based iodinated contrast media could increase the degree of lymphatic drainage while still allowing for long-term retention in lymph nodes, potentially improving SLN detection by CTL [16, 31]. Alternatively, other radiocontrast agents (e.g., Nanotrast-CF800 entrapped gold nanoparticles) have shown their potential for SLN mapping using CTL in animal studies [32–34]. These modified radiocontrast agents may enhance the utility of CTL for SLN mapping but have yet to be investigated in human studies.

Several limitations of this study have to be acknowledged. First of all, as previously mentioned, in this study a smaller volume of iodinated contrast agent was administered compared to other studies [9–14]. This discrepancy, as well as other dissimilarities (i.e., tumor site and reference standard), contribute to the fact that our results cannot easily be compared with those achieved by Kim et al. [13]. However, in our population, the vast majority of the administered Lipiodol® remained in the injection site as depicted with CTL, late CTL and follow-up imaging. Accordingly, the marginal lymphatic drainage of Lipiodol® itself, rather than the injected volume,

appears to impede adequate SLN visualization. In addition, by using similar volumes for CTL and conventional [ $^{99m}\text{Tc}$ ]Tc-nanocolloid lymphoscintigraphy (i.e.,  $\sim 0.5$  mL), a more reliable comparison in regard to lymphatic drainage and SLN identification between both techniques could be actualized.

Secondly, the histopathological examination of extirpated SLNs did not include oil-staining to detect microscopic traces of Lipiodol<sup>®</sup>. Even though this did not impact the accuracy of CTL, it might have provided more insight into the (microscopic) lymphatic distribution of Lipiodol<sup>®</sup>.

Finally, due to the small population size of this study and its limited follow-up data, the results of this study should be interpreted with caution. Especially since longer follow-up might reveal missed occult metastases as they become clinically manifest (false-negative outcome).

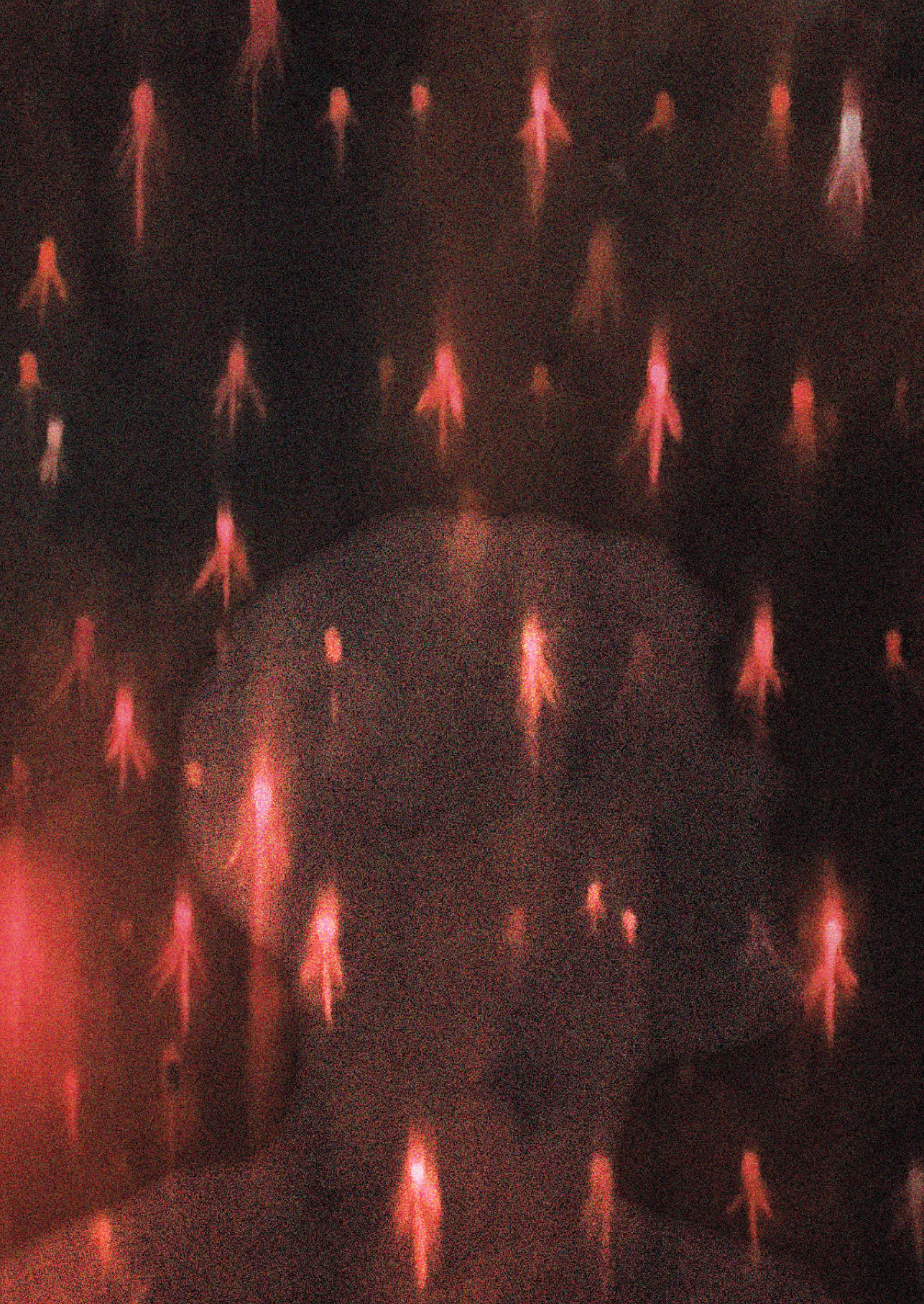
## Conclusion

In conclusion, the results of this study suggest that CTL following the peritumoral administration of Lipiodol® is not a reliable technique for SLN mapping in early-stage OSCC, on account of the low SLN identification rate compared to the current standard for SLN mapping: lymphoscintigraphy including SPECT/CT using <sup>99m</sup>Tc-labeled radiotracers. Although modified radiocontrast agents may enhance the utility of CTL for SLN mapping, they have yet to be further investigated in human studies.

## References

1. Garrel R, Poissonnet G, Moyà Plana A, et al. Equivalence randomized trial to compare treatment on the basis of sentinel node biopsy versus neck node dissection in operable T1-T2N0 oral and oropharyngeal cancer. *J Clin Oncol*. 2020;38(34):4010-4018. doi:10.1200/JCO.20.01661
2. Hasegawa Y, Tsukahara K, Yoshimoto S, et al. Neck dissections based on sentinel lymph node navigation versus elective neck dissections in early oral cancers: a randomized, multicenter, and noninferiority trial. *J Clin Oncol*. 2021;39(18):2025-2036. doi:10.1200/JCO.20.03637
3. Gupta T, Maheshwari G, Kannan S, Nair S, Chaturvedi P, Agarwal JP. Systematic review and meta-analysis of randomized controlled trials comparing elective neck dissection versus sentinel lymph node biopsy in early-stage clinically node-negative oral and/or oropharyngeal squamous cell carcinoma: Evidence-base for practice and implications for research. *Oral Oncol*. 2022;124:105642. doi:10.1016/j.oraloncology.2021.105642
4. den Toom IJ, van Schie A, van Weert S, et al. The added value of SPECT-CT for the identification of sentinel lymph nodes in early stage oral cancer. *Eur J Nucl Med Mol Imaging*. 2017;44(6):998-1004. doi:10.1007/s00259-017-3613-8
5. den Toom IJ, Boeve K, Lobeek D, et al. Elective neck dissection or sentinel lymph node biopsy in early stage oral cavity cancer patients: the Dutch experience. *Cancers (Basel)*. 2020;12(7):1783. Published 2020 Jul 3. doi:10.3390/cancers12071783
6. Bowe CM, Shastri M, Gulati A, et al. Challenges and outcomes in establishing a sentinel lymph node biopsy service for oral squamous cell carcinoma in a regional district specialist hospital. *Br J Oral Maxillofac Surg*. 2021;59(2):217-221. doi:10.1016/j.bjoms.2020.08.057
7. Mahieu R, de Maar JS, Nieuwenhuis ER, et al. New developments in imaging for sentinel lymph node biopsy in early-stage oral cavity squamous cell carcinoma. *Cancers (Basel)*. 2020;12(10):3055. Published 2020 Oct 20. doi:10.3390/cancers12103055
8. Saito M, Nishiyama H, Oda Y, Shingaki S, Hayashi T. The lingual lymph node identified as a sentinel node on CT lymphography in a patient with cN0 squamous cell carcinoma of the tongue. *Dentomaxillofac Radiol*. 2012;41(3):254-258. doi:10.1259/dmfr/61883763
9. Honda K, Ishiyama K, Suzuki S, et al. Sentinel lymph node biopsy using computed tomographic lymphography in patients with early tongue cancer. *Acta Otolaryngol*. 2015;135(5):507-512. doi:10.3109/00016489.2015.1010126
10. Honda K, Ishiyama K, Suzuki S, Kawasaki Y, Saito H, Horii A. Sentinel lymph node biopsy using preoperative computed tomographic lymphography and intraoperative indocyanine green fluorescence imaging in patients with localized tongue cancer. *JAMA Otolaryngol Head Neck Surg*. 2019;145(8):735-740. doi:10.1001/jamaoto.2019.1243
11. Sugiyama S, Iwai T, Izumi T, et al. CT lymphography for sentinel lymph node mapping of clinically N0 early oral cancer. *Cancer Imaging*. 2019;19(1):72. Published 2019 Nov 12. doi:10.1186/s40644-019-0258-9
12. Ishiguro K, Iwai T, Izumi T, et al. Sentinel lymph node biopsy with preoperative CT lymphography and intraoperative indocyanine green fluorescence imaging for N0 early tongue cancer: A long-term follow-up study. *J Craniomaxillofac Surg*. 2020;48(3):217-222. doi:10.1016/j.jcms.2020.01.007
13. Kim YH, Lee YJ, Park JH, et al. Early gastric cancer: feasibility of CT lymphography with ethiodized oil for sentinel node mapping. *Radiology*. 2013;267(2):414-421. doi:10.1148/radiol.12121527
14. Sugiyama S, Iwai T, Izumi T, et al. Sentinel lymph node mapping of clinically N0 early oral cancer: a diagnostic pitfall on CT lymphography. *Oral Radiol*. 2021;37(2):251-255. doi:10.1007/s11282-020-00442-1
15. Pieper CC, Hur S, Sommer CM, et al. Back to the future: Lipiodol in lymphography—from diagnostics to theranostics. *Invest Radiol*. 2019;54(9):600-615. doi:10.1097/RLI.0000000000000578
16. Kim H, Lee SK, Kim YM, et al. Fluorescent iodized emulsion for pre- and intraoperative sentinel lymph node imaging: validation in a preclinical model. *Radiology*. 2015;275(1):196-204. doi:10.1148/radiol.14141159
17. Amin MB, Greene FL, Edge SB, et al. The Eighth Edition AJCC Cancer Staging Manual: Continuing to build a bridge from a population-based to a more “personalized” approach to cancer staging. *CA Cancer J Clin*. 2017;67(2):93-99. doi:10.3322/caac.21388

18. Brierley JD, Gospodarowicz M, Wittekind C. UICC TNM Classification of Malignant Tumours. 8<sup>th</sup> ed. Chichester, United Kingdom: Wiley; 2017.
19. Giammarile F, Schilling C, Gnanasegaran G, et al. The EANM practical guidelines for sentinel lymph node localisation in oral cavity squamous cell carcinoma. *Eur J Nucl Med Mol Imaging*. 2019;46(3):623-637. doi:10.1007/s00259-018-4235-5
20. Stoeckli SJ, Huebner T, Huber GF, Broglie MA. Technique for reliable sentinel node biopsy in squamous cell carcinomas of the floor of mouth. *Head Neck*. 2016;38(9):1367-1372. doi:10.1002/hed.24440
21. Alkureishi LW, Burak Z, Alvarez JA, et al. Joint practice guidelines for radionuclide lymphoscintigraphy for sentinel node localization in oral/oropharyngeal squamous cell carcinoma. *Ann Surg Oncol*. 2009;16(11):3190-3210. doi:10.1245/s10434-009-0726-8
22. Dhawan I, Sandhu SV, Bhandari R, Sood N, Bhullar RK, Sethi N. Detection of cervical lymph node micrometastasis and isolated tumor cells in oral squamous cell carcinoma using immunohistochemistry and serial sectioning. *J Oral Maxillofac Pathol*. 2016;20(3):436-444. doi:10.4103/0973-029X.190946
23. Yoneyama H, Tsushima H, Kobayashi M, Onoguchi M, Nakajima K, Kinuya S. Improved detection of sentinel lymph nodes in SPECT/CT images acquired using a low- to medium-energy general-purpose collimator. *Clin Nucl Med*. 2014;39(1):e1-e6. doi:10.1097/RLU.0b013e31828da362
24. Ambrosch P, Kron M, Fischer G, Brinck U. Micrometastases in carcinoma of the upper aerodigestive tract: detection, risk of metastasizing, and prognostic value of depth of invasion. *Head Neck*. 1995;17(6):473-479. doi:10.1002/hed.2880170604
25. Rinaldo A, Devaney KO, Ferlito A. Immunohistochemical studies in the identification of lymph node micrometastases in patients with squamous cell carcinoma of the head and neck. *ORL J Otorhinolaryngol Relat Spec*. 2004;66(1):38-41. doi:10.1159/000077232
26. King C, Elsherif N, Kirwan R, et al. Serial step sections at narrow intervals with immunohistochemistry are required for accurate histological assessment of sentinel lymph node biopsy in oral squamous cell carcinoma. *Head Neck*. 2021;43(10):2985-2993. doi:10.1002/hed.26784
27. Vorburger MS, Broglie MA, Soltermann A, et al. Validity of frozen section in sentinel lymph node biopsy for the staging in oral and oropharyngeal squamous cell carcinoma. *J Surg Oncol*. 2012;106(7):816-819. doi:10.1002/jso.23156
28. Dabbagh Kakhki VR, Aliakbarian H, Fattahi A, et al. Effect of radiotracer injection volume on the success of sentinel node biopsy in early-stage breast cancer patients. *Nucl Med Commun*. 2013;34(7):660-663. doi:10.1097/MNM.0b013e3283619d07
29. Bluemel C, Herrmann K, Giammarile F, et al. EANM practice guidelines for lymphoscintigraphy and sentinel lymph node biopsy in melanoma. *Eur J Nucl Med Mol Imaging*. 2015;42(11):1750-1766. doi:10.1007/s00259-015-3135-1
30. Kim DH, Kim Y, Kim SW, Hwang SH. Usefulness of sentinel lymph node biopsy for oral cancer: a systematic review and meta-analysis. *Laryngoscope*. 2021;131(2):E459-E465. doi:10.1002/lary.28728
31. Chung YE, Hyung WJ, Kweon S, et al. Feasibility of interstitial CT lymphography using optimized iodized oil emulsion in rats. *Invest Radiol*. 2010;45(3):142-148. doi:10.1097/RLI.0b013e3181c8cf19
32. Wan J, Oblak ML, Ram AS, McKenna C, Singh A, Nykamp S. Evaluating the feasibility and efficacy of a dual-modality nanoparticle contrast agent (Nanotrast-CF800) for image-guided sentinel lymph node mapping in the oral cavity of healthy dogs. *Front Vet Sci*. 2021;8:721003. doi:10.3389/fvets.2021.721003
33. Yang Y, Shi F, Zhou J, Shi X, Sha Y, Wu H. Short-term dynamic observation of the color change and enhancement effect of polyethylenimine-entrapped gold nanoparticles used for indirect lymphography. *ORL J Otorhinolaryngol Relat Spec*. 2016;78(3):136-143. doi:10.1159/000446190
34. Shi F, Yang Y, Chen J, Sha Y, Shu Y, Wu H. Dendrimer-entrapped gold nanoparticles as potential CT contrast agents for localizing sentinel lymph node via indirect CT lymphography on rabbit model. *Biomed Res Int*. 2018;2018:1230151. doi:10.1155/2018/1230151



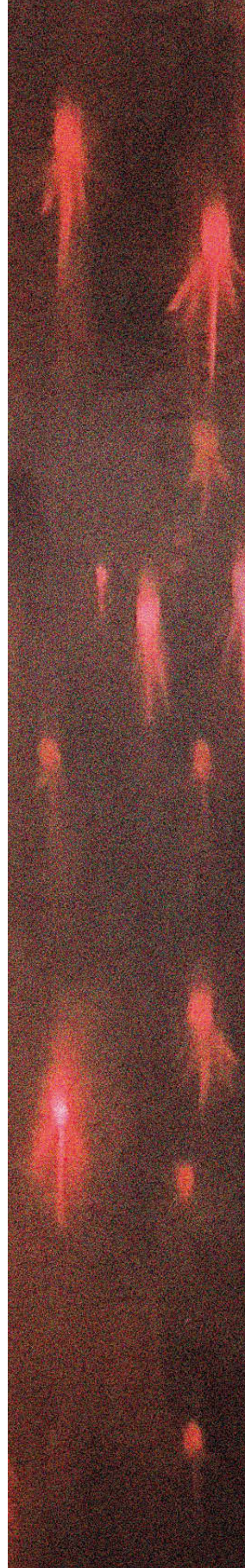
# 10

Within-patient comparison  
between [<sup>68</sup>Ga]Ga-tilmanocept  
PET/CT lymphoscintigraphy  
and [<sup>99m</sup>Tc]Tc-tilmanocept  
lymphoscintigraphy for sentinel  
lymph node detection in oral  
cancer: a pilot study

---

Rutger Mahieu, Dominique N.V. Donders, Gerard C. Krijger,  
F.F. Tessa Ververs, Remmert de Roos, John L.M.M. Bemelmans,  
Rob van Rooij, Remco de Bree, Bart de Keizer.

*Eur J Nucl Med Mol Imaging. 2022 May;49(6):2023-2036*



# Abstract

## Purpose

To compare sentinel lymph node (SLN) identification using [ $^{68}\text{Ga}$ ]Ga-tilmanocept PET/CT lymphoscintigraphy to [ $^{99\text{m}}\text{Tc}$ ]Tc-tilmanocept lymphoscintigraphy (including SPECT/CT) in early-stage oral cancer. Furthermore, to assess whether reliable intraoperative SLN localization can be performed with a conventional portable gamma-probe using [ $^{99\text{m}}\text{Tc}$ ]Tc-tilmanocept without the interference of [ $^{68}\text{Ga}$ ]Ga-tilmanocept in these patients.

## Methods

This prospective within-patient comparison pilot study evaluated SLN identification by [ $^{68}\text{Ga}$ ]Ga-tilmanocept PET/CT lymphoscintigraphy compared to conventional lymphoscintigraphy using [ $^{99\text{m}}\text{Tc}$ ]Tc-tilmanocept ( $\sim 74$  MBq) in 10 early-stage oral cancer patients scheduled for SLN biopsy. After conventional [ $^{99\text{m}}\text{Tc}$ ]Tc-tilmanocept lymphoscintigraphy, patients underwent peritumoral administration of [ $^{68}\text{Ga}$ ]Ga-tilmanocept ( $\sim 10$  MBq) followed by PET/CT acquisition initiated 15 min after injection. Intraoperative SLN localization was performed under conventional portable gamma-probe guidance the next day; the location of harvested SLNs was correlated to both lymphoscintigraphic images in each patient.

## Results

A total of 24 SLNs were identified by [ $^{99\text{m}}\text{Tc}$ ]Tc-tilmanocept lymphoscintigraphy, all except one were also identified by [ $^{68}\text{Ga}$ ]Ga-tilmanocept PET/CT lymphoscintigraphy. [ $^{68}\text{Ga}$ ]Ga-tilmanocept PET/CT lymphoscintigraphy identified 4 additional SLNs near the injection site, of which two harbored metastases. Lymphatic vessels transporting [ $^{68}\text{Ga}$ ]Ga-tilmanocept were identified by PET/CT lymphoscintigraphy in 80% of patients, while draining lymphatic vessels were visualized by [ $^{99\text{m}}\text{Tc}$ ]Tc-tilmanocept lymphoscintigraphy in 20% of patients. Of the 33 SLNs identified by [ $^{68}\text{Ga}$ ]Ga-tilmanocept PET/CT lymphoscintigraphy, 30 (91%) were intraoperatively localized under conventional gamma-probe guidance.

## Conclusion

[ $^{68}\text{Ga}$ ]Ga-tilmanocept PET/CT lymphoscintigraphy provided more accurate identification of SLNs and improved visualization of lymphatic vessels compared to [ $^{99\text{m}}\text{Tc}$ ]Tc-tilmanocept lymphoscintigraphy. When combined with peritumoral administration of [ $^{99\text{m}}\text{Tc}$ ]Tc-tilmanocept, SLNs detected by [ $^{68}\text{Ga}$ ]Ga-tilmanocept PET/CT lymphoscintigraphy can be reliably localized during surgery under conventional gamma-probe guidance.

## Introduction

Since the growing consensus concerning the need for active management of the cervical lymph node basin in early-stage (cT1-2N0) oral squamous cell carcinoma (OSCC) [1], sentinel lymph node biopsy (SLNB) is gaining interest for assessing the cervical nodal status without comprehensive removal of the at-risk nodal basins [2]. With a pooled sensitivity of 87% and negative predictive value (NPV) of 94%, SLNB has been put forward as an equally accurate, less invasive alternative to elective neck dissection for staging the clinically negative neck in early-stage OSCC patients [3–5]. Still, challenges remain for SLNB with conventional peritumorally administered  $^{99m}\text{Tc}$ -labeled radiotracers, on account of the limited resolution of conventional scintigraphy and SPECT/CT imaging [6].

First and foremost, activity residing at the radiotracer injection site may hide neighboring sentinel lymph nodes (SLN) and impede distinction between SLN and the injection site (shine-through phenomenon) [4, 7–10]. In particular, tumor subsites with close spatial relation to SLNs (e.g., floor-of-mouth) are prone to the shine-through phenomenon, thus increasing the risk of missing metastatic SLNs in these patients. Any neglected occult metastasis will inevitably develop into the clinical manifestation of disease, which usually entails comprehensive surgery as well as adjuvant radiotherapy and reduces disease-specific survival [1, 11].

Furthermore, the discrimination of hotpots between either relevant SLN or irrelevant higher echelon nodes (HEN) can be complicated. Erroneously considering HENs as SLNs induces unnecessary exploration of the neck, with its accompanying morbidity and risk of complications that may hamper a complementary neck dissection in case of metastatic involvement of SLNs [12]. More importantly, falsely designating true SLNs as HENs can result in neglecting occult nodal metastases as well.

Therefore, technical developments aimed at increasing the diagnostic accuracy of SLNB in early-stage OSCC are still of vital importance. In 2013, Heuveling et al. demonstrated that PET/CT lymphoscintigraphy, following peritumoral injection of [ $^{89}\text{Zr}$ ]Zr-nanocolloid, may provide a solution to these clinical issues addressed [13]. On the basis of its superior resolution, relative to conventional SLN imaging using [ $^{99m}\text{Tc}$ ]Tc-radiotracers, PET/CT lymphoscintigraphy can significantly decrease the shine-through phenomenon and consequently enhance the accuracy of SLN detection. In addition, PET/CT lymphoscintigraphy contributes to better differentiation between SLNs and HENs due to its high resolution and capability to visualize lymphatic vessels transporting the radiotracer [13]. In their sequel study, Heuveling et al. achieved both highly accurate SLN mapping with PET/CT lymphoscintigraphy, as

well as intraoperative SLN localization using a handheld PET-probe, after peritumoral administration of [ $^{89}\text{Zr}$ ]Zr-nanocolloid [14]. However, the PET-probe detected only 80% of SLNs as identified by PET/CT lymphoscintigraphy, owing to the PET-probe's limited sensitivity. Besides, due to the limited sensitivity and large size of the PET-probe, wider skin incisions and exploration of the neck were required for SLN localization.

To overcome the concerns with the use of a PET-probe, a radiotracer labeled with both a positron-emitter and a gamma-emitter could facilitate high-resolution PET/CT lymphoscintigraphy for SLN mapping and reliable intra-operative SLN localization using a conventional portable gamma-probe [6]. On account of the relatively long half-life of  $^{89}\text{Zr}$  (i.e., 78.4 h), high-energy photons created by the annihilation of positrons emitted by  $^{89}\text{Zr}$  will interfere with  $^{99\text{m}}\text{Tc}$ 's gamma radiation and is therefore not feasible for such a dual-isotope approach [15]. To prevent interference of high-energy photons from positron-emitting tracers, a PET-isotope with a short half-life, that has been decayed at the time of surgery the next day, could be considered. A promising alternative PET-isotope is  $^{68}\text{Ga}$ , which has a short half-life (68 min) and has been successfully conjugated with tilmanocept before [16]. Moreover, fluorescent (IRD-800CW)-labeled tilmanocept has been radiolabeled with both  $^{68}\text{Ga}$  and  $^{99\text{m}}\text{Tc}$  and has shown to allow for high-resolution preoperative PET/CT lymphoscintigraphic imaging and intraoperative SLN localization under conventional gamma-probe and fluorescence imaging guidance in animal models [17–19].

Nonetheless, the concept that a  $^{68}\text{Ga}$ -labeled radiotracer indeed provides high-resolution PET/CT lymphoscintigraphic images for preoperative SLN mapping, without interference with  $^{99\text{m}}\text{Tc}$ -detection using the conventional gamma-probe for intraoperative SLN localization, has to be investigated in patients first.

Accordingly, this prospective within-patient comparison pilot study evaluated SLN identification by means of [ $^{68}\text{Ga}$ ]Ga-tilmanocept PET/CT lymphoscintigraphy as compared to SLN identification using [ $^{99\text{m}}\text{Tc}$ ]Tc-tilmanocept lymphoscintigraphy (including SPECT/CT) in early-stage OSCC patients. Furthermore, this pilot study assessed whether reliable intraoperative SLN localization could be performed with the conventional portable gamma-probe without the interference of  $^{68}\text{Ga}$  with  $^{99\text{m}}\text{Tc}$  in these patients.

# Materials and methods

## Patients

This study was approved by the Ethics Committee of the University Medical Center Utrecht (no. 19/697); written informed consent has been obtained from all patients. This trial was registered in the Netherlands Trial Register (no. NL8433) and in EudraCT for clinical trials on medicinal products (no. 2019-004,914-32).

Between June and November 2020, a total of 10 previously untreated patients with newly diagnosed early-stage OSCC (cT1-3N0; TNM Staging AJCC UICC 8<sup>th</sup> Edition [20, 21]) scheduled for SLNB were prospectively included in this study (Table 1). Patients with a tumor clinically staged as T3 were only included when cT3 was based on depth-of-invasion of > 10 mm and tumor dimensions of > 2 cm and ≤ 4 cm [22]. Clinical negative nodal status (cN0) was confirmed by at least palpation and ultrasound in all patients. In those with suspect lymph nodes on ultrasound, ultrasound-guided fine-needle aspiration cytology was performed. In several patients, magnetic resonance imaging of the head and neck was acquired, as part of clinical staging.

Patients with a history of gross injury to the neck that would preclude reasonable surgical dissection of SLNs for this trial, neck dissection or radiotherapy to the neck were excluded from this study. Patients with prior head and neck malignancies in the past 5 years or patients who underwent other nuclear imaging within 240 h of the study procedure were excluded as well.

**Table 1.** Patient- and tumor characteristics.

Characteristics	<i>n</i> = 10
<b>Gender, n (%)</b>	
Female	6 (60%)
<b>Median age (y) (range)</b>	62.3 (51-80)
<b>Tumor location, n (%)</b>	
Tongue	7 (70%)
Floor-of-mouth	1 (10%)
Lower gum	2 (20%)
<b>Side primary tumor, n (%)</b>	
Left	5 (50%)
Right	4 (40%)
Midline	1 (10%)

**Table 1.** Continued.

Characteristics	<i>n</i> = 10
<b>Clinical T stage, n (%)*</b>	
T1	5 (50%)
T2	4 (40%)
T3	1 (10%)
<b>Pathology primary tumor</b>	
Mean diameter (mm) (SD)	21.4 (±10.5)
Mean depth-of-invasion (mm) (SD)	6.5 (±4.5)
Median harvested SLNs (range)	3 (1-5)
<b>Histopathological status SLNs, n (%)</b>	
Negative	25 (76%)
Positive	8 (24%)
<b>Pathological N stage after SLNB, n (%)*</b>	
pN0(sn)	4 (40%)
pN1(sn)	5 (50%)
pN3b(sn)	1 (10%)
<b>Complementary neck treatment, n (%)</b>	
Complementary ND	4 (40%)
Complementary RT	1 (10%)
Complementary CH-RT	1 (10%)

SLN, *sentinel lymph node*; n, *number*; y, *years*; mm, *millimeters*; SD, *standard deviation*; ND, *neck dissection*; RT, *radiotherapy*; CH-RT, *chemo-radiation*.

\*According to 8<sup>th</sup> AJCC TNM classification.

## Study design

Figure 1 provides an overview of the study procedures. On the day before surgery, included patients first underwent conventional scintigraphy (i.e., dynamic, early static, and late static) and SPECT/CT imaging following peritumoral administration of 74 MBq [<sup>99m</sup>Tc]Tc-tilmanocept. Identified SLNs by [<sup>99m</sup>Tc]Tc-tilmanocept lymphoscintigraphy were marked on the overlying skin.

Subsequently, 10 MBq [<sup>68</sup>Ga]Ga-tilmanocept was peritumorally administered at the same injection spots by the same nuclear medicine physician (B.K.) in the presence of a second observer (R.M.). At 15 min post-injection of [<sup>68</sup>Ga]Ga-tilmanocept, PET/CT was conducted for a total duration of 15 min. Any additionally identified SLNs in proximity of the primary tumor on [<sup>68</sup>Ga]Ga-tilmanocept PET/CT lymphoscintigraphy, that might be subject to the shine-through phenomenon on [<sup>99m</sup>Tc]Tc-tilmanocept lymphoscintigraphy, were marked for surgical extirpation as well on the basis of their anatomical location.

The next day, patients underwent surgical extirpation of the marked SLNs. Intraoperative SLN localization was performed under conventional portable gamma-probe guidance. In this cohort, no superselective neck dissection of cervical lymph node level I was performed in patients with floor-of-mouth tumors [9]. Harvested SLNs were histopathologically assessed using step-serial-sectioning (section thickness 150  $\mu\text{m}$ ) with hematoxylin–eosin and pan-cytokeratin anti-body (AE 1/3) staining [23, 24]. Patients with histopathologically negative SLN(s) were assigned to a wait-and-scan approach. In those with at least one SLN containing metastasis, complementary treatment of the affected and adjacent nodal basins was employed (i.e., neck dissection and/or (chemo)radiotherapy). Complementary neck dissection specimens were histopathologically examined for additional nodal metastases.

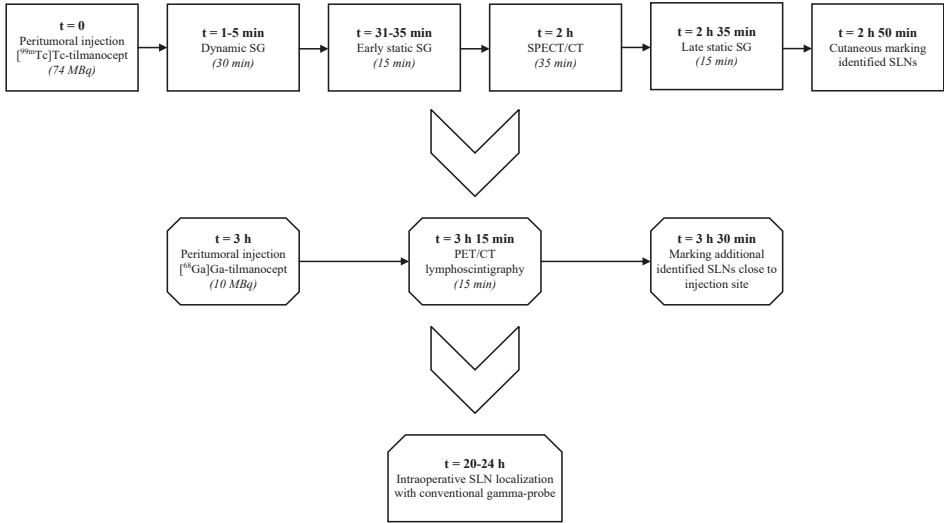


**Figure 1.** Time schedule of study events. MBq, megabecquerel; SG, scintigraphy; SPECT/CT, single photon emission computed tomography/computed tomography; SLN, sentinel lymph node; PET/CT, positron emission tomography/computed tomography.

**Preparation of [99mTc]Tc-tilmanocept and [68Ga]Ga-tilmanocept**

Radiolabeling tilmanocept with <sup>99m</sup>Tc was employed using a kit method (Lymphoseek<sup>®</sup>, Navidea Biopharmaceuticals, Inc). [<sup>99m</sup>Tc]Tc-tilmanocept was prepared according to the manufacturer’s instructions with [<sup>99m</sup>Tc]TcO<sub>4</sub>—eluted from a registered generator (Ultra-Technekow<sup>™</sup> FM, Curium Pharma, Maryland Heights, USA). Radiolabeling was complete after incubation at room temperature for 15 min; [<sup>99m</sup>Tc]Tc-tilmanocept was stable for at least 6 h. The radiolabeling yield exceeded 98%, as determined by instant thin-layer chromatography (ITLC) using ITLC-SG (Agilent Technologies) and acetone as developing solvent. [<sup>99m</sup>Tc]Tc-tilmanocept was prepared with an activity of ~74 MBq in a volume of 0.3–0.4 mL for peritumoral administration.

[<sup>68</sup>Ga]Ga-tilmanocept was prepared using the same Lymphoseek® kit and a registered <sup>68</sup>Ge/<sup>68</sup>Ga-generator (GalliaPharm®, Eckert & Ziegler, Berlin, Germany). In order to reduce the acidity of the generator's eluate, an automatic synthesis module was used (Modular-Lab EAZY®, Eckert & Ziegler, Berlin, Germany). Herewith, <sup>68</sup>Ga pre-purification and concentration was established using the strong cation exchange (SCX) column in a disposable sterile synthesis cassette. The content of the Lymphoseek® kit was dissolved in 3.5 mL 0.8 M acetate buffer (reagent kit for the synthesis of <sup>68</sup>Ga-labeled peptides, Eckert & Ziegler, Berlin, Germany) and introduced in the reaction vial. The automated synthesis was performed at room temperature with a reaction time of 30 min. Apart from radiolabeling yield (> 98%) as determined by ITLC, similar to [<sup>99m</sup>Tc]Tc-tilmanocept but using 0.1 M citrate buffer pH 5.0 as developing solvent, additional quality controls were performed. These included pH value (4–7), endotoxin content (< 17.5 IU/mL) and sterility (0 CFU). [<sup>68</sup>Ga]Ga-tilmanocept was stable for at least 2 h. All batches used for patients were approved by a local hospital pharmacist. Ultimately, a syringe with ~10 MBq [<sup>68</sup>Ga]Ga-tilmanocept in a volume of 0.2–0.3 mL was prepared for peritumoral administration. Following peritumoral administration, the syringe was measured for the amount of remaining radioactivity using a dose calibrator to determine the exact amount of activity administered (Table 2).

**Table 2.** Specifications of [<sup>68</sup>Ga]Ga-tilmanocept administration.

Parameter	<i>n</i> = 10
Mean administered volume in mL (SD)	0.255 (±0.095)
Number of peritumoral injections, <i>n</i> (%)	
3	2 (20%)
4	8 (80%)
Mean administered radioactivity in MBq (SD)	9.3 (±0.7)
Mean time until PET/CT acquisition in minutes (SD)	16.9 (±1.9)
Adverse reactions, <i>n</i> (%)	0 (0%)

mL, milliliter; SD, standard deviation; MBq, megabecquerel; PET/CT, positron emission tomography/computed tomography

### [<sup>99m</sup>Tc]Tc-tilmanocept lymphoscintigraphy

Directly post-injection of [<sup>99m</sup>Tc]Tc-tilmanocept, planar scintigraphic images were acquired in dynamic mode (128 × 128 matrix; 60 frames of 30 s) in anterior–posterior projection, followed by static mode (256 × 256 matrix; 4 min) in anterior–posterior and lateral projections (30 min and 2 h post-injection). Dynamic and static scintigraphic imaging was supplemented with 30 s flood field images. In addition to scintigraphic imaging at 2 h post-injection, SPECT/CT scans were acquired on a 128 × 128 matrix (pixel spacing, 4.8 × 4.8 mm), with 128 angles, 20 s per projection, over a noncircular 360° orbit (CT: 110 kV, 40 mAs eff., 16 × 1.2 mm). Both scintigraphic

and SPECT/CT images were acquired using a Siemens Symbia T16 SPECT/CT scanner with “low and medium energy” (LME) collimators to limit septal penetration and reduce shine-through [25]. SPECT/CT images were reconstructed using clinical reconstruction software (Siemens Flash 3D), with attenuation and scatter correction (6 iterations, 8 subsets, 5 mm Gaussian filter).

### **[<sup>68</sup>Ga]Ga-tilmanocept PET/CT lymphoscintigraphy**

At 15 min post-injection of [<sup>68</sup>Ga]Ga-tilmanocept, PET/CT acquisition was initiated using a Siemens Biograph mCT (TrueV). A 15 min single bed-position acquisition was reconstructed in three consecutive 5 min timeframes and one full 15 min frame (4 iterations, 21 subsets, using time of flight and resolution recovery and a 4 mm FWHM Gaussian filter). A low dose CT scan was acquired for attenuation correction, using CARE kV and CARE Dose4D (120 Ref. kV and 40 Ref. mAs).

### **Evaluation and analyses**

In each patient, corresponding images of both [<sup>99m</sup>Tc]Tc-tilmanocept lymphoscintigraphy (including SPECT/CT) and [<sup>68</sup>Ga]Ga-tilmanocept PET/CT lymphoscintigraphy were evaluated for similarity of depicted draining lymph node basins, number and location of SLNs, and visualization of lymphatic vessels transporting the radiotracer. Identified SLNs by either modality (i.e., [<sup>99m</sup>Tc]Tc-tilmanocept lymphoscintigraphy; [<sup>68</sup>Ga]Ga-tilmanocept PET/CT lymphoscintigraphy) were related to outcomes from histopathological assessment of harvested SLNs and any complementary neck dissection specimens.

In an effort to assess the optimal timing of PET/CT acquisition following [<sup>68</sup>Ga]Ga-tilmanocept injection within the set acquisition time frame (i.e., 15 min initiated 15 min post-injection), quantitative data on the activity of [<sup>68</sup>Ga]Ga-tilmanocept in the injection site was obtained from PET reconstructions for each 5 min timeframe. When corrected for decay, the rate of clearance from the injection site between consecutive intervals should correspond with the degree of lymphatic drainage from the injection site in each timeframe. First, the full 15 min PET reconstruction was used to automatically define a volume of interest (VOI) covering the injection site for every [<sup>68</sup>Ga]Ga-tilmanocept PET/CT study. Images were filtered with a Gaussian (sigma: 4 mm) and subsequently thresholded to 5% of the maximum intensity value in the filtered image. Then, the injection VOI was defined as the connected region which encloses the maximum. The injection VOI was applied to each subsequent 5 min timeframe image independently in order to obtain the activity within the injection site, which is presented as a percentage of total injected activity (corrected for decay) and denoted as  $A_{inj}(t)$ , with  $t = \{15, 20, 25\}$  in minutes post-injection. The total activity within the field-of-view for each 5 min timeframe was determined after

cropping the image, removing 5 slices from the bottom and top in order to remove noise at the edges of the axial field of view (where the sensitivity of the PET scanner is minimal), and is also presented as a percentage of injected activity; denoted  $A_{\text{tot}}(t)$ , with  $t = \{15, 20, 25\}$  in minutes post-injection. Finally, the rate of clearance from the injection site was determined by fitting an exponential function through the three time points, assuming  $A_{\text{inj}}(t) \propto e^{-kt}$ , with  $k$  the percentage of clearance per minute as a proportion of activity residing in the injection site.

Furthermore, quantitative data on activity in SLNs as identified by [ $^{68}\text{Ga}$ ]Ga-tilmanocept PET/CT lymphoscintigraphy were obtained from manually generated VOIs, defined by two observers (D.D.; B.K.) using syngo.via medical imaging software (Siemens Healthineers, Germany, Version 7.2), for the full 15 min [ $^{68}\text{Ga}$ ]Ga-tilmanocept PET/CT study as well as for each individual 5 min timeframe. Similar to outcomes from injection site VOIs, the activity in identified SLNs is presented as a percentage of total injected activity, corrected for decay.

In one patient (patient 8), quantitative data obtained from PET reconstruction was inconsistent, as the total activity of [ $^{68}\text{Ga}$ ]Ga-tilmanocept within both the injection site and field-of-view increased over time according to quantitative PET data and was therefore excluded from the analysis.

All data was analyzed with IBM SPSS Statistics Version 26.0. For categorical variables, the number of cases and percentages are presented. Continuous parametric variables are presented as mean ( $\pm$ SD); nonparametric variables are presented as median. Statistical tests were considered unfeasible, due to the small number of patients included in this pilot study.

## Results

Patient- and tumor characteristics of included patients are listed in Table 1. The oral tongue was the most commonly affected subsite (70%). Tumors were clinically classified as T1 or T2 in the majority of patients (90%). A total of 33 SLNs were surgically extirpated (on average 3 per patient), of which 8 were histopathologically positive for metastasis. These 8 positive SLNs were harvested from 6 patients. Thus, 60% (6 of 10) of our study population was positive for lymphatic metastasis. Most patients staged positive for lymphatic metastases underwent complementary neck dissection (n = 4; 67%).

### **[<sup>68</sup>Ga]Ga-tilmanocept administration**

A mean volume of 0.255 mL ( $\pm$  0.095) [<sup>68</sup>Ga]Ga-tilmanocept, with a mean activity of 9.27 MBq ( $\pm$  0.69), was peritumorally administered in each patient (Table 2). None of the patients experienced any adverse reactions from the administration of [<sup>68</sup>Ga]Ga-tilmanocept. PET/CT acquisition was initiated 16.9 ( $\pm$  1.9) min following peritumoral administration of [<sup>68</sup>Ga]Ga-tilmanocept.

### **Sentinel lymph node identification**

The outcomes of [<sup>99m</sup>Tc]Tc-tilmanocept lymphoscintigraphy and [<sup>68</sup>Ga]Ga-tilmanocept PET/CT lymphoscintigraphy for all included patients are presented in Table 3. A total of 24 SLNs were identified by [<sup>99m</sup>Tc]Tc-tilmanocept lymphoscintigraphy. All SLNs, except for one (patient 10; level III left), as identified by [<sup>99m</sup>Tc]Tc-tilmanocept lymphoscintigraphy were also identified by [<sup>68</sup>Ga]Ga-tilmanocept PET/CT lymphoscintigraphy. A total of 33 SLNs were identified by [<sup>68</sup>Ga]Ga-tilmanocept PET/CT lymphoscintigraphy, of which 30 (91%) were intraoperatively localized under conventional gamma-probe guidance.

[<sup>68</sup>Ga]Ga-tilmanocept PET/CT lymphoscintigraphy was able to identify 4 additional hotspots in the vicinity of the injection site in three patients (patients 3, 6, 9), all of which were considered to be SLNs. On [<sup>99m</sup>Tc]Tc-tilmanocept lymphoscintigraphy, these SLNs were not visualized, owing to the shine-through phenomenon (Figures 2, 3, and 4). Of these 4 additional SLNs close to the injection site, 3 were intraoperatively localized and harvested under conventional gamma-probe guidance. In two patients (patient 3, 6), these additionally harvested SLNs were histopathologically positive for metastasis. In one patient this additional harvested SLN was the only SLN harboring metastasis (patient 6). Due to the accompanying pathological nodal upstaging (pN0(sn)–pN1(sn)), this patient was a candidate for complementary neck treatment rather than a wait-and-scan approach.

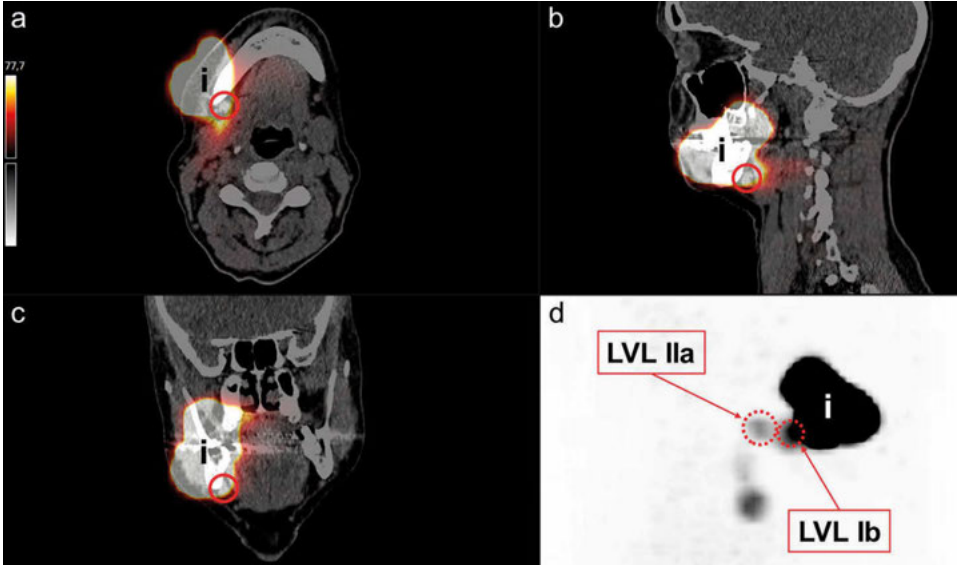


**Figure 2.** Shine-through phenomenon on [<sup>99m</sup>Tc]Tc-tilmanocept SPECT/CT imaging in patient with a cT2N0 vestibule of mouth carcinoma on the right side (*patient 6*). (a-c) Radioactivity residing in the injection site (*i*) covers a lymph node in level Ib of the ipsilateral neck on axial, sagittal and coronal planes (*circle*). (d) Maximum Intensity Projections (MIP) provides an overview of the marked SLNs based on [<sup>99m</sup>Tc]Tc-tilmanocept lymphoscintigraphy in level IIa and Ib of the ipsilateral neck (*dotted circles*). The lymph node covered by the injection site (*circle*), which was located more anterior of the marked SLN in level Ib of the ipsilateral neck (*dotted circle*), was not marked as SLN.

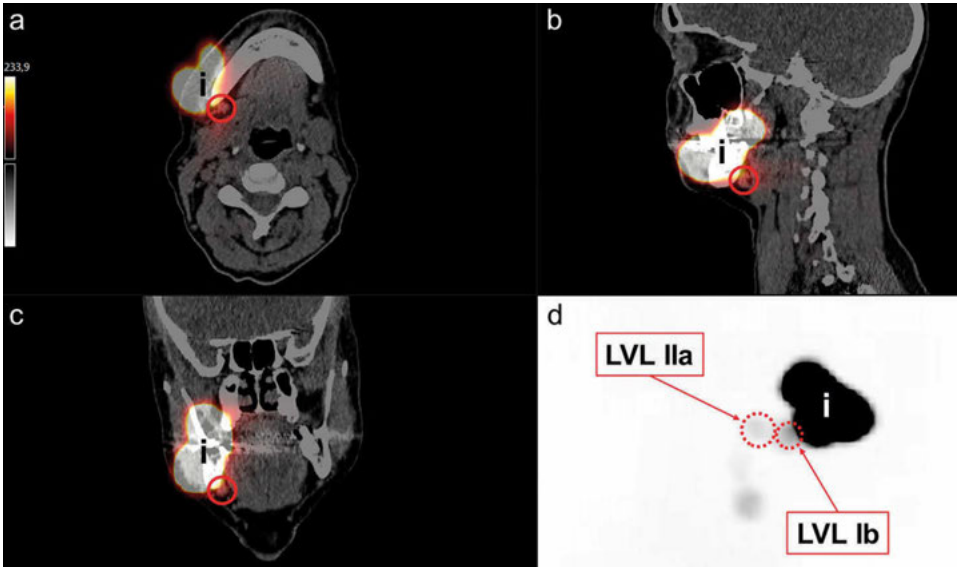


**Figure 3.** (a-c) After adjustment of the radioactivity threshold display settings on SPECT/CT images of the same patient as illustrated in Figure 2 (*patient 6*), no clear radioactive uptake was seen in the lymph node in level Ib of the ipsilateral neck that is subject to the shine-through phenomenon (*circle*). (d) Maximum Intensity Projections (MIP) did not reveal

any additional hotspots in vicinity of the injection site (*i*) following radioactivity threshold adjustment. Consequently, this lymph node was not considered a SLN based on [<sup>99m</sup>Tc]Tc-tilmanocept lymphoscintigraphy.

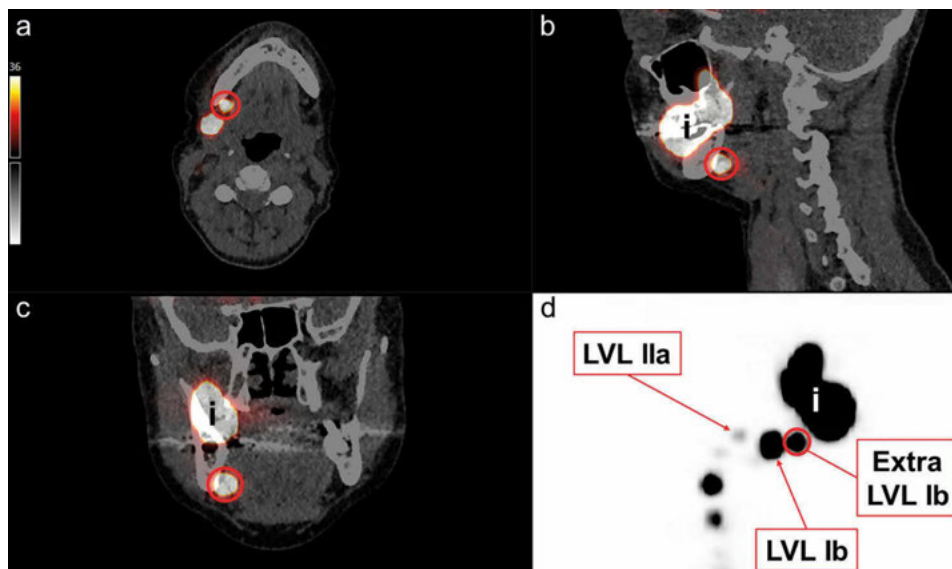


**Figure 4.** [<sup>68</sup>Ga]Ga-tilmanocept PET/CT lymphoscintigraphic images of the same patient as illustrated in Figures 2 and 3 (*patient 6*). (a-c) PET/CT lymphoscintigraphy shows evident radioactive uptake in a lymph node in level Ib of the ipsilateral neck (*circle*), located anterior of the already marked SLN in level Ib (*d; arrow*). Following comparison with [<sup>99m</sup>Tc]Tc-tilmanocept lymphoscintigraphy, it became apparent that this hotspot corresponded with the lymph node that was subject to the shine-through phenomenon on [<sup>99m</sup>Tc]Tc-tilmanocept lymphoscintigraphy. Owing to its evident radioactive uptake on [<sup>68</sup>Ga]Ga-tilmanocept PET/CT lymphoscintigraphy, this lymph node was considered an additional SLN. Intraoperatively, three SLNs were harvested (i.e., 2 × level Ib, level IIa), of which the most anteriorly located SLN in level Ib, which was only identified on [<sup>68</sup>Ga]Ga-tilmanocept PET/CT lymphoscintigraphy, was histopathologically positive for metastasis.

Furthermore, [<sup>68</sup>Ga]Ga-tilmanocept PET/CT lymphoscintigraphy showed that 4 hotspots on [<sup>99m</sup>Tc]Tc-tilmanocept lymphoscintigraphy, which were marked as SLN, actually consisted of multiple hotspots (patients 1, 3, 4, 5; Figure 5). These additional hotspots, which were covered by an all-embracing marked hotspot on [<sup>99m</sup>Tc]Tc-tilmanocept lymphoscintigraphy were designated as SLN as well.

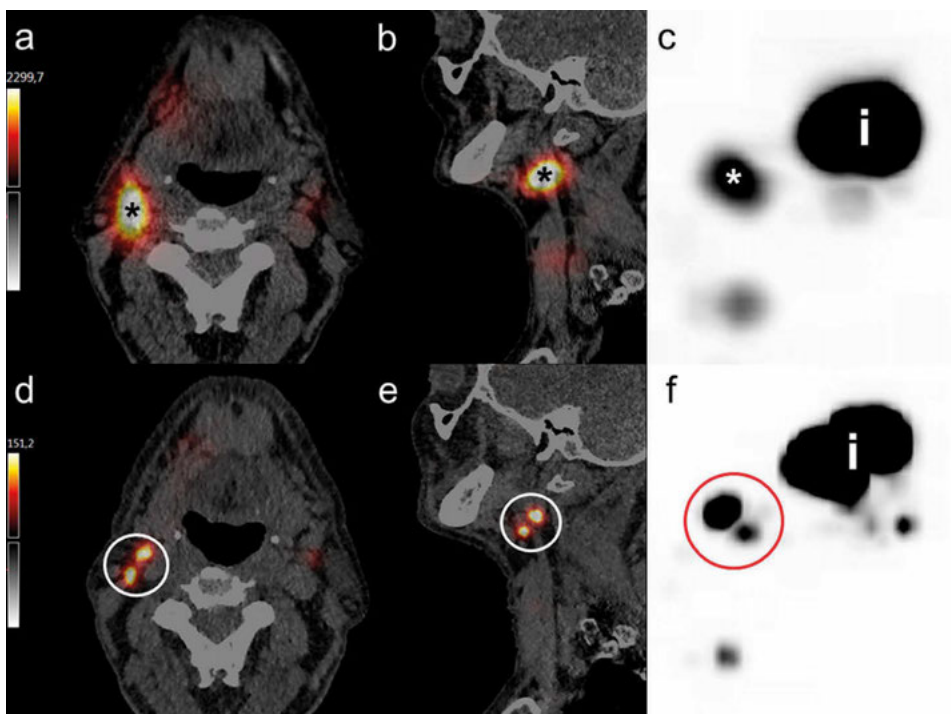


**Figure 5.** (a-c) Hotspot on [<sup>99m</sup>Tc]Tc-tilmanocept SPECT/CT (asterisk), (d-f) consisting of multiple hotspots on [<sup>68</sup>Ga]Ga-tilmanocept PET/CT lymphoscintigraphy (circle). i, injection site.

When comparing the individual 5 min timeframe images of [<sup>68</sup>Ga]Ga-tilmanocept PET/CT lymphoscintigraphy in each patient, no difference was seen in depicted hotspots between each timeframe. The median radioactive uptake of <sup>68</sup>Ga in SLNs detected by [<sup>68</sup>Ga]Ga-tilmanocept PET/CT lymphoscintigraphy was 12.55 kBq (range 0.06–245.48 kBq) for the full PET/CT study, corresponding with 0.12% of the injected activity (range  $8 \times 10^{-4}$ –3.04%; Table 3). Data on uptake of [<sup>68</sup>Ga]Ga-tilmanocept in SLNs for each individual timeframe is presented in Supplementary Table 1.

**Table 3.** Comparison of sentinel lymph node distribution between [<sup>68</sup>Ga]Ga-tilmanocept PET/CT lymphoscintigraphy and [<sup>99m</sup>Tc]Tc-tilmanocept lymphoscintigraphy.

N°	Primary tumor	Identified SLNs PET/CT	Activity identified SLNs PET/CT in kBq (%)	Identified SLNs SG & SPECT/CT	Harvested SLNs (cps)	PA	Comp. treatment	Add. meta in CND	Upstaging due to PET/CT
1	Tongue (right)	Ib	Right	Ib	Right (376)	-	MRND	None	No
		Ia	Right	Ia	Right (1186)	-	I-IV right		
		Ia	Right	III	Right (306)	+			
		Ia	Right	Ia	Right (386)	-			
		III	Right	III	Right (784)	-			
2	Tongue (left)	Ia	Left	Ia	Left (426)	-	RT I-V left	N.A.	No
		Ib	Right	Ib	Right (1038)	+	MRND	None	No
3	Tongue (right)	Ib	Right	Ia	Right (208)	+	I-V right, SSND		
		Ia	Right	Ia	Right (769)	+	Ib left		
		Ia	Right	Ia	Right (250)	-			
		Ib	Right	Ib	Right (92)	-	N.A.	N.A.	No
4	Tongue (right)	Ia	Right	Ia	Right (560)	-			
		Ia	Right	Ia	Right (406)	-			
		IV	Right	IV	Right (546)	-			
		Ia	Left	Ia	Left (62)	-			
		Ia	Left	Ia	Left (846)	+	MRND	None	No
		Ib	Left	III	Left (208)	-	I-V left		
		III	Left	Ib	Left (249)	-			
5	Tongue (left)	III	Left	III	Left (148)	-			
		Ib	Right	Ib	Right (63)	-			
		Ia	Left	Ia	Left (846)	+	MRND	None	No
		Ib	Left	III	Left (208)	-	I-V left		

Table 3. Continued.

N <sup>o</sup>	Primary tumor	Identified SLNs PET/CT	Activity identified SLNs PET/CT in kBq (%)	Identified SLNs SG & SPECT/CT	Harvested SLNs (cps)	PA	Comp. treatment	Add. meta in CND	Upstaging due to PET/CT
6	Lower gum (right)	Ib Right	44.9 (0.42)	Ib Right	Right (175)	-	CH-RT	N.A.	Yes (NO - NI)
		Ib Right	13.1 (0.12)	Ila Right	Right (126)	+	I-III right		
		Ila Right	12.8 (0.12)	Ila	Right (86)	-			
7	Tongue (left)	Ila Left	245.5 (3.04)	Ila Left	Left (1568)	-	N.A.	N.A.	No
		III Left	16.0 (0.20)	III Left	Left (480)	-			
8	Tongue (left)	Ila Left	N.A.	Ila Left	Left (1159)	-	N.A.	N.A.	No
		III Left	N.A.	III Left	Left (1741)	-			
9	FOM (midline)	Ib Right	3.8 (0.04)	IV Right	Right (64)	-	MRND	None	No
		Ib Right	11.3 (0.13)	Ila Left	Right (392)	-	I-IV left		
		IV Right	4.6 (0.05)	III Left	Left (176)	+			
		Ila Left	3.7 (0.04)						
		III Left	1.6 (0.02)						
10	Lower gum (left)	Ib Left	4.1 (0.05)	Ib Left	Left (355)	-	N.A.	N.A.	No
				III Left	Left (100)	-			
					Left (62)	-			

N<sup>o</sup>: patient number; SLN, sentinel lymph node; PET/CT, positron emission tomography/computed tomography; kBq, kilobecquerel; %, percentage of injected activity corrected for decay; SG, scintigraphy; SPECT/CT, single photon emission computed tomography/computed tomography; PA, pathological assessment; Comp., complementary; Add., additional; meta, metastasis; CND, complementary neck dissection; +, histopathologically positive for metastasis; -, histopathologically negative for metastasis; MRND, modified radical neck dissection; RT, radiotherapy; N.A., not applicable; SSND, superselective neck dissection; CH-RT, chemo-radiation; FOM, floor-of-mouth.

\*Additional metastatic SLN harvested based on information obtained from [<sup>68</sup>Ga]Ga-tilmanocept PET/CT lymphoscintigraphy.

## Identification of lymphatic vessels transporting the radiotracer

[<sup>99m</sup>Tc]Tc-tilmanocept lymphoscintigraphy visualized draining lymphatic vessels in 2 patients (patients 3, 5; 20%) on early dynamic and static scintigraphic imaging (0–45 min post-injection).

Lymphatic vessels transporting [<sup>68</sup>Ga]Ga-tilmanocept were identified by PET/CT lymphoscintigraphy in 8 patients (patients 1–8; 80%) (Figure 6). On [<sup>68</sup>Ga]Ga-tilmanocept PET/CT lymphoscintigraphy a relatively high activity was seen in draining lymphatic vessels, which was not quantitatively analyzed. No difference was seen in the number and intensity of draining lymphatic vessels between each 5 min PET/CT acquisition timeframe.

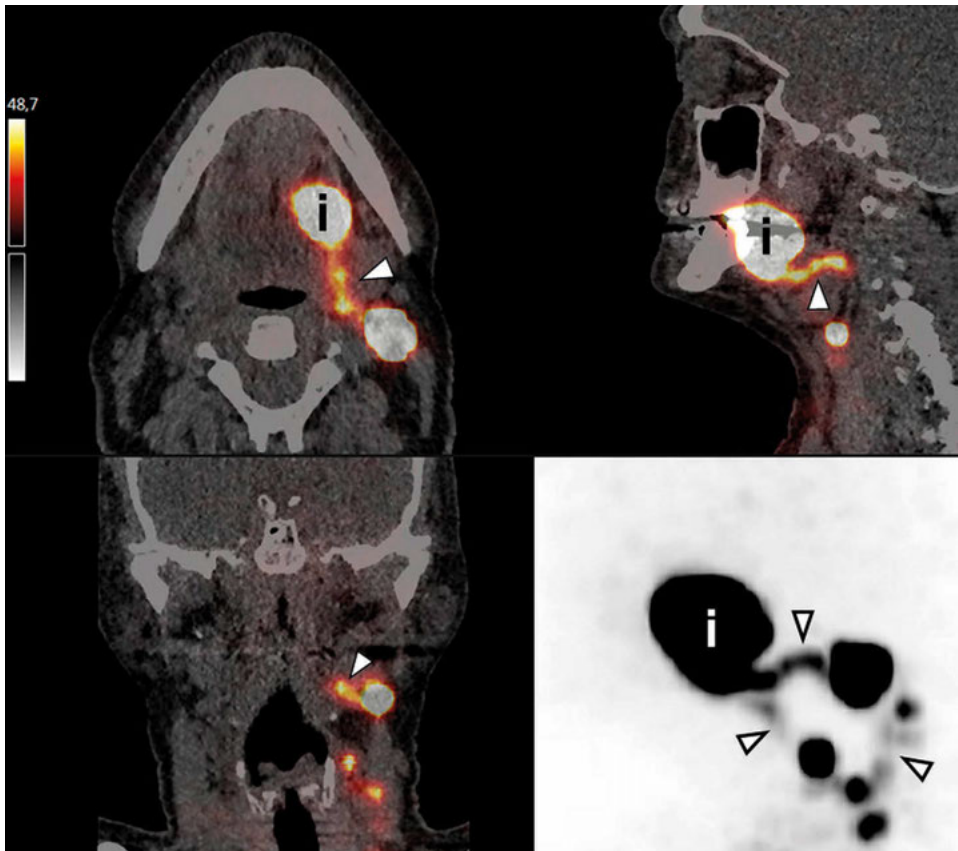


**Figure 6.** Visualization of lymphatic vessels transporting [<sup>68</sup>Ga]Ga-tilmanocept on PET/CT lymphoscintigraphy (arrowheads). i, injection site.

### Clearance of [<sup>68</sup>Ga]Ga-tilmanocept from the injection site over time

Figure 7 displays the activity of [<sup>68</sup>Ga]Ga-tilmanocept residing in the injection site of each patient, as a percentage of total injected activity and corrected for decay, for the 5 min acquisition timeframes (initiated at 15 min, 20 min, and 25 min post-injection).

At 15 min post-injection, on average, 64.2% ( $\pm 10.7$ ) of the total injected activity [<sup>68</sup>Ga]Ga-tilmanocept was detected within the field-of-view; 59.6% ( $\pm 11.2$ ) resided in the injection site. At 20 and 25 min post-injection, 62.9% ( $\pm 10.6$ ) and 61.5% (SD  $\pm 10.6$ ) was observed within the field-of-view, while 58.3% ( $\pm 11.2$ ) and 56.9% ( $\pm 11.0$ ) remained in the injection site, respectively.

The average clearance of [<sup>68</sup>Ga]Ga-tilmanocept from the injection site between 15 and 25 min post-injection was  $0.48\% \text{ min}^{-1}$  ( $\pm 0.08$ ).

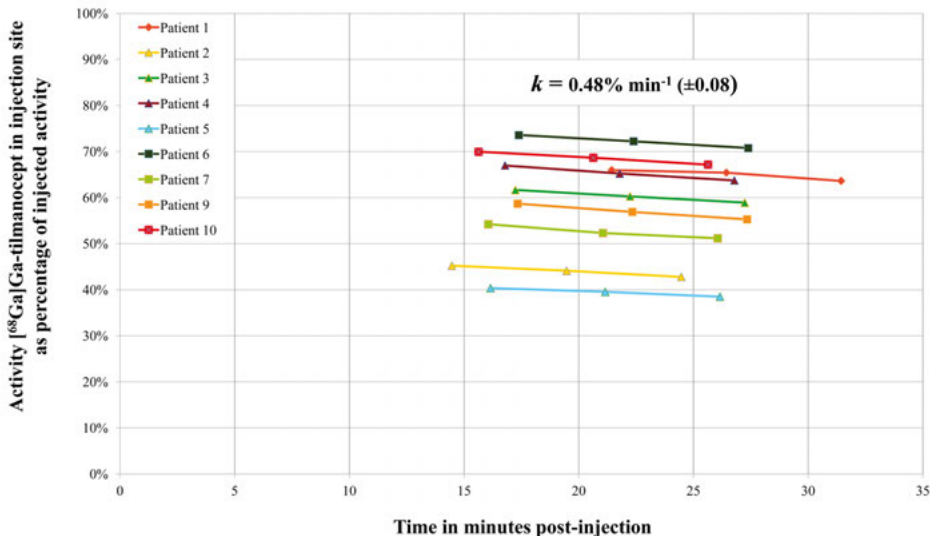


**Figure 7.** Activity of [<sup>68</sup>Ga]Ga-tilmanocept residing in the injection site of each patient, as percentage of total injected activity (corrected for decay), for each 5 minute acquisition timeframe ( $t = \{15, 20, 25\}$  in minutes post-injection).  $k$ , average clearance, as proportion of activity residing in the injection site, for the full PET/CT study;  $\text{min}^{-1}$ , per minute.

## Discussion

This is the first in-human series concerning SLN mapping by [ $^{68}\text{Ga}$ ]Ga-tilmanocept PET/CT lymphoscintigraphy. The results of this study demonstrated that, when compared to conventional lymphoscintigraphy using [ $^{99\text{m}}\text{Tc}$ ]Tc-tilmanocept, [ $^{68}\text{Ga}$ ]Ga-tilmanocept PET/CT lymphoscintigraphy provides more accurate identification of SLNs; especially those located close to the injection site. In our population, [ $^{68}\text{Ga}$ ]Ga-tilmanocept PET/CT lymphoscintigraphy visualized nearly all SLNs as identified by [ $^{99\text{m}}\text{Tc}$ ]Tc-tilmanocept lymphoscintigraphy and depicted four additional SLNs in the vicinity of the injection site. Two of these additional SLNs harbored metastasis. In one of these patients (patient 6), the additionally harvested SLN was the only histopathologically positive SLN. This patient would have been erroneously staged negative for nodal metastasis by [ $^{99\text{m}}\text{Tc}$ ]Tc-tilmanocept lymphoscintigraphy, potentially compromising the patient's prognosis [1, 11].

In 80% of our population, lymphatic vessels transporting [ $^{68}\text{Ga}$ ]Ga-tilmanocept were visualized by PET/CT lymphoscintigraphy. Besides, [ $^{68}\text{Ga}$ ]Ga-tilmanocept PET/CT lymphoscintigraphy showed that some hotspots on [ $^{99\text{m}}\text{Tc}$ ]Tc-tilmanocept lymphoscintigraphy actually covered several neighboring lymph nodes with radioactive uptake. These attributes, provided by the superior resolution of [ $^{68}\text{Ga}$ ]Ga-tilmanocept PET/CT lymphoscintigraphy, may assist in distinguishing hotspots as either actual SLN or insignificant HENs, which ought to further contribute to both the accuracy as well as the minimally invasive character of SLNB [13, 26, 27].

Owing to its short half-life of 68 min, [ $^{68}\text{Ga}$ ]Ga-tilmanocept does not interfere with gamma-radiation from  $^{99\text{m}}\text{Tc}$ -labeled radiotracers necessary for intraoperative SLN localization by conventional gamma-probe guidance, when using a 2-day protocol. The findings of the present study substantiate this theory, as the vast majority of SLNs identified by [ $^{68}\text{Ga}$ ]Ga-tilmanocept PET/CT lymphoscintigraphy were intraoperatively localized using a conventional gamma-probe (91%); even most of those near the injection site that were not visualized by [ $^{99\text{m}}\text{Tc}$ ]Tc-tilmanocept lymphoscintigraphy. Because of the dual-isotope approach in this study, a 2-day protocol is necessary to make sure that  $^{68}\text{Ga}$  has been decayed sufficiently and therefore does not interfere with the detection of  $^{99\text{m}}\text{Tc}$  using a conventional gamma-probe. For a 1-day protocol, a possible solution might be direct detection of positrons using sensitive compact  $\beta$ -probes that are emerging as a solution to detect PET tracers. However, the limited tissue penetration of positrons (1–3 mm) might complicate effective intraoperative SLN localization using this probe and may require greater amounts of administered activity, more extensive neck exploration and longer probing time [28].

Another important advantage of [ $^{68}\text{Ga}$ ]Ga-tilmanocept PET/CT lymphoscintigraphy over conventional lymphoscintigraphy using  $^{99\text{m}}\text{Tc}$ -labeled radiotracers is the potential to significantly decrease scan acquisition times for SLN mapping due to superior resolution and detection efficiency of PET compared to SPECT [29]. [ $^{68}\text{Ga}$ ]Ga-tilmanocept PET/CT lymphoscintigraphy provided more accurate SLN visualization with only 15 min of acquisition, opposed to the 92 min of acquisition required for [ $^{99\text{m}}\text{Tc}$ ]Tc-tilmanocept lymphoscintigraphy. Moreover, [ $^{68}\text{Ga}$ ]Ga-tilmanocept PET/CT lymphoscintigraphy acquisition times may even be further reduced, as no difference was seen in depicted hotspots, nor in the visualization of lymphatic vessels, between each 5 min timeframe. Since the overall clearance of [ $^{68}\text{Ga}$ ]Ga-tilmanocept from the injection site was relatively small during the 15 min time interval within which PET/CT lymphoscintigraphy was acquired (average clearance rate:  $0.48\% \text{ min}^{-1}$ ) and the absolute clearance rates between the 5 min timeframes proved to be similar (1.3% and 1.4%, respectively), the exact onset of acquisition within the set acquisition timeframe (i.e., 15–25 min post-injection) appears to be of little consequence. Accordingly, acquisition times for [ $^{68}\text{Ga}$ ]Ga-tilmanocept PET/CT lymphoscintigraphy may be reduced to 5 min, initiated between 15 and 25 min post-injection.

Still, as a result of relatively high activity in lymphatic vessels in this particular time frame, it proved challenging in some cases to differentiate between activity in lymphatic vessels and radioactive uptake in (sentinel) lymph nodes on [ $^{68}\text{Ga}$ ]Ga-tilmanocept PET/CT lymphoscintigraphy. Furthermore, in tumors featuring slow or limited lymphatic drainage (e.g., lower gum, retromolar area, buccal mucosa), lymphoscintigraphic imaging acquired at 15–30 min post-injection might be inadequate [12]. Specifically, in one patient (patient 10; lower gum) the SLN in level III, as determined by [ $^{99\text{m}}\text{Tc}$ ]Tc-tilmanocept SPECT/CT (acquired  $\sim 2$  h post-injection), was not depicted by [ $^{68}\text{Ga}$ ]Ga-tilmanocept PET/CT lymphoscintigraphy. This illustrates that in some patients more time is required for the radiotracer to accumulate in SLNs. Both these issues addressed may be resolved by acquiring an additional late PET/CT lymphoscintigram. The additional value of late PET/CT lymphoscintigraphic acquisition at 1 h post-injection is currently under investigation in a sequel study.

Limitations of this study include its small population size and lack of follow-up data. Secondly, as this study was designed to compare PET/CT lymphoscintigraphy with conventional lymphoscintigraphy, [ $^{99\text{m}}\text{Tc}$ ]Tc-tilmanocept and [ $^{68}\text{Ga}$ ]Ga-tilmanocept had to be administered sequentially, rather than concomitantly as a single agent, to avoid interference of  $^{68}\text{Ga}$  with conventional lymphoscintigraphic imaging. Resulting from the inherent risk of inter-injection variability, differences in depicted lymphatic drainage patterns between [ $^{99\text{m}}\text{Tc}$ ]Tc-tilmanocept lymphoscintigraphy and [ $^{68}\text{Ga}$ ]Ga-

tilmanocept PET/CT lymphoscintigraphy may occur. Besides, a substantial proportion of the injected dosage [<sup>68</sup>Ga]Ga-tilmanocept was not detected within the field-of-view at the time of PET/CT acquisition (36–39%), which could be explained by clearance from procedural rinsing of the oral cavity and unintentional swallowing after peritumoral [<sup>68</sup>Ga]Ga-tilmanocept injection [26]. Moreover, although the clearance rate from the injection site should correlate with the degree of lymphatic drainage, it is worth noting that the small molecular diameter of tilmanocept (7 nm) facilitates diffusion into blood capillaries as well [10, 30]. Therefore, it is uncertain to what degree the clearance rate from the injection site corresponds with the exact clearance by lymphatic drainage.

Subsequent studies should be aimed at assessing the diagnostic accuracy of [<sup>68</sup>Ga]Ga-tilmanocept PET/CT lymphoscintigraphy for SLN mapping in a larger population, with sufficient follow-up time for false-negative SLNB outcomes to become clinically manifest (i.e., ≥ 24 months) [31, 32]. In addition, the reliability of IRD-800CW-<sup>68</sup>Ga]Ga-<sup>99m</sup>Tc]Tc-tilmanocept as a single agent for SLN mapping in early-stage OSCC should be evaluated, as it may diminish inter-injection variability and allow for high-resolution pre-operative PET/CT lymphoscintigraphic imaging and intraoperative SLN localization under conventional gamma-probe and fluorescence imaging guidance [18].

In conclusion, our results suggest that [<sup>68</sup>Ga]Ga-tilmanocept PET/CT lymphoscintigraphy provides more accurate identification of SLNs, improved visualization of lymphatic vessels and considerably shorter acquisition times compared to [<sup>99m</sup>Tc]Tc-tilmanocept lymphoscintigraphy in early-stage OSCC patients. Furthermore, [<sup>68</sup>Ga]Ga-tilmanocept PET/CT lymphoscintigraphy can be combined with [<sup>99m</sup>Tc]Tc-tilmanocept for reliable intraoperative SLN localization using the conventional portable gamma-probe.

## References

1. d'Cruz AK, Vaish R, Kapre N, et al. Elective versus therapeutic neck dissection in node-negative oral cancer. *N Engl J Med*. 2015;373(6):521-529. doi:10.1056/NEJMoa1506007
2. de Bree R, de Keizer B, Civantos FJ, et al. What is the role of sentinel lymph node biopsy in the management of oral cancer in 2020? *Eur Arch Otorhinolaryngol*. 2021;278(9):3181-3191. doi:10.1007/s00405-020-06538-y
3. Garrel R, Poissonnet G, Moyà Plana A, et al. Equivalence randomized trial to compare treatment on the basis of sentinel node biopsy versus neck node dissection in operable T1-T2N0 oral and oropharyngeal cancer. *J Clin Oncol*. 2020;38(34):4010-4018. doi:10.1200/JCO.20.01661
4. den Toom IJ, Boeve K, Lobeek D, et al. Elective neck dissection or sentinel lymph node biopsy in early stage oral cavity cancer patients: the Dutch experience. *Cancers (Basel)*. 2020;12(7):1783. doi:10.3390/cancers12071783
5. Murer K, Huber GF, Haile SR, Stoeckli SJ. Comparison of morbidity between sentinel node biopsy and elective neck dissection for treatment of the n0 neck in patients with oral squamous cell carcinoma. *Head Neck*. 2011;33(9):1260-1264. doi:10.1002/hed.21622
6. Mahieu R, de Maar JS, Nieuwenhuis ER, et al. New developments in imaging for sentinel lymph node biopsy in early-stage oral cavity squamous cell carcinoma. *Cancers (Basel)*. 2020;12(10):3055. doi:10.3390/cancers12103055
7. Alkureishi LW, Ross GL, Shoaib T, et al. Sentinel node biopsy in head and neck squamous cell cancer: 5-year follow-up of a European multicenter trial. *Ann Surg Oncol*. 2010;17(9):2459-2464. doi:10.1245/s10434-010-1111-3
8. Pedersen NJ, Jensen DH, Hedbäck N, et al. Staging of early lymph node metastases with the sentinel lymph node technique and predictive factors in T1/T2 oral cavity cancer: A retrospective single-center study. *Head Neck*. 2016;38 Suppl 1:E1033-E1040. doi:10.1002/hed.24153
9. Stoeckli SJ, Huebner T, Huber GF, Broglie MA. Technique for reliable sentinel node biopsy in squamous cell carcinomas of the floor of mouth. *Head Neck*. 2016;38(9):1367-1372. doi:10.1002/hed.24440
10. den Toom IJ, Mahieu R, van Rooij R, et al. Sentinel lymph node detection in oral cancer: a within-patient comparison between [<sup>99m</sup>Tc]Tc-tilmanocept and [<sup>99m</sup>Tc]Tc-nanocolloid. *Eur J Nucl Med Mol Imaging*. 2021;48(3):851-858. doi:10.1007/s00259-020-04984-8
11. Flach GB, Tenhagen M, de Bree R, et al. Outcome of patients with early stage oral cancer managed by an observation strategy towards the N0 neck using ultrasound guided fine needle aspiration cytology: No survival difference as compared to elective neck dissection. *Oral Oncol*. 2013;49(2):157-164. doi:10.1016/j.oraloncology.2012.08.006
12. Heuveling DA, Flach GB, van Schie A, et al. Visualization of the sentinel node in early-stage oral cancer: limited value of late static lymphoscintigraphy. *Nucl Med Commun*. 2012;33(10):1065-1069. doi:10.1097/MNM.0b013e3283571089
13. Heuveling DA, van Schie A, Vugts DJ, et al. Pilot study on the feasibility of PET/CT lymphoscintigraphy with <sup>89</sup>Zr-nanocolloidal albumin for sentinel node identification in oral cancer patients. *J Nucl Med*. 2013;54(4):585-589. doi:10.2967/jnumed.112.115188
14. Heuveling DA, Karagozoglu KH, Van Lingen A, Hoekstra OS, Van Dongen GAMS, De Bree R. Feasibility of intraoperative detection of sentinel lymph nodes with 89-zirconium-labelled nanocolloidal albumin PET-CT and a handheld high-energy gamma probe. *EJNMMI Res*. 2018;8(1):15. doi:10.1186/s13550-018-0368-6
15. Kasbollah A, Eu P, Cowell S, Deb P. Review on production of <sup>89</sup>Zr in a medical cyclotron for PET radiopharmaceuticals. *J Nucl Med Technol*. 2013;41(1):35-41. doi:10.2967/jnmt.112.111377
16. Stroup SP, Kane CJ, Farchshchi-Heydari S, et al. Preoperative sentinel lymph node mapping of the prostate using PET/CT fusion imaging and Ga-68-labeled tilmanocept in an animal model. *Clin Exp Metastasis*. 2012;29(7):673-680. doi:10.1007/s10585-012-9498-9
17. Lee HJ, Barback CV, Hoh CK, et al. Fluorescence-based molecular imaging of porcine urinary bladder sentinel lymph nodes. *J Nucl Med*. 2017;58(4):547-553. doi:10.2967/jnumed.116.178582
18. Qin Z, Hoh CK, Hall DJ, Vera DR. A tri-modal molecular imaging agent for sentinel lymph node mapping. *Nucl Med Biol*. 2015;42(12):917-922. doi:10.1016/j.nuclmedbio.2015.07.011

19. Anderson KM, Barback CV, Qin Z, et al. Molecular imaging of endometrial sentinel lymph nodes utilizing fluorescent-labeled Tilmanocept during robotic-assisted surgery in a porcine model. *PLoS One*. 2018;13(7):e0197842. doi:10.1371/journal.pone.0197842
20. Amin MB, Greene FL, Edge SB, et al. The Eighth Edition AJCC Cancer Staging Manual: Continuing to build a bridge from a population-based to a more “personalized” approach to cancer staging. *CA Cancer J Clin*. 2017;67(2):93-99. doi:10.3322/caac.21388
21. Brierley JD, Gospodarowicz M, Wittekind C. UICC TNM Classification of Malignant Tumours. 8<sup>th</sup> ed. Chichester, United Kingdom: Wiley; 2017.
22. International Consortium for Outcome Research (ICOR) in Head and Neck Cancer, Ebrahimi A, Gil Z, et al. Primary tumor staging for oral cancer and a proposed modification incorporating depth of invasion: an international multicenter retrospective study. *JAMA Otolaryngol Head Neck Surg*. 2014;140(12):1138-1148. doi:10.1001/jamaoto.2014.1548
23. Alkureishi LW, Burak Z, Alvarez JA, et al. Joint practice guidelines for radionuclide lymphoscintigraphy for sentinel node localization in oral/oropharyngeal squamous cell carcinoma. *Ann Surg Oncol*. 2009;16(11):3190-3210. doi:10.1245/s10434-009-0726-8
24. Dhawan I, Sandhu SV, Bhandari R, Sood N, Bhullar RK, Sethi N. Detection of cervical lymph node micrometastasis and isolated tumor cells in oral squamous cell carcinoma using immunohistochemistry and serial sectioning. *J Oral Maxillofac Pathol*. 2016;20(3):436-444. doi:10.4103/0973-029X.190946
25. Yoneyama H, Tsushima H, Kobayashi M, Onoguchi M, Nakajima K, Kinuya S. Improved detection of sentinel lymph nodes in SPECT/CT images acquired using a low- to medium-energy general-purpose collimator. *Clin Nucl Med*. 2014;39(1):e1-e6. doi:10.1097/RLU.0b013e31828da362
26. Giammarile F, Schilling C, Gnanasegaran G, et al. The EANM practical guidelines for sentinel lymph node localisation in oral cavity squamous cell carcinoma. *Eur J Nucl Med Mol Imaging*. 2019;46(3):623-637. doi:10.1007/s00259-018-4235-5
27. Flach GB, van Schie A, Witte BI, et al. Practice variation in defining sentinel lymph nodes on lymphoscintigrams in oral cancer patients. *Eur J Nucl Med Mol Imaging*. 2014;41(12):2249-2256. doi:10.1007/s00259-014-2843-2
28. Collamati F, Bocci V, Castellucci P, et al. Radioguided surgery with  $\beta$  radiation: a novel application with Ga<sup>68</sup>. *Sci Rep*. 2018;8(1):16171. doi:10.1038/s41598-018-34626-x
29. Hicks RJ, Hofman MS. Is there still a role for SPECT-CT in oncology in the PET-CT era? *Nat Rev Clin Oncol*. 2012;9(12):712-720. doi:10.1038/nrclinonc.2012.188
30. Ellner SJ, Hoh CK, Vera DR, Darrah DD, Schulteis G, Wallace AM. Dose-dependent biodistribution of [<sup>99m</sup>Tc]DTPA-mannosyl-dextran for breast cancer sentinel lymph node mapping. *Nucl Med Biol*. 2003;30(8):805-810. doi:10.1016/j.nucmedbio.2003.10.001
31. Flach GB, Tenhagen M, de Bree R, et al. Outcome of patients with early stage oral cancer managed by an observation strategy towards the N0 neck using ultrasound guided fine needle aspiration cytology: No survival difference as compared to elective neck dissection. *Oral Oncol*. 2013;49(2):157-164. doi:10.1016/j.oraloncology.2012.08.006
32. Brands MT, Smeekens EAJ, Takes RP, et al. Time patterns of recurrence and second primary tumors in a large cohort of patients treated for oral cavity cancer. *Cancer Med*. 2019;8(12):5810-5819. doi:10.1002/cam4.2124



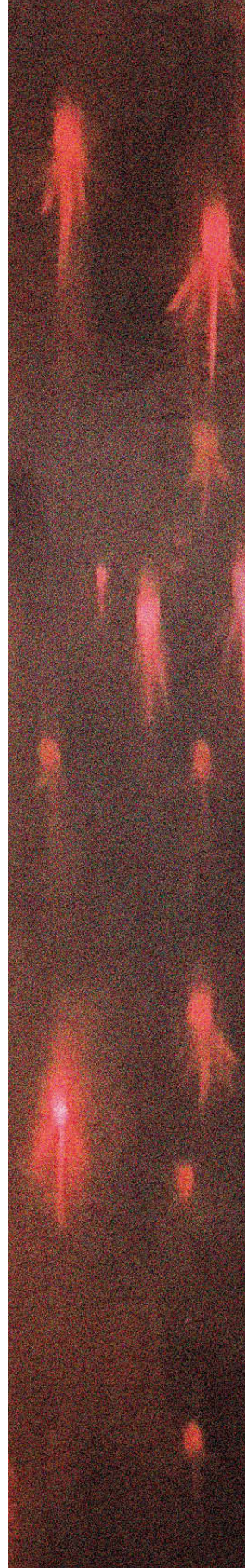
# 11

## [<sup>68</sup>Ga]Ga-tilmanocept PET/CT lymphoscintigraphy: a novel technique for sentinel lymph node imaging

---

Rutger Mahieu, Gerard C. Krijger, F.F. Tessa Ververs,  
Remmert de Roos, Remco de Bree, Bart de Keizer.

*Eur J Nucl Med Mol Imaging. 2021 Apr;48(4):963-965 – Editorial*



Sentinel lymph node biopsy (SLNB) has been implemented in most Dutch Head and Neck Cancer institutions as a standard oncological care for staging the clinically negative neck in early-stage (cT1/2N0) oral squamous cell carcinoma (OSCC) [1]. As SLNB has shown to accurately stage the clinically negative neck in these patients, with a pooled sensitivity of 87% and negative predictive value of 94%, SLNB offers a reliable, less invasive alternative for elective neck dissection with overall lower morbidity rates, better quality-of-life, and lower healthcare costs [1–10].

Nevertheless, SLNB with conventional peritumorally administered  $^{99m}\text{Tc}$ -labeled radiotracers has its predicaments in OSCC, arising from the limited resolution of conventional scintigraphy and SPECT/CT imaging. Especially in cases where sentinel lymph nodes (SLNs) are located in proximity of the primary tumor, the activity residing at the radiotracer injection site can conceal these adjacent SLNs and impede distinction between SLN and injection site. This so-called shine-through phenomenon is notably manifest in floor-of-mouth OSCC, resulting in a significant lower accuracy of SLNB in floor-of-mouth tumors (sensitivity 63%; NPV 90%) compared to other OSCC subsites (sensitivity 86%; NPV 95%) [1]. Such decline in diagnostic accuracy increases the risk of neglecting occult lymph node metastasis that will inevitably develop into clinical manifestation of disease and consequently induce a poor oncological prognosis [11, 12].

Furthermore, on conventional scintigraphy and SPECT/CT imaging, distinguishing hotspots as either real SLN or higher echelon node (HEN) can pose a challenge. Consequently, in clinical practice, presumably an excessive amount of lymph nodes is harvested, as some will actually represent HENs. Extirpation of HENs may lead to unnecessary morbidity and risk of complications and may even hamper a complementary surgical treatment in case of metastatic involvement of SLNs [13]. In this issue of the *European Journal of Nuclear Medicine and Molecular Imaging*, we present a promising novel imaging technique that may solve the clinical issues addressed: [ $^{68}\text{Ga}$ ]Ga-tilmanocept PET/CT lymphoscintigraphy [14]. The superior spatial resolution of PET/CT lymphoscintigraphy, when compared to SPECT/CT using  $^{99m}\text{Tc}$ -labeled radiotracers, enables identification of SLNs located close to the radiotracer injection site and improves anatomic localization of SLNs, which is of particular importance in the complex anatomy of the neck and its abundant lymph nodes. Hence, PET/CT lymphoscintigraphy using [ $^{68}\text{Ga}$ ]Ga-tilmanocept might lead to a reduction of false-negative SLNB outcomes by diminishing the shine-through phenomenon. In addition, its high temporal resolution and ability to visualize lymphatic vessels could improve differentiation between true SLNs and HENs, thereby decreasing unnecessary HEN extirpation and reducing the risk of surgical complications and morbidity [14, 15].

Further merits of [ $^{68}\text{Ga}$ ]Ga-tilmanocept PET/CT lymphoscintigraphy, relative to SPECT/CT with [ $^{99\text{m}}\text{Tc}$ ]Tc-radiotracers, include its potential to considerably shorten acquisition time with similar signal-to-noise ratios, as well as the concomitant opportunities provided by using a tri-modal agent (IRD-800CW-[ $^{68}\text{Ga}$ ]Ga-[ $^{99\text{m}}\text{Tc}$ ]Tc-tilmanocept) [16–19]. This tri-modal agent should facilitate high-resolution PET/CT lymphoscintigraphic images for preoperative SLN mapping and, the following day, intraoperative localization of SLNs with both the conventional portable gamma-probe and fluorescence imaging, without interference from  $^{68}\text{Ga}$ 's positron emission due to its short half-life (68 min). Although high-energy handheld PET probes are available, designed for intraoperative localization of SLNs containing a positron-emitting isotope-labeled radiotracer (e.g., [ $^{89}\text{Zr}$ ]Zr-nanocolloid), their use is not recommended due to their large size and limited sensitivity [20]. Therefore, intraoperative localization of SLNs should still depend on at least conventional gamma-probe guidance, which remains feasible when combining [ $^{68}\text{Ga}$ ]Ga- and [ $^{99\text{m}}\text{Tc}$ ]Tc-radiotracers [14].

Finally, in contrast to other commonly used positron emitting isotopes (e.g.,  $^{11}\text{C}$ ,  $^{18}\text{F}$ ,  $^{89}\text{Zr}$ ), production of  $^{68}\text{Ga}$  does not require a nearby cyclotron, but can be obtained from a portable  $^{68}\text{Ge}/^{68}\text{Ga}$  generator, allowing on-demand preparation of [ $^{68}\text{Ga}$ ]Ga-tilmanocept in a standard hospital radiopharmacy [21–23].

Yet, the materialistic costs associated with [ $^{68}\text{Ga}$ ]Ga-tilmanocept PET/CT lymphoscintigraphy may remain a hindrance for the global spread of this innovative technique. First of all, as labeling of  $^{68}\text{Ga}$  with nanocolloids is unfeasible due to instability of their bond at physiological pH, this technique relies on using the more expensive tracer tilmanocept. Secondly, the additional costs for labeling tilmanocept with  $^{68}\text{Ga}$  should be taken into account. The necessary commercial automated synthesis units are relatively expensive, although more economical options with minimal operator radiation exposure are available [23]. In addition,  $^{68}\text{Ge}/^{68}\text{Ga}$ -generators typically cost in excess of €50.000 and expire after 1 year. However, it should be emphasized that the interest in  $^{68}\text{Ga}$ -labeled tracers (e.g., [ $^{68}\text{Ga}$ ]Ga-DOTATOC, [ $^{68}\text{Ga}$ ]Ga-PSMA) continues to increase. Accordingly, the costs per preparation decrease, while  $^{68}\text{Ge}/^{68}\text{Ga}$ -generators have already proven to provide a cost-effective alternative to radionuclides obtained from reactors and cyclotrons [23–25]. Finally, the operating costs for PET acquisition are still higher than scintigraphy and SPECT acquisition, despite the fact that the costs of purchasing and operating PET scanners have been halved over the past 10 years [25]. All considered, the costs for performing [ $^{68}\text{Ga}$ ]Ga-tilmanocept PET/CT lymphoscintigraphy in our institution are estimated at €1.700 per patient, not including expenses for additional  $^{99\text{m}}\text{Tc}$  and fluorescent labeling in light of future perspectives. In contrast, in our institution, costs for conventional

lymphoscintigraphy including SPECT/CT using [<sup>99m</sup>Tc]Tc nanocolloid are estimated at €1.200 per patient, when performed in a research setting.

In spite of these higher materialistic costs, [<sup>68</sup>Ga]Ga-tilmanocept PET/CT lymphoscintigraphy may even be cost-effective, apart from its potential to raise the standard of care, especially when enabling a depletion of false-negative SLNB outcomes, considering that patients with regional failure (i.e., false-negative) generally require comprehensive healthcare, including more extensive surgery and adjuvant radiotherapy, compared to patients who are correctly staged positive for disease by SLNB [9, 11, 26]. Furthermore, the potential of [<sup>68</sup>Ga]Ga-tilmanocept PET/CT lymphoscintigraphy to significantly decrease acquisition times for SLN imaging may substantially decline relative personnel costs [25]. Since [<sup>68</sup>Ga]Ga-tilmanocept PET/CT lymphoscintigraphy may diminish unnecessary HEN extirpation, expenses for meticulous histopathological assessment (i.e., step-serial-sectioning, immunohistochemistry) of irrelevant HENs might also be avoided [27].

For now, [<sup>68</sup>Ga]Ga-tilmanocept PET/CT lymphoscintigraphy for SLN mapping in early-stage OSCC is both promising and encouraging, although the number of studied patients requires a considerable increase before any definite conclusions can be drawn. Still, the first results are inspiring for future prospects, including adoption of a trimodal agent for SLNB (IRD-800CW-[<sup>68</sup>Ga]Ga-[<sup>99m</sup>Tc]Tc-tilmanocept), implementation in other malignancies, and employing highly accurate targeted radiotherapy by PET/CT lymphoscintigraphic-guided nodal irradiation.

## References

1. den Toom IJ, Boeve K, Lobeek D, et al. Elective neck dissection or sentinel lymph node biopsy in early stage oral cavity cancer patients: the Dutch experience. *Cancers (Basel)*. 2020;12(7):1783. Published 2020 Jul 3. doi:10.3390/cancers12071783
2. Liu M, Wang SJ, Yang X, Peng H. Diagnostic efficacy of sentinel lymph node biopsy in early oral squamous cell carcinoma: a meta-analysis of 66 studies. *PLoS One*. 2017;12(1):e0170322. Published 2017 Jan 20. doi:10.1371/journal.pone.0170322
3. Schilling C, Stoeckli SJ, Haerle SK, et al. Sentinel European Node Trial (SENT): 3-year results of sentinel node biopsy in oral cancer. *Eur J Cancer*. 2015;51(18):2777-2784. doi:10.1016/j.ejca.2015.08.023
4. Flach GB, Bloemena E, Klop WM, et al. Sentinel lymph node biopsy in clinically N0 T1-T2 staged oral cancer: the Dutch multicenter trial. *Oral Oncol*. 2014;50(10):1020-1024. doi:10.1016/j.oraloncology.2014.07.020
5. Schiefke F, Akdemir M, Weber A, Akdemir D, Singer S, Frerich B. Function, postoperative morbidity, and quality of life after cervical sentinel node biopsy and after selective neck dissection. *Head Neck*. 2009;31(4):503-512. doi:10.1002/hed.21001
6. Murer K, Huber GF, Haile SR, Stoeckli SJ. Comparison of morbidity between sentinel node biopsy and elective neck dissection for treatment of the n0 neck in patients with oral squamous cell carcinoma. *Head Neck*. 2011;33(9):1260-1264. doi:10.1002/hed.21622
7. Govers TM, Schreuder WH, Klop WM, et al. Quality of life after different procedures for regional control in oral cancer patients: cross-sectional survey. *Clin Otolaryngol*. 2016;41(3):228-233. doi:10.1111/coa.12502
8. Govers TM, Takes RP, Baris Karakullukcu M, et al. Management of the N0 neck in early stage oral squamous cell cancer: a modeling study of the cost-effectiveness. *Oral Oncol*. 2013;49(8):771-777. doi:10.1016/j.oraloncology.2013.05.001
9. Hernando J, Villarreal P, Álvarez-Marcos F, García-Consuegra L, Gallego L, Junquera L. Sentinel node biopsy versus elective neck dissection. Which is more cost-effective? A prospective observational study. *J Craniomaxillofac Surg*. 2016;44(5):550-556. doi:10.1016/j.jcms.2016.01.017
10. Garrel R, Poissonnet G, Moyà Plana A, et al. Equivalence randomized trial to compare treatment on the basis of sentinel node biopsy versus neck node dissection in operable T1-T2N0 oral and oropharyngeal cancer. *J Clin Oncol*. 2020;38(34):4010-4018. doi:10.1200/JCO.20.01661
11. D'Cruz AK, Vaish R, Kapre N, et al. Elective versus therapeutic neck dissection in node-negative oral cancer. *N Engl J Med*. 2015;373(6):521-529. doi:10.1056/NEJMoa1506007
12. de Bree R, Takes RP, Shah JP, et al. Elective neck dissection in oral squamous cell carcinoma: Past, present and future. *Oral Oncol*. 2019;90:87-93. doi:10.1016/j.oraloncology.2019.01.016
13. Heuveling DA, Flach GB, van Schie A, et al. Visualization of the sentinel node in early-stage oral cancer: limited value of late static lymphoscintigraphy. *Nucl Med Commun*. 2012;33(10):1065-1069. doi:10.1097/MNM.0b013e3283571089
14. Mahieu R, Krijger GC, Ververs FFT, de Roos R, de Bree R, de Keizer B. [<sup>68</sup>Ga]Ga-tilmanocept PET/CT lymphoscintigraphy for sentinel lymph node detection in early-stage oral cavity carcinoma. *Eur J Nucl Med Mol Imaging*. 2021;48(4):1246-1247. doi:10.1007/s00259-020-05060-x
15. Heuveling DA, van Schie A, Vugts DJ, et al. Pilot study on the feasibility of PET/CT lymphoscintigraphy with <sup>89</sup>Zr-nanocolloidal albumin for sentinel node identification in oral cancer patients. *J Nucl Med*. 2013;54(4):585-589. doi:10.2967/jnumed.112.115188
16. Rahmim A, Zaidi H. PET versus SPECT: strengths, limitations and challenges. *Nucl Med Commun*. 2008;29(3):193-207. doi:10.1097/MNM.0b013e3282f3a515
17. Qin Z, Hoh CK, Hall DJ, Vera DR. A tri-modal molecular imaging agent for sentinel lymph node mapping. *Nucl Med Biol*. 2015;42(12):917-922. doi:10.1016/j.nucmedbio.2015.07.011
18. Lee HJ, Barback CV, Hoh CK, et al. Fluorescence-based molecular imaging of porcine urinary bladder sentinel lymph nodes. *J Nucl Med*. 2017;58(4):547-553. doi:10.2967/jnumed.116.178582
19. Anderson KM, Barback CV, Qin Z, et al. Molecular imaging of endometrial sentinel lymph nodes utilizing fluorescent-labeled Tilmanocept during robotic-assisted surgery in a porcine model. *PLoS One*. 2018;13(7):e0197842. Published 2018 Jul 2. doi:10.1371/journal.pone.0197842

20. Heuveling DA, Karagozoglu KH, Van Lingen A, Hoekstra OS, Van Dongen GAMS, De Bree R. Feasibility of intraoperative detection of sentinel lymph nodes with <sup>89</sup>Zr-labelled nanocolloidal albumin PET-CT and a handheld high-energy gamma probe. *EJNMMI Res.* 2018;8(1):15. Published 2018 Feb 14. doi:10.1186/s13550-018-0368-6
21. Kasbollah A, Eu P, Cowell S, Deb P. Review on production of <sup>89</sup>Zr in a medical cyclotron for PET radiopharmaceuticals. *J Nucl Med Technol.* 2013;41(1):35-41. doi:10.2967/jnmt.112.111377
22. Martiniova L, Palatis L, Etchebehere E, Ravizzini G. Gallium-68 in medical imaging. *Curr Radiopharm.* 2016;9(3):187-207. doi:10.2174/1874471009666161028150654
23. Heidari P, Szretter A, Rushford LE, et al. Design, construction and testing of a low-cost automated <sup>68</sup>Gallium-labeling synthesis unit for clinical use. *Am J Nucl Med Mol Imaging.* 2016;6(3):176-184.
24. Velikyán I. Prospective of <sup>68</sup>Ga-radiopharmaceutical development. *Theranostics.* 2013;4(1):47-80. Published 2013 Dec 10. doi:10.7150/thno.7447
25. Hicks RJ, Hofman MS. Is there still a role for SPECT-CT in oncology in the PET-CT era? *Nat Rev Clin Oncol.* 2012;9(12):712-720. doi:10.1038/nrclinonc.2012.188
26. Flach GB, Tenhagen M, de Bree R, et al. Outcome of patients with early stage oral cancer managed by an observation strategy towards the N0 neck using ultrasound guided fine needle aspiration cytology: No survival difference as compared to elective neck dissection. *Oral Oncol.* 2013;49(2):157-164. doi:10.1016/j.oraloncology.2012.08.006
27. Dhawan I, Sandhu SV, Bhandari R, Sood N, Bhullar RK, Sethi N. Detection of cervical lymph node micrometastasis and isolated tumor cells in oral squamous cell carcinoma using immunohistochemistry and serial sectioning. *J Oral Maxillofac Pathol.* 2016;20(3):436-444. doi:10.4103/0973-029X.190946

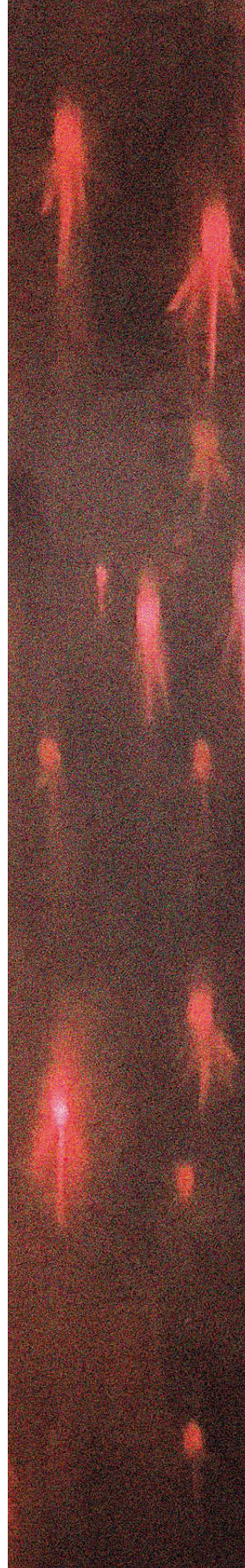




# 12

Summary, general discussion and  
future perspectives

---



In a changing landscape concerning management of the clinically negative neck in early-stage oral cancer, SLNB has emerged as a rational proposition [1]. Despite its promising results in several recent trials [2-4], SLNB is met with mixed responses within the head-and-neck oncological community and is still offered at a limited number of health-care centers across the globe [1, 5-8]. Admittedly, technological and logistical challenges of SLNB may contribute to the lack of a more widespread adoption in patients with early-stage OSCC [5]. On the other hand, logistical limitations associated with SLNB, such as the need for radiopharmaceutical and nuclear medicine facilities as well as the recommended labor-intensive advanced histopathology, may diminish over time on account of the momentum SLNB is gaining for other tumor-sites (e.g., breast cancer, melanoma), improving the availability of the required infrastructure. Furthermore, the possibility to outsource nuclear medicine or histopathological services, if the expertise is not available in the respecting center, could facilitate the implementation of SLNB [7-10]. The corresponding technological constraints, which form the foundation of the shine-through-phenomenon and confine the diagnostic accuracy of SLNB, constitute a greater challenge. These, however, may be resolved by technological advancements and refinements. This thesis is dedicated to addressing these issues of SLNB, in pursuit of improving diagnostic accuracy and oncologic prognosis as well as quality-of-life for early-stage OSCC patients (**chapter 1**).

Since the first Dutch OSCC patient was treated according to the SLNB principle in 2007, SLNB has been embraced by an increasing number of head-and-neck cancer institutions domestically. The transition from an elective neck dissection approach to a SLNB approach, provided the opportunity for retrospective analysis of outcomes in patients with early-stage OSCC following either elective neck dissection or SLNB as performed in daily practice. In **chapter 2**, the results of a nationwide retrospective multicenter study provide clinical evidence that assessment of the tumor's individual lymphatic drainage pattern by SLNB is indeed particularly beneficial for patients with lateralized OSCC, allowing for improved control over the contralateral neck. Although the overall incidence of contralateral metastases is low in lateralized OSCC (3.7%), and thus the significance of identifying and treating occult contralateral nodal metastases at an early stage seems to be modest on a population-based level, the development of contralateral regional recurrences appears to have a major impact on affected individuals due to the poor salvage rate and prognosis. Besides, SLNB has the advantage of simultaneously staging the ipsilateral and contralateral neck with the same procedure, while in case of an elective neck dissection the treating surgeon has to decide whether the contralateral neck should be included based on patient- and tumor characteristics, with due consideration of the additional morbidity inflicted. As shown in this chapter, it proves exceptionally difficult to assess whether the contralateral clinically negative neck should be electively treated in

lateralized OSCC. In the elective neck dissection cohort, of those who only underwent ipsilateral neck dissection ( $n = 337$ ), 14 patients eventually developed contralateral nodal recurrence during follow-up. Of those who underwent bilateral neck dissection ( $n = 28$ ), contralateral nodal metastasis was correctly identified and treated in only 2 patients. Conversely, 26/28 patients (93%) underwent unnecessary contralateral neck dissection. These results do not only provide an important argument in favor of SLNB for staging the clinically negative neck, but also highlight the utility of lymphatic mapping itself, which can be used in many different ways to tailor (oncologic) therapy based on lymph drainage patterns. For instance, de Veij Mestdagh et al. were able to show that lymphoscintigraphy can guide elective nodal irradiation in head-and-neck cancer patients, selecting those in whom radiation of the contralateral neck can be safely omitted [11-14]. As a consequence, the incidence and severity of radiation-related toxicities were reduced, which are notoriously known to negatively and permanently affect quality-of-life [11-15]. Aiming to further avoid futile irradiation of the neck, a multicenter randomized clinical trial has been initiated to assess the safety and efficacy of SLNB guided neck irradiation in node negative pharyngeal and laryngeal squamous cell carcinoma. In this current ongoing study, the irradiated tissue volumes are customized based on the histopathological outcome of harvested SLNs, rather than adapted based on lymphoscintigraphy alone [15]. Lymphoscintigraphy, and possibly even SLNB entirely, may become a valuable addition to radiotherapy practice standards by enabling more targeted radiotherapy and consequently allow for a reduction of radiation treatment volumes and associated radiation-related toxicities.

Still, it should be realized that lymphoscintigraphy is a comprehensive and consequently time-consuming and costly procedure, which may prevent its implementation in other fields. In **chapter 3**, the opportunities to streamline this imaging procedure, without interfering with its diagnostic accuracy, are investigated. The results of this study show that lymphoscintigraphy, as performed at our institute, can be significantly shortened by considerably reducing the duration of early dynamic acquisition and by eliminating late static acquisition in the vast majority of OSCC patients. In those with OSCC featuring slow or marginal lymphatic drainage (i.e., tumors involving the inferior alveolar process or retromolar area) as well as in those who underwent previous oncological treatment of the neck, it is advisable to acquire late static lymphoscintigraphy nonetheless. The substantial decrease in acquisition time for lymphoscintigraphy (from 92 to 58.5 minutes) in the majority of OSCC patients permits a reduction of patient burden and costs for lymphoscintigraphy and facilitates the availability of nuclear imaging devices on a day-to-day basis. This enables access to lymphoscintigraphy for other indications without the need to obtain additional gamma-cameras, SPECT/CT imaging devices and trained personnel.

Further efforts should be made to assess whether the advocated streamlined imaging protocol is sufficient, to evaluate whether the imaging procedure can be further abbreviated and to what extent the acquisition time of lymphoscintigraphy in other tumor (sub)sites could be reduced. Other approaches to reduce patient burden, costs and patient load for lymphoscintigraphy include the development of a system that is able to improve the selection of patients for either SLNB (cN0) or a therapeutic neck dissection (cN+). As mentioned in the introduction (**chapter 1**), the sensitivity of current conventional staging techniques (i.e., palpation, CT, MRI, [<sup>18</sup>F]FDG-PET/CT, USgFNAC) for detecting small nodal metastasis is poor. Recently, a multicenter study has been designed to develop [<sup>18</sup>F]FDG-PET/CT scoring criteria with a high positive predictive value for the presence of lymph node metastasis. Similarly, another ongoing study investigates the implementation of artificial intelligence in the evaluation of MRI's performed as part of clinical cervical nodal staging, developing a model that is able to predict, with a high positive predictive value, whether the neck is metastatically involved. Accordingly, patients with a high positive predictive value for nodal metastasis can then be scheduled for tumor resection combined with a therapeutic neck dissection as a single stage procedure, thus avoiding a futile diagnostic SLNB procedure.

Although a more streamlined lymphoscintigraphy imaging protocol or improved patient selection for SLNB might reduce the logistical challenges of SLNB and could facilitate the utilization of lymphoscintigraphy for other indications, the technological concerns of SLNB remain. In order to overcome these issues and improve the diagnostic accuracy of SLNB, innovations are required. Current histopathological SLN evaluation (i.e., step-serial-sectioning, hematoxylin-eosin staining and immunohistochemistry) is undisputed in terms of accuracy, allowing even the detection of isolated tumor cells, [16-19]. Whereas there are several opportunities to enhance preoperative identification and as well as the intraoperative localization of SLNs. Over the last decade, the adjunction of a fluorescent dye to well-known radiotracers (e.g., ICG- [<sup>99m</sup>Tc]Tc-nanocolloid) has gained increasing interest both internationally and domestically by improving intraoperative SLN localization when used concomitantly with gamma-tracing methods such as the gamma-probe [20, 21]. However, since fluorescence guidance remains hampered by limited tissue penetration and the conventional handheld gamma-probe lacks the ability for visual feedback, portable gamma-detecting imaging devices can also be of additional benefit [20, 22-24]. Nonetheless, obtaining a handheld gamma-probe, near-infrared camera as well as a portable gamma-camera can be a steep financial investment. Besides, near-infrared cameras and portable gamma-cameras can be large in size, sometimes requiring an articulated arm or even an additional operator to manage, and can take up a significant amount of space near the operating table. In **chapter 4**, the use of a

relatively inexpensive, small and light-weight portable gamma-camera is described. This prospective study demonstrates that the Crystal Cam handheld gamma-camera offers reliable intraoperative SLN localization and can reduce the risk of missing a malignant SLN. The information provided by the handheld gamma-camera was even considered helpful in 40% of the patients in whom fluorescence guidance was also available. Furthermore, the dual-isotope capability of this handheld gamma-camera has been particularly helpful in the preoperative marking of designated SLNs by the nuclear physician. On account of these benefits, this handheld gamma-camera has been incorporated within the clinical care of our institution. It is still worth emphasizing that detecting SLNs close to the injection site or with low radioactive uptake can remain challenging when solely using gamma-tracing methods (i.e., handheld gamma-probe, portable gamma-camera, freehand SPECT). In those situations, the complementary use of near-infrared fluorescence imaging can be of additional value. Ideally, optical navigation by both gamma-tracing as well as fluorescence guidance are combined using only one device, which can be achieved by either a robotic surgical system (e.g., daVinci Xi) or by an augmented reality headset (e.g., Microsoft HoloLens) [25-27]. As the place of robotic-assisted surgery in the neck is a matter of debate, especially sustained by its financial burden and increased operative time respective to its minor benefits [28], it is conceivable that augmented reality headsets will gain traction in the upcoming years for intraoperative SLN localization in the head and neck region [27].

Nevertheless, even with advanced and upcoming techniques for intraoperative SLN localization, accurate preoperative identification of SLNs remains key to assess which SLNs should be harvested and to acquire detailed topographical information on the location of the designated SLNs. Therefore, to establish a higher accuracy for SLNB, it is paramount that the limitations of conventional lymphoscintigraphy are overcome. In 2013 a novel radiotracer, [<sup>99m</sup>Tc]Tc-tilmanocept (Lymphoseek<sup>®</sup>, Navidea Biopharmaceuticals Inc.), specifically designed for SLN identification was introduced. Its proposed rapid clearance from the injection site, rapid uptake and high retention within the SLN, as well as low uptake by the remaining (higher echelon) lymph nodes, lead us to hypothesize that [<sup>99m</sup>Tc]Tc-tilmanocept may particularly be of benefit in tumors with complex drainage patterns and close spatial relation to SLNs. The remarkable results of Agrawal et al. on SLNB in early-stage OSCC using [<sup>99m</sup>Tc]Tc-tilmanocept (false-negative rate 2.6%, NPV 97.8%) strengthened the idea that [<sup>99m</sup>Tc]Tc-tilmanocept would possibly diminish the shine-through phenomenon and improve the SLN detection rate [29]. Unfortunately, a head-to-head (within-patient) comparison study between [<sup>99m</sup>Tc]Tc-tilmanocept and our conventionally used radiotracer ([<sup>99m</sup>Tc]Tc-nanocolloid), shows no superiority of [<sup>99m</sup>Tc]Tc-tilmanocept over [<sup>99m</sup>Tc]Tc-nanocolloid (**chapter 5**). No difference was observed in the median rate of detected HENs and SLNs between [<sup>99m</sup>Tc]Tc-tilmanocept and [<sup>99m</sup>Tc]Tc-nanocolloid,

nor was there a difference in the SLN to injection site ratio (i.e., radioactive uptake in SLN relative to activity remaining in the injection site) between both radiotracers. The follow-up study (**chapter 6**) confirms that [ $^{99m}\text{Tc}$ ]Tc-tilmanocept is not superior to [ $^{99m}\text{Tc}$ ]Tc-nanocolloid for SLNB, since the accuracy of SLN detection using [ $^{99m}\text{Tc}$ ]Tc-tilmanocept proved similar to that of [ $^{99m}\text{Tc}$ ]Tc-nanocolloid. On the basis of these studies, taking the much higher costs of tilmanocept into consideration, [ $^{99m}\text{Tc}$ ]Tc-tilmanocept was not recommended for SLNB in clinical practice. Admittedly, it cannot be denied that the small sample size of these studies might obscure subtle, yet clinically relevant, differences and that higher powered studies are needed to conclusively determine [ $^{99m}\text{Tc}$ ]Tc-tilmanocept's value for SLNB in OSCC. A European expert panel recently concluded that multicenter trials are still needed to assess if [ $^{99m}\text{Tc}$ ]Tc-tilmanocept is superior to other radiotracers used in clinical routine [30]. It is our considered opinion that, because of individual lymphatic drainage patterns, randomized controlled trials are not feasible to clearly clarify discrepancies between tracers with respect to drainage patterns, injection site clearance and uptake in SLNs and HENs, and would therefore not ascertain much more proof. Larger prospective head-to-head comparison studies, on the other hand, have the potential to assess whether [ $^{99m}\text{Tc}$ ]Tc-tilmanocept is actually superior to other radiotracers and to what extent its higher costs are justified. In the meantime, as our findings rendered it unlikely that [ $^{99m}\text{Tc}$ ]Tc-tilmanocept will outperform [ $^{99m}\text{Tc}$ ]Tc-nanocolloid for SLNB in early-stage OSCC, a further investigation for novel SLNB techniques was instigated by literature review (**chapter 7**).

In **chapter 7**, several novel preoperative SLN imaging techniques are reviewed: MR lymphography using either superparamagnetic iron oxide nanoparticles (SPIOs) or a gadolinium-based contrast agent, CT lymphography with iodine-based contrast agents, PET lymphoscintigraphy requiring a tracer labeled with a positron emitting radionuclide and contrast-enhanced lymphosonography using microbubbles. Based on a limited number of studies, each with small samples, most of these techniques appear inferior compared to SLNB using conventional  $^{99m}\text{Tc}$ -labeled radiotracers, owing to the rapid lymphatic transportation of the corresponding tracer, their dependency on separate unconjugated tracers for intraoperative SLN localization (dual-tracer methods) or the limitations of the detection probe. Several of these flaws, however, may be overcome with some adaptations, without impairing the inherent advantages of the modality itself. For instance, Waanders et al. recently developed the DiffMag magnetometer, especially designed to detect SPIOs without being interfered by the magnetic signals deriving from surgical instruments, metal elements such as (dental) prothesis or the diamagnetic human body [31, 32]. Although this magnetometer eliminates the need for frequent balancing of the probe and provides improved differentiation between injection site and SLN compared to

a conventional gamma-probe, some shortcomings of the magnetic SLNB procedure using SPIOs remain. In particular the limited performance on longitudinal distance of the magnetometer, which can hamper the detection of deeper located SLNs, the dependence on dual-tracer methods to allow for intraoperative optical guidance and the inability to visualize connecting lymphatic vessels should be addressed in further studies [32]. When considering contrast-enhanced lymphosonography, albeit highly promising for enhancing USgFNAC and consequently increasing the accuracy of preoperative clinical staging, in its present state this technique seems less suitable for SLNB [33-35]. First of all, the short duration of microbubble enhancement (Sonovue: 2 – 4 minutes) negatively affects the reproducibility of the procedure and often multiple repetitive injections are required to identify SLNs [36]. As a result, similar to USgFNAC, the success of contrast-enhanced lymphosonography is highly dependent on the skills and experience of the operator. Presently, this technique also suffers from the lack of a reliable system to mark the exact location of SLNs and is dependent on the supplementation of separate tracers to allow for intraoperative SLN localization [36, 37]. Further development of microbubbles that are retained and detectable in SLNs for a longer period of time, such as Sonazoid, which can be conjugated with ICG or technetium-99m, could make contrast-enhanced lymphosonography more compelling as an alternative technique for SLNB [37-41].

MR lymphography using a gadolinium-based contrast agent shares several limitations with contrast-enhanced lymphosonography (i.e., lacking a reliable system to mark location of SLNs, dependent on dual-tracer methods for intraoperative SLN localization). Certainly, these issues should be resolved before MR lymphography with gadolinium-based contrast agents could be considered a valid alternative technique for SLNB. Even so, the promising results as achieved by Bae et al. sustained the hypothesis that MR lymphography using gadobutrol might be a valuable addition to radiotherapy planning, by performing MR lymphography, as part of MRI already increasingly used for radiotherapy planning in head and neck cancer [42, 43]. The superior soft-tissue contrast, spatial resolution and signal-to-noise ratio of MR lymphography using gadobutrol, even when compared to MR lymphography with SPIOs, could facilitate more targeted radiotherapy, by applying a higher radiation dose on SLNs and reducing doses on surrounding tissues. Nevertheless, given obvious limitations to the study of Bae et al., mainly comprising of insufficient reference standards and lack of follow-up data, the actual accuracy of MR lymphography using gadobutrol for SLN identification was yet to be established [42]. With this in mind, another head-to-head comparison study was initiated, with the intent to directly compare MR lymphography using gadobutrol with conventional lymphoscintigraphy (**chapter 8**). The disappointing results of MR lymphography using gadobutrol, especially compared to conventional lymphoscintigraphy, were predominantly

attributed to the instant and fast lymphatic drainage of gadobutrol, along with its insufficient retention within SLNs. Optimization of the imaging protocol, with acquisition timeframes adapted to its swift lymphatic drainage, or the administration of larger volumes might improve the SLN identification rate of MR lymphography. Regardless, even with the most optimal settings achievable, it is implausible that MR lymphography with gadobutrol would transcend conventional lymphoscintigraphy with respect to lymphatic mapping. Alternate positive MR contrast agents, which have the benefit of increasing signal intensity contrary to negative MR contrast agents such as SPIOs, that have achieved encouraging results in preclinical models, are gadolinium-loaded polyethylenimine-entrapped gold nanoparticles and gadomer-17. The increased SLN retention and long-term enhancement that was established with these alternate positive MR contrast agents could be favorable for MR lymphography, but should first be further investigated in human subjects [44-47].

Meanwhile, in the continuing search for a high-resolution alternative for SLN mapping, the readily available and registered oil-based iodized contrast agent Lipiodol<sup>®</sup>, that has been successfully prepared with ICG as a single emulsion, was thought to resolve the problems that CT lymphography with water-soluble iodine-based contrast agents encountered [48, 49]. Its higher viscosity compared to water-soluble iodine-based contrast media anticipated prolonged retention in SLNs and was supposed to benefit SLN identification by CT lymphography [50, 51]. Whereas the predicted prolonged retention of Lipiodol<sup>®</sup> in SLNs was substantiated in the study described in **chapter 9**, the hypothesis that it would lead to improved SLN identification was refuted. In this study, designed to compare CT lymphography using Lipiodol<sup>®</sup> to conventional [<sup>99m</sup>Tc]Tc-nanocolloid lymphoscintigraphy, CT lymphography failed to identify any SLNs in 40% of the population and was not able to identify additional SLNs to those identified by [<sup>99m</sup>Tc]Tc-nanocolloid lymphoscintigraphy. Overall, only 33% of SLNs that were identified by conventional [<sup>99m</sup>Tc]Tc-nanocolloid lymphoscintigraphy showed uptake of Lipiodol<sup>®</sup> on SPECT/CT lymphography fusion images. With a sensitivity of no more than 50% and a NPV of 75%, CT lymphography using Lipiodol<sup>®</sup> was not considered a reliable technique for SLN mapping. In contrast to gadobutrol for MR lymphography (**chapter 8**) and water-soluble iodine-based contrast agents for CT lymphography, which suffer from rash lymphatic drainage and deficient SLN retention, the observed poor lymphatic drainage and prolonged deposition of Lipiodol<sup>®</sup> was held responsible for its disappointing performance. The dilution of Lipiodol<sup>®</sup> has been suggested to resolve the long-term accumulation of Lipiodol<sup>®</sup>, but may also accommodate in its lymphatic drainage [51, 52]. Still, diluting Lipiodol<sup>®</sup> is a delicate balance; in the pursuit to facilitate its lymphatic drainage, the long-term retention in SLNs may falter and tracer wash-out could be accelerated.

Ultimately, even with these small samples, MR lymphography using gadobutrol (**chapter 8**) and CT lymphography using Lipiodol® (**chapter 9**) were considered inadequate for SLN mapping. Even if some modifications might improve these procedures, it became apparent that the kinetics of both gadobutrol and Lipiodol® are unfeasible for lymphatic mapping in the head and neck region. As described in **chapter 7** and emphasized by the results of **chapters 8 and 9**, PET/CT lymphoscintigraphy clearly has the benefit that it permits the use of commonly administered tracers for SLNB, whose kinetics have proven to be particularly suitable for SLNB. In 2013, Heuveling et al. already demonstrated the high potential of PET/CT lymphoscintigraphy using [<sup>89</sup>Zr]Zr-nanocolloid, but adjustments were warranted to overcome the poor performance of the PET-probe for reliable intraoperative SLN localization [53, 54]. While the long half-life of zirconium-89 (78 hours) prevents the use of technetium-99m for intraoperative localization of SLNs, due to the interference of high-energy photons still being emitted by zirconium-89 at the time of surgery, a radiotracer labeled with both gallium-68 (half-life 68 minutes) and technetium-99m was considered a promising solution. This would enable high-resolution PET/CT lymphoscintigraphic images for preoperative SLN mapping, and the next day, following full decay of gallium-68, intraoperative SLN localization under conventional gamma-tracing guidance without interference by high-energy photons. Regrettably, labelling of nanocolloids with gallium-68 proved unfeasible, due to instability of the bond between gallium-68 and nanocolloids, however it has been successfully labeled to tilmanocept [55, 56]. The successful labelling of gallium-68 to tilmanocept enabled the investigation of [<sup>68</sup>Ga]Ga-tilmanocept PET/CT lymphoscintigraphy for SLN identification, which was directly compared to [<sup>99m</sup>Tc]Tc-tilmanocept lymphoscintigraphy (**chapter 10**). First and foremost, [<sup>68</sup>Ga]Ga-tilmanocept PET/CT lymphoscintigraphy provided more accurate SLN identification and improved visualization of lymphatic vessels with only 15 minutes of acquisition, as opposed to the ~90 minutes of acquisition required for [<sup>99m</sup>Tc]Tc-tilmanocept lymphoscintigraphy. Of note, [<sup>68</sup>Ga]Ga-tilmanocept PET/CT lymphoscintigraphy was able to identify 4 additional SLNs in vicinity of the injection site, which were not visualized on [<sup>99m</sup>Tc]Tc-tilmanocept lymphoscintigraphy due to the shine-through phenomenon. Furthermore, since 91% of the SLNs that were preoperatively identified by [<sup>68</sup>Ga]Ga-tilmanocept PET/CT lymphoscintigraphy were intraoperatively localized and harvested under gamma-probe guidance, the theory that [<sup>68</sup>Ga]Ga-tilmanocept does not interfere with the gamma-radiation from <sup>99m</sup>Tc-labeled radiotracers, required for reliable intraoperative SLN localization, was supported. To further enhance the accuracy of [<sup>68</sup>Ga]Ga-tilmanocept PET/CT lymphoscintigraphy, a late static PET/CT lymphoscintigram at 60 minutes post-injection was recommended to improve differentiation between the relatively high activity residing in lymphatic vessels at early timeframes and uptake in (sentinel) lymph nodes. Currently, as a result of the

auspicious performance of [<sup>68</sup>Ga]Ga-tilmanocept PET/CT lymphoscintigraphy in this pilot study, a large prospective multicenter within-patient comparison study, which includes the suggested late static PET/CT lymphoscintigram, is in preparation to start soon. Furthermore, [<sup>68</sup>Ga]Ga-tilmanocept PET/CT lymphoscintigraphy is already being adopted in other tumor sites and has demonstrated equally impressive results in a small cohort of thyroid carcinoma patients [57, 58].

If the upcoming studies confirm that [<sup>68</sup>Ga]Ga-tilmanocept PET/CT lymphoscintigraphy identifies SLNs more accurately by limiting the shine-through phenomenon and by allowing better differentiation between true SLNs and HENs, [<sup>68</sup>Ga]Ga-tilmanocept PET/CT lymphoscintigraphy has the potential to replace conventional lymphoscintigraphy and SPECT/CT with [<sup>99m</sup>Tc]Tc-radiotracers. Ideally, the tri-modal fluorescent agent IRD-800CW-tilmanocept radiolabeled with both gallium-68 and technetium-99m can be incorporated in clinical practice for SLNB by then. This would enable high-resolution PET/CT lymphoscintigraphic preoperative SLN mapping and intraoperative localization of SLNs using conventional gamma-tracing methods (e.g., gamma-probe, portable gamma-camera) as well as fluorescence guidance, without being affected by limitations of dual-tracer methods or inter-injection variability. Furthermore, with the emergence of PET/MRI and its undeniable advantages in terms of superior soft tissue contrast compared to PET/CT, it is imaginable that PET/MRI will be investigated in the near future for lymphatic mapping purposes and may eventually substitute PET/CT as the imaging modality for [<sup>68</sup>Ga]Ga-tilmanocept lymphoscintigraphy [59, 60].

Even though the prospects of SLNB using IRD-800CW-[<sup>68</sup>Ga]Ga-[<sup>99m</sup>Tc]Tc-tilmanocept are profound, one ought to be aware of the higher material costs associated with this technique (**chapter 11**). Nonetheless, these costs may be compensated by the shorter acquisition time, a reduction of relative personnel costs and, if able to realize a depletion in false-negative SLNB outcomes, a decrease in the number of patients requiring comprehensive healthcare at a later stage (e.g., more extensive surgery, adjuvant radiotherapy). The cost-effectiveness, with due consideration of the gain in quality-of life, of SLNB using IRD-800CW-[<sup>68</sup>Ga]Ga-[<sup>99m</sup>Tc]Tc-tilmanocept should be assessed in cost-utility studies.

All considered, SLNB has the capability to exceed elective neck dissection in the management of the clinically negative neck in early oral cancer patients. Conventional SLNB has already proven to be non-inferior to an elective neck dissection strategy in multiple randomized clinical trials, with superior postoperative functional outcomes. The less-invasive character and ability to reveal aberrant lymphatic drainage patterns and consequently identify occult metastasis located beyond the nodal levels

addressed by elective neck dissection prove to be particularly beneficial features of SLNB. Although currently confined by the limited resolution of lymphoscintigraphy and the disturbing shine-through phenomenon, advances in SLNB may overcome its present limitations. While most of the novel SLN imaging techniques investigated in this thesis still need to be developed further to evolve into a viable alternative, [<sup>68</sup>Ga]Ga-tilmanocept PET/CT lymphoscintigraphy has shown encouraging results and might become the new standard for SLNB in early-stage OSCC. Constraints for the global implementation of SLNB remain, especially in developing countries, yet it may be a matter of time before SLNB becomes the recommended treatment strategy for the clinically negative neck in early-stage OSCC worldwide.

## References

1. Bylapudi B, Rao VUS, Subash A, Thakur S. Does SLNB substitute END in the future with the sole advantage of preventing shoulder morbidity? *Oral Oncol.* 2021;123:105628. doi:10.1016/j.oraloncology.2021.105628
2. Garrel R, Poissonnet G, Moyà Plana A, et al. Equivalence randomized trial to compare treatment on the basis of sentinel node biopsy versus neck node dissection in operable T1-T2N0 oral and oropharyngeal cancer. *J Clin Oncol.* 2020;38(34):4010-4018. doi:10.1200/JCO.20.01661
3. Hasegawa Y, Tsukahara K, Yoshimoto S, et al. Neck dissections based on sentinel lymph node navigation versus elective neck dissections in early oral cancers: a randomized, multicenter, and noninferiority trial. *J Clin Oncol.* 2021;39(18):2025-2036. doi:10.1200/JCO.20.03637
4. Gupta T, Maheshwari G, Kannan S, Nair S, Chaturvedi P, Agarwal JP. Systematic review and meta-analysis of randomized controlled trials comparing elective neck dissection versus sentinel lymph node biopsy in early-stage clinically node-negative oral and/or oropharyngeal squamous cell carcinoma: Evidence-base for practice and implications for research. *Oral Oncol.* 2022;124:105642. doi:10.1016/j.oraloncology.2021.105642
5. Lai SY, Ferris RL. Evolving evidence in support of sentinel lymph node biopsy for early-stage oral cavity cancer. *J Clin Oncol.* 2020;38(34):3983-3986. doi:10.1200/JCO.20.02716
6. Jang SS, Davis ME, Vera DR, Lai SY, Guo TW. Role of sentinel lymph node biopsy for oral squamous cell carcinoma: Current evidence and future challenges. *Head Neck.* 2023;45(1):251-265. doi:10.1002/hed.27207
7. Puthiyottil IV, Subash A, Thakur S, Rao VUS. Elective neck dissection versus sentinel node biopsy in early oral cavity cancer - Are we ready for transition? *Oral Oncol.* 2021;123:105597. doi:10.1016/j.oraloncology.2021.105597
8. Schilling C, Shaw R, Schache A, et al. Sentinel lymph node biopsy for oral squamous cell carcinoma. Where are we now? *Br J Oral Maxillofac Surg.* 2017;55(8):757-762. doi:10.1016/j.bjoms.2017.07.007
9. Patel HN, Bowe C, Garg M, et al. Centralised pathology service for sentinel node biopsy in oral cavity cancer: The Southeast England Consortium experience. *J Oral Pathol Med.* 2022;51(4):315-321. doi:10.1111/jop.13291
10. Vaish R, Mittal N, Mahajan A, Rane SU, Agrawal A, D'Cruz AK. Sentinel node biopsy in node negative early oral cancers: Solution to the conundrum! *Oral Oncol.* 2022;134:106070. doi:10.1016/j.oraloncology.2022.106070
11. de Veij Mestdagh PD, Jonker MCJ, Vogel WV, et al. SPECT/CT-guided lymph drainage mapping for the planning of unilateral elective nodal irradiation in head and neck squamous cell carcinoma. *Eur Arch Otorhinolaryngol.* 2018;275(8):2135-2144. doi:10.1007/s00405-018-5050-0
12. de Veij Mestdagh PD, Schreuder WH, Vogel WV, et al. Mapping of sentinel lymph node drainage using SPECT/CT to tailor elective nodal irradiation in head and neck cancer patients (SUSPECT-2): a single-center prospective trial. *BMC Cancer.* 2019;19(1):1110. doi:10.1186/s12885-019-6331-8
13. de Veij Mestdagh PD, Walraven I, Vogel WV, et al. SPECT/CT-guided elective nodal irradiation for head and neck cancer is oncologically safe and less toxic: A potentially practice-changing approach. *Radiother Oncol.* 2020;147:56-63. doi:10.1016/j.radonc.2020.03.012
14. de Veij Mestdagh PD, Janssen T, Lamers E, et al. SPECT/CT-guided elective nodal irradiation for head and neck cancer: Estimation of clinical benefits using NTCP models. *Radiother Oncol.* 2019;130:18-24. doi:10.1016/j.radonc.2018.07.023
15. van den Bosch S, Takes RP, de Ridder M, et al. Personalized neck irradiation guided by sentinel lymph node biopsy in patients with squamous cell carcinoma of the oropharynx, larynx or hypopharynx with a clinically negative neck: (Chemo)radiotherapy to the PRIMARY tumor only. Protocol of the PRIMO study. *Clin Transl Radiat Oncol.* 2023;44:100696. doi:10.1016/j.ctro.2023.100696
16. Chone CT, Aniteli MB, Magalhães RS, et al. Impact of immunohistochemistry in sentinel lymph node biopsy in head and neck cancer. *Eur Arch Otorhinolaryngol.* 2013;270(1):313-317. doi:10.1007/s00405-012-2032-5
17. King C, Elsherif N, Kirwan R, et al. Serial step sections at narrow intervals with immunohistochemistry are required for accurate histological assessment of sentinel lymph node biopsy in oral squamous cell carcinoma. *Head Neck.* 2021;43(10):2985-2993. doi:10.1002/hed.26784

18. Ross GL, Shoaib T, Scott J, et al. The impact of immunohistochemistry on sentinel node biopsy for primary cutaneous malignant melanoma. *Br J Plast Surg*. 2003;56(2):153-155. doi:10.1016/s0007-1226(03)00038-9
19. Elsheikh MN, Rinaldo A, Hamakawa H, et al. Importance of molecular analysis in detecting cervical lymph node metastasis in head and neck squamous cell carcinoma. *Head Neck*. 2006;28(9):842-849. doi:10.1002/hed.20368
20. KleinJan GH, van Werkhoven E, van den Berg NS, et al. The best of both worlds: a hybrid approach for optimal pre- and intraoperative identification of sentinel lymph nodes. *Eur J Nucl Med Mol Imaging*. 2018;45(11):1915-1925. doi:10.1007/s00259-018-4028-x
21. Jeremiasse B, van den Bosch CH, Wijnen MWA, Terwisscha van Scheltinga CEJ, Fiocco MF, van der Steeg AFW. Systematic review and meta-analysis concerning near-infrared imaging with fluorescent agents to identify the sentinel lymph node in oncology patients. *Eur J Surg Oncol*. 2020;46(11):2011-2022. doi:10.1016/j.ejso.2020.07.012
22. Schilling C, Stoeckli SJ, Vigili MG, et al. Surgical consensus guidelines on sentinel node biopsy (SNB) in patients with oral cancer. *Head Neck*. 2019;41(8):2655-2664. doi:10.1002/hed.25739
23. Giammarile F, Schilling C, Gnanasegaran G, et al. The EANM practical guidelines for sentinel lymph node localisation in oral cavity squamous cell carcinoma. *Eur J Nucl Med Mol Imaging*. 2019;46(3):623-637. doi:10.1007/s00259-018-4235-5
24. Heuveling DA, van Weert S, Karagozoglu KH, de Bree R. Evaluation of the use of freehand SPECT for sentinel node biopsy in early stage oral carcinoma. *Oral Oncol*. 2015;51(3):287-290. doi:10.1016/j.oraloncology.2014.12.001
25. Azargoshab S, Houwing KHM, Roos PR, et al. Optical navigation of the drop-in  $\gamma$ -probe as a means to strengthen the connection between robot-assisted and radioguided surgery. *J Nucl Med*. 2021;62(9):1314-1317. doi:10.2967/jnumed.120.259796
26. Wu Y, Jing J, Wang J, Xu B, Du M, Chen M. Robotic-assisted sentinel lymph node mapping with indocyanine green in pelvic malignancies: a systematic review and meta-analysis. *Front Oncol*. 2019;9:585. doi:10.3389/fonc.2019.00585
27. von Niederhäusern PA, Seppi C, Sandkühler R, Nicolas G, Haerle SK, Cattin PC. Augmented reality for sentinel lymph node biopsy. *Int J Comput Assist Radiol Surg*. 2024;19(1):171-180. doi:10.1007/s11548-023-03014-w
28. Lira RB, Kowalski LP. Robotic Head and Neck Surgery: Beyond TORS. *Curr Oncol Rep*. 2020;22(9):88. doi:10.1007/s11912-020-00950-7
29. Agrawal A, Civantos FJ, Brumund KT, et al. [ $^{99m}\text{Tc}$ ]Tilmanocept accurately detects sentinel lymph nodes and predicts node pathology status in patients with oral squamous cell carcinoma of the head and neck: results of a phase III multi-institutional trial. *Ann Surg Oncol*. 2015;22(11):3708-3715. doi:10.1245/s10434-015-4382-x
30. Rovera G, de Koster EJ, Rufini V, et al.  $^{99m}\text{Tc}$ -Tilmanocept performance for sentinel node mapping in breast cancer, melanoma, and head and neck cancer: a systematic review and meta-analysis from a European expert panel. *Eur J Nucl Med Mol Imaging*. 2023;50(11):3375-3389. doi:10.1007/s00259-023-06290-5
31. Waanders S, Visscher M, Oderkerk TOB, Krooshoop HJG, Haken B. Method and apparatus for measuring an amount of superparamagnetic material in an object. (Patent No. EP 12194029.0. 2012.)
32. Nieuwenhuis ER, Mir N, Horstman-van de Loosdrecht MM, et al. Performance of a nonlinear magnetic handheld probe for intraoperative sentinel lymph node detection: a phantom study. *Ann Surg Oncol*. 2023;30(13):8735-8742. doi:10.1245/s10434-023-14166-z
33. Sever AR, Mills P, Weeks J, et al. Preoperative needle biopsy of sentinel lymph nodes using intradermal microbubbles and contrast-enhanced ultrasound in patients with breast cancer. *AJR Am J Roentgenol*. 2012;199(2):465-470. doi:10.2214/AJR.11.7702
34. Zhong J, Sun DS, Wei W, et al. Contrast-enhanced ultrasound-guided fine-needle aspiration for sentinel lymph node biopsy in early-stage breast cancer. *Ultrasound Med Biol*. 2018;44(7):1371-1378. doi:10.1016/j.ultrasmedbio.2018.03.005
35. Nielsen Moody A, Bull J, Culpan AM, et al. Preoperative sentinel lymph node identification, biopsy and localisation using contrast enhanced ultrasound (CEUS) in patients with breast cancer: a systematic review and meta-analysis. *Clin Radiol*. 2017;72(11):959-971. doi:10.1016/j.crad.2017.06.121

36. Gvetadze SR, Xiong P, Lv M, et al. Contrast-enhanced ultrasound mapping of sentinel lymph nodes in oral tongue cancer—a pilot study. *Dentomaxillofac Radiol.* 2017;46(3):20160345. doi:10.1259/dmfr.20160345
37. Kogashiwa Y, Sakurai H, Akimoto Y, et al. Sentinel node biopsy for the head and neck using contrast-enhanced ultrasonography combined with indocyanine green fluorescence in animal models: a feasibility study. *PLoS One.* 2015;10(7):e0132511. doi:10.1371/journal.pone.0132511
38. Li Y, Huang W, Li C, Huang X. Indocyanine green conjugated lipid microbubbles as an ultrasound-responsive drug delivery system for dual-imaging guided tumor-targeted therapy. *RSC Adv.* 2018;8(58):33198-33207. doi:10.1039/c8ra03193b
39. Wang L, Hu Y, Peng Q, et al. Correction: Indocyanine-green-loaded microbubbles for localization of sentinel lymph node using near-infrared fluorescence/ultrasound imaging: a feasibility study. *RSC Adv.* 2023;13(35):24319. doi:10.1039/d3ra90075d
40. Han YH, Kankala RK, Wang SB, Chen AZ. Leveraging engineering of indocyanine green-encapsulated polymeric nanocomposites for biomedical applications. *Nanomaterials (Basel).* 2018;8(6):360. doi:10.3390/nano8060360
41. Lazarova N, Causey PW, Lemon JA, et al. The synthesis, magnetic purification and evaluation of <sup>99m</sup>Tc-labeled microbubbles. *Nucl Med Biol.* 2011;38(8):1111-1118. doi:10.1016/j.nucmedbio.2011.04.008
42. Bae S, Lee HJ, Nam W, Koh YW, Choi EC, Kim J. MR lymphography for sentinel lymph node detection in patients with oral cavity cancer: Preliminary clinical study. *Head Neck.* 2018;40(7):1483-1488. doi:10.1002/hed.25167
43. Wong KH, Panek R, Bhide SA, Nutting CM, Harrington KJ, Newbold KL. The emerging potential of magnetic resonance imaging in personalizing radiotherapy for head and neck cancer: an oncologist's perspective. *Br J Radiol.* 2017;90(1071):20160768. doi:10.1259/bjr.20160768
44. Yang Y, Zhou J, Shi X, Sha Y, Wu H. Long-term observation of indirect lymphography using gadolinium-loaded polyethylenimine-entrapped gold nanoparticles as a dual mode CT/MR contrast agent for rabbit lingual sentinel lymph node identification. *Acta Otolaryngol.* 2017;137(2):207-214. doi:10.1080/00016489.2016.1222550
45. Yang Y, Zhou B, Zhou J, Shi X, Sha Y, Wu H. Assessment of lingual sentinel lymph nodes metastases using dual-modal indirect CT/MR lymphography with gold-gadolinium-based nanoprobe in a tongue VX<sub>2</sub> carcinoma model. *Acta Otolaryngol.* 2018;138(8):727-733. doi:10.1080/00016489.2018.1441544
46. Torchia MG, Misselwitz B. Combined MR lymphangiography and MR imaging-guided needle localization of sentinel lymph nodes using Gadomer-17. *AJR Am J Roentgenol.* 2002;179(6):1561-1565. doi:10.2214/ajr.179.6.1791561
47. Nason RW, Torchia MG, Morales CM, Thliveris J. Dynamic MR lymphangiography and carbon dye for sentinel lymph node detection: a solution for sentinel lymph node biopsy in mucosal head and neck cancer. *Head Neck.* 2005;27(4):333-338. doi:10.1002/hed.20173
48. Kim H, Lee SK, Kim YM, et al. Fluorescent iodized emulsion for pre- and intraoperative sentinel lymph node imaging: validation in a preclinical model. *Radiology.* 2015;275(1):196-204. doi:10.1148/radiol.14141159
49. Sugiyama S, Iwai T, Izumi T, et al. Sentinel lymph node mapping of clinically N0 early oral cancer: a diagnostic pitfall on CT lymphography. *Oral Radiol.* 2021;37(2):251-255. doi:10.1007/s11282-020-00442-1
50. Kim YH, Lee YJ, Park JH, et al. Early gastric cancer: feasibility of CT lymphography with ethiodized oil for sentinel node mapping. *Radiology.* 2013;267(2):414-421. doi:10.1148/radiol.12121527
51. Lee JH, Park DJ, Kim YH, Shin CM, Lee HS, Kim HH. Clinical implementations of preoperative computed tomography lymphography in gastric cancer: a comparison with dual tracer methods in sentinel node navigation surgery. *Ann Surg Oncol.* 2013;20(7):2296-2303. doi:10.1245/s10434-012-2855-8
52. Chung YE, Hyung WJ, Kweon S, et al. Feasibility of interstitial CT lymphography using optimized iodized oil emulsion in rats. *Invest Radiol.* 2010;45(3):142-148. doi:10.1097/RLI.0b013e3181c8cf19
53. Heuveling DA, van Schie A, Vugts DJ, et al. Pilot study on the feasibility of PET/CT lymphoscintigraphy with <sup>89</sup>Zr-nanocolloidal albumin for sentinel node identification in oral cancer patients. *J Nucl Med.* 2013;54(4):585-589. doi:10.2967/jnumed.112.115188

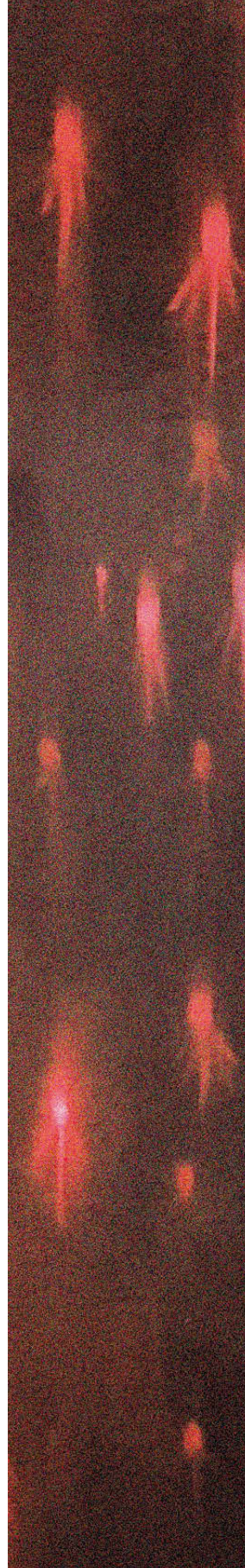
54. Heuveling DA, Karagozoglu KH, Van Lingen A, Hoekstra OS, Van Dongen GAMS, De Bree R. Feasibility of intraoperative detection of sentinel lymph nodes with 89-zirconium-labelled nanocolloidal albumin PET-CT and a handheld high-energy gamma probe. *EJNMMI Res.* 2018;8(1):15. doi:10.1186/s13550-018-0368-6
55. Persico MG, Marengo M, De Matteis G, et al. <sup>99m</sup>Tc-<sup>68</sup>Ga-ICG-labelled macroaggregates and nanocolloids of human serum albumin: synthesis procedures of a trimodal imaging agent using commercial kits. *Contrast Media Mol Imaging.* 2020;2020:3629705. doi:10.1155/2020/3629705
56. Stroup SP, Kane CJ, Farchshchi-Heydari S, et al. Preoperative sentinel lymph node mapping of the prostate using PET/CT fusion imaging and Ga-68-labeled tilmanocept in an animal model. *Clin Exp Metastasis.* 2012;29(7):673-680. doi:10.1007/s10585-012-9498-9
57. de Vries LH, Lodewijk L, de Keizer B, Borel Rinkes IH, Vriens MR. Sentinel lymph node detection in thyroid carcinoma using <sup>68</sup>Ga-tilmanocept PET/CT: a proof-of-concept study protocol. *Future Oncol.* 2022;18(31):3493-3499. doi:10.2217/fon-2022-0165
58. de Vries LH, Lodewijk L, Ververs T, et al. Sentinel lymph node detection in thyroid carcinoma using [<sup>68</sup>Ga]Ga-tilmanocept PET/CT: a proof-of-concept study. *Eur J Nucl Med Mol Imaging.* 2024;51(2):512-520. doi:10.1007/s00259-023-06449-0
59. Pampaloni MH, Nardo L. PET/MRI radiotracer beyond <sup>18</sup>F-FDG. *PET Clin.* 2014;9(3):345-349. doi:10.1016/j.cpet.2014.03.010
60. Ehman EC, Johnson GB, Villanueva-Meyer JE, et al. PET/MRI: Where might it replace PET/CT? *J Magn Reson Imaging.* 2017;46(5):1247-1262. doi:10.1002/jmri.25711



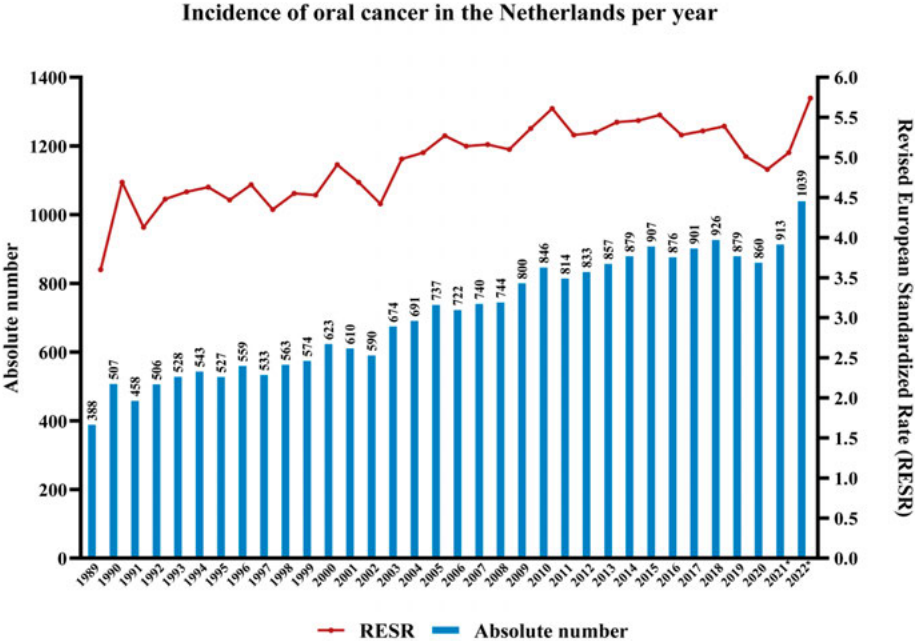
# 13

Nederlandse samenvatting

---



In Nederland worden elk jaar ongeveer 1000 mensen gediagnosticeerd met mondholtekanker, wat het de meest voorkomende vorm van hoofd-halskanker maakt. Roken is de voornaamste risicofactor voor het ontwikkelen van mondholtekanker. Echter, ondanks een halvering van het percentage dagelijkse rokers in de afgelopen 30 jaar, blijft het aantal mensen die per jaar in Nederland gediagnosticeerd worden met mondholtekanker toch stijgen (**hoofdstuk 1; figuur 1**). Een duidelijke verklaring voor deze aanhoudende stijging in de incidentie van mondholtekanker ontbreekt nog.



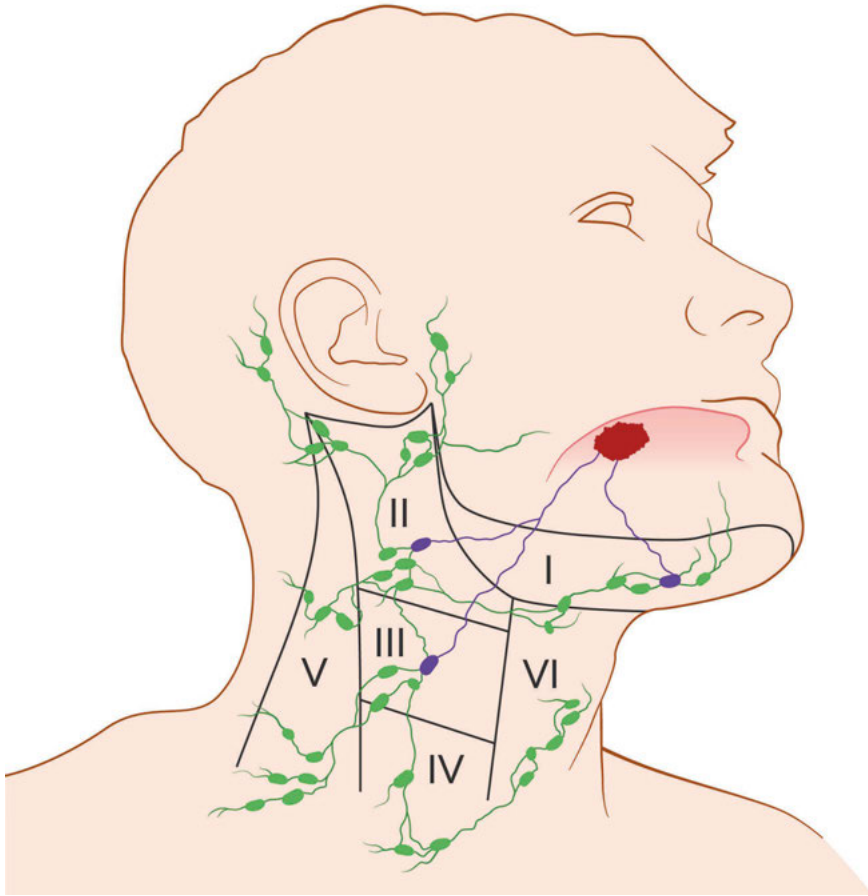
**Figuur 1.** Incidentie van mondholtekanker in Nederland per jaar. Het absolute aantal patiënten dat elk jaar wordt gediagnosticeerd met mondholtekanker wordt weergegeven middels de blauwe staven; de rode lijn vertegenwoordigt het aantal nieuwe gevallen per 100.000 personen per jaar, gecorrigeerd voor de leeftijdsdistributie in de Europese populatie in 2010. \**Voorlopige data*. Data afkomstig van Integraal Kankercentrum Nederland (IKNL).

Eén van de belangrijkste factoren voor zowel de behandeling als prognose van mondholtekanker is de aanwezigheid van uitzaaiingen in de lymfeklieren in de hals. Om deze reden is gedegen onderzoek naar de aanwezigheid van lymfeklieruitzaaiingen, door middel van lichamelijk en beeldvormend onderzoek (echogeleide punctie, CT, MRI en/of [<sup>18</sup>F]FDG-PET/CT), van groot belang. Deze technieken zijn echter niet betrouwbaar genoeg om kleine lymfeklieruitzaaiingen te detecteren. Dit blijkt uit het aanzienlijke aandeel patiënten dat toch verborgen lymfeklieruitzaaiingen heeft (20-30%), ondanks dat lichamelijk en beeldvormend onderzoek geen lymfeklieruitzaaiingen hebben gedetecteerd.

Hoe deze specifieke patiënten met mondholtekanker het beste kunnen worden behandeld is een wederkerend dilemma. Enerzijds kan ervoor worden gekozen om uit voorzorg de lymfeklieren in de hals te verwijderen met een electieve halsklierdissectie, waarbij 70-80% van de patiënten dus onnodig deze omvangrijke operatie ondergaan. Anderzijds kan de hals ongemoeid worden gelaten, waarna patiënten nauwlettend worden vervolgd. Een halsklierdissectie wordt verricht indien zich alsnog lymfeklieruitzaaiingen voordoen. Onderzoek heeft echter uitgewezen dat behandeling van lymfeklieruitzaaiingen op een later moment, wanneer deze klinisch manifest geworden zijn (regionaal recidief), veelal uitgebreider is en aanzienlijke morbiditeit alsmede een slechtere prognose tot gevolg heeft. Dit dilemma doet zich met name voor wanneer de hals niet benaderd hoeft te worden voor het verwijderen van de tumor, zoals het geval is bij kleine (vroeg-stadium) mondholtetumoren die door de mond verwijderd kunnen worden.

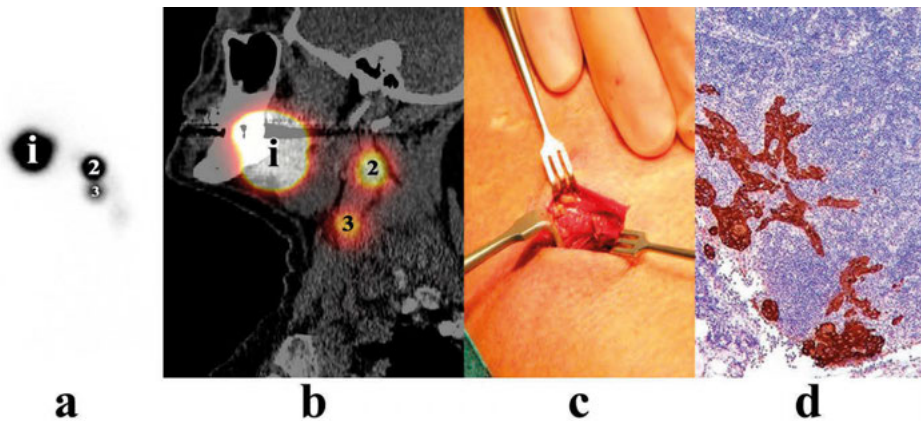
In de afgelopen decennia kwam er echter een nieuwe techniek aan het licht, die mogelijk een oplossing kan bieden voor deze kwestie: de schildwachtklierprocedure. De schildwachtklierprocedure, ook wel poortwachtersklierprocedure of *sentinel node procedure* genoemd, is een procedure die inmiddels bij meerdere kankersoorten wordt toegepast, waaronder vroeg-stadium mondholtekanker, met het doel om alleen de patiënten te selecteren die baat hebben bij een behandeling van de regionale lymfeklieren.

De schildwachtklierprocedure gaat uit van het gegeven dat de tumor eerst naar één of een beperkt aantal lymfeklieren uitzaait, voordat uitzaaiing naar de lymfeklieren verderop gelegen in het drainagesysteem plaatsvindt. Deze eerste drainerende lymfeklieren, de schildwachtklieren, hebben een directe relatie met de tumor via lymfebanen en daarmee het hoogste risico op het bevatten van eventuele uitzaaiingen (**hoofdstuk 1; figuur 2**).



**Figuur 2.** Drainage van een tongtumor via het lymfatische systeem in de hals waarbij, in dit voorbeeld, drie lymfeklieren een directe relatie hebben met de tumor (de schildwachtklieren: *paars*). De lymfeklieren verderop gelegen in het drainagesysteem zijn de zogeheten hogere echelonklieren (*groen*). De locatie van schildwachtklieren en hogere echelonklieren wordt aangegeven op basis van het lymfeklierstation waarin de lymfeklieren gelegen zijn (*level I-VI*), zoals gehanteerd door de American Academy of Otolaryngology and Head and Neck Surgery.

Wanneer rondom de tumor een radioactieve vloeistof (een technetium-99m ( $^{99m}\text{Tc}$ ) gelabelde radiotracer) wordt ingespoten, zal deze vloeistof via lymfebanen eerst naar de schildwachtklier(en) gaan. Vervolgens kunnen deze schildwachtklier(en) in beeld gebracht worden met een serie scans: lymfoscintigrafie. Tot slot wordt de schildwachtklier(en) met behulp van de radioactieve stof tijdens een operatie opgezocht en verwijderd, waarna deze wordt ingestuurd voor pathologisch onderzoek (**hoofdstuk 1; figuur 3**).



**Figuur 3.** Onderdelen van de schildwachtklierprocedure. Nadat de radiotracer is ingespoten rondom de tumor worden de schildwachtklieren in beeld gebracht met behulp van lymfoscintigrafie (a,b). Bij deze patiënt zijn met statische scintigrafie (a) en SPECT/CT (b) de injectieplaats (i) en twee schildwachtklieren (2,3) geïdentificeerd. De geïdentificeerde schildwachtklieren worden vervolgens tijdens een operatie opgezocht en verwijderd via een kleine incisie in de hals (c). De verwijderde schildwachtklieren worden ingestuurd voor pathologisch onderzoek (d).

Bevat minstens één schildwachtklier een uitzaaiing, dan mogen de opeenvolgende lymfe-klieren ook niet vertrouwd worden en is een aanvullende behandeling van het lymfeklierpakket in de hals nodig (lymfeklierdissectie of radiotherapie). Bevat(ten) de schildwachtklier(en) géén uitzaaiingen, dan is aanvullende behandeling van de lymfeklieren niet nodig. Op deze manier kan de schildwachtklierprocedure onnodige lymfeklierdissecties voorkomen, zonder in te boeten op de prognose van patiënten.

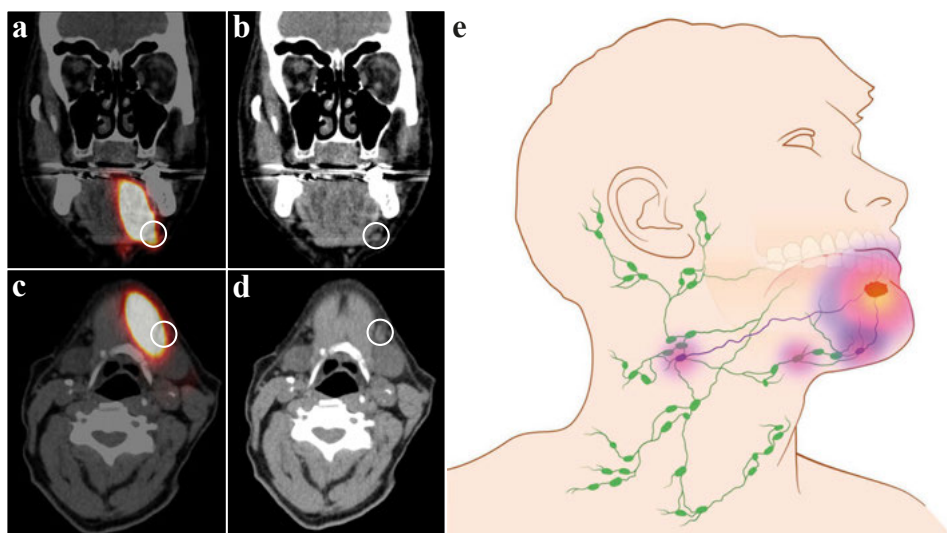
In 2007 werd in Nederland voor het eerst de schildwachtklierprocedure toegepast bij een patiënt met mondholtekanker. In de opvolgende jaren werd in de meeste Nederlandse hoofd-halskankercentra de schildwachtklierprocedure steeds meer routinematig toegepast bij deze groep patiënten en werd de electieve halsklierdissectie langzaam maar zeker verlaten. De transitie van een electieve halsklierdissectie naar de schildwachtklierprocedure in de behandeling van deze patiënten bood de mogelijkheid om in retrospect uitkomsten te vergelijken tussen patiënten die een electieve halsklierdissectie ondergingen en patiënten die werden behandeld volgens de principes van de schildwachtklierprocedure (**hoofdstuk 2**). In deze grote groep patiënten ( $n = 816$ ) bleek dat degenen die een tumor hadden in de zijkant van de mondholte, zonder betrokkenheid van de middenlijn, in 3,7% van de gevallen lymfeklieruitzaaiingen hadden in de andere (contralaterale) zijde van de hals. Waar de schildwachtklierprocedure individuele lymfebanen volgt en zo eventuele schildwachtklieren in de contralaterale hals kan detecteren, moet bij een electieve halsklierdissectie op basis van karakteristieken van de tumor ingeschat worden of

deze contralaterale hals ook geopereerd moet worden. Patiënten die een electieve (meestal eenzijdige) halsklierdissectie ondergingen ( $n = 365$ ) hadden dan ook een significant hoger risico op het ontwikkelen van een regionaal recidief in de contralaterale hals, vermoedelijk door het missen van verborgen lymfeklieruitzaaiingen in de contralaterale hals ten tijde van de behandeling, vergeleken met patiënten die werden behandeld met behulp van de schildwachtklierprocedure ( $n = 451$ , HR = 2,922;  $p = 0,030$ ). De prognose van de patiënten die een regionaal recidief in de contralaterale hals ontwikkelden was slechter, doch niet significant ( $p = 0,066$ ), ten opzichte van de patiënten waarbij de lymfeklieruitzaaiingen in de contralaterale hals werden gedetecteerd en behandeld ten tijde van de ingreep. Slechts 33% van de patiënten met een regionaal recidief in de contralaterale hals kon nog effectief behandeld worden (succesvolle salvage behandeling). Dat het ingewikkeld blijkt om op basis van tumorkarakteristieken alleen te bepalen of de contralaterale hals behandeld moet worden, blijkt uit het feit dat 26 van de 28 patiënten (93%) die een electieve halsklierdissectie aan beide kanten van de hals ondergingen, geen lymfeklieruitzaaiingen in de contralaterale hals hadden en dus onnodig een contralaterale halsklierdissectie hadden ondergaan. Dit is niet alleen een argument voor het gebruik van de schildwachtklierprocedure bij vroeg-stadium mondholtekanker, maar pleit ook voor het gebruik van de schildwachtklierprocedure om andere kankerbehandelingen van de lymfeklieren in de hals doelgerichter te maken, zoals bestralingsbehandelingen.

De scans die worden gebruikt voor de schildwachtklierprocedure (lymfoscintigrafie) zijn echter uitgebreid en tijdrovend. In **hoofdstuk 3** werd bij 77 patiënten met vroeg-stadium mondholtekanker onderzocht of het scan-protocol voor lymfoscintigrafie verkort kon worden, zonder daarmee zijn nauwkeurigheid te ondermijnen. Door een aanzienlijke verkorting van de vroege dynamische scan (10 minuten i.p.v. 30 minuten) en het weglaten van de late statische scan kon de totale scantijd ingekort worden van 92 naar 58.5 minuten in de grote meerderheid van deze patiëntenpopulatie, zonder daarmee de nauwkeurigheid van de schildwachtklierprocedure in te perken. Bij patiënten waarbij het transport van de radiotracer via de lymfebanen trager verloopt of verminderd is, zoals bij patiënten met tumoren uitgaande van het tandvlees of bij patiënten die eerder een kankerbehandeling van de hals hadden ondergaan, kon de scantijd niet verkort worden.

Hoewel een kortere scantijd het gebruik van de schildwachtklierprocedure kan faciliteren, mede voor andere kankerbehandelingen, behelzen de technologische beperkingen van de schildwachtklierprocedure nog steeds de belangrijkste uitdaging. Een van de voornaamste beperkingen van de schildwachtklierprocedure doet zich namelijk voor in situaties waarbij schildwachtklier(en) dichtbij de tumor liggen. Door

de lage resolutie van de huidige scans kan de radioactiviteit van de injectieplaats de activiteit in nabijgelegen schildwachtklier(en) overstralen, waardoor deze niet zichtbaar worden op de scans. Dit zogeheten ‘shine-through fenomeen’ is vooral aanwezig bij mondbodemtumoren waarbij schildwachtklieren vaak dicht in de buurt van de injectieplaats liggen (**hoofdstuk 1; figuur 5**). Hierdoor is bij deze tumoren de schildwachtklierprocedure minder betrouwbaar (sensitiviteit 63%; negatief voorspellende waarde 90%) vergeleken met andere mondholtetumoren (sensitiviteit 86%; negatief voorspellende waarde 95%).



**Figuur 5.** Shine-through fenomeen bij een patiënt met mondbodemkanker. (a-d) SPECT/CT beelden waarop te zien is de radioactiviteit van de injectieplaats een nabij gelegen schildwachtklier overschaduwde (witte cirkel). (e) Schematische illustratie van het shine-through fenomeen.

Een lagere nauwkeurigheid in het detecteren van schildwachtklieren kan resulteren in het achterlaten van verborgen lymfeklieruitzaaiingen, door onterecht de lymfeklieren in de hals als “schoon” te bestempelen (negatief voor uitzaaiingen). Deze achtergelaten lymfeklieruitzaaiingen zullen vervolgens onvermijdelijk groeien en zich verder verspreiden, met een uitgebreidere behandeling en slechtere prognose tot gevolg.

Daarnaast is het met de huidige scans uitdagend om onderscheid te maken tussen schildwachtklieren en opeenvolgende lymfeklieren (hogere echelonklieren). Hierdoor worden waarschijnlijk te veel lymfeklieren verwijderd, aangezien sommige hogere echelonklieren onterecht als schildwachtklier worden aangemerkt. Operatieve verwijdering van hogere echelonklieren kan onnodige complicaties veroorzaken en een eventuele aanvullende operatie van het lymfeklierpakket belemmeren. Bovendien

kan het onterecht aanmerken van schildwachtklieren als hogere echelonklieren ook resulteren in het achterlaten van verborgen lymfeklieruitzaaiingen.

Tot deze beperkingen van de schildwachtklierprocedure zijn opgelost, blijven verborgen lymfeklieruitzaaiingen onopgemerkt en daarmee onbehandeld bij 5-6% van de patiënten met vroeg-stadium mondholtekanker. **Hoofdstukken 4 – 11** zijn toegewijd aan het verbeteren van de nauwkeurigheid van de schildwachtklierprocedure en daarmee de prognose en kwaliteit van leven voor patiënten met vroeg-stadium mondholtekanker te bevorderen.

In **hoofdstuk 4** werd bij 53 patiënten met vroeg-stadium mondholtekanker tijdens de schildwachtklierprocedure gebruik gemaakt van een relatief goedkope en handzame gamma-camera, met als doel om tijdens de operatie schildwachtklieren nauwkeuriger te kunnen opzoeken. Geblindeerd voor de uitkomsten van de scans (lymfoscintigrafie) kon deze gamma-camera 91% van de schildwachtklieren detecteren. De schildwachtklieren die op deze manier niet gedetecteerd konden worden met deze gamma-camera waren met name dicht in de buurt van de injectieplaats gelegen. Geen van deze gemiste schildwachtklieren bleek uitzaaiingen te bevatten. Het gebruik van deze gamma-camera tijdens de operatie zorgde voor het verwijderen van 16 extra lymfeklieren waarvan 4 uitzaaiingen bevatten. In 2 patiënten voorkwam de gamma-camera dat de hals onterecht als ‘schoon’ werd afgegeven. De chirurg vond het gebruik van deze handzame gamma-camera tijdens de operatie in 55% van de patiënten van toegevoegde waarde. Zelfs met dergelijke geavanceerde technieken voor het nauwkeuriger lokaliseren van schildwachtklieren tijdens de operatie, blijft de identificatie van schildwachtklieren door de scans voor de operatie van cruciaal belang. Deze scans zijn namelijk essentieel om te beoordelen welke schildwachtklieren moeten worden verwijderd en om gedetailleerde informatie te verkrijgen over de anatomische locatie van de schildwachtklieren.

In 2013 werd een nieuwe radiotracer op de markt gebracht: [<sup>99m</sup>Tc]Tc-tilmanocept. De veronderstelde vlotte klaring vanuit de injectieplaats en snelle opname alsmede de hoge retentie in schildwachtklieren van deze radiotracer, leidde tot de hypothese dat [<sup>99m</sup>Tc]Tc-tilmanocept het ‘shine-through fenomeen’ zou inperken en de detectiegraad van schildwachtklieren zou bevorderen. In het vergelijkende onderzoek tussen de standaard radiotracer ([<sup>99m</sup>Tc]Tc-nanocolloïd) en deze nieuwe radiotracer ([<sup>99m</sup>Tc]Tc-tilmanocept), bleek [<sup>99m</sup>Tc]Tc-tilmanocept echter niet beter te zijn ten opzichte van de standaard gebruikte radiotracer ([<sup>99m</sup>Tc]Tc-nanocolloïd; **hoofdstuk 5 en 6**). In deze onderzoeken werd geen significant verschil gezien tussen beide radiotracers met betrekking tot het gemiddeld aantal gedetecteerde schildwachtklieren en hogere echelonklieren, noch in de opname van de radiotracer in de schildwachtklieren ten

opzichte van de injectieplaats (injectieplaats tot schildwachtklier ratio). Uiteindelijk, na een gemiddelde follow-up van 22,6 maanden, bleek de nauwkeurigheid van de nieuwe radiotracer ( $[^{99m}\text{Tc}]$ Tc-tilmanocept) in het detecteren van schildwachtklieren overeen te komen met die van de standaard gebruikte radiotracer ( $[^{99m}\text{Tc}]$ Tc-nanocolloid). Wegens de aanzienlijk hogere kosten van deze nieuwe radiotracer ( $[^{99m}\text{Tc}]$ Tc-tilmanocept), kon het gebruik hiervan niet worden aanbevolen.

Aangezien op basis van deze onderzoeken het onwaarschijnlijk leek dat  $[^{99m}\text{Tc}]$ Tc-tilmanocept de standaard radiotracer  $[^{99m}\text{Tc}]$ Tc-nanocolloid zal overtreffen, werd de zoektocht naar nieuwe technieken voor de schildwachtklierprocedure voortgezet. In **hoofdstuk 7** werden enkele nieuwe schildwachtkliertechnieken in een literatuuronderzoek onderzocht: MR lymfografie (MRI scan; tracer op gadolinium-basis of op superparamagnetisch ijzer-basis), CT lymfografie (CT scan; tracer op jodium-basis), PET/CT lymfoscintigrafie (PET scan; radiotracer met positron-emissie) en lymfasonografie (echo; tracer met microbubbel). De meeste van deze technieken leken echter ondergeschikt aan de huidige schildwachtklierprocedure met technetium-99m gelabelde radiotracers. De voornaamste beperkingen van deze technieken bleken met name het snelle transport van de corresponderende tracer door de lymfebanen zonder adequaat behoud in de schildwachtklieren, de afhankelijkheid van afzonderlijke ongebonden tracers voor het opzoeken van schildwachtklieren tijdens de operatie of de beperkingen van de detectie-probe voor het lokaliseren van de tracer (c.q. de schildwachtklieren). Sommige van de bovengenoemde beperkingen kunnen echter worden opgelost met enkele aanpassingen, zonder de inherente voordelen van deze technieken aan te tasten.

Alhoewel MR lymfografie met een tracer op gadolinium-basis ingrijpende en complexe aanpassingen behoeft voordat deze techniek een valide alternatief is voor de standaard schildwachtklierprocedure, kan deze techniek in zijn huidige vorm wel gebruikt worden om bestralingsbehandelingen doelgerichter te maken. De veelbelovende resultaten van het enige onderzoek die MR lymfografie met een tracer op gadolinium-basis (gadobutrol) had toegepast bij patiënten met mondholletumoren (Bae et al. 2018), deed vermoeden dat MR lymfografie met gadobutrol een waardevolle aanvulling kon zijn voor bestralingsbehandelingen. Door vlak voor de MRI-scans, die al routinematig worden gebruikt om te bepalen welke gebieden bestraald moeten worden, gadobutrol rondom de tumor in te spuiten, zou nog gericht bestraald kunnen worden op de lymfeklieren die het hoogste risico hebben op het bevatten van eventuele uitzaaiingen (de schildwachtklieren). Echter, aan het onderzoek van Bae et al. zaten meerdere haken en ogen, waardoor de daadwerkelijke nauwkeurigheid van MR lymfografie met gadobutrol voor het detecteren van schildwachtklieren nog ter discussie stond. Hierop werd besloten om MR lymfografie met gadobutrol te

vergelijken met de standaard schildwachtklierprocedure in 10 patiënten met vroeg-stadium mondholtekanker (**hoofdstuk 8**). MR lymfografie detecteerde echter maar 16 van de 27 schildwachtklieren (59%) die gedetecteerd waren door standaard lymfoscintigrafie met [<sup>99m</sup>Tc]Tc-nanocolloïd. Bovendien had MR lymfografie slechts 3 van de 7 schildwachtklieren (43%) gedetecteerd die uitzaaiingen bevatten. Op basis van deze teleurstellende resultaten werd geconcludeerd dat MR lymfografie met gadobutrol, in zijn huidige vorm, geen betrouwbare methode is voor het detecteren van schildwachtklieren.

Ondertussen werd gedacht dat het gemakkelijk verkrijgbare en reeds hiervoor geregistreerde Lipiodol® de problemen zou oplossen waaraan CT lymfografie met een wateroplosbare jodiumhoudende tracer onderhevig was. Lipiodol® is een jodiumhoudend contrastmiddel op oliebasis, waardoor deze tracer een hogere viscositeit heeft dan wateroplosbare jodiumhoudende tracers. De hogere viscositeit zou ervoor kunnen zorgen dat de tracer minder snel door de lymfebanen transporteert en langer in de schildwachtklieren aanwezig blijft, wat de detectie van schildwachtklieren ten goede zou komen. Bovendien is Lipiodol® succesvol bereid met indocyanine groen (ICG) als één homogene emulsie, waardoor de schildwachtklieren die gedetecteerd zijn op CT lymfografie ook tijdens de operatie opgezocht kunnen worden met een nabij-infrarood camera. Alhoewel de langdurige retentie van Lipiodol® in schildwachtklieren werd bevestigd in **hoofdstuk 9**, werd verworpen dat CT lymfografie met Lipiodol® zou resulteren in nauwkeurigere detectie van schildwachtklieren. In dit hoofdstuk werd CT lymfografie met Lipiodol® vergeleken met standaard lymfoscintigrafie met [<sup>99m</sup>Tc]Tc-nanocolloïd in 10 patiënten met vroeg-stadium mondholtekanker. CT lymfografie met Lipiodol® kon in 4 van de 10 patiënten (40%) geen enkele schildwachtklier identificeren. Slechts 7 van de 21 schildwachtklieren (33%) die gedetecteerd waren met de standaard [<sup>99m</sup>Tc]Tc-nanocolloïd lymfoscintigrafie konden worden geïdentificeerd op gefuseerde beelden van CT lymfografie en SPECT (onderdeel van standaard lymfoscintigrafie). Waar de nauwkeurigheid in het detecteren van schildwachtklieren bij MR lymfografie en CT lymfografie met een wateroplosbare jodiumhoudende tracer worden benadeeld door het snelle transport van de tracer door het lymfeklierstelsel, bleek het geringe transport van Lipiodol® door de lymfebanen verantwoordelijk voor deze teleurstellende resultaten.

13 Uiteindelijk, zelfs met deze kleine patiëntpopulaties ( $n = 10$ ), werd geconcludeerd dat MR lymfografie met gadobutrol (**hoofdstuk 8**) en CT lymfografie met Lipiodol® (**hoofdstuk 9**) onbetrouwbare alternatieve methoden zijn voor de schildwachtklierprocedure ten gevolge van de nadelige eigenschappen van de corresponderende tracers.

PET/CT lymfoscintigrafie, daarentegen, heeft het voordeel gebruik te kunnen maken van standaard gebruikte radiotracers die bewezen geschikt zijn gebleken voor de schildwachtklierprocedure. In 2013 demonstreerde Heuveling et al. al de potentie van PET/CT lymfoscintigrafie met zirconium-89 ( $^{89}\text{Zr}$ ) gelabeld nanocolloïd. Aanpassingen waren echter nodig om betrouwbaar de gedetecteerde schildwachtklieren op te kunnen zoeken tijdens de operatie. Door gebruik te maken van gallium-68 ( $^{68}\text{Ga}$ ) in plaats van zirconium-89, welke een kortere halfwaardetijd heeft (68 minuten versus 78 uur), kan gebruik gemaakt worden van een radiotracer die gelabeld is met zowel gallium-68 als technetium-99m. Dit zou PET/CT lymfoscintigrafische beelden met een hoge resolutie mogelijk maken en de volgende dag, na volledig verval van gallium-68, het opzoeken van de afgebeelde schildwachtklieren met behulp van het technetium-99m signaal, zoals ook het geval is bij de standaard schildwachtklierprocedure. Gallium-68 kon echter niet gelabeld worden aan nanocolloïd vanwege de instabiele verbinding tussen gallium-68 en nanocolloïd, maar kon wel betrouwbaar gelabeld worden aan tilmanocept. In **hoofdstuk 10** werd PET/CT lymfoscintigrafie met behulp van [ $^{68}\text{Ga}$ ]Ga-tilmanocept vergeleken met standaard lymfoscintigrafie met [ $^{99\text{m}}\text{Tc}$ ]Tc-tilmanocept in 10 patiënten met vroeg-stadium mondholttekanker. [ $^{68}\text{Ga}$ ]Ga-tilmanocept PET/CT lymfoscintigrafie kon nauwkeuriger schildwachtklieren detecteren dan [ $^{99\text{m}}\text{Tc}$ ]Tc-tilmanocept lymfoscintigrafie en kon bovendien 4 schildwachtklieren detecteren dicht bij de injectieplaats die niet gedetecteerd konden worden met [ $^{99\text{m}}\text{Tc}$ ]Tc-tilmanocept lymfoscintigrafie. Door de hogere resolutie van [ $^{68}\text{Ga}$ ]Ga-tilmanocept PET/CT lymfoscintigrafie kon in 8 van de 10 patiënten (80%) lymfbanen in beeld worden gebracht die de radiotracer transporteren; met [ $^{99\text{m}}\text{Tc}$ ]Tc-tilmanocept lymfoscintigrafie was dat slechts mogelijk in 2 van de 10 patiënten (20%). Het in beeld brengen van lymfbanen die de radiotracer transporteren is behulpzaam in het onderscheid maken tussen schildwachtklieren en hogere echelonklieren. Uiteindelijk konden 30 van de 33 schildwachtklieren (91%) die gedetecteerd waren met [ $^{68}\text{Ga}$ ]Ga-tilmanocept PET/CT lymfoscintigrafie gelokaliseerd worden tijdens de operatie met behulp van het technetium-99m signaal. Deze veelbelovende resultaten, ook al in een kleine patiëntenpopulatie, illustreren de potentie van [ $^{68}\text{Ga}$ ]Ga-tilmanocept PET/CT lymfoscintigrafie. Men moet zich echter bewust zijn van de hogere materiële kosten die met deze techniek gepaard gaan (**hoofdstuk 11**). Deze hogere materiële kosten kunnen echter mogelijk gecompenseerd worden door de kortere scantijd van [ $^{68}\text{Ga}$ ]Ga-tilmanocept PET/CT lymfoscintigrafie ten opzichte van standaard lymfoscintigrafie, waardoor het onderzoek overigens ook minder belastend is voor de patiënt, en de daaruit voortkomende reductie in relatieve personeelskosten. Bovendien, als deze techniek ook in vervolgonderzoek nauwkeuriger blijkt en zo het aantal patiënten kan reduceren waarbij onterecht de lymfeklieren in de hals als “schoon” afgegeven worden (fout-negatieve uitslag), zal het aantal patiënten die uitgebreide en kostbare zorg in een later stadium nodig heeft, afnemen.

Al met al heeft de schildwachtklierprocedure de capaciteit om de electieve halsklierdissectie te overtreffen in de behandeling van patiënten met vroegstadium mondholtekanker. De standaard schildwachtklierprocedure heeft reeds in meerdere gerandomiseerde klinische trials bewezen niet onder te doen voor een behandelingsstrategie met een electieve halsklierdissectie. Verder zijn het minder invasieve karakter, met minder morbiditeit tot gevolg, en het vermogen om individuele patronen voor lymfeklieruitzaaiingen te detecteren, belangrijke voordelen van de schildwachtklierprocedure ten opzichte van de electieve halsklierdissectie. Hoewel de schildwachtklierprocedure momenteel beperkt wordt door zijn matige resolutie en hinderlijke 'shine-through fenomeen', kunnen nieuwe ontwikkelingen deze beperkingen overwinnen. De meeste nieuwe technieken die worden beschreven in dit proefschrift dienen echter nog verder ontwikkeld te worden om een reëel alternatief te zijn voor de huidige schildwachtklierprocedure. [<sup>68</sup>Ga]Ga-tilmanocept PET/CT lymfoscintigrafie daarentegen blijkt een veelbelovende techniek die de potentie heeft om de nieuwe standaard te worden voor de schildwachtklierprocedure bij vroegstadium mondholtekanker.



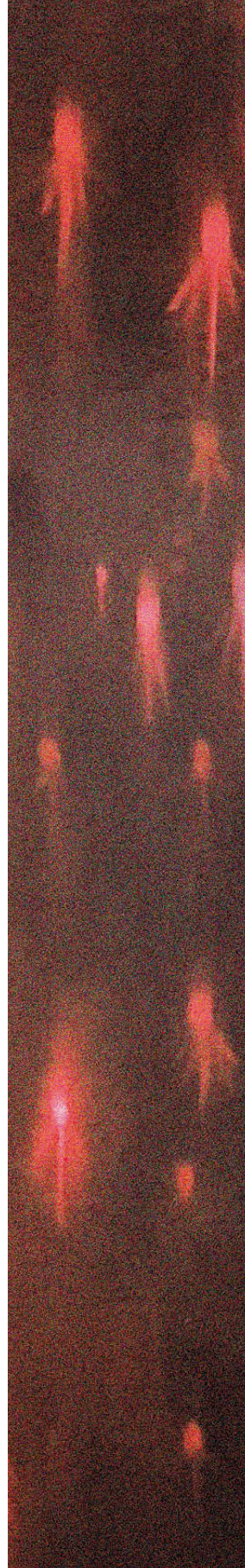




List of publications

Acknowledgments | *Dankwoord*

About the author | *Curriculum Vitae*



## LIST OF PUBLICATIONS

- Mahieu R**, Russo S, Gualtieri T, Colletti G, Deganello A. Oral cavity reconstruction with the masseter flap. *Acta Otorhinolaryngol Ital.* 2016;36(2):139-143. doi:10.14639/0392-100X-890
- Mahieu R**, Coenen MN, van Bommel T, van der Zaag-Loonen HJ, Theuvenet WJ. Detecting intrinsic muscle weakness of the hallux as an addition to early-stage screening of the feet in patients with diabetes. *Diabetes Res Clin Pract.* 2016;119:83-87. doi:10.1016/j.diabres.2016.07.007
- Mahieu R**, Colletti G, Bonomo P, et al. Head and neck reconstruction with pedicled flaps in the free flap era. *Acta Otorhinolaryngol Ital.* 2016;36(6):459-468. doi:10.14639/0392-100X-1153
- Mahieu R**, Heuveling D, Mahieu H. Superomedial partial arytenoidectomy for voice improvement by correction of posterior glottic insufficiency. *Eur Arch Otorhinolaryngol.* 2020;277(5):1417-1426. doi:10.1007/s00405-020-05859-2
- Mahieu R**, de Maar JS, Nieuwenhuis ER, et al. New developments in imaging for sentinel lymph node biopsy in early-stage oral cavity squamous cell carcinoma. *Cancers (Basel).* 2020;12(10):3055. doi:10.3390/cancers12103055
- den Toom IJ, **Mahieu R**, van Rooij R, et al. Sentinel lymph node detection in oral cancer: a within-patient comparison between [<sup>99m</sup>Tc]Tc-tilmanocept and [<sup>99m</sup>Tc]Tc-nanocolloid. *Eur J Nucl Med Mol Imaging.* 2021;48(3):851-858. doi:10.1007/s00259-020-04984-8
- Mahieu R**, den Toom IJ, Boeve K, et al. Contralateral regional recurrence in lateralized or paramedian early-stage oral cancer undergoing sentinel lymph node biopsy-comparison to a historic elective neck dissection cohort. *Front Oncol.* 2021;11:644306. doi:10.3389/fonc.2021.644306
- Mahieu R**, Krijger GC, Ververs FFT, de Roos R, de Bree R, de Keizer B. [<sup>68</sup>Ga]Gatilmanocept PET/CT lymphoscintigraphy for sentinel lymph node detection in early-stage oral cavity carcinoma. *Eur J Nucl Med Mol Imaging.* 2021;48(4):1246-1247. doi:10.1007/s00259-020-05060-x
- Mahieu R**, Krijger GC, Ververs FFT, de Roos R, de Bree R, de Keizer B. [<sup>68</sup>Ga]Gatilmanocept PET/CT lymphoscintigraphy: a novel technique for sentinel lymph node imaging. *Eur J Nucl Med Mol Imaging.* 2021;48(4):963-965. doi:10.1007/s00259-020-05101-5
- Mahieu R**, Thomeer HGXM, Straatman LV. Chronisch loopoor door liquorlekkage. *Ned Tijdschr Geneeskd.* 2021;165:D5456.
- Mahieu R**, den Toom IJ, van Rooij R, et al. Diagnostic accuracy of [<sup>99m</sup>Tc]Tc-tilmanocept compared to [<sup>99m</sup>Tc]Tc-nanocolloid for sentinel lymph node identification in early-stage oral cancer. *Clin Otolaryngol.* 2021;46(6):1383-1388. doi:10.1111/coa.13798

- Zeeuw M, **Mahieu R**, de Keizer B, de Bree R. Evaluation of a streamlined sentinel lymph-node imaging protocol in early-stage oral cancer. *Ann Nucl Med*. 2021;35(12):1353-1360. doi:10.1007/s12149-021-01677-6
- Mahieu R**, Donders DNV, Krijger GC, et al. Within-patient comparison between [<sup>68</sup>Ga]Ga-tilmanocept PET/CT lymphoscintigraphy and [<sup>99m</sup>Tc]Tc-tilmanocept lymphoscintigraphy for sentinel lymph node detection in oral cancer: a pilot study. *Eur J Nucl Med Mol Imaging*. 2022;49(6):2023-2036. doi:10.1007/s00259-021-05645-0
- de Bree R, **Mahieu R**, Donders DNV, de Keizer B. Detection of sentinel lymph nodes by tilmanocept in oral squamous cell carcinoma. *Clin Exp Metastasis*. 2022;39(3):417-419. doi:10.1007/s10585-022-10159-6
- Mahieu R**, Donders DNV, Dankbaar JW, de Bree R, de Keizer B. CT Lymphography Using Lipiodol® for Sentinel Lymph Node Biopsy in Early-Stage Oral Cancer. *J Clin Med*. 2022;11(17):5129. doi:10.3390/jcm11175129
- Mahieu R**, Tijink BM, van Es RJJ, et al. The potential of the Crystal Cam handheld gamma-camera for preoperative and intraoperative sentinel lymph node localization in early-stage oral cancer. *Eur Arch Otorhinolaryngol*. 2023;280(12):5519-5529. doi:10.1007/s00405-023-08138-y
- Mahieu R**, Rijken JA, Jansen TTG, Groen AH. KNOck KNOck cast: de podcast over KNO en hoofd-halschirurgie. *NTvKNO*. 2024;30(4):125-126
- Donders DNV, **Mahieu R**, Tellman RS, et al. Sentinel lymph node detection in early-stage oral squamous cell carcinoma using magnetic resonance lymphography: a pilot study. *J Clin Med*. 2024;13(23):7052. doi:10.3390/jcm13237052
- Tellman RS, Donders DNV, **Mahieu R**, et al. Evaluation of the 10 %-rule in sentinel lymph node biopsy for clinically node-negative oral squamous cell carcinoma. *Oral Oncol*. 2025;160:107110. doi:10.1016/j.oraloncology.2024.107110

## ACKNOWLEDGMENTS | DANKWOORD

Dit proefschrift is tot stand gekomen dankzij hulp en steun van vele kanten, waardoor ik, al zijnde het 't laatste loodje, met veel plezier dit dankwoord schrijf. Het biedt de gelegenheid om nog één keer terug te mogen blikken op een geweldige periode en degenen die direct, dan wel indirect, een bijdrage aan dit proefschrift hebben geleverd in het zonnetje te mogen zetten. Ik heb het voorrecht gehad om in mijn vooralsnog korte medische en wetenschappelijke carrière met hele bijzondere mensen samen te mogen werken, die ik dan ook expliciet wil bedanken.

Op de eerste plaats zou ik graag alle patiënten willen bedanken die hebben bijgedragen aan dit onderzoek. In een voor hen onzekere en turbulente periode zijn zij bereid geweest om bij te dragen aan wetenschappelijk onderzoek. Voor velen van hen behelsde deelname een extra serie injecties op een dikwijls gevoelige plek, rondom de tumor in de mond, waar diezelfde dag al injecties hadden plaatsgevonden. Het is bewonderenswaardig dat zoveel patiënten gemotiveerd zijn geweest om dit te ondergaan, in de hoop dat patiënten in de toekomst gebaat zijn bij de uitkomsten van het onderzoek. Dit proefschrift had niet kunnen bestaan zonder hun onbaatzuchtigheid, inzet en vertrouwen.

Daarnaast natuurlijk mijn promotoren, prof. dr. R. de Bree en dr. B. de Keizer. Beste Remco en Bart, een beter promotieteam had ik niet durven wensen. Samen vormden jullie een onuitputtelijk duo. Pragmatisch, efficiënt, kritisch, een bron van eindeloze inspiratie en ideeën en bovenal verdraaid vlot. De geruchten van mijn voorgangers dat elk stuk binnen een etmaal weer nagekeken en wel zijn retour zou vinden in mijn inbox, ongeacht het moment van versturen, bleek niets minder dan waar. Het is dankzij jullie gedrevenheid dat wij zoveel studies hebben kunnen opzetten en aantoonbare stappen hebben kunnen zetten naar een betere schildwachtklierprocedure. Het plezier wat ik heb gehad in dit onderzoek heb ik voor een aanzienlijk deel aan jullie te danken. Remco, graag wil ik jou bedanken dat jij mij de kans hebt geboden om dit project aan te gaan. Het bleek niet alleen een prachtig klinisch onderzoeksproject waar mijn hart sneller van is gaan kloppen, maar was uiteindelijk ook het opstapje naar een opleidingsplaats bij de KNO en hoofd-halschirurgie in het UMC Utrecht. Bedankt voor jouw vertrouwen en begeleiding, zowel wetenschappelijk als nu ook klinisch. Bart, graag wil ik jou bedanken voor mijn introductie in de wondere wereld van de nucleaire geneeskunde. Ook jij maakt altijd tijd voor mij en weet mij direct op weg te helpen als er iets moet gebeuren op radiologisch of nucleair gebied. Tot op de dag van vandaag geniet ik van onze samenwerking.

&

Leden van de beoordelings- en promotiecommissie, beste prof. dr. P.J. van Diest, prof. dr. M.G.E.H. Lam, prof. dr. M.R. Vriens, prof. dr. M.J.H. Witjes, prof. dr. R.P. Takes, prof. dr. C.H.J. Terhaard en dr. R.A. Valdès Olmos, dank voor het kritisch doornemen van dit proefschrift.

Beste Najiba, Klijs en Maartje, bedankt voor de goede sfeer die jullie hebben gebracht als collega-onderzoekers van de Hoofd-Hals Chirurgische Oncologie in het Q-gebouw. Het was een waar genoegen om met jullie het nauwe evenwicht op te zoeken tussen serieus wetenschappen, klagen en zuchten over de toenemende mate van bureaucratie die het onderzoek behelst en gezelligheid. Beste Inne, ik mag mij absoluut gelukkig prijzen dat ik jou op heb mogen volgen als sentinel node onderzoeker. Met al het werk wat jij reeds had verricht stapte ik op een rijdende trein op volle toeren. Het is mede dankzij jouw inzet en punctualiteit dat wij feilloos en met dezelfde vaart het onderzoek voort konden zetten. Veel succes met jouw verdere carrière als chirurg. Beste Dominique en Roosmarijn, bedankt voor de manier waarop jullie het sentinel node onderzoek voortzetten. Het is fijn om te weten dat de onderzoekslijn in goede handen is. Jullie worden geteisterd door de administratieve rompslomp die multicenter onderzoek met zich meebrengt, alsmede door leveringsproblemen van de noodzakelijke tracers, maar ik heb alle vertrouwen dat voor jullie een prachtig proefschrift in het verschiet ligt.

Hoofd-halschirurgen en fellows van het UMC Utrecht: Weibel Braunius, Bernard Tijink, Johannes Rijken, Luuk Janssen, Remco de Bree, Robert van Es, Ellen van Cann, François Dieleman, Thomas Klein Nulent en Reinoud Klijn; dank voor jullie inzet, betrokkenheid en geduld bij het implementeren van onderzoek binnen de kliniek. Bedankt dat jullie altijd bereid waren om de tijd te nemen voor de inclusie van patiënten of voor het gebruik van ‘weer’ een nieuwe camera op de operatiekamer. Beste Weibel, Bernard, Johannes, Luuk, Remco en David, ik mag mijn maat 7 handjes dichtknijpen met de training en begeleiding die jullie mij bieden als AIOS en differentiant. Het is mede dankzij jullie dat mijn enthousiasme voor de hoofd-halschirurgie elke dag verder toeneemt.

NUG-seniors en laboranten van de Nucleaire Geneeskunde, zonder jullie was het nooit wat geworden. Bedankt voor jullie flexibiliteit en tomeloze inzet. Geïnccludeerde patiënten kwamen altijd met meerderen tegelijk en jullie wisten het zo in te passen dat het precies kon. Ik wil jullie ontzettend bedanken dat jullie altijd bereid waren om een stap extra te zetten voor het onderzoek, altijd geïnteresseerd waren, deden voorkomen alsof het nooit een probleem was wat wij van jullie vroegen en vooral ook in waren voor een gezellige babbel. Dit proefschrift heb ik mede aan jullie te danken. Beste Rob van Rooij, Casper Beijst en Bastiaan van Nierop, bedankt dat wij gebruik

mochten maken van jullie expertise als klinisch fysici. Bovendien was het heel fijn dat ik altijd binnen mocht komen waaien om nog een keer in jip-en-janneketaal uitleg te krijgen over hoe het allemaal nou precies werkt. Jullie input, rekenkracht en visie zijn van grote waarde geweest en hebben het onderzoek naar een hoger niveau gebracht. Beste Alex Poot, Tessa Ververs, Gerard Krijger, John Bemelmans en Remmert de Roos, bedankt voor alle ondersteuning in het opzetten en aanvragen van het geneesmiddelenonderzoek en het valideren en bereiden van de radionucliden. Jullie wisten regelmatig weer licht in de duisternis te scheppen voor iemand die volslagen onbekend was in de radionucliden-wereld. Het was soms een flinke klus, maar uiteindelijk hebben wij prachtige resultaten bereikt samen.

Beste Nicole en Ingeborg, bedankt voor jullie hulp bij de soms nagenoeg onmogelijke planning van onze studiepatiënten. Alhoewel het een enorme uitdaging kon zijn om alles in te plannen voor de operatie, waarbij het essentieel was dat de behandeling geen vertraging opliep, kregen jullie het telkens toch weer voor elkaar. Het is dankzij jullie dat de inclusie zo vlot verliep en dat dit proefschrift nu compleet is.

Bea den Hollander, ook jou wil ik heel graag bedanken voor alles wat jij voor ons als onderzoekers hebt gedaan. Het is een groot gemis dat jij het UMC Utrecht achter je hebt gelaten, maar ik was verheugd om te zien dat je toch nog langskwam bij het afscheid van José. Hopelijk kruisen onze paden zich binnenkort weer.

Graag wil ik ook van de gelegenheid gebruik maken om alle co-auteurs te bedanken van de in dit proefschrift opgenomen artikelen. Dank voor de prettige samenwerking, betrokkenheid bij het onderzoek, ideeën en feedback op de manuscripten.

Naast de mensen die een directe bijdrage hebben geleverd aan dit proefschrift, zou ik ook graag een aantal andere mensen willen bedanken waarmee ik in de afgelopen jaren heb samen mogen werken of die mij hebben geïnspireerd. Te beginnen met Robert Stokroos en Ivonne Ligtenberg, bedankt dat jullie mij de mogelijkheid hebben geboden om, na mijn rol als arts-onderzoeker, opgeleid te mogen worden tot KNO-arts. Ook de KNO-stafleden van het UMC Utrecht, St. Antonius Ziekenhuis en Gelre Ziekenhuizen wil ik ontzettend bedanken voor hun tijd en investering in mij als mens en toekomstig KNO-arts. Dankzij jullie training, wijze lessen en supervisie heb ik in de afgelopen jaren een enorme groei doorgemaakt, waar ik jullie altijd heel dankbaar voor zal zijn.

Waarde KNO-llega's, lieve mede-AIOS, bedankt voor de geweldige jaren samen en voor de tijd die nog komen gaat. Het is een waar genot om onderdeel te zijn van deze groep. Bedankt voor het sparren en voor de steun waar het nodig was, maar vooral

bedankt voor de gezelligheid en mooie herinneringen samen. In het bijzonder dank aan Jan en Rick, lichtingsgenoten, vrienden en nu ook paranimfen. De afgelopen jaren heb ik, ondanks jullie eigen drukke leven, zowel op werk als thuis, altijd op jullie kunnen rekenen. Ook nu kan ik weer op jullie bouwen. Sinds ik jullie heb leren kennen zijn jullie waardevolle vrienden gebleken waarmee ik kan niet alleen kan lachen, zeuren en borrelen, maar zijn jullie ook het klankbord dat mij telkens weer prikkelt om te presteren en alles uit de kast te halen. Het is mooi om te zien hoe jullie beiden een eigen pad bewandelen en laten zien dat alles mogelijk is als je er maar hard voor werkt. Het kan niet anders dan dat jullie een prachtige carrière tegemoet gaan en ik ben absoluut trots dat jullie mijn paranimfen willen zijn.

Beste Wim Theuvenet, onder jouw vleugels is de basis gelegd voor mijn wetenschappelijke carrière en daarmee voor dit proefschrift. Ook al is het destijds niet gelukt om samen een PhD-traject op te tuigen, ligt er nu uiteindelijk toch een boekje en daar houd ik jou mede verantwoordelijk voor. Ik ben ontzettend dankbaar dat jij mij zo vroeg in mijn studie op sleeptouw hebt willen nemen, voor alle tijd die jij in mij hebt geïnvesteerd en voor alle oprechte belangstelling die jij in mij hebt getoond. Lang heb ik gedacht in jouw voetsporen te willen treden als plastisch chirurg, maar uiteindelijk moest ik toch toegeven aan mijn passie voor de KNO en hoofd-halschirurgie. Bedankt voor de dierbare herinneringen die ik heb overgehouden aan onze samenwerking en aan onze reis naar Washington (en Baltimore).

Caro prof. dott. Alberto Deganello, vorrei ringraziarti per il mio periodo indimenticabile in Italia. Con il tuo entusiasmo contagioso per la professione e una guida eccezionale, hai gettato le basi per la mia carriera nella otorinolaringoiatria e nella chirurgia della testa e del collo. Ti sono eternamente grato per questo. Grazie per il tuo incoraggiamento, per l'ospitalità senza pari e per il trasferimento di conoscenze. Non dimenticherò mai che sotto la tua supervisione ho effettuato la mia prima incisione (pectoral major flap, lato destro). Infine, sono grato che tu possa dimostrare meglio di chiunque altro che la vita non è solo lavoro e che è importante anche godersela: grazie per la bellissima festa con Zero Tituli. Ti auguro buona fortuna come Direttore dell'Istituto Nazionale dei Tumori di Milano e spero di rivederti presto. Grazie!

Enrico Muratori, ook jij verdient absoluut een plek in dit dankwoord. Tijdens mijn tijd in Florence heb jij mij onder je hoede genomen, wat mijn tijd daar onvergetelijk heeft gemaakt. Zelfs toen ik noodgedwongen uit mijn kamer in Florence moest, regelde jij direct dat ik in jouw huis mocht komen wonen. Jij schroomde nooit om mij op sleeptouw te nemen, zoals naar de World Expo in Milan, naar jouw familie en zelfs op wintersport. Bedankt dat jij mij telkens kwam ophalen bij de Lorenzi skilift. Bedankt voor alle gezellige etentjes samen met jou en Ali. Bedankt voor alle mooie

herinneringen samen en bovenal bedankt voor deze buitengewone vriendschap. Lieve vrienden, familieleden en schoonfamilie, nu is het eindelijk klaar. Bedankt voor jullie altijd aanwezige interesse en gezelschap. Ik voel mij bevoorrecht met zo'n fijne groep mensen om mij heen.

Lieve Erik, grote broer, wat geweldig om te merken dat wij opnieuw weer meer naar elkaar toe groeien. Het is zo leuk om te zien dat de gedeelde interesses vanuit onze jeugd weer worden aangewakkerd, ondanks dat wij zo'n ander pad des levens hebben bewandeld en daarom ook zo verschillend kunnen zijn. Ik ben ontzettend dankbaar dat Tamara en Emma onderdeel zijn geworden van de familie en trots op de band die wij met jullie als gezin hebben. Ik geniet elke keer weer immens van de momenten die wij met jullie mogen delen en verheug mij telkens weer op de volgende.

Lieve mam en pap, dit proefschrift is een eerbetoon aan jullie als ouders. Jullie zijn verantwoordelijk voor de man die ik geworden ben; ik hoop maar dat jullie dat als een compliment beschouwen. Jullie hebben mij altijd alle ruimte en vrijheid geboden om mij te ontwikkelen als mens, maar wisten ook precies op de juiste momenten net dat steuntje in de rug te bieden die ik nodig had. Nooit heb ik jullie kunnen betrappen op het sturen van mijn keuzes en ik ben er dan ook heilig van overtuigd dat jullie even geïnteresseerd zouden zijn, misschien zelfs een beetje meer, als dit proefschrift niet een medische inhoud had. Jullie blijken een ijzersterk team en vullen elkaar, mede vanwege jullie verschillen, feilloos aan. Dat maakt ook dat jullie voor mij allebei op een eigen manier onmisbaar zijn. Van jullie beiden heb ik nog eindeloos veel te leren en dat hoop ik nog heel lang te mogen doen.

Lieve Rian, het moment waarvan jij wist dat het ging komen, alleen nog niet precies wanneer. Uit goede hoop kwam jij al bijna twee jaar geleden met een cadeau voor mijn aanstaande promotie, maar toch bleef die weer wat langer op zich wachten. Nu is het dan eindelijk zover. Bedankt voor jouw geduld en voor al die avonden dat jij mij wist aan te moedigen om aan de slag te gaan, in de wetenschap dat jij jezelf maar weer moest zien te vermaken. Overigens, terwijl jij al jouw handen vol had aan jouw eigen carrière, was jij bereid om de motor in huis te zijn, waardoor ik de gelegenheid kreeg om al het nodige werk voor dit proefschrift te doen. Ik had hier niet gestaan zonder jou. Graag wil ik je bedanken voor het feit dat het leven al ruim 10 jaar leuker en beter is met jou. Niet alleen ben jij mijn maatje, mijn steun en toeverlaat, maar heb jij mij ook sinds ons samenzijn in vrijwel elk opzicht naar een hoger niveau getild. Bedankt dat jij mijn betere wederhelft wil zijn, bedankt dat jij mij laat lachen en alvast bedankt voor wat wij samen nog mee gaan maken.

## ABOUT THE AUTHOR | CURRICULUM VITAE

Rutger Mahieu was born on the 1<sup>st</sup> of April 1993 in Blaricum, the Netherlands. He grew up in Bussum with his parents Hans and Margriet and his older brother Erik. In 2011 he graduated from the Willem de Zwijger College in Bussum and started his medical study at the Rijksuniversiteit Groningen.



His first experience with medical research took place during his bachelor under supervision of dr. Wim Theuvenet, as he investigated intrinsic muscle weakness in the feet of diabetic patients. After finishing his bachelor's degree, he moved to Florence, Italy, for seven months to carry out a research clerkship on the reconstruction of head and neck defects under supervision of prof. dr. Alberto Deganello. In the course of his subsequent internships back in the Netherlands, motivated by his experience in Italy, he decided to pursue a career in otorhinolaryngology and head and neck surgery.

In 2019 he obtained his master's degree after fulfilling his senior internship at the departments Otorhinolaryngology and Head and Neck Surgical Oncology of the University Medical Center Utrecht. There he got the opportunity by prof. dr. Remco de Bree to continue his research journey and start the PhD project that led to this thesis.

Following two years of conducting research, he enrolled in the residency program of otorhinolaryngology and head and neck surgery at the University Medical Center Utrecht, under supervision of drs. Ivonne Ligtenberg – van der Drift and prof. dr. Robert Stokroos. During his training he joined the Dutch Head and Neck Surgery and Skull Base Pathology committee and co-founded a Dutch medical podcast on otorhinolaryngology and head and neck surgery. Currently, Rutger is finishing his residency program with a projected graduation in October 2025.





